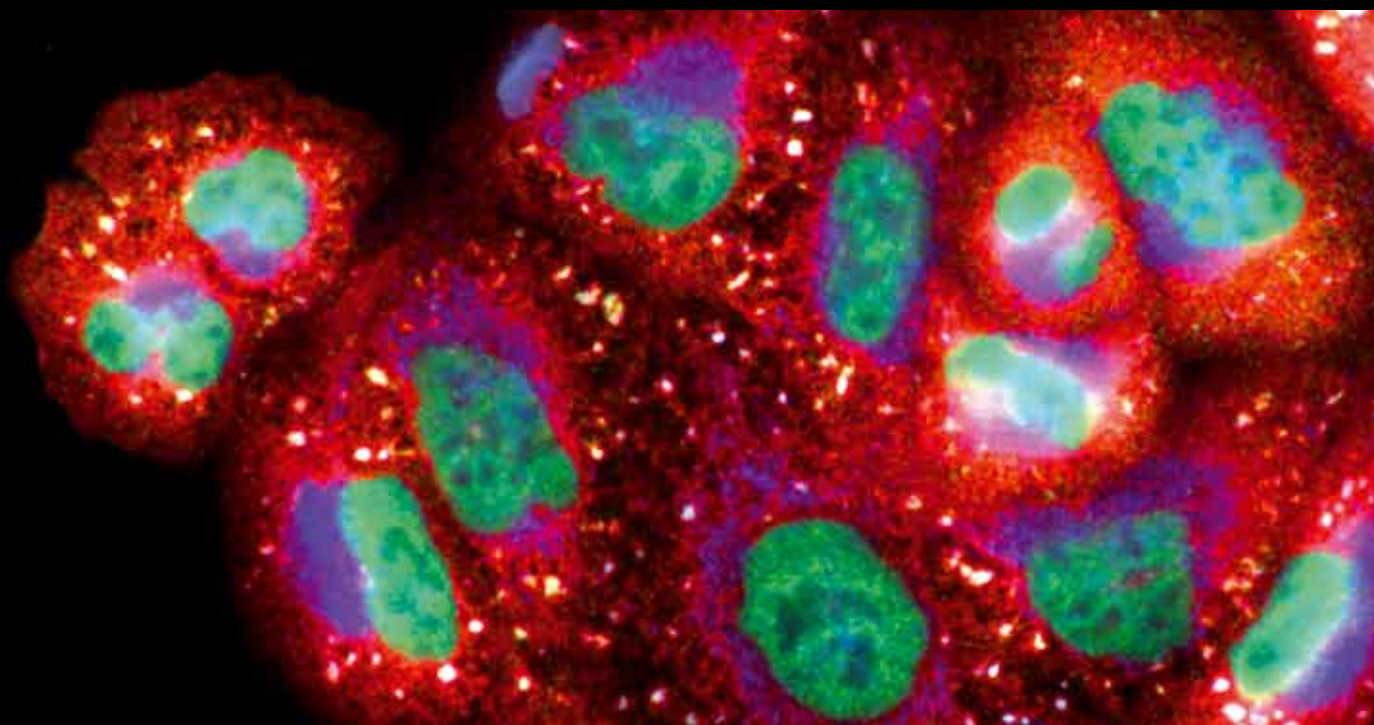


Oxidative Stress in Cardiovascular Pathologies: Genetics, Cellular, and Molecular Mechanisms and Future Antioxidant Therapies

Guest Editors: Adrian Manea, Ana Fortuno, and Jose Luis Martin-Ventura





Oxidative Stress in Cardiovascular Pathologies: Genetics, Cellular, and Molecular Mechanisms and Future Antioxidant Therapies

Oxidative Medicine and Cellular Longevity

Oxidative Stress in Cardiovascular Pathologies: Genetics, Cellular, and Molecular Mechanisms and Future Antioxidant Therapies

Guest Editors: Adrian Manea, Ana Fortuno,
and Jose Luis Martin-Ventura



Copyright © 2012 Hindawi Publishing Corporation. All rights reserved.

This is a special issue published in “Oxidative Medicine and Cellular Longevity.” All articles are open access articles distributed under the Creative Commons Attribution License, which permits unrestricted use, distribution, and reproduction in any medium, provided the original work is properly cited.

Editorial Board

Mohammad Abdollahi, Iran
Antonio Ayala, Spain
Peter Backx, Canada
Consuelo Borrás, Spain
Elisa Cabiscol, Spain
Vittorio Calabrese, Italy
Shao-yu Chen, USA
Zhao Zhong Chong, USA
Felipe Dal-Pizzol, Brazil
Ozcan Erel, Turkey
Ersin Fadillioglu, Turkey
Qingping Feng, Canada
Swaran J. S. Flora, India
Janusz Gebicki, Australia
Husam Ghanim, USA
Daniela Giustarini, Italy
Hunjo Ha, Republic of Korea
Giles E. Hardingham, UK

Michael R. Hoane, USA
Vladimir Jakovljevic, Serbia
Raouf A. Khalil, USA
Neelam Khaper, Canada
Mike Kingsley, UK
Eugene A. Kiyatkin, USA
Lars-Oliver Klotz, Canada
Ron Kohen, Israel
Jean-Claude Lavoie, Canada
Christopher Horst Lillig, Germany
Kenneth Maiese, USA
Bruno Meloni, Australia
Luisa Minghetti, Italy
Ryuichi Morishita, Japan
Donatella Pietraforte, Italy
Aurel Popa-Wagner, Germany
José L. Quiles, Spain
Pranela Rameshwar, USA

Sidhartha D. Ray, USA
Francisco Javier Romero, Spain
Gabriele Saretzki, UK
Honglian Shi, USA
Cinzia Signorini, Italy
Richard Siow, UK
Sidney J. Stohs, USA
Oren Tirosh, Israel
Madia Trujillo, Uruguay
Jeannette Vasquez-Vivar, USA
Donald A. Vessey, USA
Victor M. Victor, Spain
Michal Wozniak, Poland
Sho-ichi Yamagishi, Japan
Liang-Jun Yan, USA
Jing Yi, China
Guillermo Zalba, Spain

Contents

Oxidative Stress in Cardiovascular Pathologies: Genetics, Cellular, and Molecular Mechanisms and Future Antioxidant Therapies, Adrian Manea, Ana Fortuno, and Jose Luis Martin-Ventura
Volume 2012, Article ID 373450, 3 pages

Sodium-Glucose Cotransporter Inhibition Prevents Oxidative Stress in the Kidney of Diabetic Rats, Horacio Osorio, Israel Coronel, Abraham Arellano, Ursino Pacheco, Rocío Bautista, Martha Franco, and Bruno Escalante
Volume 2012, Article ID 542042, 7 pages

Oxygen Concentration-Dependent Oxidative Stress Levels in Rats, Fumiko Nagatomo, Hidemi Fujino, Hiroyo Kondo, and Akihiko Ishihara
Volume 2012, Article ID 381763, 5 pages

Intensification of Doxorubicin-Related Oxidative Stress in the Heart by Hypothyroidism Is Not Related to the Expression of Cytochrome P450 NADPH-Reductase and Inducible Nitric Oxide Synthase, As Well As Activity of Xanthine Oxidase, Jaroslaw Dudka, Franciszek Burdan, Agnieszka Korga, Magdalena Iwan, Barbara Madej-Czerwona, Monika Cendrowska-Pinkosz, Agnieszka Korobowicz-Markiewicz, Barbara Jodlowska-Jedrych, and Włodzimierz Matysiak
Volume 2012, Article ID 139327, 11 pages

Evaluation of Oxidative Stress and Antioxidant Status in Diabetic and Hypertensive Women during Labor, Mashaal M. Al-Shebly and Mahmoud A. Mansour
Volume 2012, Article ID 329743, 6 pages


Effect of Antioxidant Mineral Elements Supplementation in the Treatment of Hypertension in Albino Rats, S. A. Muhammad, L. S. Bilbis, Y. Saidu, and Y. Adamu
Volume 2012, Article ID 134723, 8 pages

Protective Effects of Aspirin from Cardiac Hypertrophy and Oxidative Stress in Cardiomyopathic Hamsters, Rong Wu, David Yin, Nataliya Sadekova, Christian F. Deschepper, Jacques de Champlain, and Helene Girouard
Volume 2012, Article ID 761710, 8 pages

Cell Stress Proteins in Atherothrombosis, Julio Madrigal-Matute, Roxana Martinez-Pinna, Carlos Ernesto Fernandez-Garcia, Priscila Ramos-Mozo, Elena Burillo, Jesus Egido, Luis Miguel Blanco-Colio, and Jose Luis Martin-Ventura
Volume 2012, Article ID 232464, 10 pages

Blockade of TGF- β 1 Signalling Inhibits Cardiac NADPH Oxidase Overactivity in Hypertensive Rats, José Luis Miguel-Carrasco, Ana Baltanás, Carolina Cebrián, María U. Moreno, Begoña López, Nerea Hermida, Arantxa González, Javier Dotor, Francisco Borrás-Cuesta, Javier Díez, Ana Fortuño, and Guillermo Zalba
Volume 2012, Article ID 726940, 8 pages

Ginkgo Biloba Extract EGB761 Protects against Aging-Associated Diastolic Dysfunction in Cardiomyocytes of D-Galactose-Induced Aging Rat, Jing Liu, Junhong Wang, Xiangjian Chen, Changqing Guo, Yan Guo, and Hui Wang
Volume 2012, Article ID 418748, 7 pages



Phytochemical Activation of Nrf2 Protects Human Coronary Artery Endothelial Cells against an Oxidative Challenge, Elise L. Donovan, Joe M. McCord, Danielle J. Reuland, Benjamin F. Miller, and Karyn L. Hamilton

Volume 2012, Article ID 132931, 9 pages

Metformin Rescues the Myocardium from Doxorubicin-Induced Energy Starvation and Mitochondrial Damage in Rats, Abdelkader E. Ashour, Mohamed M. Sayed-Ahmed, Adel R. Abd-Allah, Hesham M. Korashy, Zaid H. Maayah, Hisham Alkhalidi, Mohammed Mubarak, and Abdulqader Alhaider

Volume 2012, Article ID 434195, 13 pages

Editorial

Oxidative Stress in Cardiovascular Pathologies: Genetics, Cellular, and Molecular Mechanisms and Future Antioxidant Therapies

Adrian Manea,¹ Ana Fortuno,² and Jose Luis Martin-Ventura³

¹ *Department of Genomics, Transcriptomics, and Molecular Therapies, Molecular and Cellular Pharmacology, Functional Genomics Laboratory, Institute of Cellular Biology and Pathology "Nicolae Simionescu," 8 BP Hasdeu Street, 050568 Bucharest, Romania*

² *Division of Cardiovascular Sciences, Center for Applied Medical Research, University of Navarra, Pio XII, 31008 Pamplona, Spain*

³ *Vascular Research Laboratory, Fundación Jiménez Díaz, Autonomous University of Madrid, Avenida Reyes Católicos 2, 28040 Madrid, Spain*

Correspondence should be addressed to Adrian Manea, adrian.manea@icbp.ro

Received 23 December 2012; Accepted 23 December 2012

Copyright © 2012 Adrian Manea et al. This is an open access article distributed under the Creative Commons Attribution License, which permits unrestricted use, distribution, and reproduction in any medium, provided the original work is properly cited.

Reactive oxygen species (ROS) are generated during normal cell physiology; however increased ROS formations are highly detrimental in many cardiometabolic disorders, including atherosclerosis, hypertension, diabetes, obesity, neurodegenerative diseases, and aneurism [1–3]. Despite the numerous existing data the role of ROS and the associated redox mechanisms of the disease inception and progression remain elusive. A common feature of all cardiovascular disorders is the occurrence of oxidative stress, a condition characterized by an imbalance between ROS production and the ability of biological systems to detoxify the reactive intermediates [4]. Produced in excess, ROS react indiscriminately and cause irreversible damage of the majority of biological molecules, thereby altering cell functions [5]. Although extensive studies have focused on the redox control of vascular response to inflammatory and metabolic insults, the molecular mechanisms ROS generation and the way that this class of molecules contributes to vascular damage are not entirely clear. Therefore, uncovering the intimate molecular control mechanisms involved in regulation of the delicate balance of ROS formation and neutralization in the vascular wall cells is a prerequisite for the development of an effective antioxidant stress therapy.

The topic of this special issue focuses on recent advances in experimental aspects of oxidative stress in cardiovascular disorders. In the current issue, H. Osorio et al. have addressed the role of sodium-glucose cotransporter (SGLT2) in the oxidative and nitrative stress processes taking place in the kidney of diabetic rats. The authors have shown that

SGLT2 inhibition reverse streptozotocin-induced diabetes and redox disbalance in the kidney, suggesting the potential therapeutic role of SGLT2 inhibitors in diabetic nephropathy. The role of oxygen supplementation in systemic redox balance in rats has been investigated in the paper by F. Nagatomo et al. The authors demonstrated that exposure to oxygen concentrations higher than 40% leads to a prooxidant response able to produce morphological changes in red blood cells, whereas antioxidant response does not seem to be modified in the 24 h period of the study. J. Dudka et al. have evaluated the implication of hypothyreosis on the oxidative stress induced by doxorubicin. The authors also analyzed the effect of both hypothyreosis and the drug on cytochrome P450 NADPH-reductase and inducible nitric oxide synthase expression. The results of this study bring additional support that hypothyroid conditions may increase the cardiac oxidative stress caused by doxorubicin. In the paper by M. Al-Shebly and M. Mansour the authors have analyzed whether oxidative stress status is modified in hypertensive/diabetic women during labor. The findings of this study clearly demonstrate that different biomarkers of redox balance-altered in hypertensive/diabetic women during labor and suggest that this redox imbalance could increase the risk of fetal abnormalities. In the paper of S. Muhammad et al., the authors aimed at investigating the antioxidant effects of mineral elements supplementation using a rat model of hypertension. They showed that copper, manganese, and zinc supplementation reduces the blood pressure as compared with hypertensive control.

In addition, a significant reduction in the plasma total cholesterol, triglyceride, low density lipoprotein-cholesterol, very low density lipoprotein-cholesterol, malondialdehyde, and insulin level, as well as increases in the high density lipoprotein cholesterol, total antioxidant activities, and nitric oxide have been demonstrated in the supplemented groups relative to the hypertensive control. Together, the present report highlights that various minerals may play a role in preventing oxidative stress, dyslipidemia, and insulin resistance associated with hypertension. Interestingly, R. Wu et al. demonstrated the beneficial effects of chronic acetylsalicylic acid (ASA) treatment on cardiac hypertrophy and oxidative stress in cardiomyopathic hamsters. The authors concluded that ASA present a therapeutic potential to prevent cardiac dysfunction.

The review of J. Madrigal-Matute et al. is focused on the thioredoxin (TRX) system, which is composed of several proteins such as TRX and Peroxiredoxin (PRDX). In addition to their main role as antioxidants, recent data highlights their function in several processes involved on the development of atherothrombosis. In fact, since TRX and PRDX are present in the atherosclerotic plaque and can be secreted under prooxidative conditions to the circulation, their role as diagnostic, prognostic, and therapeutic biomarkers of cardiovascular diseases (CVD) has been addressed. In conclusion, J. Madrigal-Matute et al. summarized several findings that demonstrate the major role of the TRX system in the maintenance of the redox status in CVD. Furthermore, the extracellular levels of PRDX/TRX seem to be related with a pro-oxidative scenario suggesting their potential role as biomarkers for oxidative related diseases. Nevertheless, their value as useful therapeutic tools is being tested and future studies are necessary to validate its prospective beneficial effects in CVD.

Vascular NADPH oxidases (Nox) are a class of heterooligomeric enzymes, whose unique function is the generation of ROS in a highly regulated manner [6]; conversely, the specific role of each enzyme is yet to be discovered. Nox expression and activity are significantly upregulated in the vasculature of hypertensive subjects and are associated with the development of macro- and microvascular diseases [7]. Since the members of the Nox family are major triggers of oxidative stress they have a prominent role in the pathology of diabetes-induced vasculopathies [8, 9]; thus, Nox and their upstream regulators may become important therapeutic targets [10]. In the paper of J. Miguel-Carrasco et al., the authors investigated the effects of the profibrotic factor TGF-beta 1 in mediating Nox overactivity and oxidative stress in hypertensive rats. The results showed that pharmacological inhibition of TGF-beta 1 pathway greatly reduces the Nox activity, expression of the Nox2 and Nox4 isoforms, and nitrotyrosine levels in hypertensive rats compared to control animals. Collectively, the data of this study provides conclusive evidence on the involvement of this enzyme in the profibrotic actions of TGF-beta 1.

The major cause for diastolic heart failure is cardiac aging, which is referred to a dramatic decline in cardiac pump function with advanced age and resulted in diastolic dysfunction. Current clinical treatment for patients with

diastolic heart failure is disappointing. The cardioprotective effects of EGB761, a standard extract from the leaves of Ginkgo biloba, have been demonstrated already. The aim of the present study was to investigate the potential antiaging-associated cellular diastolic dysfunction effects of EGB761, exploring underlying molecular mechanisms. Cardiomyocyte aging model was established by treating with D-galactose. Treatment with EGB761 attenuated the intracellular formation of AGEs, delays the cellular senescence, and increase reuptake of Ca^{2+} stores in the sarcoplasmic reticulum. J. Liu et al. have suggested that EGB761 may protect against aging-associated diastolic dysfunction in cardiomyocytes. Furthermore, it was possible that EGB761 could upregulate SERCA2a function through improvement of the amount of Ser16 sites PLN phosphorylation. In conclusion, EGB761 significantly improved the diastolic function in cardiomyocytes, through the regulation of myocardial sarcoplasmic reticulum calcium transport regulatory.

NF-E2-related factor 2 (Nrf2) represents a promising therapeutic target to prevent oxidative stress and oxidative damage in various pathologies, including cardiovascular diseases. In the study of E. Donovan et al., the beneficial effects of phytochemicals included in dietary supplements might be an effective strategy to protect the cells against the detrimental effects of oxidative stress. The authors have demonstrated the Protandim activates Nrf2, a condition that ultimately influenced the protection of human coronary artery endothelial cells against an oxidative challenge.

In the paper by A. Ashour et al., the authors have addressed the potential use of metformin to prevent cardiotoxic effects of doxorubicin, a potent antitumor agent, in an experimental model of cardiomyopathy in rats. The adverse effects of doxorubicin include biochemical and morphological cardiac markers of injury, associated to decreasing antioxidant systems. Interestingly, the authors demonstrated that treatment with metformin prevents deleterious changes associated to doxorubicin mainly by modulation of redox balance.

Collectively, the original articles published in this special issue stimulate the ongoing efforts to identify the basic molecular mechanisms regulating the oxidative stress that may be used to find ways to manage its occurrence and correct its adverse effects.

Acknowledgments

We thank all the authors, the referees, and the staff of Hindawi's Editorial Office for their remarkable contribution that made this special issue possible.

Adrian Manea

Ana Fortuno

Jose Luis Martin-Ventura

References

- [1] D. D. Heistad, Y. Wakisaka, J. Miller, Y. Chu, and R. Pena-Silva, "Novel aspects of oxidative stress in cardiovascular diseases," *Circulation Journal*, vol. 73, no. 2, pp. 201–207, 2009.

- [2] M. Simionescu, "Implications of early structural-functional changes in the endothelium for vascular disease," *Arteriosclerosis, Thrombosis, and Vascular Biology*, vol. 27, no. 2, pp. 266–274, 2007.
- [3] J. Madrigal-Matute, C. E. Fernandez-Garcia, C. Gomez-Guerrero et al., "HSP90 inhibition by 17-DMAG attenuates oxidative stress in experimental atherosclerosis," *Cardiovascular Research*, vol. 95, no. 1, pp. 116–123, 2012.
- [4] A. Fortuño, J. Bidegain, A. Baltanás et al., "Is leptin involved in phagocytic NADPH oxidase overactivity in obesity? Potential clinical implications," *Journal of Hypertension*, vol. 28, no. 9, pp. 1944–1950, 2010.
- [5] A. Manea and M. Simionescu, "Nox enzymes and oxidative stress in atherosclerosis," *Frontiers in Bioscience*, vol. 4, pp. 651–670, 2012.
- [6] A. Manea, "NADPH oxidase-derived reactive oxygen species: involvement in vascular physiology and pathology," *Cell and Tissue Research*, vol. 342, no. 3, pp. 325–339, 2010.
- [7] A. C. Montezano and R. M. Touyz, "Molecular mechanisms of hypertension—reactive oxygen species and antioxidants: a basic science update for the clinician," *Canadian Journal of Cardiology*, vol. 28, no. 3, pp. 288–295, 2012.
- [8] U. Förstermann, "Oxidative stress in vascular disease: causes, defense mechanisms and potential therapies," *Nature Clinical Practice Cardiovascular Medicine*, vol. 5, no. 6, pp. 338–349, 2008.
- [9] I. M. Fearon and S. P. Faux, "Oxidative stress and cardiovascular disease: novel tools give (free) radical insight," *Journal of Molecular and Cellular Cardiology*, vol. 47, no. 3, pp. 372–381, 2009.
- [10] I. M. Fenyo, I. C. Florea, M. Raicu, and A. Manea, "Tyrophostin AG490 reduces NADPH oxidase activity and expression in the aorta of hypercholesterolemic apolipoprotein E-deficient mice," *Vascular Pharmacology*, vol. 54, no. 3–6, pp. 100–106, 2011.

Research Article

Sodium-Glucose Cotransporter Inhibition Prevents Oxidative Stress in the Kidney of Diabetic Rats

Horacio Osorio,¹ Israel Coronel,² Abraham Arellano,¹ Ursino Pacheco,¹ Rocío Bautista,¹ Martha Franco,¹ and Bruno Escalante^{3,4}

¹Renal Pathophysiology Laboratory, Department of Nephrology, Instituto Nacional de Cardiología “Ignacio Chávez”, Juan Badiano 1, 14080 Mexico City, DF, Mexico

²Health Science Faculty, Universidad Anáhuac, México Norte, 57286 Huixquilucan, State of Mexico, Mexico

³Department of Molecular Biomedicine, Centro de Investigación y de Estudios Avanzados del Instituto Politécnico Nacional (CINVESTAV), 07360 Mexico City, Mexico

⁴Department of Molecular Biomedicine, CINVESTAV-Monterrey, 66600 Apodaca, NL, Mexico

Correspondence should be addressed to Horacio Osorio, horace_33@yahoo.com.mx

Received 7 June 2012; Accepted 13 October 2012

Academic Editor: José Luis Martín-Ventura

Copyright © 2012 Horacio Osorio et al. This is an open access article distributed under the Creative Commons Attribution License, which permits unrestricted use, distribution, and reproduction in any medium, provided the original work is properly cited.

The hyperglycemia triggers several chronic diabetic complications mediated by increased oxidative stress that eventually causes diabetic nephropathy. The aim of this study was to examine if the sodium-glucose cotransporter (SGLT2) inhibition prevents the oxidative stress in the kidney of diabetic rats. *Methods.* The diabetic rat model was established by intraperitoneal injection of streptozotocin (50 mg/kg). The inhibition of SGLT2 was induced by daily subcutaneous administration of phlorizin (0.4 g/kg). Oxidative stress was assessed by catalase (CAT), glutathione peroxidase (GPx), and superoxide dismutase (SOD) activities and by immunohistochemical analysis of 3-nitrotyrosine (3-NT). *Results.* Streptozotocin-induced diabetes caused hyperglycemia and lower body weight. The CAT activity decreased in cortex and medulla from diabetic rats; in contrast, the GPx activity increased. Furthermore the 3-NT staining of kidney from diabetic rats increased compared to control rats. The inhibition of SGLT2 decreased hyperglycemia. However, significant diuresis and glucosuria remain in diabetic rats. The phlorizin treatment restores the CAT and GPx activities and decreases 3-NT staining. *Conclusion.* The inhibition of SGLT2 by phlorizin prevents the hyperglycemia and oxidative stress in kidney of diabetic rats, suggesting a prooxidative mechanism related to SGLT2 activity.

1. Introduction

Diabetic nephropathy (DN) is a leading cause of end-stage renal failure, accounting for 35% to 40% of all new cases that require dialysis therapy worldwide. Clinical studies have demonstrated that hyperglycemia is an important causal factor that mediates the development and progression of diabetic kidney disease [1]. Several evidences suggest that the controlling of glucose in the renal proximal tubular could play a major role in the genesis of diabetic systemic complications [2, 3].

On the other hand it has been shown that increases in glucose uptake in the kidney during diabetes could lead to high intracellular glucose levels, inducing an enhanced

production of reactive oxygen species (ROS), which probably can be amplified by the decreased capacity of the cellular antioxidant defense system in this condition [4, 5]. Recently, we have reported increased sodium glucose cotransporter (SGLT2) activity and expression in rats with diabetes and salt sensitivity [6, 7]. Also, we showed that the increase in oxidative stress and SGLT2 expression was prevented by ursodeoxycholic acid treatment in diabetic rats [8].

The excessive production of ROS has been suggested as a common outcome from the pathways leading to increased oxidative damage, which culminates in DN [5]. Under this condition compounds which are able to diminish or modulate hyperglycemia and oxidative stress could be a plausible target to delay the onset of DN.

The SGLT2 inhibition by phlorizin exerts a hypoglycemic effect in diabetic rodents via induction of glycosuria [9] and prevents elevated blood glucose levels in Zucker diabetic fatty rats [10]. The renal glucose transport inhibition induced by phlorizin treatment leads to glucose plasma levels close to the normal values without significant alteration in insulin plasma levels. These observations suggest that SGLT2 inhibitors may be effective agents to normalize high blood glucose levels, which are associated with diseases such as type 1 and type 2 diabetes mellitus [11].

In the present study we hypothesized that increased SGLT2 activity may contribute to hyperglycemic chronic state leading to the development of oxidative stress during diabetes. Therefore, the present study was undertaken to assess if phlorizin as a sodium glucose cotransporter inhibitor could be effective reducing the alterations in the oxidative stress in kidney in streptozotocin-induced diabetic rat model.

2. Methods

2.1. Reagents. Streptozotocin (STZ), phlorizin, xanthine, nitroblue tetrazolium (NBT), BSA, xanthine oxidase, NADPH, glutathione reductase (GR), and reduced glutathione (GSH) were purchased from Sigma (St. Louis, MO, USA). Rabbit anti-3-nitrotyrosine polyclonal antibodies were from Upstate, Lake Placid, NY, USA. All other chemicals used were of the highest analytical grade available.

2.2. Experimental Design. Male adult Wistar rats (10–14 weeks of age) weighing 250–300 g were used. Animals were randomly divided into four groups: control (C), diabetic (D), diabetic treated with phlorizin (DP), and diabetic treated with insulin (DI). Diabetes was induced by a single administration of STZ (50 mg/kg i.p.) dissolved in citrate buffer (0.1 M, pH 4.5). Control group received the same volume of citrate buffer.

After 72 h of STZ administration, the blood glucose concentration was determined (Accu-Chek sensor comfort, Roche Diagnostics), and only rats having over 20.0 mmol/L were considered diabetic for further studies.

Phlorizin was administered (0.4 g/kg/day/4 weeks, s.c. in a 20% of propylene glycol solution) subcutaneous injection in two equally divided doses that were given at 12 h intervals to ensure continuous inhibition of renal tubular glucose reabsorption.

Insulin treatment was administered i.p. (Humulin; Eli Lilly and Company, Indianapolis, IN). Insulin was given in initial dose of 6 IU followed by 8 to 10 IU depending on morning blood glucose values.

After diabetes confirmation, the treatments started and were maintained during 30 days. All experimental groups were maintained on laboratory diet and water *ad libitum*.

Thirty days after STZ administration, urine samples (24 h) were collected in metabolic cages; the urinary variables measures were diuresis and glucose (IL 300 plus, clinical chemistry analyzer). Later, all the animals were anesthetized

with sodium pentobarbital (50 mg/kg). The kidneys were perfused and rapidly removed. The cortex and medulla were isolated and submerged in liquid nitrogen before enzyme activity measurements. Some kidneys were placed in paraformaldehyde 4% for nitrosative stress analysis, measured by immunohistochemical analysis of 3-nitrotyrosine modified proteins.

All animal procedures were performed in accordance with the Mexican Federal Regulation for Animal Experimentation and Care (NOM-062-ZOO-2001) and were approved by the Bioethics and Investigation Committees of the Instituto Nacional de Cardiología “Ignacio Chávez.”

2.3. Evaluation of Oxidative Stress

2.3.1. Preparation of Renal Tissue. Cortex and medulla were washed thoroughly with ice cold saline, 10% (w/v); each tissue was homogenized separately in a Potter Elvehjem homogenizer in ice-cold 50 mM phosphate buffer pH 7.4 containing mammalian protease inhibitor cocktail. The homogenates were centrifuged at $10,000 \times g$ for 30 min at 4°C. The supernatants were used for measuring the enzyme activities. A portion of the supernatant was used for the determination of total protein concentration by Bradford method [12] using bovine serum albumin as standard.

2.3.2. Catalase Assay. Renal catalase (CAT) activity was assayed at 25°C by Aebi method which is based on the disappearance of H_2O_2 from a solution containing 30 mmol/L H_2O_2 in 10 mmol/L potassium phosphate buffer (pH 7) at 240 nm [13]. The results were expressed as U/mL/min.

2.3.3. Glutathione Peroxidase Assay. Renal glutathione peroxidase (GPx) activity was assessed by a method previously described [14]. The results were expressed as U/mL/min.

2.3.4. Superoxide Dismutase Assay. Superoxide dismutase (SOD) activity in kidney homogenates was measured by a competitive inhibition assay using xanthine-xanthine oxidase system to reduce NBT, a previously reported method [15]. Results were expressed as U/mg protein.

2.3.5. Immunohistochemical Localization of 3-Nitrotyrosine (3-NT). For immunohistochemistry, paraffin-embedded kidney tissues were sectioned (5 μm) and transferred to positively charged slides. Samples were treated with H_2O_2 (4.5%) to quench/inhibit endogenous peroxidase. After blocking, the sections were reacted with anti-3-NT antibody (Upstate Biotechnology Inc., Lake Placid, NY) for 1 h at room temperature. After extensive washing with PBS, the sections were incubated with antibody peroxidase conjugated for 1 h and finally incubated with diaminobenzidine for 30 min. Quantitative image analysis was performed with image analysis software (Image-Pro Plus 6.0, Media Cybernetics Inc, Bethesda, Maryland, MD, USA). The software determines densitometry mean values of selected tissue regions. Thus, 10 fields/rats were randomly

TABLE 1: Physiological parameters in experimental groups.

	Body weight (g)	Blood glucose (mg dL ⁻¹)	Diuresis (mL 24 hrs)	Urinary glucose (mg dL ⁻¹ 24 hrs)
Control	408.8 ± 1.750	88.00 ± 5.119	16.81 ± 2.113	20.00 ± 7.638
Diabetic	271.2 ± 4.964*	527.4 ± 8.834*	44.88 ± 4.569*	1748 ± 176.6*
Diabetic phlorizin	316.3 ± 5.609*†	133.2 ± 7.929*†	55.33 ± 6.015*	1920 ± 179.7*
Diabetic insulin	408.5 ± 9.192*†	118.0 ± 10.18*†	16.10 ± 2.578†	71.67 ± 36.71*†

Data are mean ± SEM of 8 animals in each group. * $P < 0.05$ versus control, † $P < 0.05$ versus D.

selected, and the intensity of the 3-NT immunostaining was determined.

2.4. Statistics. The data were expressed as the mean ± SEM. Data were analyzed with a nonpaired t -test or with ANOVA followed by multiple comparisons by Bonferroni t -test, when applicable (Prism 3.0; GraphPad Software, San Diego, CA, USA). Statistical significance was assumed at $P \leq 0.05$.

3. Results

3.1. Animal Characteristics. STZ-induced diabetes caused significant increases in blood glucose concentration, diuresis and glucosuria and a significant decrease in body weight (Table 1).

After 30 days of treatment in diabetic rats, phlorizin reduced blood glucose levels; however, significant diuresis, glucosuria, and low body weight remain (Table 1). The insulin treatment in diabetic rats induced a significant increase in body weight compared to nontreated diabetic rats. Moreover, insulin treatment completely reversed hyperglycemia, diuresis, and glucosuria (Table 1).

3.2. Evaluation of Oxidative Stress

3.2.1. Renal Activity of Antioxidant Enzymes. The antioxidant enzyme CAT, GPx, and total SOD activities were determined in the cortex and medulla of diabetic, phlorizin-treated, insulin-treated rats and control group.

Figures 1 to 3 showed that in the cortex and medulla of diabetic rats, CAT activity was decreased (Figures 1(a) and 1(b)), whereas GPx level was increased when compared with the control group (Figures 2(a) and 2(b)). Interestingly the treatment with phlorizin or insulin restores to normal levels CAT and GPx enzyme activities in cortex and medulla (Figures 1 and 2). SOD activity in cortex and medulla was similar in the four groups studied (Figures 3(a) and 3(b)).

3.2.2. Immunohistochemical Localization of 3-Nitrotyrosine (3-NT). The 3-NT levels were significantly increased in diabetic rats (Figures 4(a) and 4(b)). The phlorizin or insulin treatments were able to reverse the oxidative damage to normal values. These results indicate that tyrosine nitration of proteins is enhanced in the kidney of diabetic rats, and the blood glucose control was able to prevent these hyperglycemia-induced effects.

4. Discussion

In the present study, diabetes induction was followed by significant increases in renal oxidative stress evidenced by low CAT activity, whereas GPx was increased; moreover, diabetic rats showed increase in nitrotyrosine levels in cortex and medulla. Four-week phlorizin treatment restores blood glucose levels, enzymatic activities, and nitrotyrosine levels. These effects were observed without any influence on the metabolic control. Insulin treatment prevents the alterations that are diabetes-induced with normalization of the metabolic derangement unbalance.

Increased formation of ROS and diabetic nephropathy may occur in diabetes possibly associated with increased glucose concentration in plasma, tissues, and renal intracellular glucose levels [2, 16, 17]. High proximal tubular glucose concentration in poorly controlled diabetes may lead to excessive glucose, sodium, and water reabsorption, which could be mediated by enhanced activity of the Na⁺-glucose cotransporter (SGLT); this might contribute to development of diabetic complications [3, 6–8, 18–20]. The main goal of this study was to investigate the effect of phlorizin (a SGLT2 inhibitor) on oxidative stress in diabetic rats. Therefore, we examined the antioxidant enzymes activity and tyrosine nitration in cortex and medulla from control, diabetic, diabetic treated with phlorizin, and diabetic rats treated with insulin.

One month of STZ-induced diabetes resulted in a reduced CAT activity in cortex and medulla. In contrast, the GPx activity increased in cortex and medulla from diabetic rats to protect cellular and tissue injury. The increase in GPx and the decrease in the CAT activities in the kidney cortex suggest a compensatory mechanism in the different antioxidant enzymes in response to oxidative stress.

Although Cu/Zn SOD mRNA has been shown to be significantly induced in the total kidney of diabetic rats [21], we were not able to find any change in total SOD activity neither cortex or medulla. However, we are not discarding the possibility that diabetes change the activity of Cu-Zn SOD or Mn SOD.

The functional and pathophysiological role of excessive oxidative stress in diabetic kidney disease was indicated by the presence of increased levels of lipid peroxides and 8-hydroxydeoxyguanosine in the kidney of STZ-induced diabetic rats [22, 23]. These observations are lacking in the direct evidence for the presence of oxidative stress in cortex or medulla and might reflect a common consequence of diabetic kidney damage. Here we provide the evidence

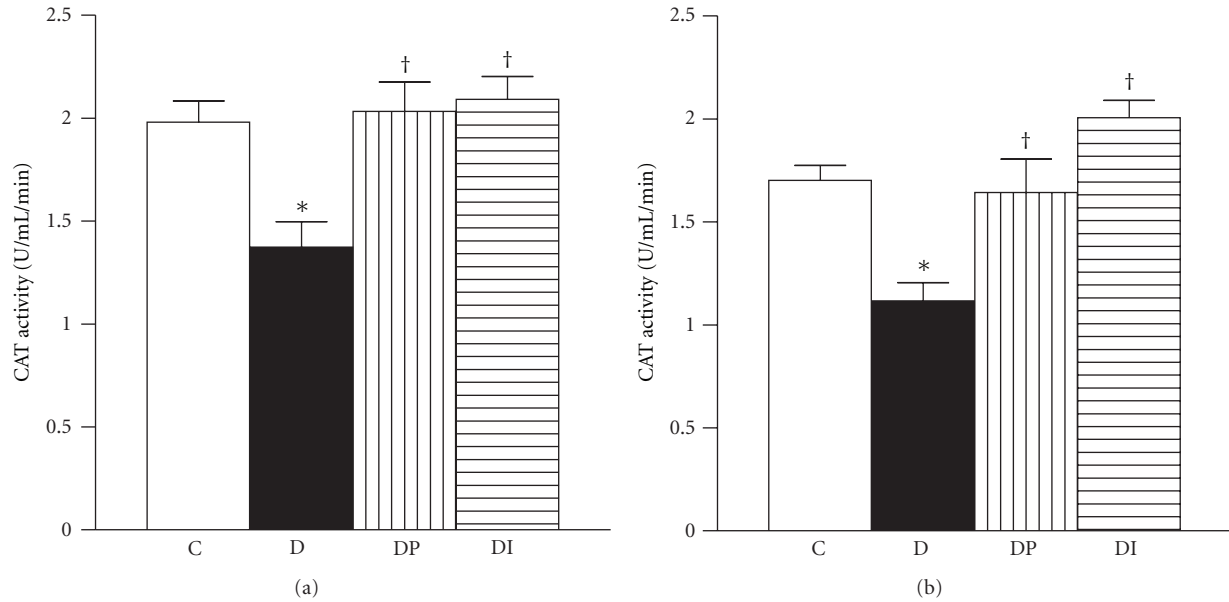


FIGURE 1: Catalase activity was measured in kidney from control (C), diabetic (D), diabetic treated with phlorizin (DP), and diabetic treated with insulin (DI). (a) cortex and (b) medulla. Data are mean \pm SEM of eight animals in each group; * $P < 0.05$ versus C, † $P < 0.05$ versus D.

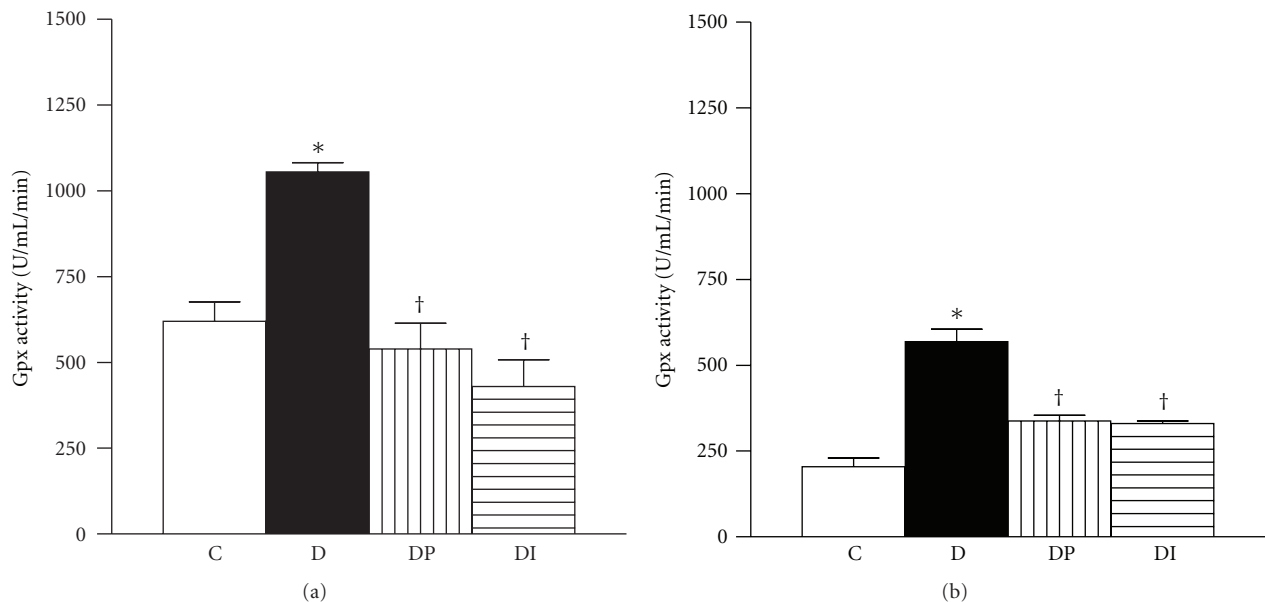


FIGURE 2: Glutathione peroxidase activity was measured in kidney from control (C), diabetic (D), diabetic treated with phlorizin (DP), and diabetic treated with insulin (DI). (a) cortex and (b) medulla. Data are mean \pm SEM of eight animals in each group; * $P < 0.05$ versus C, † $P < 0.05$ versus D.

for the presence of oxidative stress in cortex and medulla by two methods, enzymatic activity measurements and 3-NT immunostaining, which has been used to estimate the formation of nitrogen reactive species.

Peroxynitrite, formed by the reaction between superoxides and nitric oxide (NO), modifies tyrosine in proteins to form nitrotyrosine, and this stable end-product is involved in the inactivation of mitochondrial and cytosolic proteins, resulting in damage of cellular constituents [24]. Our results

showed that diabetes is associated with an increased tyrosine nitration in cortex and medulla, which is consistent with the previous studies in patients and experimental models with DM [25–28]. Presently, it is unclear if nitrotyrosine represents only a marker for oxidative stress from NO-induced oxidants or whether it alters protein structure sufficiently to cause abnormal enzyme, receptor, or signaling function. The phlorizin treatment in diabetic animals decreased the nitrotyrosine stain in cortex and medulla, consistent with

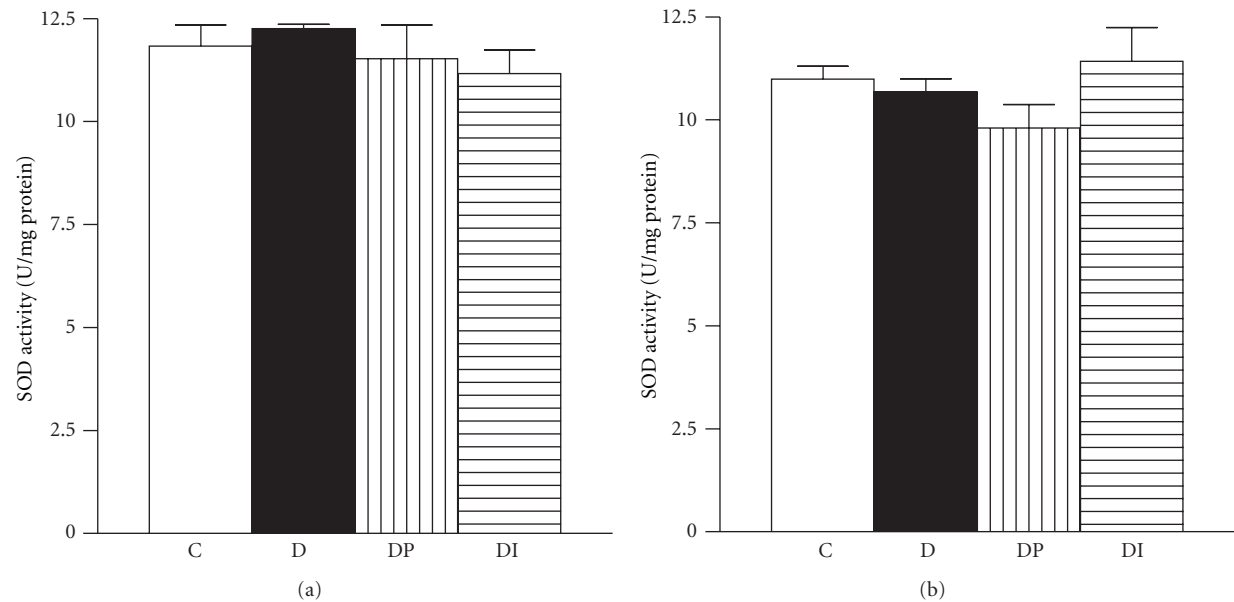


FIGURE 3: Superoxide dismutase activity was measured in kidney from control (C), diabetic (D), diabetic treated with phlorizin (DP), and diabetic treated with insulin (DI). (a) cortex and (b) medulla. Data are mean \pm SEM of eight animals in each group; * $P < 0.05$ versus C, $^{\dagger}P < 0.05$ versus D.

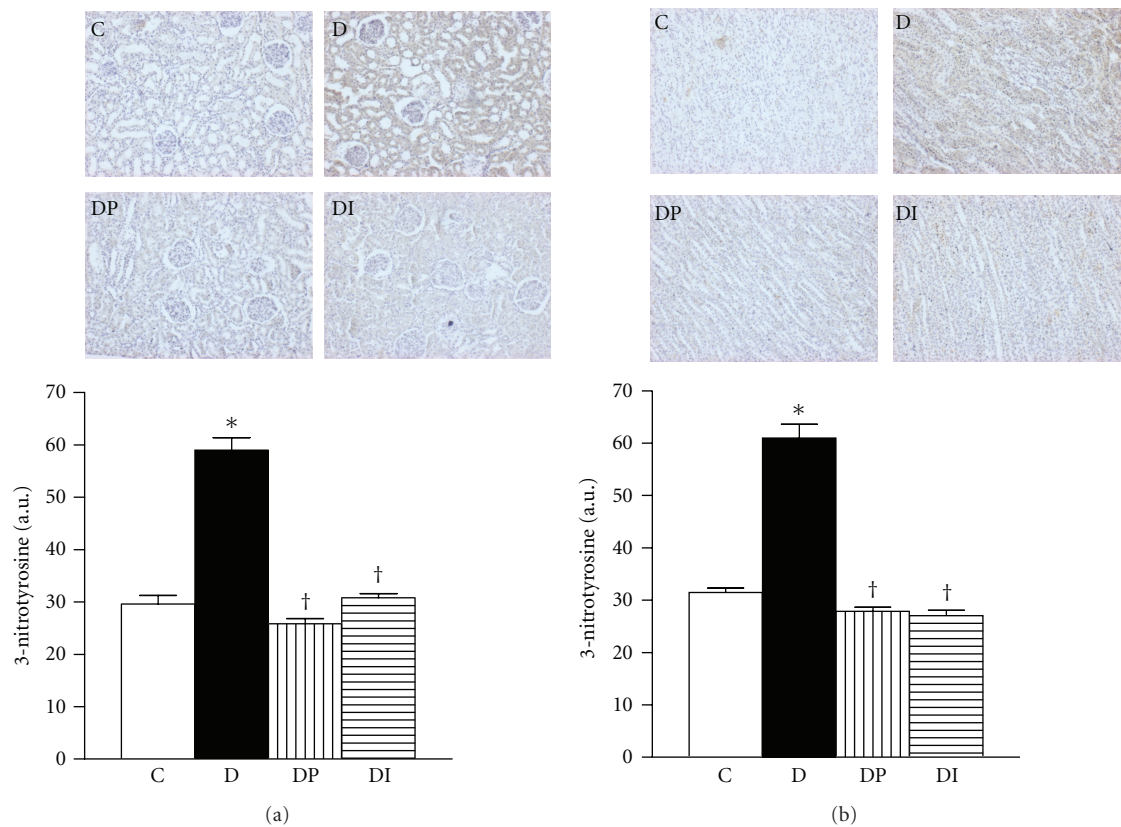


FIGURE 4: Immunohistochemistry and semiquantitative analysis of nitrotyrosine levels in kidney from control (C), diabetic (D), diabetic treated with phlorizin (DP), and Diabetic treated with insulin (DI). (a) cortex and (b) medulla. Data are mean \pm SEM of eight animals in each group; * $P < 0.05$ versus C, $^{\dagger}P < 0.05$ versus D.

their effects in preventing hyperglycemia and restoring the antioxidant enzyme activity. These data have also been shown by insulin treatment.

In previous studies, phlorizin treatment of diabetic rats has been shown to normalize the blood glucose levels, blood pressure, proteinuria, and hyperfiltration [7, 11, 29]. Previously it has been reported that phlorizin treatment increases glycosuria [29]; however, in this study we were not able to observe these effects.

In the present study phlorizin and insulin treatments were almost equally effective in their ability to prevent the decrease in CAT activity and increase in GPX activity and nitrotyrosine levels observed in diabetic rats. Our data clearly demonstrate an SGLT2 participation in the development of oxidative stress during diabetes. We hypothesize that phlorizin may inhibit SGLT2 activity *in vivo*. That means that phlorizin treatment can reduce the glucose reabsorption and therefore hyperglycemia, consequently the potential glycation of enzymes or probably reducing reactive oxygen-free radicals formation improving the activities of antioxidant enzymes.

The results obtained in this approach performed *in vitro* and *in vivo* suggest that the SGLT2 inhibition might be used in diabetic patients to alleviate the dysfunctions caused by diabetes and to lower oxidative stress via inhibition of SGLT2 activity.

Previously, we have demonstrated increase in SGLT2 activity and expression in cortex of diabetic and hypertensive rats [6, 7]. It has been suggested that the consequences of the SGLT2 induction not only represent responses designed to adjust the transtubular glucose reabsorption in different filtration rates, but also play an active role in renal injury, such as oxidative stress, diabetic nephropathy, hypertension, and Na⁺ reabsorption. Thus, SGLT2 inhibitors may be potential antidiabetic agents [9–11, 30–32] with a renoprotective effect by specifically mitigating transcellular epithelial glucose flux [32], which may prevent some of the cellular mechanisms leading to diabetic renal complications [32].

In conclusion, our evidence demonstrated that SGLT2 inhibition prevents oxidative and nitrative stress in kidney of diabetic rats, which was significantly influenced by glycemic control. Furthermore, our data confirm that early continuous aggressive treatment of glycemia is important to avoid future complications.

Conflict of Interests

There are no conflict of interests.

Acknowledgments

This project was supported by the Mexican Council of Science and Technology (CONACYT), Research Grant 155604 to Dr. H. Osorio, and by Fondos del Gasto Directo Autorizado a la Subdirección de Investigación Básica INC “Ignacio Chávez.” Dra. Claudia Rangel-Barajas critically revised the paper.

References

- [1] H. Shamon, H. Duffy, N. Fleischer et al., “The effect of intensive treatment of diabetes on the development and progression of long-term complications in insulin-dependent diabetes mellitus,” *New England Journal of Medicine*, vol. 329, no. 14, pp. 977–986, 1993.
- [2] S. P. Bagby, “Diabetic nephropathy and proximal tubule ROS: challenging our glomerulocentricity,” *Kidney International*, vol. 71, no. 12, pp. 1199–1202, 2007.
- [3] V. Vallon, “The proximal tubule in the pathophysiology of the diabetic kidney,” *The American Journal of Physiology*, vol. 300, no. 5, pp. R1009–R1022, 2011.
- [4] M. C. Garg, S. Ojha, and D. D. Bansal, “Antioxidant status of streptozotocin diabetic rats,” *Indian Journal of Experimental Biology*, vol. 34, no. 3, pp. 264–266, 1996.
- [5] H. Ha and H. B. Lee, “Reactive oxygen species amplify glucose signalling in renal cells cultured under high glucose and in diabetic kidney,” *Nephrology*, vol. 10, supplement 2, pp. S7–S10, 2005.
- [6] H. Osorio, R. Bautista, A. Rios, M. Franco, J. Santamaría, and B. Escalante, “Effect of treatment with losartan on salt sensitivity and SGLT2 expression in hypertensive diabetic rats,” *Diabetes Research and Clinical Practice*, vol. 86, no. 3, pp. e46–e49, 2009.
- [7] H. Osorio, R. Bautista, A. Rios et al., “Effect of phlorizin on SGLT2 expression in the kidney of diabetic rats,” *Journal of Nephrology*, vol. 23, no. 5, pp. 541–546, 2010.
- [8] H. Osorio, I. Coronel, A. Arellano, M. Franco, B. Escalante, and R. Bautista, “Ursodeoxycholic acid decreases sodium-glucose cotransporter (SGLT2) expression and oxidative stress in the kidney of diabetic rats,” *Diabetes Research and Clinical Practice*, vol. 97, no. 2, pp. 276–282, 2012.
- [9] T. Asano, M. Anai, H. Sakoda et al., “SGLT as a therapeutic target,” *Drugs of the Future*, vol. 29, no. 5, pp. 461–466, 2004.
- [10] A. L. Handlon, “Sodium glucose co-transporter 2 (SGLT2) inhibitors as potential antidiabetic agents,” *Expert Opinion on Therapeutic Patents*, vol. 15, no. 11, pp. 1531–1540, 2005.
- [11] S. W. Janssen, G. J. Martens, C. G. Sweep, P. N. Span, A. A. J. Verhofstad, and A. R. M. M. Hermus, “Phlorizin treatment prevents the decrease in plasma insulin levels but not the progressive histopathological changes in the pancreatic islets during aging of Zucker diabetic fatty rats,” *Journal of Endocrinological Investigation*, vol. 26, no. 6, pp. 508–515, 2003.
- [12] M. M. Bradford, “A rapid and sensitive method for the quantitation of microgram quantities of protein utilizing the principle of protein dye binding,” *Analytical Biochemistry*, vol. 72, no. 1–2, pp. 248–254, 1976.
- [13] H. Aebi, “Catalase *in vitro*,” *Methods in Enzymology*, vol. 105, pp. 121–126, 1984.
- [14] R. A. Lawrence and R. F. Burk, “Glutathione peroxidase activity in selenium deficient rat liver,” *Biochemical and Biophysical Research Communications*, vol. 71, no. 4, pp. 952–958, 1976.
- [15] Y. Sun, L. W. Oberley, and Y. Li, “A simple method for clinical assay of superoxide dismutase,” *Clinical Chemistry*, vol. 34, no. 3, pp. 497–500, 1988.
- [16] M. Brownlee, “Biochemistry and molecular cell biology of diabetic complications,” *Nature*, vol. 414, no. 6865, pp. 813–820, 2001.
- [17] H. Ha and K. H. Kim, “Pathogenesis of diabetic nephropathy: the role of oxidative stress and protein kinase C,” *Diabetes*

- Research and Clinical Practice*, vol. 45, no. 2-3, pp. 147–151, 1999.
- [18] R. E. Gilbert and M. E. Cooper, “The tubulointerstitium in progressive diabetic kidney disease: more than an aftermath of glomerular injury?” *Kidney International*, vol. 56, no. 5, pp. 1627–1637, 1999.
- [19] N. Bank and H. S. Aynedjian, “Progressive increases in luminal glucose stimulate proximal sodium absorption in normal and diabetic rats,” *Journal of Clinical Investigation*, vol. 86, no. 1, pp. 309–316, 1990.
- [20] W. T. Noonan, V. M. Shapiro, and R. O. Banks, “Renal glucose reabsorption during hypertonic glucose infusion in female streptozotocin-induced diabetic rats,” *Life Sciences*, vol. 68, no. 26, pp. 2967–2977, 2001.
- [21] L. A. Sechi, A. Ceriello, C. A. Griffin et al., “Renal antioxidant enzyme mRNA levels are increased in rats with experimental diabetes mellitus,” *Diabetologia*, vol. 40, no. 1, pp. 23–29, 1997.
- [22] K. Horie, T. Miyata, K. Maeda et al., “Immunohistochemical colocalization of glycoxidation products and lipid peroxidation products in diabetic renal glomerular lesions. Implication for glycoxidative stress in the pathogenesis of diabetic nephropathy,” *Journal of Clinical Investigation*, vol. 100, no. 12, pp. 2995–3004, 1997.
- [23] H. Ha, C. Kim, Y. Son, M. H. Chung, and K. H. Kim, “DNA damage in the kidneys of diabetic rats exhibiting microalbuminuria,” *Free Radical Biology and Medicine*, vol. 16, no. 2, pp. 271–274, 1994.
- [24] B. Halliwell, “What nitrates tyrosine? Is nitrotyrosine specific as a biomarker of peroxynitrite formation in vivo,” *FEBS Letters*, vol. 411, no. 2-3, pp. 157–160, 1997.
- [25] P. Pacher, I. Obrosova, J. Mabley, and C. Szabó, “Role of nitrosative stress and peroxynitrite in the pathogenesis of diabetic complications: emerging new therapeutical strategies,” *Current Medicinal Chemistry*, vol. 12, no. 3, pp. 267–275, 2005.
- [26] N. Ishii, K. P. Patel, P. H. Lane et al., “Nitric oxide synthesis and oxidative stress in the renal cortex of rats with diabetes mellitus,” *Journal of the American Society of Nephrology*, vol. 12, no. 8, pp. 1630–1639, 2001.
- [27] M. L. Onozato, A. Tojo, A. Goto, T. Fujita, and C. S. Wilcox, “Oxidative stress and nitric oxide synthase in rat diabetic nephropathy: effects of ACEI and ARB,” *Kidney International*, vol. 61, no. 1, pp. 186–194, 2002.
- [28] R. C. Thuraishingham, C. A. Nott, S. M. Dodd, and M. M. Yaqoob, “Increased nitrotyrosine staining in kidneys from patients with diabetic nephropathy,” *Kidney International*, vol. 57, no. 5, pp. 1968–1972, 2000.
- [29] S. Malatiali, I. Francis, and N. M. Barac, “Phlorizin prevents glomerular hyperfiltration but not hypertrophy in diabetic rats,” *Experimental Diabetes Research*, vol. 2008, Article ID 305403, 7 pages, 2008.
- [30] T. Adachi, K. Yasuda, Y. Okamoto et al., “T-1095, A renal Na⁺-glucose transporter inhibitor, improves hyperglycemia in streptozotocin-induced diabetic rats,” *Metabolism*, vol. 49, no. 8, pp. 990–995, 2000.
- [31] A. Oku, K. Ueta, K. Arakawa et al., “T-1095, an inhibitor of renal Na⁺-glucose cotransporters, may provide a novel approach to treating diabetes,” *Diabetes*, vol. 48, no. 9, pp. 1794–1800, 1999.
- [32] K. Arakawa, T. Ishihara, A. Oku et al., “Improved diabetic syndrome in C57BL/KsJ-db/db mice by oral administration of the Na⁺-glucose cotransporter inhibitor T-1095,” *British Journal of Pharmacology*, vol. 132, no. 2, pp. 578–586, 2001.

Research Article

Oxygen Concentration-Dependent Oxidative Stress Levels in Rats

Fumiko Nagatomo,¹ Hidemi Fujino,² Hiroyo Kondo,³ and Akihiko Ishihara¹

¹ Laboratory of Cell Biology and Life Science, Graduate School of Human and Environmental Studies, Kyoto University, Kyoto 606-8501, Japan

² Department of Rehabilitation Science, Kobe University Graduate School of Health Sciences, Kobe 654-0142, Japan

³ Department of Food Sciences and Nutrition, Nagoya Women's University, Nagoya 467-8610, Japan

Correspondence should be addressed to Akihiko Ishihara, ishihara.akihiro.8s@kyoto-u.ac.jp

Received 19 April 2012; Revised 5 August 2012; Accepted 8 August 2012

Academic Editor: Jose Luis Martin-Ventura

Copyright © 2012 Fumiko Nagatomo et al. This is an open access article distributed under the Creative Commons Attribution License, which permits unrestricted use, distribution, and reproduction in any medium, provided the original work is properly cited.

Introduction. We determined derivatives of reactive oxygen metabolites (dROMs) as an index of oxidative stress level (oxidant capacity) and biochemical antioxidant potential (BAP) as an index of antioxidant capacity in rats exposed to different oxygen concentrations. **Methods.** Male Wistar rats were exposed to 14.4%, 20.9%, 35.5%, 39.8%, 62.5%, and 82.2% oxygen at 1 atmosphere absolute for 24 h. Serum levels of dROMs and BAP were examined by using a free radical and antioxidant potential determination device. The morphological characteristics of red blood cells were examined by phase contrast microscopy. **Results.** There were no differences in the levels of dROMs in rats exposed to 14.4%, 20.9%, and 35.5% oxygen. However, the levels of dROMs increased in the rats exposed to 39.8% and 62.5% oxygen. The levels of dROMs were the highest in the rats exposed to 82.2% oxygen. There were no differences in the levels of BAP with respect to the oxygen concentration. Morphological changes in the red blood cells induced by oxidative attack from reactive oxygen species were observed in the rats exposed to 39.8%, 62.5%, and 82.2% oxygen. **Conclusion.** Our results suggest that exposure to oxygen concentrations higher than 40% for 24 h induces excessive levels of oxidative stress in rats.

1. Introduction

Supplemental oxygen is used in treatment and as a countermeasure for acute and chronic diseases. When pilots of unpressurized aircrafts fly to areas at high altitudes, when climbers ascend high-altitude peaks and outpace their ability to acclimatize, or when divers inhaling compressed air return to the surface, the external pressure on the body decreases and the dissolved inert gases come out of solution in the form of bubbles in the body on depressurization [1, 2]. The resulting decompression sicknesses and air embolisms are initially treated by inhalation of oxygen-enriched air or exposure to mild hyperbaric oxygen at 1.25 atmospheres absolute (ATA) until hyperbaric oxygen therapy (100% oxygen delivered at 2-3 ATA) is administered [3-6]. Hypoxic or breathless patients with chronically obstructive pulmonary disease (COPD), who have low levels of oxygen in their blood, require oxygen at concentrations greater than that in

room air to achieve arterial oxygen saturations between 88% and 92% [7].

Oxygen therapy with or without pressure is associated with the risk of oxygen toxicity and excessive oxidative stress. Oxidative stress plays a key role in the pathogenesis of many diseases and their complications; the generation of free radicals and increased levels of oxidative stress are associated with atherosclerosis, cataract, retinopathy, myocardial infarction, hypertension, diabetes, renal failure, and uremia [8-10]. However, there are no data available on changes in the oxidative stress level and antioxidant capacity after exposure to different concentrations of oxygen. The analytical measurement of oxidative stress markers has been difficult because of the short half-life and high reactivity of the majority of reactive oxygen species and the applicability of measurement methods [11]. Blood samples are the appropriate biological materials for assessing the status of oxidants and antioxidants. A unique system for the

evaluation of oxidative stress levels and antioxidant capacity in the blood has been developed [12]. This evaluation approach is based on the free radical analytical system that mainly analyzes lipid hydroperoxides, which are relatively stable in the blood. This system has been used for both animal and human sera, which confirms its applicability [13–15].

In this study, we examined the derivatives of reactive oxygen metabolites (dROMs) as an index of oxidative stress levels (oxidant capacity) and the biochemical antioxidant potential (BAP) as an index of antioxidant capacity in rats exposed to different concentrations of oxygen at 1 ATA for 24 h.

2. Materials and Methods

2.1. Experimental Animals. All experimental and animal care procedures were performed in accordance with the guidelines stated in the Guide for the Care and Use of Laboratory Animals issued by the Institutional Animal Experiment Committee of Kyoto University (Kyoto, Japan).

2.2. Exposure to Different Concentrations of Oxygen. Ten-week-old male Wistar rats weighing between 200 g and 226 g were divided into 6 groups ($n = 5$ for each group). The individual groups were exposed to air containing low or high concentration of oxygen in a chamber ($75 \times 130 \times 85$ cm) at 1 ATA for 24 h by using a low-oxygen inhaler (Terucom Corp., Yokohama, Japan) or an oxygen concentrator (Ikiken Corp., Sayama, Japan), respectively. When the air chamber contained less or more than 20.9% oxygen, air with 2 different concentrations of oxygen from 2 tubes was transported to the aspirator: one tube contained normal air (20.9% oxygen) and the other tube had air containing 13% or 84% oxygen, which was procured from the low-oxygen inhaler or the oxygen concentrator, respectively. Then, the aspirator pumped mixed air into the chamber at the rate of 1 L/min. The low or high oxygen concentration in the chamber was adjusted by separately regulating the air flow from these 2 tubes. Normal air was transported by only 1 tube, while the air containing 20.9% oxygen was retained in the chamber. The oxygen concentration in the chamber was determined by using an oxygen monitor (Max O₂+AE; Maxtec Inc., UT, USA) attached to the chamber. The rats were maintained in individual, uniformly sized standard cages ($30 \times 40 \times 20$ cm) in the chamber. The room was maintained at $22 \pm 2^\circ\text{C}$ with 45%–55% relative humidity. Food and water were provided *ad libitum*.

2.3. Measurements of dROMs and BAP. The levels of dROMs and BAP were determined after the rats were exposed to different concentrations of oxygen. Blood samples were obtained from the tail of fully conscious rats and evaluated photometrically. A free radical and antioxidant potential determination device (Free Radical Analytical System 4; Health & Diagnostics, Grosseto, Italy) was used to automatically measure the levels of dROMs and BAP.

The dROMs are used as an index to determine the level of oxidative stress (oxidant capacity) by measuring the amount of organic hydroperoxide (ROOH) converted into radicals that oxidize *N,N*-diethyl-*p*-phenylenediamine [12, 16]. The levels of dROMs were expressed in Carr units (1 U·Carr corresponds to 0.08 mg hydroperoxide/100 mL H₂O₂). The BAP is used as an index to determine the biological antioxidant capacity and is measured on the basis of the capacity of the plasma sample to reduce ferric ions to ferrous ions. After blood samples were obtained, the rats were killed by intraperitoneal overdose of sodium pentobarbital.

2.4. Red Blood Cell Morphology. Using blood samples, the morphological profiles of red blood cells were observed by phase contrast microscopy (Nikon 80iF-PH-15; Tokyo, Japan).

2.5. Statistics. Means and standard deviations were calculated from the individual values by using standard procedures. One-way analysis of variance (ANOVA) was used to evaluate the mean differences among the 6 groups. When ANOVA analyses revealed significant differences in mean values, the groups were further compared using Scheffé's *post hoc* tests. A probability level of 0.05 was considered significant.

3. Results

The levels of dROMs in rats exposed to 39.8% and 62.5% oxygen were higher than those in the rats exposed to 14.4%, 20.9%, and 35.5% oxygen (Figure 1(a)). The level of dROMs in the rats exposed to 82.2% oxygen was the highest among the 6 groups. There were no differences in the levels of BAP among the 6 groups (Figure 1(b)). Morphological changes in red blood cells were observed in the rats exposed to 39.8%, 62.5%, and 82.2% oxygen (Figure 2).

4. Discussion

4.1. Exposure to Low Concentration of Oxygen. Acclimatization at high altitude results in changes in the respiratory, cardiovascular, and hematologic systems, which enhance oxygen delivery to the cells and tissues [17]. Decompression sickness occurs between initial hypoxic conditions and the onset of acclimatization, and the incidence and severity of the sickness depend on the rate of ascent, the altitude attained, and physiological susceptibility of individuals [5].

There is little data available regarding the oxidative stress level under low concentrations of oxygen. In this study, we examined the oxidative stress levels in rats exposed to low concentrations of oxygen. In rats exposed to 14.4% oxygen for 24 h, which is equivalent to the oxygen concentration at 3500 m/11500 feet altitude, no change was observed in the oxidative stress level (Figure 1(a)). Therefore, we conclude that low concentrations of oxygen do not induce excessive oxidative stress.

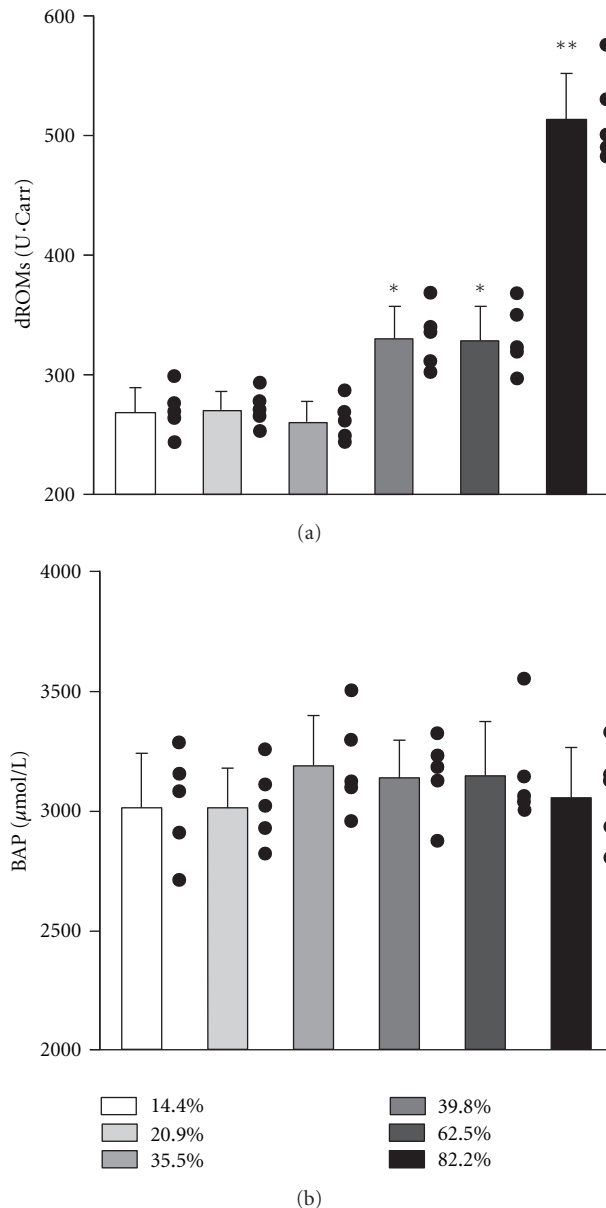


FIGURE 1: Levels of derivatives of reactive oxygen metabolites (a) and biochemical antioxidant potential (b) of rats after exposure to different concentrations of oxygen for 24 h. Values are expressed as the mean and standard deviation ($n = 5$ for each group). Five dots on the right side of the bar are the individual values of rats in each group. dROMs: derivatives of reactive oxygen metabolites; BAP: biochemical antioxidant potential. * $P < 0.05$ compared with values of 14.4%, 20.9%, and 35.5% oxygen; ** $P < 0.05$ compared with values of 14.4%, 20.9%, 35.5%, 39.8%, and 62.5% oxygen.

4.2. Exposure to High Concentration of Oxygen. Hyperbaric oxygen at 2–3 ATA with 100% oxygen induces acute changes, such as increased blood pressure and further reduction in heart rate [18], and causes chronic diseases like cataract formation [19–22]; hyperbaric oxygen is generally safe when pressures do not exceed 3 ATA and the length of treatment is less than 120 min [23, 24]. However, hyperbaric oxygen has

been reported to increase the levels of reactive oxygen species [25–27].

Patients with COPD inhale high concentrations of oxygen, generally up to 50% oxygen (fraction of inspired oxygen, FIO_2) when the partial pressure of oxygen in the arterial blood (PaO_2) is below 55 mmHg; these patients occasionally exhibit voluntary respiration failure, consciousness disturbance, and atelectasis when inhaling high concentrations of oxygen.

Oxygen therapy with or without pressure might induce excessive levels of oxidative stress. Excessive levels of oxidative stress are associated with many diseases, including atherosclerosis, cataract, retinopathy, myocardial infarction, hypertension, renal failure, and uremia [8–10]. In this study, we examined the oxidative stress levels in rats exposed to high concentrations of oxygen.

No change in the oxidative stress level was observed at 35.5% oxygen for 24 h (Figure 1(a)). We previously examined the effects of mild hyperbaric oxygen at 1.25 ATA with 36% oxygen on the neuromuscular system, including spinal motoneurons and their innervating muscle fibers [28, 29], type 2 diabetes [30–33], hypertension [34], type II collagen-induced arthritis [35], age-related decline in muscle oxidative capacity [36], and diabetes-induced cataracts [37] in mice and rats. Therefore, the data observed in this study suggest that mild hyperbaric oxygen at 1.25 ATA with 36% oxygen is effective for the inhibition and improvement of many metabolic diseases [28–37], without producing excessive levels of oxidative stress.

In contrast, 39.8% and 62.5% oxygen for 24 h induced excessive levels of oxidative stress, and the level of dROMs was the highest at 82.2% oxygen (Figure 1(a)). Oxidative stress level increases when the production of reactive oxygen species is markedly greater than the intrinsic antioxidant defenses. Patients with COPD inhale high concentrations of oxygen, and the possibility of accumulating excessive levels of oxidative stress will be greater when the inhaled oxygen concentration (FIO_2) is high. Therefore, we conclude that exposure to 40% oxygen for 24 h is a threshold for inducing an excessive level of oxidative stress.

In our previous study [15], we observed that obese rats with metabolic syndrome accompanied by insulin resistance, impaired glucose metabolism, and dyslipidemia had lower levels of BAP than normal Wistar rats. In addition, we observed that mild hyperbaric exposure at 1.25 ATA with 36% oxygen improves the levels of BAP in rats with hypertension [34]. These studies [15, 34] suggest that changes in the levels of BAP are reflected as an index of antioxidant capacity. In this study, we expected that exposure to higher concentrations of oxygen would decrease the levels of BAP compared with exposure to 20.9% oxygen because the levels of dROMs were increased by exposure to 39.8%, 62.5%, and 82.2% oxygen (Figure 1(a)). However, there was no difference in the levels of BAP among different concentrations of oxygen (Figure 1(b)). These results suggest that the antioxidant capacity is not affected by both low and high concentrations of oxygen, and thus, the antioxidant capacity did not change, at least after 24 h. However, we did not examine antioxidant enzyme levels of rats exposed to different concentrations

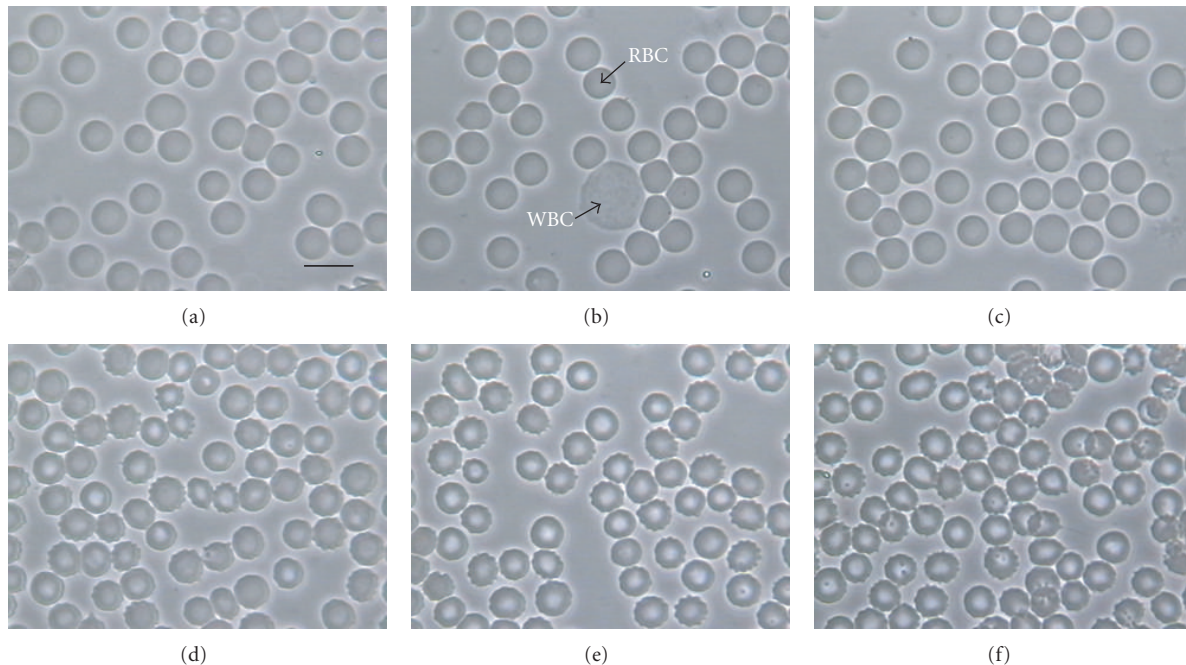


FIGURE 2: Morphological features of red blood cells after 24 h of exposure to different concentrations of oxygen: (a) 14.4%, (b) 20.9%, (c) 35.5%, (d) 39.8%, (e) 62.5%, and (f) 82.2%. RBC: red blood cell; WBC: white blood cell. Scale bar is 10 μm .

of oxygen. In our subsequent study, we plan to examine the levels of BAP and antioxidant enzymes, for example, superoxide dismutase, catalase, and glutathione peroxidase, in rats exposed to different concentrations of oxygen for more than 24 h.

Transformed red blood cells, which were induced by oxidative attack from reactive oxygen species, were observed by exposure to 39.8%, 62.5%, and 82.2% oxygen (Figure 2); these findings are consistent with the increased levels of dROMs at these oxygen concentrations (Figure 1(a)). Therefore, we conclude that morphological changes in the red blood cells are linked to increased levels of oxidative stress.

5. Conclusion

Exposure to oxygen concentrations higher than 40% for 24 h induces excessive levels of oxidative stress.

Conflict of Interests

The authors declare that they have no conflict of interests.

References

- [1] E. C. Parker, S. S. Survanshi, P. B. Massell, and P. K. Weathersby, "Probabilistic models of the role of oxygen in human decompression sickness," *Journal of Applied Physiology*, vol. 84, no. 3, pp. 1096–1102, 1998.
- [2] A. J. F. Macmillan, "Chapter 3. Sub-atmospheric decompression sickness," in *Aviation Medicine*, pp. 19–25, Butterworth Heinemann, Oxford, UK, 3rd edition, 1999.
- [3] J. F. Kasic, H. M. Smith, and R. I. Gamow, "A self-contained life support system designed for use with a portable hyperbaric chamber," *Biomedical Sciences Instrumentation*, vol. 25, pp. 79–81, 1989.
- [4] J. F. Kasic, M. Yaron, R. A. Nicholas, J. A. Lickteig, and R. Roach, "Treatment of acute mountain sickness: hyperbaric versus oxygen therapy," *Annals of Emergency Medicine*, vol. 20, no. 10, pp. 1109–1112, 1991.
- [5] C. Imray, A. Wright, A. Subudhi, and R. Roach, "Acute mountain sickness: pathophysiology, prevention, and treatment," *Progress in Cardiovascular Diseases*, vol. 52, no. 6, pp. 467–484, 2010.
- [6] G. J. Butler, N. Al-Waili, D. V. Passano et al., "Altitude mountain sickness among tourist populations: a review and pathophysiology supporting management with hyperbaric oxygen," *Journal of Medical Engineering & Technology*, vol. 35, no. 3–4, pp. 197–207, 2011.
- [7] M. A. Austin, K. E. Wills, L. Blizzard, E. H. Walters, and R. Wood-Baker, "Effect of high flow oxygen on mortality in chronic obstructive pulmonary disease patients in prehospital setting: randomised controlled trial," *British Medical Journal*, vol. 341, p. c5462, 2010.
- [8] C. M. Maier and P. H. Chan, "Role of superoxide dismutases in oxidative damage and neurodegenerative disorders," *Neuroscientist*, vol. 8, no. 4, pp. 323–334, 2002.
- [9] K. K. Griendling and G. A. FitzGerald, "Oxidative stress and cardiovascular injury. Part I: basic mechanisms and in vivo monitoring of ROS," *Circulation*, vol. 108, no. 16, pp. 1912–1916, 2003.
- [10] I. Dalle-Donne, R. Rossi, R. Colombo, D. Giustarini, and A. Milzani, "Biomarkers of oxidative damage in human disease," *Clinical Chemistry*, vol. 52, no. 4, pp. 601–623, 2006.

- [11] D. Pitocco, F. Zaccardi, E. Di Stasio et al., "Oxidative stress, nitric oxide, and diabetes," *Review of Diabetic Studies*, vol. 7, no. 1, pp. 15–25, 2010.
- [12] A. Alberti, L. Bolognini, D. Macciantelli, and M. Caratelli, "The radical cation of *N,N*-diethyl-*para*-phenylendiamine: a possible indicator of oxidative stress in biological samples," *Research on Chemical Intermediates*, vol. 26, no. 3, pp. 253–267, 2000.
- [13] C. Vassalle, C. Boni, P. Di Cecco, R. Ndreu, and G. C. Zucchelli, "Automation and validation of a fast method for the assessment of in vivo oxidative stress levels," *Clinical Chemistry and Laboratory Medicine*, vol. 44, no. 11, pp. 1372–1375, 2006.
- [14] A. Pasquini, E. Luchetti, V. Marchetti, G. Cardini, and E. L. Iorio, "Analytical performances of d-ROMs test and BAP test in canine plasma. Definition of the normal range in healthy Labrador dogs," *Veterinary Research Communications*, vol. 32, no. 2, pp. 137–143, 2008.
- [15] F. Nagatomo, N. Gu, H. Fujino, I. Takeda, K. Tsuda, and A. Ishihara, "Skeletal muscle characteristics of rats with obesity, diabetes, hypertension, and hyperlipidemia," *Journal of Atherosclerosis and Thrombosis*, vol. 16, no. 5, pp. 576–585, 2009.
- [16] R. Trotti, M. Carratelli, and M. Barbieri, "Performance and clinical application of a new, fast method for the detection of hydroperoxides in serum," *Panminerva Medica*, vol. 44, no. 1, pp. 37–40, 2002.
- [17] S. J. Paralikar and J. H. Paralikar, "High-altitude medicine," *Indian Journal of Occupational and Environmental Medicine*, vol. 14, no. 1, pp. 6–12, 2010.
- [18] N. S. Al-Waili, G. J. Butler, J. Beale et al., "Influences of hyperbaric oxygen on blood pressure, heart rate and blood glucose levels in patients with diabetes mellitus and hypertension," *Archives of Medical Research*, vol. 37, no. 8, pp. 991–997, 2006.
- [19] B. M. Palmquist, B. Philipson, and P. O. Barr, "Nuclear cataract and myopia during hyperbaric oxygen therapy," *British Journal of Ophthalmology*, vol. 68, no. 2, pp. 113–117, 1984.
- [20] F. J. Giblin, V. A. Padgaonkar, V. R. Leverenz et al., "Nuclear light scattering, disulfide formation and membrane damage in lenses of older guinea pigs treated with hyperbaric oxygen," *Experimental Eye Research*, vol. 60, no. 3, pp. 219–235, 1995.
- [21] V. A. Padgaonkar, V. R. Leverenz, K. E. Fowler, V. N. Reddy, and F. J. Giblin, "The effects of hyperbaric oxygen on the crystallins of cultured rabbit lenses: a possible catalytic role for copper," *Experimental Eye Research*, vol. 71, no. 4, pp. 371–383, 2000.
- [22] L. B. Gesell and A. Trott, "De novo cataract development following a standard course of hyperbaric oxygen therapy," *Undersea and Hyperbaric Medicine*, vol. 34, no. 6, pp. 389–392, 2007.
- [23] P. M. Tibbles and J. S. Edelsberg, "Hyperbaric-oxygen therapy," *New England Journal of Medicine*, vol. 334, no. 25, pp. 1642–1648, 1996.
- [24] R. M. Leach, P. J. Rees, and P. Wilmshurst, "ABC of oxygen: hyperbaric oxygen therapy," *British Medical Journal*, vol. 317, no. 7166, pp. 1140–1143, 1998.
- [25] C. K. Narkowicz, J. H. Vial, and P. W. McCartney, "Hyperbaric oxygen therapy increases free radical levels in the blood of humans," *Free Radical Research Communications*, vol. 19, no. 2, pp. 71–80, 1993.
- [26] S. Öter, A. Korkmaz, T. Topal et al., "Correlation between hyperbaric oxygen exposure pressures and oxidative parameters in rat lung, brain, and erythrocytes," *Clinical Biochemistry*, vol. 38, no. 8, pp. 706–711, 2005.
- [27] S. Öter, T. Topal, S. Sadir et al., "Oxidative stress levels in rats following exposure to oxygen at 3 atm for 0–120 min," *Aviation, Space, and Environmental Medicine*, vol. 78, no. 12, pp. 1108–1113, 2007.
- [28] A. Ishihara, F. Kawano, T. Okiura, F. Morimatsu, and Y. Ohira, "Hyperbaric exposure with high oxygen concentration enhances oxidative capacity of neuromuscular units," *Neuroscience Research*, vol. 52, no. 2, pp. 146–152, 2005.
- [29] A. Matsumoto, T. Okiura, F. Morimatsu, Y. Ohira, and A. Ishihara, "Effects of hyperbaric exposure with high oxygen concentration on the physical activity of developing rats," *Developmental Neuroscience*, vol. 29, no. 6, pp. 452–459, 2007.
- [30] K. Yasuda, N. Aoki, T. Adachi et al., "Hyperbaric exposure with high oxygen concentration inhibits growth-associated increase in the glucose level of diabetic Goto-Kakizaki rats," *Diabetes, Obesity and Metabolism*, vol. 8, no. 6, pp. 714–715, 2006.
- [31] K. Yasuda, T. Adachi, N. Gu et al., "Effects of hyperbaric exposure with high oxygen concentration on glucose and insulin levels and skeletal muscle-fiber properties in diabetic rats," *Muscle & Nerve*, vol. 35, no. 3, pp. 337–343, 2007.
- [32] A. Matsumoto, F. Nagatomo, K. Yasuda, K. Tsuda, and A. Ishihara, "Hyperbaric exposure with high oxygen concentration improves altered fiber types in the plantaris muscle of diabetic Goto-Kakizaki rats," *Journal of Physiological Sciences*, vol. 57, no. 2, pp. 133–136, 2007.
- [33] N. Gu, F. Nagatomo, H. Fujino, I. Takeda, K. Tsuda, and A. Ishihara, "Hyperbaric oxygen exposure improves blood glucose level and muscle oxidative capacity in rats with type 2 diabetes," *Diabetes Technology & Therapeutics*, vol. 12, no. 2, pp. 125–133, 2010.
- [34] F. Nagatomo, H. Fujino, I. Takeda, and A. Ishihara, "Effects of hyperbaric oxygenation on blood pressure levels of spontaneously hypertensive rats," *Clinical and Experimental Hypertension*, vol. 32, no. 3, pp. 193–197, 2010.
- [35] F. Nagatomo, N. Gu, H. Fujino et al., "Effects of exposure to hyperbaric oxygen on oxidative stress in rats with type II collagen-induced arthritis," *Clinical and Experimental Medicine*, vol. 10, no. 1, pp. 7–13, 2010.
- [36] T. Nishizaka, F. Nagatomo, H. Fujino et al., "Hyperbaric oxygen exposure reduces age-related decrease in oxidative capacity of the tibialis anterior muscle in mice," *Enzyme Research*, vol. 2010, Article ID 824763, 2010.
- [37] F. Nagatomo, R. R. Roy, H. Takahashi, V. R. Edgerton, and A. Ishihara, "Effect of exposure to hyperbaric oxygen on diabetes-induced cataracts in mice," *Journal of Diabetes*, vol. 3, no. 4, pp. 301–308, 2011.

Research Article

Intensification of Doxorubicin-Related Oxidative Stress in the Heart by Hypothyroidism Is Not Related to the Expression of Cytochrome P450 NADPH-Reductase and Inducible Nitric Oxide Synthase, As Well As Activity of Xanthine Oxidase

Jaroslav Dudka,¹ Franciszek Burdan,² Agnieszka Korga,¹ Magdalena Iwan,¹
Barbara Madej-Czerwonka,² Monika Cendrowska-Pinkosz,²
Agnieszka Korobowicz-Markiewicz,³ Barbara Jodłowska-Jedrych,⁴
and Włodzimierz Matysiak⁴

¹ Medical Biology Unit, Medical University of Lublin, 20-059 Lublin, Poland

² Department of Human Anatomy, Medical University of Lublin, 20-059 Lublin, Poland

³ Department of Pulmonary Diseases and Pediatric Rheumatology, Medical University of Lublin, 20-059 Lublin, Poland

⁴ Department of Histology and Embryology, Medical University of Lublin, 20-059 Lublin, Poland

Correspondence should be addressed to Jaroslav Dudka, ave123@wp.pl

Received 21 May 2012; Accepted 5 July 2012

Academic Editor: Ana Fortuno

Copyright © 2012 Jaroslav Dudka et al. This is an open access article distributed under the Creative Commons Attribution License, which permits unrestricted use, distribution, and reproduction in any medium, provided the original work is properly cited.

Cytochrome P450 NADPH-reductase (P450R), inducible synthase (iNOS) and xanthine oxidase play an important role in the antacycline-related cardiotoxicity. The expression of P450R and iNOS is regulated by triiodothyronine. The aim of this study was to evaluate the effect of methimazole-induced hypothyroidism on oxidative stress secondary to doxorubicin administration. 48 hours after methimazole giving cessation, rats were exposed to doxorubicin (2.0, 5.0 and 15 mg/kg). Blood and heart were collected 4, 48 and 96 h after the drug administration. Animals exposed exclusively to doxorubicin or untreated ones were also assessed. The hypothyroidism (0.025% of methimazole) significantly increased the doxorubicin effect on the cardiac carbonyl group and they may increase the glutathione level. An insignificant effect of methimazole was noticed in case of the cardiac lipid peroxidation product, the amount of DNA oxidative damages, iNOS and xanthine oxidase-enzymes responsible for red-ox activation of doxorubicin. However, the concentration of P450R was affected by a lower dose of methimazole in rats administered with doxorubicin. Since in rats receiving doxorubicin changes in oxidative stress caused by methimazole were not accompanied by elevation of bioreductive enzymes, it may be concluded that these changes in the oxidative stress were not related to the tested enzymes.

1. Introduction

Doxorubicin is widely used as a chemotherapeutic agent, but its usefulness is limited by cardiotoxicity [1]. Cardiotoxicity is manifested as incurable congestive heart failure that may appear months or years after completion of chemotherapy [2]. Free radicals synthesised during the doxorubicin redox

cycling are considered to be the starting point responsible for biochemical, morphological, and clinical symptoms [3–8].

Doxorubicin is enzymatically reduced with one electron which is transmitted to O_2 (Figure 1). This cycle may be repeated many times, resulting in overproduction of superoxide anion radical ($O_2^{\cdot-}$). $O_2^{\cdot-}$ implies in synthesis of more toxic oxygen (H_2O_2 , HO^{\cdot}) and nitrogen ($ONOO^-$)

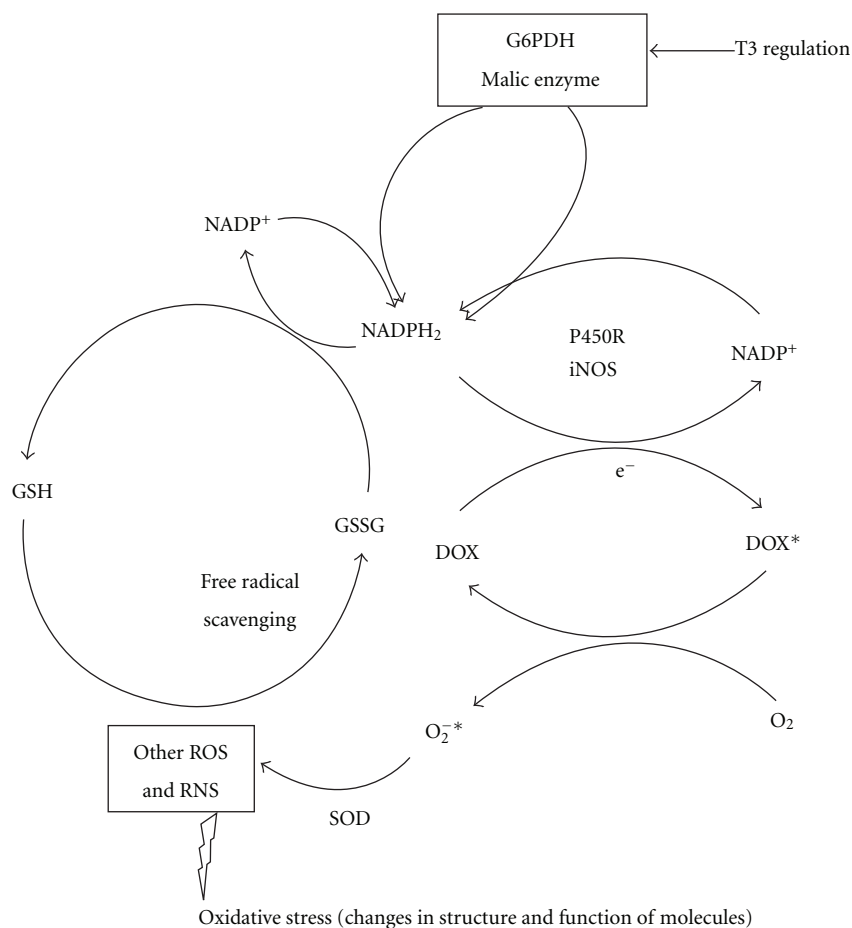


FIGURE 1: Mechanism expressed doxorubicin-dependent free radical generation and reportedly proposed role of triiodothyronine in redox equilibrium. P450R and iNOS transfer one electron to doxorubicin (DOX) from NADPH₂ leading to synthesis of doxorubicin radical (DOX^{*}). Subsequently, electron is taken by O₂ and to produce superoxide anion radical (O₂^{-*}). That is starting point to oxidative stress. Seemingly paradoxically NADPH₂ is indispensable to antioxidative activity, and its synthesis is transcriptionally regulated by triiodothyronine (T3).

species [9]. In those conditions, oxidation of lipids, protein, and DNA or nitration of amino acids of enzymes may appear [10]. Among enzymes affected by nitration, there is superoxide dismutase, a key enzyme of antioxidative defence [11].

The oxidative stress in cardiomyocytes triggered by doxorubicin is initiated by one-electron reduction, catalyzed mainly by microsomal cytochrome P450 NADPH-reductase (P-450R) [12, 13], nitric oxide synthases (NOS) [14], cytosolic xanthine oxidase (XO) [15, 16], and mitochondrial NADH dehydrogenase [17].

Interestingly, the animal and human data indicates that triiodothyronine (T3)—an active metabolite of thyroxine (T4)—upregulates P450R synthesis [18–20]. A similar mechanism has been suggested for thyroxine in case of iNOS [21]. Moreover, thyroxine regulates the crucial enzymes responsible for synthesis of NADPH—a cofactor for both P450R and iNOS and seemingly paradoxically the key factor in cellular redox balance (Figure 1).

The aim of the study was to evaluate the effect of hypothyreosis on the oxidative stress induced by doxorubicin and

to estimate the effect of both hypothyreosis and the drug on P450 and iNOS protein level.

2. Materials and Methods

2.1. Animals and Treatment. The study was approved by the Local Ethical Committee at the Medical University of Lublin. Male Wistar rats (180–220 g) were kept under conventional laboratory conditions (temperature 22°C, humidity 60–70%, 12 hours light/dark cycle) and fed with standard rodent granulated fodder LSM (AGROPOL, Poland). Food and water were freely available. The rats were randomly divided into groups, and each group contained seven subjects. The rats received thyreostatic drug—methimazole (methizole; ICN, Poland) in drinking water for three weeks at two concentrations (0.001 or 0.025%; group MET_L or MET_H, resp.). For the remaining time of the experiment, only filtrate municipal water was administered. 48 hours after completing methimazole administration, the rats received doxorubicin

(EBEWE Arzneimittel Ges.m.b.H., Austria) at the concentrations of 2.0, 5.0, and 15 mg/kg of the body weight (groups 2DOX + MET_L, 5DOX + MET_L, 15DOX + MET_L and 2DOX + MET_H, 5DOX + MET_H, 15DOX + MET_H). Doxorubicin hydrochloric was dissolved (1:1; v/v) in a saline solution (Cefarm, Poland). The other groups were exposed exclusively to doxorubicin but without inducing hypothyreosis (groups 2DOX, 5DOX, and 15DOX). The biological materials (blood and hearts) were collected 4, 48, and 96 hours after doxorubicin administration. In groups MET_L and MET_H, 48 hours after cessation of methimazole, rats were administered with saline, and, after the next 96 hours, the biological material was collected for further biochemical analyses. A similar procedure was applied in control group, in which 96 hours after the saline injection the rats were sacrificed.

The blood was aspirated from the left ventricle during the pentobarbital anaesthesia, and the obtained plasma was kept at -75°C . Immediately afterwards, the heart was removed during autopsy, washed with 20 mL of saline, and sectioned along the interventricular and coronal grooves. The wall of the left ventricle was placed in a liquid nitrogen and stored at -75°C until the biochemical and molecular analysis. The right ventricular wall was fixed in the buffered 10% formalin and routinely histologically processed to paraffin blocks.

2.2. Determination of Biochemical Parameters

2.2.1. Serum Triiodothyronine and Tetraiodothyronine. Triiodothyronine (FT₃) and tetraiodothyronine (FT₄) concentrations in rat plasma were measured using commercial reagents (AxSYM; Abbott, USA). The sample and antibody-coated microparticles added with reagent form an antibody-antigen complex. The T₃ or T₄ alkaline phosphatase conjugate binds to the available site on the anti-T₃ (anti-T₄) coated microparticles. Finally, 4-methylumbelliferyl phosphate was added and the fluorescent intensiveness of the obtained product was measured.

2.2.2. Determination of Tissue Markers for Redox Imbalance. All measurements were conducted on homogenates obtained from ~200 mg of frozen cardiac samples using the extraction buffer provided by the manufacturer of each commercial kit and homogeniser with teflon pistil (Glas-Col, USA). Plate reader PowerWave XS (Bio-tek, USA), was used to assess oxidative product of lipids (as a sum malondialdehyde and 4-hydroxyalkenals), proteins (carbonyl groups), DNA (basic sites), and the total glutathione.

2.2.3. Lipid Peroxidation Products. The evaluation of lipid peroxidation in cardiac homogenates was based on malondialdehyde and 4-hydroxyalkenals concentration (MDA + 4HAE). The commercial kit Biotech LPO-586 for MDA + 4HAE (OxisResearch, USA) was used for the assessment. The concept of the method is based on the reaction between MDA and 4HAE with N-methyl-2-phenylindol. After mixing N-methyl-2-phenylindole and methanol with the supernatant acquired from the homogenization, methanesulfonic acid

was added and all reagents were placed at the temperature 45°C for 60 minutes. Next, the solution was centrifuged and the supernatant containing the product was transferred to the plastic plate used in the spectrophotometric reader PowerWave XS (BioTek USA) at 586 nm. Subsequently, the procedure was conducted according to the manufacturer's description, and the concentration of MDA + 4HNE in the tested samples was calculated from the formula of the calibration curve $y = 0.0896x - 0.008$. The obtained data was calculated taking into account recommendations described in the procedure. The obtained results were expressed in nm/g of cardiac sample.

2.2.4. Protein Carbonyl Groups. Determination of protein carbonyl groups was conducted using the commercial kit (Cayman's Protein Carbonyl Assay; Cayman, USA). The obtained supernatant absorbance was checked at 260 and 280 nm to determine if the contaminating nucleic acid is present in the sample. The homogenisation buffer was used as a blank. The absorbance ratio 280/260 was more than 1.0; thus, the further step to remove nucleic acid was not necessary. The methods utilize the reaction of protein carbonyl groups with 2,4-dinitrophenylhydrazine. The product of the reaction was measured at 360 nm. The concentration of the carbonyl group was standardised on the protein unit (nmol carbonyl group/mg protein). The amount of protein was calculated from the bovine serum albumin dissolved in guanidine hydrochloride and read at 280 nm.

2.2.5. DNA Oxidative Damage. The commercial kit for isolation of genomic DNA (Fermentas, Lithuania) was used for isolation of the cardiac DNA according to the manufacturer's manual. The frozen cardiac sample was pulverized in liquid nitrogen and suspended in TRIS-EDTA buffer. Then, the sample was incubated in a lysis buffer at 65°C . Released DNA was extracted with the use of chloroform and then precipitated with a precipitation factor. DNA oxidative damage in cardiac muscles was evaluated by measuring the amount of basic sites (the so called AP) with a commercial kit (Dojindo, Japan). Isolated DNA was labeled with ARP reagent which can recognize the aldehyde group of the open ring in AP sites and can combine with biotin. Then, biotin-avidin specific connection and horseradish peroxidase were used for the colorimetric detection at 650 nm.

2.2.6. Total Glutathione. Glutathione determination was conducted using a commercial kit Bioxytech GSH/GSSG-412 (OxisResearch, USA). The total glutathione (GSH_t; GSH (reduced glutathione) + GSSG (oxidized glutathione)) was determined in the enzymatic reaction, where Ellman's reagent (5,5'-dithio-bis-2-nitrobenzoic acid) reacts with GSH forming color product with the maximum of absorbance at 412 nm. The concentrations of GSH, GSSG, and GSH/GSSG ratio were assessed after measuring the speed of the reaction and establishing calibrations curves. Concentrations of GSH and GSSG were determined based on the calibration curve described by the following formula:

$y = 0.1447x + 0.0004$ and $y = 0.1475x$, respectively. The obtained data was used to calculate the GSH/GSSG ratio.

2.3. Xanthine Oxidase Activity. The determination of xanthine oxidase activity (XO, EC 1.1.3.22) in the heart homogenates was conducted on the basis of the kinetic reaction of transformation xanthine to uric acid (Sigma Aldrich, USA) [22]. The increase of absorbance per unit of time at 290 nm was measured using a spectrophotometric reader PowerWave XT (BioTek, USA) at the light path 1 cm, at 25°C and pH 7.5. The absorbance was recorded every minute during 5 minutes. The phosphate buffet (pH 7.5) was added to the blank instead of the supernatant. The calculated enzyme activity was expressed on the mass unit of the sample of heart.

2.4. Molecular Analysis

2.4.1. Cytochrome P450 NADPH-Reductase. The content of cytochrome P450 NADPH-reductase (E.C. 1.6.2.4) protein was measured using WesternBreeze chromogenic Western Blot immunodetection kit (Invitrogen, USA). The left ventricular sample was homogenized in a phosphate-buffered saline with protease inhibitor cocktail (Sigma). After 30 min of blocking the nonspecific binding sites, the nitrocellulose membrane was incubated for 1 h with a rabbit anti-rat cytochrome P450 reductase polyclonal antibody (QED Bioscience) (1 : 1000) followed by a 30 min incubation with an alkaline phosphatase-conjugated anti-rabbit IgG secondary antibody. Immunoblots were developed using chromogenic substrate for 10 min, and the membrane was air-dried overnight. The chromogenic substrate was a mixture of BCIP (5-bromo-4-chloro-3-indolyl phosphate) and nitroblue tetrazolium salt.

2.4.2. Immunoexpression of iNOS. Immunohistochemical reaction for inducible nitric oxide synthase (iNOS; E.C. 1.14.13.39) was performed on the 4 μ m slides obtained from the paraffin blocks. After dewaxing and rehydration, the slides were placed for three cycles of heating in a microwave oven (750 W) for 5 min in the citrate buffer (0.01 M, pH 6.0) for antigen retrieval. Then, endogenous peroxidase activity was blocked with 3% hydrogen peroxide for 5 min, and the slides were incubated for 60 min with the primary polyclonal rabbit anti-mouse antibodies (LabVision, USA) against iNOS (clone Ab-1, dilution 1 : 50). The next step was the incubation with DakoEnvision+/HRP, Mouse kit (DakoCytomation; Glostrup, Denmark) according to the manufacturer's directions. The specific immune reaction was visualized by 3',3'-diaminobenzidine tetrahydrochloride (DAB) (DakoCytomation; Glostrup, Denmark), and finally the sections were counterstained with Mayer's hematoxylin. TBS buffer rinsing was used after each step. The whole procedure was performed at room temperature. In all cases, the appropriate positive and negative controls were performed. The sections were treated in the same way, but with mouse preimmune serum except that examined primary antibodies were used as negative controls. For the positive control, the rat lung sample was applied. All slides were eval-

uated, without the knowledge of the treated group, under light microscope (Olympus BX45; Tokyo, Japan).

2.5. Statistical Analysis. The obtained data were analysed using STATISTICA 5.0. (Statsoft Inc., USA). Statistical significance was evaluated by *U* Mann-Witney test (versus saline control) and by one-way analysis of variance (ANOVA Kruskala-Wallis). The post hoc test (Newmana-Keuls) was used to verify null hypothesis, according to which the lowered thyroid hormones status influence the evaluated parameters. All data are expressed as mean \pm SD. The value of $P < 0.05$ was considered statistically significant.

3. Results

The average plasma FT4 and FT3 concentrations of animals receiving methimazole in a lower dosage were significantly lower in comparison to the control subjects (Table 1). In the group exposed to higher drug concentration, both parameters were below the level of detection.

Comparing to the control, higher levels of MDA + 4HNE were observed in groups 15DOX/96 h, 15DOX + MET_H/48 h, and 15DOX + MET_H/96 h (Table 2). Unexpectedly, group MET_L diminished MDA + 4HNE concentration 96 h after doxorubicin administration (2 mg/kg) comparing to the proper group of DOX. Doxorubicin as a single agent applied in the highest dose significantly increased carbonyl groups concentration in animals after 4, 48, and 96 hours (Table 3). Statistically significant differences were also found between the carbonyl groups concentrations in euthyroid and hypothyroid rats receiving doxorubicin. Comparing to respective DOX group, significantly higher values were observed when doxorubicin was given to rats receiving the earlier higher dose of methimazole. Similar variables were noted for the middle and highest doses of doxorubicin, when, before the administration of the drug animals, were pretreated with a lower dose of methimazole. However, significantly lower concentrations of the carbonyl groups occurred in 15DOX + MET_L.

After the administration of the middle dose of doxorubicin, the amount of oxidative damage in DNA was rising significantly at 4 and 48 hours comparing to control (Table 4). The highest tested dose of doxorubicin triggered a significant increase in DNA damage in all tested periods. Similar changes comparing to control were observed in almost every comparable hypothyroid-like group administered with doxorubicin. However, significant changes were not revealed between any DOX + MET and DOX pairs.

The total glutathione concentration was not affected in any groups exposed to doxorubicin only when compared to the control (Table 5). However, a substantial increase of the parameter at 48 hours was observed when animals were pretreated with methimazole before the administration of the middle and highest doses of doxorubicin. Interestingly, the changes in GSH_T in rats receiving doxorubicin were related to the stage of hypothyreosis. A increase in 5DOX + MET_L/96 h and a decrease in 5DOX + MET_H/96 were observed when compared with the control. Importantly, this

TABLE 1: The concentration (pmol/L; $X \pm S.D.$) of free tetraiodothyronine (FT4) and triiodothyronine (FT3) in rats serum 48 h after withdrawal of methimazole.

	Methimazole (%)		
	0.000	0.001 (MET _L)	0.025 (MET _H)
FT4	10.48 \pm 1.12	6.10 \pm 1.55 ($P = 0.0009$)	Below limit of detection (<2.60)
FT3	3.52 \pm 0.49	2.39 \pm 0.57 ($P = 0.0092$)	Below limit of detection (<1.67)

TABLE 2: Malonyldialdehyd and 4-hydroxynonenal concentration (nmol/g of cardiac sample; $X \pm S.D.$) in rat cardiac homogenates 4, 48, and 96 h after doxorubicin administration.

Time from DOX injection (h)	DOX (mg/kg) or saline	Methimazole (%)			ANOVA P
		0.0000	0.001 (MET _L)	0.025 (MET _H)	
4	2	28.01 \pm 3.07	30.33 \pm 4.06	29.12 \pm 4.73	0.6977
	5	30.36 \pm 2.52	31.42 \pm 3.58	26.11 \pm 3.82	0.0706
	15	31.81 \pm 3.67	35.21 \pm 7.40	33.93 \pm 4.09	0.7163
48	2	25.84 \pm 4.26	23.37 \pm 3.94	22.01 \pm 4.14	0.5945
	5	26.85 \pm 1.39	25.06 \pm 3.90	25.84 \pm 0.96	0.6288
	15	29.85 \pm 6.50	29.63 \pm 7.85	38.50 \pm 4.5*	0.7520
96	2	31.36 \pm 10.45	22.43 \pm 1.99 [#]	28.49 \pm 4.83	0.0358
	5	31.25 \pm 4.33	32.20 \pm 7.48	26.12 \pm 4.93	0.2535
	15	39.36 \pm 3.39*	35.43 \pm 4.38	44.99 \pm 13.87*	0.2783
	0.9% NaCl	24.89 \pm 6.71 (control)	26.32 \pm 3.24	22.48 \pm 3.42	—

* $P < 0.05$ versus control; [#]DOX + MET versus DOX.TABLE 3: Carbonyl group concentration (nmol/mg of of cardiac protein; $X \pm S.D.$) in rat cardiac homogenates 4, 48, and 96 h after doxorubicin administration.

Time from DOX injection (h)	DOX (mg/kg) or saline	Methimazole (%)			ANOVA P
		0.0000	0.001 (MET _L)	0.025 (MET _H)	
4	2	19.55 \pm 5.12	28.18 \pm 6.11* [#]	45.45 \pm 16.15* [#] , [†]	0.0098
	5	19.41 \pm 9.41	38.65 \pm 13.45* [#]	103.08 \pm 46.03* [#] , [†]	0.0050
	15	57.52 \pm 16.05*	20.08 \pm 7.59 [#]	75.77 \pm 14.25* [#]	0.0060
48	2	18.92 \pm 5.30	29.46 \pm 6.92* [#]	42.75 \pm 12.46* [#]	0.0098
	5	21.29 \pm 6.62	40.43 \pm 22.04* [#]	109.95 \pm 84.48* [#]	0.0063
	15	54.73 \pm 1434*	14.70 \pm 6.57 [#]	124.24 \pm 62.84* [#]	0.0045
96	2	15.39 \pm 4.24	28.49 \pm 10.61* [#]	37.21 \pm 6.67* [#]	0.0081
	5	15.05 \pm 4.30	19.51 \pm 4.37 [#]	89.22 \pm 42.42* [#] , [†]	0.0052
	15	39.30 \pm 10.14*	15.06 \pm 4.98 [#]	91.76 \pm 56.76* [#] , [†]	0.0025
	0.9% NaCl	17.68 \pm 5.92 (control)	17.87 \pm 3.35	20.87 \pm 4.29	—

* $P < 0.05$ versus control; [#]DOX + MET versus DOX; [†]DOX + MET_H + versus DOX + MET_L.TABLE 4: The amount of oxidative damages of DNA (for 10⁶ base pairs; $X \pm S.D.$) in rat cardiac homogenates 4, 48, and 96 h after doxorubicin administration.

Time from DOX injection (h)	DOX (mg/kg) or saline	Methimazole (%)			ANOVA P
		0.0000	0.001 (MET _L)	0.025 (MET _H)	
4	2	1.22 \pm 0.14	1.16 \pm 0.11	1.23 \pm 0.11	0.4706
	5	1.54 \pm 0.21*	1.26 \pm 0.12*	1.60 \pm 0.22* [†]	0.0478
	15	1.82 \pm 0.17*	1.64 \pm 0.17*	1.90 \pm 0.31*	0.2645
48	2	1.13 \pm 0.05	1.14 \pm 0.07	1.12 \pm 0.04	0.8670
	5	1.21 \pm 0.07*	1.14 \pm 0.06	1.29 \pm 0.03* [†]	0.0183
	15	1.55 \pm 0.13*	1.38 \pm 0.15*	1.63 \pm 0.17*	0.0517
96	2	1.11 \pm 0.06	1.10 \pm 0.05	1.10 \pm 0.04	0.9900
	5	1.15 \pm 0.35	1.10 \pm 0.03	1.23 \pm 0.09* [†]	0.0271
	15	1.35 \pm 0.13*	1.29 \pm 0.08*	1.38 \pm 0.06*	0.2645
	0.9% NaCl	1.10 \pm 0.05 (control)	1.13 \pm 0.06	1.11 \pm 0.06	—

* $P < 0.05$ versus control; [†]DOX + MET_H versus DOX + MET_L.

TABLE 5: Total glutathione concentration (nmol/g of cardiac sample; $X \pm S.D.$) in rat cardiac homogenates 4, 48, and 96 h after doxorubicin administration.

Time from DOX injection (h)	DOX (mg/kg) or saline	Methimazole (%)			ANOVA <i>P</i>
		0.0000	0.001 (MET _L)	0.025 (MET _H)	
4	2	369.27 \pm 29.45	353.04 \pm 30.24	363.68 \pm 37.97	0.6505
	5	405.83 \pm 77.76	356.66 \pm 26.28	394.16 \pm 39.15	0.3356
	15	348.33 \pm 22.55	418.33 \pm 52.50	363.33 \pm 39.46	0.0514
48	2	361.54 \pm 43.76	395.52 \pm 31.92	378.85 \pm 29.82	0.4449
	5	353.33 \pm 70.73	454.16 \pm 46.68 ^{*,#}	455.83 \pm 41.10 ^{*,#}	0.0418
	15	395.83 \pm 69.53	564.16 \pm 72.08 ^{*,#}	439.17 \pm 16.82 ^{*,†}	0.0080
96	2	339.16 \pm 43.16	328.33 \pm 27.54	362.50 \pm 35.84	0.2101
	5	340.00 \pm 31.54	421.66 \pm 49.07 [*]	300.83 \pm 62.04 ^{*,†}	0.0081
	15	322.92 \pm 55.54	367.71 \pm 34.42	365.00 \pm 38.14	0.3813
	0.9% NaCl	368.33 \pm 34.43 (control)	342.71 \pm 83.57	395.83 \pm 25.68	—

* $P < 0.05$ versus control; #DOX + MET versus DOX; †DOX + MET_H versus DOX + MET_L.

TABLE 6: Xanthine oxidase activity (μ U/g of cardiac sample; $X \pm S.D.$) in rat cardiac homogenates 4, 48, and 96 h after doxorubicin administration.

Time from DOX injection (h)	Dose of DOX (mg/kg b.w.)	Methimazole			ANOVA <i>P</i>
		0.0000	0.001%	0.025%	
4	2	52.00 \pm 14.00	56.00 \pm 17.10	47.00 \pm 18.00	0.6229
	5	43.00 \pm 8.00	43.00 \pm 14.50	47.00 \pm 18.60	0.9680
	15	57.00 \pm 8.00	34.00 \pm 2.90 ^{*,#}	101.00 \pm 6.91 ^{*,†}	0.0171
48	2	38.00 \pm 17.10	56.00 \pm 14.30	54.00 \pm 16.60	0.1998
	5	34.00 \pm 10.60	66.00 \pm 50.00	64.00 \pm 17.4	0.0602
	15	65.00 \pm 37.00	54.00 \pm 9.40	58.00 \pm 15.7	0.9324
96	2	50.00 \pm 16.80	67.00 \pm 19.00	55.00 \pm 24.6	0.3705
	5	54.00 \pm 32.70	60.00 \pm 10.90	49.00 \pm 18.00	0.3724
	15	68.00 \pm 33.60	52.00 \pm 7.10	60.00 \pm 12.60	0.6057
	0.9% NaCl	70.00 \pm 35.80 (control)	52.00 \pm 10.70	46.00 \pm 6.60	

* $P < 0.05$ versus control; #DOX + MET versus DOX; †DOX + MET_H versus DOX + MET_L.

rise in GSH_T level in rats with hypothyreosis receiving doxorubicin (5, 15DOX + MET_{L,H}/48) was also significant when compared to DOX group.

The activity of xanthine oxidase in the heart muscle of the rats receiving doxorubicin was not affected when compared with control groups (Table 6). However, in groups 15DOX + MET_L/4 h and 15DOX + MET_H/4 h, respectively, lower and higher activity of the studied enzyme was found in relation to the observed values in the DOX group. Lack of differences in protein P450R expression using Western Blot technique was observed in the cardiac muscle among animals receiving doxorubicin alone when compared with the control group (Figure 2). On the contrary, the expression of protein was higher in groups of rats administered with a lower dose of methimazole with all tested doses of doxorubicin versus control and DOX groups. However, in all DOX groups receiving a higher dose of methimazole, insignificant changes were observed comparing to control and DOX groups as well.

A diffuse cytoplasmic immunostaining for iNOS and higher iNOS gene expression was found in the cardiac muscle, especially in the group examined at 96 hours and exposed exclusively to the lowest and middle doses of

doxorubicin (Figures 3 and 4). In case of animals exposed to doxorubicin with previously induced hypothyreosis, the level of iNOS mRNA and protein was lower and comparable to the control.

4. Discussion

The conducted study revealed that hypothyreosis had an important effect on the cardiac oxidative stress in rats exposed to doxorubicin. The direction of these changes was dependent on the concentration of iodothyronine hormones and the cytostatic dose. In case of hypothyreosis, the intensity of the doxorubicin-dependent oxidative stress was not related to the P450R, iNOS, and OX level.

The oxidative stress in cardiomyocytes triggered by doxorubicin is a widely accepted hypothesis in cardiotoxicity leading to the fatal congestive failure of the heart. As it was pointed above (Figure 1), the one-electron doxorubicin reduction, a key process in oxidative stress development, is catalyzed by microsomal [12, 13], cytoplasmic [12, 14, 15], and mitochondrial enzymes [17]. Among microsomal and

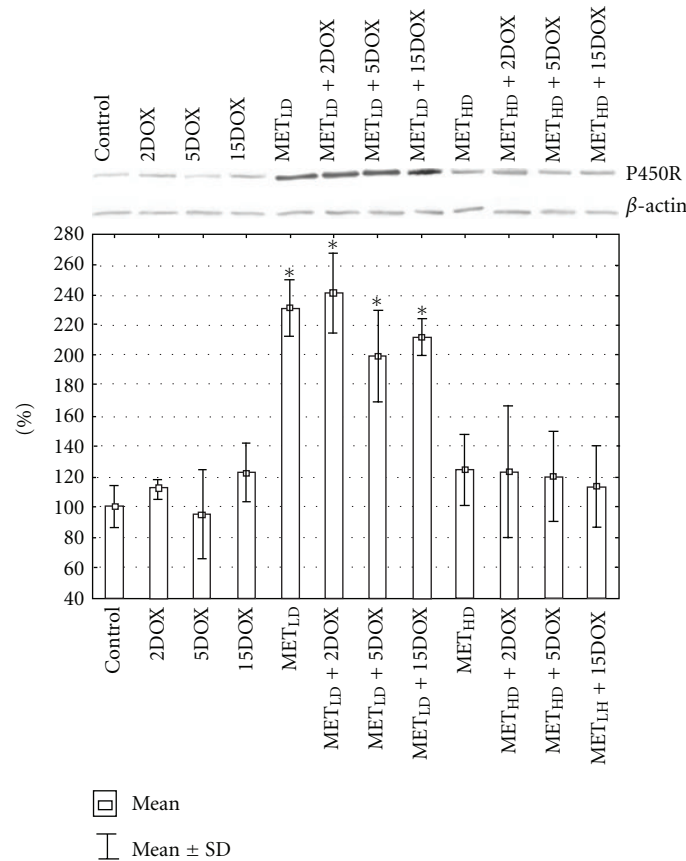


FIGURE 2: Representative Western Blot analysis for P450R protein in cardiac muscle homogenates. Beta-actin is shown as a loading control. Densitometric analysis (mean \pm SD) of total P450R content, expressed as percent changes with respect to the control group, which has been set at 100%. * $P < 0.05$ versus control and proper DOX group.

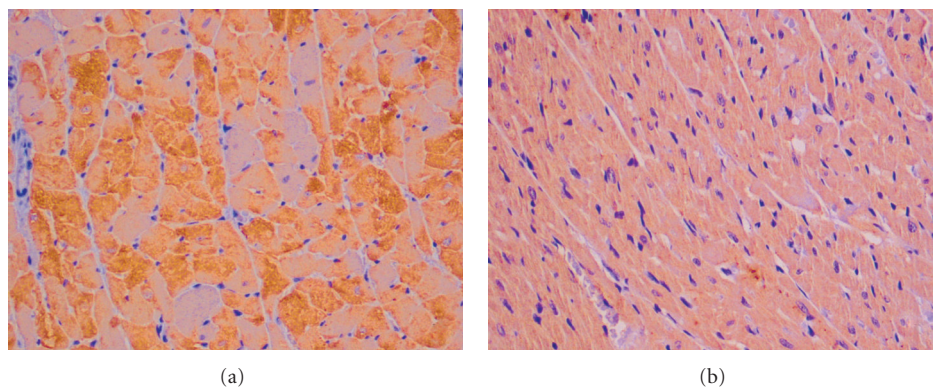


FIGURE 3: Strong positive cytoplasmic immunostaining for inducible nitric oxide synthase (iNOS) in cardiomyocytes. (a) 5DOX/96 h. (b) 5DOX + MET_L/96 h; (DakoEnvision+HRP; objective magnification (a) and (b): 20x).

cytoplasmic enzymes, the P450R [12, 13], iNOS [23, 24], and XO [15, 16] play important roles. As it was mentioned in the introduction, T3 and T4 via genome mechanism may change the activity of various enzymes engaged in doxorubicin redox activation [18, 20, 21] and in antioxidative defence [19, 25–27].

To confirm the proper dose of methimazole, the plasma FT₃ and FT₄ was determined and thyroid histology (data

not shown) was examined. The significant dose-dependent reduction of both FT₃ and FT₄ level and decreased amounts of colloid in thyroid follicles confirmed the properly chosen regimen of methimazole.

Clinical sensitivity of the analyzed oxidative stress markers varies in the order oxDNA > CG > MDA + 4HNE > GSH_T since an increase in oxidative DNA damages was observed in all tested periods in the group of 15DOX and

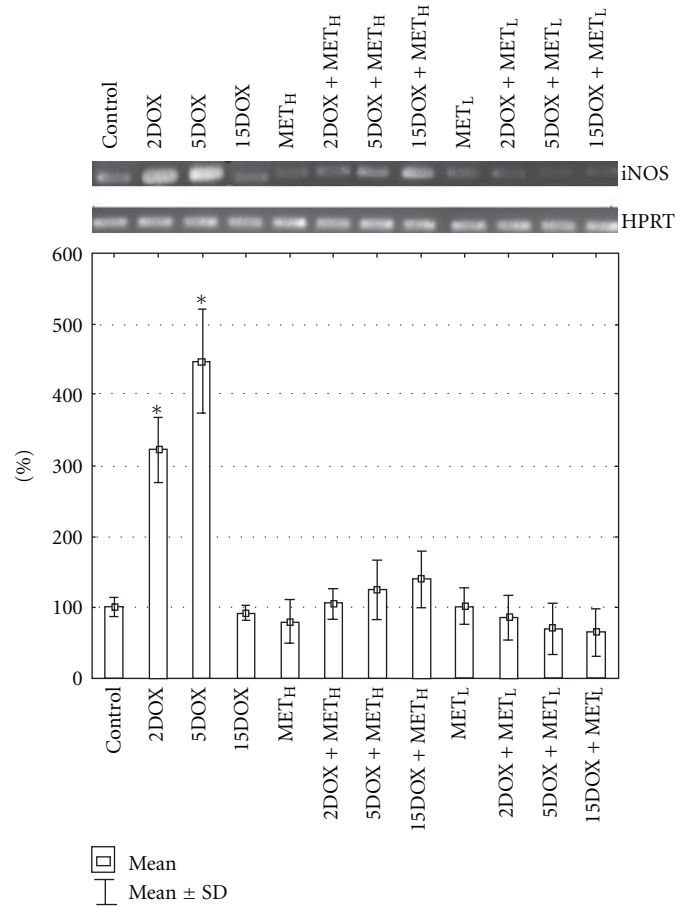


FIGURE 4: Representative mRNA iNOS content in cardiac muscle. HPRT was used as endogenous control. The results express percent changes (mean \pm SD) with respect to the control group, which has been set at 100%. * $P < 0.05$ versus control.

after treatment with the middle dose of DOX (5 mg) in 4 and 48 h. A significant doxorubicin-dependent increase in CG concentration was also observed at 4, 48, and 96 h but only in groups administered with the highest dose of DOX. An important increase in the lipid peroxidation was revealed exclusively at 96 h from the administration of the highest doxorubicin dose. Moreover, a lack of the GSH_T cardiac level changes was found.

Similar data was previously found in other studies. Palmeira et al. [28] observed that a single bolus of doxorubicin (15 mg/kg) caused a significant increase of the cardiac level of 8-hydroxydeoxyguanosine (8OHdG), another marker of DNA oxidative changes. The abundance of adducts was highest at the earliest time-point examined (24 h) and decreased to control values within 2 weeks. On the other hand, a significant increase in the level of the cardiac carbonyl group 10 days from single administration of doxorubicin in the dose of 20 mg was also pointed out [29]. Moreover, the single doxorubicin dose in the range of 10–20 mg/kg caused an increase of lipid peroxidation products, which was revealed after several days from the drug injection [29–32], whereas a lower single dose of doxorubicin (2.5 mg/kg) caused an increase of MDA level during the first

four hours and normalised within 24 h [33]. It seems that the dose of 2 mg, which was used in the current study, is too low to elicit a marked increase of the lipid peroxidation after single injection.

The question arises about the cause of different sensitivity determined markers after doxorubicin treatment. Based on the current knowledge, it is not possible to explain incompatible changes of various biochemical markers in case of the doxorubicin exposition. However, a biological half-life and sensitiveness to different kinds of reactive oxygen species should be considered. The carbonyl group appears relatively early and is stable during hours, and even days [34, 35], while the lifespan of the main lipid peroxidation products is estimated for minutes [36]. Lipid peroxidation products (e.g., MDA) form DNA adducts, which may explain the observed disproportion between the level of MDA and oxDNA in this study [37–40]. Moreover, oxidative destruction of lipids, protein, and DNA depends on the type of reactive oxygen species, for example, HOCl, a product of the reaction catalysed by myeloperoxidase, easily elevates the carbonyl group concentration but has a very little or no activity to create oxidative changes in lipids and DNA in the intracellular environment [41]. It should be also stressed that

in a study conducted by Fadillioglu et al. [29] a single dose of DOX (20 mg/kg) caused a significant increase of the cardiac myeloperoxidase activity.

It was previously assumed that hypothyreosis may change redox status in the heart of rats receiving doxorubicin, since triiodothyronine regulates P450R [18, 20] and is suspected to regulate iNOS expression [21], which plays an important role in bioreductive activation of DOX. Furthermore, the hormone upregulates the genes responsible for synthesis of G6PDH, malic enzyme, and 6-phosphogluconate dehydrogenase [27, 42]. These enzymes are a crucial cellular source of NADPH which via P450 and iNOS trigger ROS synthesis and, at the same time seemingly paradoxically, are indispensable in cell's antioxidative defence by reduced glutathione regeneration.

The current study revealed that hypothyroid conditions may increase the cardiac oxidative stress caused by doxorubicin. The most affected oxidative stress marker by hypothyreosis in rats treated with doxorubicin was CG. Similar result was also found for GSH_T that was influenced by the lowest and middle doses of DOX at 48 h and in the lowest dose at 96 h after drug administration.

The significant influence of hypothyreosis on cardiac lipid peroxidation in rats administered with doxorubicin appears only one time, and no such changes were observed in the case of oxDNA damages. For that reason, the comments will be focused on changes in carbonyl groups.

After treatment with the lowest and middle doses of doxorubicin only, there were no significant changes in CG in any period of time comparing to the control. However, when both mentioned doses of the drug were given to rats with hypothyreosis, a significant increase of oxidative protein damages was revealed. That rise was even 2-3 times higher than in proper DOX group. In cases when rats were treated with doxorubicin only, oxidative protein damages were higher comparing to control in all periods of time. The protein oxidative damages in rats administered with the highest dose of the drug changed depending on hypothyreosis state. When doxorubicin was administered to the rats exposed to a lower methimazole concentration, the level of carbonyl groups dramatically dropped, but in animals with more intense hypothyreosis the carbonyl groups levels were significantly elevated.

The obtained finding referring to the P450R protein level is somewhat surprising because referring to the assumption based on Ram and Waxman's [20] results, who observed that T3 upregulates gene expression of this enzyme, and on the basis of their study, it might be expected that inhibition of T3 synthesis caused by methimazole should diminish the concentration of the enzyme.

Taking into consideration that a very high increase in protein oxidative damages in all groups receiving the higher dose of methimazole with DOX was not accompanied by any changes in P450R protein level comparing to the DOX only proper group, it may be concluded that the oxidative stress is not related to the expression of the enzyme.

Similarly, iNOS was not responsible for the increased oxidative protein level because these elevations in group DOX + MET_H were not accompanied by an increase of the

enzyme concentration. Moreover, for the lowest and middle doses of doxorubicin, the immunoexpression of iNOS was lower in group DOX + MET_H comparing to euthyroid rats (proper group of DOX only).

Generally, there were no effects of iodothyronine hormone status on the activity of xanthine oxidase in rats receiving doxorubicin. Furthermore, this enzyme cannot be responsible for the observed oxidative protein elevation in all groups of DOX + MET_H.

Collectively, hypothyroid-like state may intensify the oxidative stress caused by doxorubicin, but P450R, iNOS, and XO may be excluded as being responsible for these phenomena. Further studies are needed to explain the role of other doxorubicin biactivating enzymes, especially of the mitochondrial fraction.

Acknowledgment

The authors would like to thank Ms. Mariola Michalczuk for technical support.

References

- [1] G. Minotti, P. Menna, E. Salvatorelli, G. Cairo, and L. Gianni, "Anthracyclines: molecular advances and pharmacologic developments in antitumor activity and cardiotoxicity," *Pharmacological Reviews*, vol. 56, no. 2, pp. 185–229, 2004.
- [2] A. L. A. Ferreira, L. S. Matsubara, and B. B. Matsubara, "Anthracycline-induced cardiotoxicity," *Cardiovascular and Hematological Agents in Medicinal Chemistry*, vol. 6, no. 4, pp. 278–281, 2008.
- [3] A. E. Ashour, M. M. Sayed-Ahmed, A. R. Abd-Allah et al., "Metformin rescues the myocardium from doxorubicin-induced energy starvation and mitochondrial damage in rats," *Oxidative Medicine and Cellular Longevity*, vol. 2012, Article ID 434195, 13 pages, 2012.
- [4] J. Dudka, F. Burdan, A. Korga et al., "The diagnosis of anthracycline-induced cardiac damage and heart failure," *Postępy Higieny i Medycyny Doświadczalnej*, vol. 63, pp. 225–233, 2009.
- [5] Y. W. Zhang, J. Shi, Y. J. Li, and L. Wei, "Cardiomyocyte death in doxorubicin-induced cardiotoxicity," *Archivum Immunologiae et Therapiae Experimentalis*, vol. 57, pp. 435–445, 2009.
- [6] V. A. Sardão, P. J. Oliveira, J. Holy, C. R. Oliveira, and K. B. Wallace, "Morphological alterations induced by doxorubicin on H9c2 myoblasts: nuclear, mitochondrial, and cytoskeletal targets," *Cell Biology and Toxicology*, vol. 25, no. 3, pp. 227–243, 2009.
- [7] J. M. Berthiaume and K. B. Wallace, "Persistent alterations to the gene expression profile of the heart subsequent to chronic doxorubicin treatment," *Cardiovascular Toxicology*, vol. 7, no. 3, pp. 178–191, 2007.
- [8] M. Tokarska-Schlattner, T. Wallimann, and U. Schlattner, "Alterations in myocardial energy metabolism induced by the anti-cancer drug doxorubicin," *Comptes Rendus Biologies*, vol. 329, no. 9, pp. 657–668, 2006.
- [9] J. Dudka, "The role of reactive oxygen and nitrogen species in calcium and iron homeostasis dysregulation in anthracycline cardiotoxicity," *Postępy Higieny i Medycyny Doświadczalnej*, vol. 60, pp. 241–247, 2006.
- [10] M. J. Mihm, F. Yu, D. M. Weinstein, P. J. Reiser, and J. A. Bauer, "Intracellular distribution of peroxynitrite during doxorubicin

- cardiomyopathy: Evidence for selective impairment of myofibrillar creatine kinase," *British Journal of Pharmacology*, vol. 135, no. 3, pp. 581–588, 2002.
- [11] N. B. Surmeli, N. K. Litterman, A. F. Miller, and J. T. Groves, "Peroxynitrite mediates active site tyrosine nitration in manganese superoxide dismutase. evidence of a role for the carbonate radical anion," *Journal of the American Chemical Society*, vol. 132, no. 48, pp. 17174–17185, 2010.
 - [12] S. Deng, A. Kruger, A. L. Kleschyov, L. Kalinowski, A. Daiber, and L. Wojnowski, "Gp91phox-containing NAD(P)H oxidase increases superoxide formation by doxorubicin and NADPH," *Free Radical Biology and Medicine*, vol. 42, no. 4, pp. 466–473, 2007.
 - [13] N. R. Bachur, S. L. Gordon, and M. V. Gee, "A general mechanism for microsomal activation of quinone anticancer agents to free radicals," *Cancer Research*, vol. 38, no. 6, pp. 1745–1750, 1978.
 - [14] S. Fogli, P. Nieri, and M. C. Breschi, "The role of nitric oxide in anthracycline toxicity and prospects for pharmacologic prevention of cardiac damage," *FASEB Journal*, vol. 18, no. 6, pp. 664–675, 2004.
 - [15] P. Mukhopadhyay, M. Rajesh, S. B tkai et al., "Role of superoxide, nitric oxide, and peroxynitrite in doxorubicin-induced cell death in vivo and in vitro," *American Journal of Physiology*, vol. 296, no. 5, pp. H1466–H1483, 2009.
 - [16] D. L. Gustafson, J. D. Swanson, and C. A. Pritsos, "Role of xanthine oxidase in the potentiation of doxorubicin-induced cardiotoxicity by mitomycin C," *Cancer Communications*, vol. 3, no. 9, pp. 299–304, 1991.
 - [17] K. J. A. Davies and J. H. Doroshow, "Redox cycling of anthracyclines by cardiac mitochondria. I. Anthracycline radical formation by NADH dehydrogenase," *Journal of Biological Chemistry*, vol. 261, no. 7, pp. 3060–3067, 1986.
 - [18] M. K. Tee, N. Huang, I. Damm, and W. L. Miller, "Transcriptional regulation of the human p450 oxidoreductase gene: Hormonal regulation and influence of promoter polymorphisms," *Molecular Endocrinology*, vol. 25, no. 5, pp. 715–731, 2011.
 - [19] H. C. Li, D. Liu, and D. J. Waxman, "Transcriptional induction of hepatic NADPH: cytochrome P450 oxidoreductase by thyroid hormone," *Molecular Pharmacology*, vol. 59, no. 5, pp. 987–995, 2001.
 - [20] P. A. Ram and D. J. Waxman, "Thyroid hormone stimulation of NADPH P450 reductase expression in liver and extrahepatic tissues. Regulation by multiple mechanisms," *Journal of Biological Chemistry*, vol. 267, no. 5, pp. 3294–3301, 1992.
 - [21] A. Virdis, R. Colucci, M. Fornai et al., "Inducible nitric oxide synthase is involved in endothelial dysfunction of mesenteric small arteries from hypothyroid rats," *Endocrinology*, vol. 150, no. 2, pp. 1033–1042, 2009.
 - [22] H. U. Bergmeyer, K. Gawehn, and M. W. Grassel, *Methods of Enzymatic Analysis*, vol. 1, Edited by H. U. Bergmeyer, Academic Press, New York, NY, USA, 1974.
 - [23] A. P. Garner, M. J. I. Paine, I. Rodriguez-Crespo et al., "Nitric oxide synthases catalyze the activation of redox cycling and bioreductive anticancer agents," *Cancer Research*, vol. 59, no. 8, pp. 1929–1934, 1999.
 - [24] J. V squez-Vivar, P. Martasek, N. Hogg, B. S. S. Masters, K. A. Pritchard Jr., and B. Kalyanaraman, "Endothelial nitric oxide synthase-dependent superoxide generation from adriamycin," *Biochemistry*, vol. 36, no. 38, pp. 11293–11297, 1997.
 - [25] S. Chattopadhyay, G. Zaidi, K. Das, and G. B. N. Chainy, "Effects of hypothyroidism induced by 6-n-propylthiouracil and its reversal by T3 on rat heart superoxide dismutase, catalase and lipid peroxidation," *Indian Journal of Experimental Biology*, vol. 41, no. 8, pp. 846–849, 2003.
 - [26] M. Jain, D. A. Brenner, L. Cui et al., "Glucose-6-phosphate dehydrogenase modulates cytosolic redox status and contractile phenotype in adult cardiomyocytes," *Circulation Research*, vol. 93, no. 2, pp. e9–16, 2003.
 - [27] A. Lombardi, L. Beneduce, M. Moreno et al., "3,5-Diiodo-L-thyronine regulates glucose-6-phosphate dehydrogenase activity in the rat," *Endocrinology*, vol. 141, no. 5, pp. 1729–1734, 2000.
 - [28] C. M. Palmeira, J. Serrano, D. W. Kuehl, and K. B. Wallace, "Preferential oxidation of cardiac mitochondrial DNA following acute intoxication with doxorubicin," *Biochimica et Biophysica Acta*, vol. 1321, no. 2, pp. 101–106, 1997.
 - [29] E. Fadilliglu, E. Oztas, H. Erdogan et al., "Protective effects of caffeic acid phenethyl ester on doxorubicin-induced cardiotoxicity in rats," *Journal of Applied Toxicology*, vol. 24, no. 1, pp. 47–52, 2004.
 - [30] M. A. Mansour, A. G. El-Din, M. N. Nagi, O. A. Al-Shabanah, and A. M. Al-Bekairi, "N^ω-Nitro-L-Arginine Methyl ester Ameliorates Myocardial Toxicity Induced by Doxorubicin," *Journal of Biochemistry and Molecular Biology*, vol. 36, no. 6, pp. 593–596, 2003.
 - [31] Z. Bolaman, C. Cicek, G. Kadikoylu et al., "The protective effects of amifostine on adriamycin-induced acute cardiotoxicity in rats," *Tohoku Journal of Experimental Medicine*, vol. 207, no. 4, pp. 249–253, 2005.
 - [32] X. Sun and Y. J. Kang, "Prior increase in metallothionein levels is required to prevent doxorubicin cardiotoxicity," *Experimental Biology and Medicine*, vol. 227, no. 8, pp. 652–657, 2002.
 - [33] T. Li, I. Danelisen, and P. K. Singal, "Early changes in myocardial antioxidant enzymes in rats treated with adriamycin," *Molecular and Cellular Biochemistry*, vol. 232, no. 1-2, pp. 19–26, 2002.
 - [34] T. Grune, T. Reinheckel, and K. J. A. Davies, "Degradation of oxidized proteins in K562 human hematopoietic cells by proteasome," *Journal of Biological Chemistry*, vol. 271, no. 26, pp. 15504–15509, 1996.
 - [35] T. Grune, T. Reinheckel, M. Joshi, and K. J. A. Davies, "Proteolysis in cultured liver epithelial cells during oxidative stress. Role of the multicatalytic proteinase complex, proteasome," *Journal of Biological Chemistry*, vol. 270, no. 5, pp. 2344–2351, 1995.
 - [36] W. G. Siems, H. Zollner, T. Grune, and H. Esterbauer, "Metabolic fate of 4-hydroxynonenal in hepatocytes: 1,4-dihydroxynonenone is not the main product," *Journal of Lipid Research*, vol. 38, no. 3, pp. 612–622, 1997.
 - [37] W. M. Przybylski, J. Kasperczyk, K. Stoklosa, and A. Bkhiyan, "DNA damage induced by products of lipid peroxidation," *Postępy Higieny i Medycyny Doświadczalnej*, vol. 59, pp. 75–81, 2005.
 - [38] L. J. Marnett, J. N. Riggins, and J. D. West, "Endogenous generation of reactive oxidants and electrophiles and their reactions with DNA and protein," *Journal of Clinical Investigation*, vol. 111, no. 5, pp. 583–593, 2003.
 - [39] L. J. Marnett, "Lipid peroxidation - DNA damage by malondialdehyde," *Mutation Research*, vol. 424, no. 1-2, pp. 83–95, 1999.
 - [40] P. M ller and H. Wallin, "Adduct formation, mutagenesis and nucleotide excision repair of DNA damage produced by reactive oxygen species and lipid peroxidation product," *Mutation Research*, vol. 410, no. 3, pp. 271–290, 1998.

- [41] I. Dalle-Donne, R. Rossi, D. Giustarini, A. Milzani, and R. Colombo, "Protein carbonyl groups as biomarkers of oxidative stress," *Clinica Chimica Acta*, vol. 329, no. 1-2, pp. 23–38, 2003.
- [42] A. Flores-Morales, H. Gullberg, L. Fernandez et al., "Patterns of liver gene expression governed by TR β ," *Molecular Endocrinology*, vol. 16, no. 6, pp. 1257–1268, 2002.

Research Article

Evaluation of Oxidative Stress and Antioxidant Status in Diabetic and Hypertensive Women during Labor

Mashaël M. Al-Shebl¹ and Mahmoud A. Mansour²

¹ Department of Obstetrics and Gynecology, College of Medicine, King Saud University, P.O. Box 2925, Riyadh 11461, Saudi Arabia

² Department of Pharmacology and Toxicology, College of Pharmacy, King Saud University, P.O. Box 2457, Riyadh 11451, Saudi Arabia

Correspondence should be addressed to Mahmoud A. Mansour, mansour1960us@yahoo.com

Received 5 February 2012; Revised 26 May 2012; Accepted 10 June 2012

Academic Editor: Martin-Ventura Jose Luis

Copyright © 2012 M. M. Al-Shebl and M. A. Mansour. This is an open access article distributed under the Creative Commons Attribution License, which permits unrestricted use, distribution, and reproduction in any medium, provided the original work is properly cited.

Pregnancy in insulin-dependent diabetes mellitus is associated with a greater incidence of fetal abnormality. Animal studies suggested that increased free-radical production and antioxidant depletion may contribute to this risk. The objective of this work was to evaluate oxidative stress and antioxidant capacity in hypertensive, diabetics, and healthy control women during labor. Simultaneous determination of antioxidant enzymes activities, namely glutathione peroxidase (GSH-Px), glutathione reductase (GSH-red), superoxide dismutase (SOD), total antioxidant, and lipid peroxides measured as thiobarbituric acid-reactive substances (TBARS) levels, were carried out in maternal plasma during labor. Plasma GSH-Px activity was found to be significantly increased as it doubled in hypertensive, and diabetic women when compared with healthy control women ($P < 0.05$). In contrast, plasma SOD activity was significantly decreased in both groups when compared to the control group ($P < 0.05$). No significant differences were detected in GSH-Red activity between diabetic, hypertensive and control groups. Alterations in antioxidant enzyme activities were accompanied by a significant increase in the levels of plasma lipid peroxides in hypertensive and diabetic women during labor. Plasma levels of total antioxidants were significantly increased in diabetic women as compared with the control group. Based on our results, it may be concluded that enhanced generation of oxidative stress causes alteration of antioxidant capacity in diabetic and hypertensive women during labor. Alterations in antioxidant and prooxidant components may result in various complications including peroxidation of vital body molecules which may be regarded as an increased risk factor for pregnant women as well as the fetus.

1. Introduction

Lipid peroxidation is an oxidative process which occurs at low levels in all cells and tissues. Under normal conditions, a variety of antioxidant mechanisms serve to control this peroxidative process [1]. The generation of free radicals is a normal physiological process, but increased production of free radicals can act on lipids causing lipid peroxidation. The cells have evolved a number of counter acting antioxidant defenses. Free radical scavenging mechanisms includes enzymatic and nonenzymatic antioxidants which limit the cellular concentration of free radical and prevent excessive oxidative stress.

Pregnancy is a stressful condition in which many physiological and metabolic functions are altered to a considerable

extent. Consequently, remarkable and dramatic events occur during this period [2]. Moreover, pregnancy is a physiological state, accompanied by a high-energy demand and an increased oxygen utilization, both of which may lead to increased oxidative stress. Oxidative stress occurs when there is an imbalance between free-radical production and the radical scavenging capacity of antioxidant systems [3]. Recently, Leal et al. [4] showed that there was a change in the prooxidant and antioxidant defenses that are inherent to pregnancy process.

There is evidence that both free-radical production and antioxidant defenses are disturbed in diabetes [5]. Therefore, it has been suggested over the last few years that oxidative stress in diabetes may be partly responsible for the development of diabetic complications [6]. The role of

oxidative stress in the pathogenesis of insulin dependent diabetes mellitus has been implicated in several studies [7–9]. Increased lipid peroxidation products and altered antioxidative enzyme activities were also reported in non-insulin-dependent diabetes mellitus [10]. However, there are limited numbers of investigations in diabetic pregnancy [11–13]. Congenital malformations in diabetic pregnancies may be regarded in this context as a complication of maternal disease. Exposure of the developing rat embryo to free-radical generating systems *in vitro* will cause fetal abnormalities [14], and an increased oxygen tension is also associated with abnormal neural fold and crest development [15].

Little information is available regarding the early human development of antioxidant defenses, but the fetus is likely to be particularly sensitive to free-radical damage early in development when the major organ systems are developing. Therefore, it is likely that antioxidant status is especially important during this period.

In the present study, our aim was to investigate oxidative stress as an indicator of oxygen radical activity and antioxidant defenses in diabetic and hypertensive women and to compare the results with those obtained for healthy control women during labor.

2. Results

2.1. Blood Parameters. The blood parameters of all the three groups are summarized in Table 1. Our results show that all blood parameters including RBCs count, WBCs count, platelets counts, and HB concentration in control, diabetic, and hypertensive women during labor were found to be statistically the same.

2.2. Plasma Concentrations of Urea, Creatinine, and Fasting Blood Glucose. Table 2 represents kidney function tests and fasting blood sugar. Plasma urea and creatinine concentrations were found to be significantly higher during labor in hypertensive women as compared to the control group concentrations. As expected, fasting blood sugar was significantly higher in diabetic women.

2.3. Enzymatic Antioxidant Parameters and Oxidative Stress Parameters. The antioxidant enzyme activities of all the three groups are summarized in Table 3. Plasma SOD levels of diabetic and hypertensive women during labor were significantly low as compared with the control group. In contrast, plasma GSH-Px levels of diabetic and hypertensive women were found to be significantly higher as compared to the control group. In addition, our results show that plasma GSH-red activity during labor in control, diabetic, and hypertensive women was found to be statistically the same.

Plasma levels of total antioxidants of diabetic women were found to be significantly higher than the respective control group, while there was no difference between control and hypertensive women.

Oxidative stress parameters of all the three groups are summarized in Table 4. Results show that the level of LPO of diabetic and hypertensive women during labor was found to be significantly higher than the control women.

3. Discussion

Pregnancy is a physiological state accompanied by a high energy demand and an increased oxygen requirement. Various compensatory adaptive changes, including increased ventilation for enhanced oxygen demand, occur with advancing pregnancy to meet the increasing requirements for proper bodily functions of the mother to fulfill the needs of the fetus [16]. Such a condition may be responsible for raised oxidative stress in pregnancy. The hypothesis underpinning this study was that impaired antioxidant status in diabetic and hypertensive women during labor might contribute to an increased risk of fetal abnormality. As outlined earlier, substantial evidence from animal models suggested that increased oxidative stress in the developing embryo is an important cause of abnormality, and that this can be prevented by antioxidants [17].

Our aim in the present study was to show the possibility of using the measured parameters as indicators of oxidative stress and antioxidant status during labor in diabetic, hypertensive, and healthy control women. In previous studies of antioxidant status in diabetics, abnormalities have usually been reported in the presence of diabetic complications or poor metabolic control. Indeed, in several studies antioxidant status and markers of lipid peroxidation have been normal in well-controlled diabetic subjects with no evidence of micro- or macroangiopathic complications [18, 19].

In the present study, we observed an increased level of plasma lipid peroxidation products (LPO) during labor in diabetic and hypertensive women. This may be attributed to over production of reactive oxygen species (ROS) or a deficiency of antioxidant defense. The results of the present study are in harmony with previous studies by Orhan et al. [20] and Tiwari et al. [21] who reported that the significant increase in plasma LPO in diabetic and anemic pregnant women, respectively, were parallel with a depletion of antioxidant enzymes as these enzymes are the major defense system of cells in normal aerobic reactions [22].

Similarly, during labor, plasma GSH-Px activity in diabetic and hypertensive women was increased significantly when compared to control women. This finding was in accordance with previous reports [23, 24] and the finding of Orhan et al. [20] who reported that erythrocyte GSH-Px activity was found to be significantly increased in hypertensive preeclamptic pregnancy and in insulin-dependent diabetic pregnancy. However, there are a number of conflicting reports as well [25, 26]. It can be assumed that at low levels of oxidants the enzyme is deactivated, but after a certain higher level it gets activated by same oxidant(s). Therefore, an increase in GSH-Px activity coupled with an increase in plasma lipid peroxides in the same groups can be interpreted as a compensatory mechanism of the enzyme in order to quench the increased levels of hydrogen

TABLE 1: Hemoglobin concentration, RBCs, WBCs, and platelets counts in control, diabetic, and hypertensive women during labor. Results are expressed as mean \pm SE.

Groups	HB g/L	RBCs $10^{12}/L$	WBCs $10^9/L$	Platelet $10^9/L$
Control	11.8 ± 0.4	4.17 ± 0.1	10.2 ± 0.76	229 ± 11.2
Diabetic	10.9 ± 0.2	3.88 ± 0.079	10.8 ± 0.26	237 ± 15
Hypertensive	10.9 ± 1.1	3.7 ± 0.44	10.4 ± 2.6	247 ± 51

TABLE 2: Plasma urea, creatinine, and fasting blood glucose concentration in control, diabetic, and hypertensive women during labor.

Groups	Urea mmol/L	Creatinine $\mu\text{mol}/L$	Fasting blood sugar mmol/L
Control	2.5 ± 0.17	47.6 ± 3.1	4.4 ± 0.14
Diabetic	2.5 ± 0.15	46.2 ± 1.6	$5.7 \pm 0.38^*$
Hypertensive	$3.77 \pm 0.65^*$	$61.1 \pm 5.1^*$	5 ± 0.4

Results are expressed as mean \pm SE.

*Significant difference from control group.

$P < 0.05$.

peroxide. Therefore, elevated levels of GSH-Px activity in hypertensive and diabetic women during labor may be linked to increased oxidative stress, because it is well known that ROS, especially hydrogen peroxide stimulate GSH-Px activity. This is an expected outcome during the delivery of a fetus, since the high oxygen challenge occurring at birth might lead to increased formation of reactive oxygen species and subsequently hydrogen peroxide.

Our present data show that there was no statistically significant difference in plasma GSH-Red activity during labor in diabetic, hypertensive, and control women. However, Miranda Guisado et al. [27] recently clarified glutathione redox cycle in hypertensive disorders of pregnancy and found a significant decrease in its reduced form GSH with a parallel increase in the oxidized form GSSG and an increment in both GSH-Px and GSH-Red activities. In our study, we observed that the plasma level of GSH-red activity in hypertensive group is higher than control group but the difference did not reach significant level. The reason for the discrepancy may be due to difference between activity level of GSH-Red in RBCs and plasma or may be explained by the physiological properties of the enzyme GSH-red. Moreover the pentose phosphate pathway may not be perturbed, as the availability of NADPH, a cofactor for GSH-red functioning be may still sufficient.

Glutathione is a major intracellular antioxidant. Glutathione and other thiols maintain the redox balance of cells, thereby preventing oxidative damage. GSH-Px catalyzes the oxidation of GSH to GSSG and reduces hydrogen peroxides (H_2O_2) to water. To maintain the balance between GSH and GSSG, the oxidized form of glutathione (GSSG) is reduced to GSH by GSH-red. For our future research, further assessment of GSH/GSSG ratio and hydrogen peroxides (H_2O_2) could give us more information about oxidant and antioxidant status in diabetic and hypertensive women during labor. Therefore, we will take that in our consideration and it will be verified in the erythrocytes and plasma of diabetic and hypertensive women during labor.

Plasma SOD activity of diabetic and hypertensive women during labor was significantly lower than its corresponding level in control women although erythrocytes possess highly efficient antioxidant enzymes, such as SOD and GSH-Px compared to other cell types [28]. In the present study there were no differences in RBCs, WBCs, and platelet counts, and HB concentrations in different groups during labor. However, our results showed that diabetic and hypertensive women have lower SOD and higher GSH-Px activities than healthy control. Our results are in accordance with an earlier report [29]. The observed reduction in SOD activity in hypertensive and diabetic women to that of normal control women could be associated with deleterious effect of hypertension and diabetes, as the superoxide anion that is being generated continuously by numerous sources throughout the body would not be inactivated effectively and lead to an increase in its concentration. Enhanced generation of superoxide anion would result in greater oxidative stress and lipid peroxidation. Decreased SOD activity during labor in diabetic, and hypertensive groups may be linked to increased hydrogen peroxide since it is well known that ROS, especially superoxide anion and hydrogen peroxide (H_2O_2), inhibit SOD activity [30]. SOD is a metalloprotein and accomplishes its antioxidant function by enzymatically detoxifying the peroxides ($-OOH$) and $O_2^{\bullet-}$, respectively.

Plasma total antioxidants were significantly higher only in diabetic women as compared with the control group. Clinical biochemical parameters, such as urea and creatinine, were higher only in the hypertensive group when compared to the control. The significantly high level of urea and creatinine of these patients seem to be a result of a renal damage due to hypertension. On the other hand, plasma levels of fasting blood sugar were higher in diabetic women as compared with normal controls.

The present study shows elevated oxidative stress/lipid peroxidation in diabetic and hypertensive women during labor. Besides, SOD, GSH-Px, and total antioxidants seem to be appropriate biomarkers reflecting the status of antioxidant

TABLE 3: Plasma antioxidant enzymes activities and total antioxidant in control, diabetic, and hypertensive women during labor.

Groups	SOD U/mL	GSH-Px U/L	GSH-red U/L	Total antioxidant mmol/L
Control	49.76 ± 1.8	35.6 ± 3.4	208 ± 11.8	0.59 ± 0.04
Diabetic	32.76 ± 2.4*	60.7 ± 9.6*	194 ± 13.3	1.5 ± 0.38*
Hypertensive	32 ± 3*	69.3 ± 12.8*	253.5 ± 49.7	1 ± 0.14

Results are expressed as mean ± SE.

*Significant difference from control group.

$P < 0.05$.

TABLE 4: Plasma lipid peroxides measured as in control, diabetic, and hypertensive women during labor.

Groups	MDA (nmol/mL)
Control	2.3 ± 0.47
Diabetic	3.34 ± 0.28*
Hypertensive	3.1 ± 0.33*

Results are expressed as mean ± SE.

*Significant difference from control group.

$P < 0.05$.

capacity in these diseases. The validation of these biomarkers for monitoring the efficiency of antioxidant supplementation during pregnancy should be further investigated. This supplementation may provide the prevention and/or attenuation of oxidative stress and enhancement of antioxidant status.

4. Material and Methods

4.1. Chemicals. All chemicals used in this study were of analytical grade.

4.2. Subjects. The present study was comprised of 62 pregnant women [namely control (24), diabetic (27) and hypertensive (11)] aged between 20–40 years. The subjects were selected amongst those attending the Department of Obstetrics and Gynaecology, King Khaled Hospital, King Saud University, Riyadh, Saudi Arabia. They were divided into groups of healthy controls, hypertensive, and insulin-dependent diabetic subject. Hypertension was defined according to the criteria of the Committee on Terminology of the American College of Obstetricians and Gynecologists, which has defined hypertension as a blood pressure greater than 140/90 mmHg before pregnancy or before 20 weeks of gestation. We defined insulin dependent diabetics diagnosed when not pregnant as Type I diabetes mellitus according to the National Diabetes Data Group Classification [31]. The diagnosis of the disease was made when two or more of the following plasma glucose concentrations were met or exceeded: fasting, 105 mg/dL; 1 h, 190 mg/dL; 2 h, 165 mg/dL; and 3 h, 145 mg/dL.

All groups were non-alcoholic and non-smoking subjects having no history of diseases such as malignancy, heart disease, or having infections such as tuberculosis and HIV. Informed consent was obtained from each subject. The

present study was approved by the Institutional Ethical Committee of King Saud University, Riyadh, Saudi Arabia.

4.3. Sample Collection. Venous blood (6 mL) was taken from each subject at the time of delivery and divided into three aliquots. Blood (2 mL) was transferred to an EDTA containing evacuated tube and was used to determine hemoglobin (Hb), red blood cells (RBC), white blood cells (WBC), and platelets counts. 2 mL of whole blood was also transferred into a heparin containing tube and then centrifuged, plasma was separated and used for the estimation of lipid peroxide levels (LPO), antioxidant enzymes, namely superoxide dismutase (SOD), glutathione peroxidase (GSH-Px), glutathione reductase (GSH-red), and total antioxidant. The remaining 2 mL of venous blood was also centrifuged at 3000 rpm for 15 min, serum separated and used for the estimation of urea, creatinine and glucose.

4.4. Biochemical Estimation

4.4.1. Blood Cell Counting. Blood haemoglobin was determined by using the cyanomethemoglobin method [32]. Red blood cell, white blood cells and platelets counts were determined by using the Sysmax A-380 automated cell counter.

4.4.2. Measurement of the Antioxidant Enzyme Activities. Plasma SOD activity was determined as previously described by McCord and Fridovich [33] in a kinetic assay at 37°C using a test reagent kit for SOD (RANSOD-Randox, UK). The absorbance was measured at 505 nm and the results were expressed as U/mL.

GSH-Px activity was estimated in the plasma according to Paglia and Valentine [34] by a kinetic assay at 37°C using a test reagent kit (RANSEL-Randox, UK). The absorbance was measured at 340 nm and the results were expressed as U/L. The GSH-red was assayed by the method of Hazelton and Lang [35]. The absorbance was measured at 340 nm and the results were expressed as U/L. Total antioxidant was measured according to Miller et al. [36]. The absorbance was measured at 600 nm and the results were expressed as mmol/L.

4.4.3. Estimation of Lipid Peroxidation. Plasma levels of lipid peroxides were determined as TBARS and calculated as malondialdehyde (MDA) according to the method of

Ohkawa et al. [37]. The absorbance was measured at 532 nm and the concentrations were expressed as nmol MDA/mL.

4.5. Statistical Analysis. Results are expressed as mean \pm SEM. Differences between obtained values were carried out by one way analysis of variance (ANOVA) followed by the Tukey-Kramer multiple comparison test. A *P* value of 0.05 or less was considered as a statistically significant difference.

Abbreviations

ROS: Reactive oxygen species
SOD: Superoxide dismutase
GSH-Px: Glutathione peroxidase
GSH-Red: Glutathione reductase
LP: Lipid peroxide.

Acknowledgment

The present work was supported by operating grant from Research Center, College of Medicine, King Saud University (CMRC130146).

References

- [1] H. Sies, "Oxidative stress: oxidants and antioxidants," *American Journal of Medicine*, vol. 91, no. 3, 1991.
- [2] S. Qanungo and M. Mukherjee, "Ontogenic profile of some antioxidants and lipid peroxidation in human placental and fetal tissues," *Molecular and Cellular Biochemistry*, vol. 215, no. 1-2, pp. 11-19, 2000.
- [3] E. Granot and R. Kohen, "Oxidative stress in childhood—in health and disease states," *Clinical Nutrition*, vol. 23, no. 1, pp. 3-11, 2004.
- [4] C. A. M. Leal, M. R. C. Schetinger, D. B. R. Leal et al., "Oxidative stress and antioxidant defenses in pregnant women," *Redox Report*, vol. 16, no. 6, pp. 230-236, 2011.
- [5] T. J. Lyons, "Oxidized low density lipoproteins: a role in the pathogenesis of atherosclerosis in diabetes?" *Diabetic Medicine*, vol. 8, no. 5, pp. 411-419, 1991.
- [6] J. W. Baynes, "Role of oxidative stress in development of complications in diabetes," *Diabetes*, vol. 40, no. 4, pp. 405-412, 1991.
- [7] S. K. Jain, "Hyperglycemia can cause membrane lipid peroxidation and osmotic fragility in human red blood cells," *Journal of Biological Chemistry*, vol. 264, no. 35, pp. 21340-21345, 1989.
- [8] H. Orhan and G. Sahin, "Erythrocyte glutathione S-transferase activity in diabetes mellitus: the effect of the treatment," *Fabad Journal of Pharmaceutical Sciences*, vol. 24, no. 3, pp. 127-131, 1999.
- [9] Y. Sato, N. Hotta, and N. Sakamoto, "Lipid peroxide level in plasma of diabetic patients," *Biochemical Medicine*, vol. 21, no. 1, pp. 104-107, 1979.
- [10] H. Kaji, M. Kurasaki, and K. Ito, "Increased lipoperoxide value and glutathione peroxidase activity in blood plasma of type 2 (non-insulin-dependent) diabetic women," *Klinische Wochenschrift*, vol. 63, no. 16, pp. 765-768, 1985.
- [11] D. Carone, G. Loverro, P. Greco, F. Capuano, and L. Selvaggi, "Lipid peroxidation products and antioxidant enzymes in red blood cells during normal and diabetic pregnancy," *European Journal of Obstetrics Gynecology and Reproductive Biology*, vol. 51, no. 2, pp. 103-109, 1993.
- [12] U. Kamath, G. Rao, C. Raghothama, L. Rai, and P. Rao, "Erythrocyte indicators of oxidative stress in gestational diabetes," *Acta Paediatrica*, vol. 87, no. 6, pp. 676-679, 1998.
- [13] A. Loven, Y. Romem, I. Z. Pelly, G. Holcberg, and G. Agam, "Copper metabolism—a factor in gestational diabetes?" *Clinica Chimica Acta*, vol. 213, no. 1-3, pp. 51-59, 1992.
- [14] P. C. Jenkinson, D. Anderson, and S. D. Gangolli, "Malformations induced in cultured rat embryos by enzymically generated active oxygen species," *Teratogenesis Carcinogenesis and Mutagenesis*, vol. 6, no. 6, pp. 547-554, 1986.
- [15] G. M. Morriss and D. A. T. New, "Effect of oxygen concentration on morphogenesis of cranial neural folds and neural crest in cultured rat embryos," *Journal of Embryology and Experimental Morphology*, vol. 54, pp. 17-35, 1979.
- [16] E. Gitto, R. J. Reiter, M. Karbownik et al., "Causes of oxidative stress in the pre- and perinatal period," *Biology of the Neonate*, vol. 81, no. 3, pp. 146-157, 2002.
- [17] U. J. Eriksson and L. A. H. Borg, "Protection by free oxygen radical scavenging enzymes against glucose-induced embryonic malformations in vitro," *Diabetologia*, vol. 34, no. 5, pp. 325-331, 1991.
- [18] P. E. Jennings and A. H. Barnett, "New approaches to the pathogenesis and treatment of diabetic microangiopathy," *Diabetic Medicine*, vol. 5, no. 2, pp. 111-117, 1988.
- [19] S. V. McLennan, S. Heffernan, L. Wright et al., "Changes in hepatic glutathione metabolism in diabetes," *Diabetes*, vol. 40, no. 3, pp. 344-348, 1991.
- [20] H. Orhan, L. Önderoglu, A. Yücel, and G. Sahin, "Circulating biomarkers of oxidative stress in complicated pregnancies," *Archives of Gynecology and Obstetrics*, vol. 267, no. 4, pp. 189-195, 2003.
- [21] A. K. M. Tiwari, A. A. Mahdi, F. Zahra, S. Chandyan, V. K. Srivastava, and M. P. S. Negi, "Evaluation of oxidative stress and antioxidant status in pregnant anemic women," *Indian Journal of Clinical Biochemistry*, vol. 25, no. 4, pp. 411-418, 2010.
- [22] H. D. Scheibmeir, K. Christensen, S. H. Whitaker, J. Jegaethesan, R. Clancy, and J. D. Pierce, "A review of free radicals and antioxidants for critical care nurses," *Intensive and Critical Care Nursing*, vol. 21, no. 1, pp. 24-28, 2005.
- [23] J. T. Uotila, R. J. Tuimala, T. M. Aarnio, K. A. Pyykko, and M. O. Ahotupa, "Findings on lipid peroxidation and antioxidant function in hypertensive complications of pregnancy," *British Journal of Obstetrics and Gynaecology*, vol. 100, no. 3, pp. 270-276, 1993.
- [24] J. Uotila, R. Tuimala, and K. Pyykko, "Erythrocyte glutathione peroxidase activity in hypertensive complications of pregnancy," *Gynecologic and Obstetric Investigation*, vol. 29, no. 4, pp. 259-262, 1990.
- [25] C. A. Hubel, J. M. Roberts, R. N. Taylor, T. J. Musci, G. M. Rogers, and M. K. McLaughlin, "Lipid peroxidation in pregnancy: new perspectives on preeclampsia," *American Journal of Obstetrics and Gynecology*, vol. 161, no. 4, pp. 1025-1034, 1989.
- [26] D. Wickens, M. H. Wilkins, and J. Lunec, "Free-radical oxidation (peroxidation) products in plasma in normal and abnormal pregnancy," *Annals of Clinical Biochemistry*, vol. 18, no. 3, pp. 158-162, 1981.
- [27] M. L. Miranda Guisado, A. J. Vallejo-Vaz, P. Stiefel García Junco et al., "Abnormal levels of antioxidant defenses in a large sample of patients with hypertensive disorders of pregnancy," *Hypertension Research*, vol. 35, no. 3, pp. 274-278, 2012.

- [28] A. Kumerova, A. Lece, A. Skesters, A. Silova, and V. Petuhovs, "Anaemia and antioxidant defence of the red blood cells," *Materia Medica Polona*, vol. 30, no. 1-2, pp. 12–15, 1998.
- [29] E. Kurtoglu, A. Ugur, A. K. Baltaci, and L. Undar, "Effect of iron supplementation on oxidative stress and antioxidant status in iron-deficiency anemia," *Biological Trace Element Research*, vol. 96, no. 1-3, pp. 117–123, 2003.
- [30] M. Isler, N. Delibas, M. Guclu et al., "Superoxide dismutase and glutathione peroxidase in erythrocytes of patients with iron deficiency anemia: effects of different treatment modalities," *Croatian Medical Journal*, vol. 43, no. 1, pp. 16–19, 2002.
- [31] National Diabetes Data Group, "Classification and diagnosis of diabetes mellitus and other categories of glucose intolerance," *Diabetes*, vol. 28, no. 12, pp. 1039–1057, 1979.
- [32] International Nutritional Anemia Consultative Group, *Measurements of Iron Status*, INACG, Washington, DC, USA, 1985.
- [33] J. M. McCord and I. Fridovich, "Superoxide dismutase. An enzymic function for erythrocyte hemocuprein (hemocuprein)," *Journal of Biological Chemistry*, vol. 244, no. 22, pp. 6049–6055, 1969.
- [34] D. E. Paglia and W. N. Valentine, "Studies on the quantitative and qualitative characterization of erythrocyte glutathione peroxidase," *The Journal of Laboratory and Clinical Medicine*, vol. 70, no. 1, pp. 158–169, 1967.
- [35] G. A. Hazelton and C. A. Lang, "Glutathione contents of tissues in the aging mouse," *Biochemical Journal*, vol. 188, no. 1, pp. 25–30, 1980.
- [36] N. J. Miller, C. Rice-Evans, M. J. Davies, V. Gopinathan, and A. Milner, "A novel method for measuring antioxidant capacity and its application to monitoring the antioxidant status in premature neonates," *Clinical Science*, vol. 84, no. 4, pp. 407–412, 1993.
- [37] H. Ohkawa, N. Ohishi, and K. Yagi, "Assay for lipid peroxides in animal tissues by thiobarbituric acid reaction," *Analytical Biochemistry*, vol. 95, no. 2, pp. 351–358, 1979.

Research Article

Effect of Antioxidant Mineral Elements Supplementation in the Treatment of Hypertension in Albino Rats

S. A. Muhammad,¹ L. S. Bilbis,¹ Y. Saidu,¹ and Y. Adamu²

¹ Biochemistry Department, Usmanu Danfodiyo University, PMB, Sokoto 2346, Nigeria

² Faculty of Veterinary Medicine, Usmanu Danfodiyo University, PMB, Sokoto 2346, Nigeria

Correspondence should be addressed to S. A. Muhammad, salhajimuhammad@yahoo.com

Received 15 April 2012; Accepted 21 May 2012

Academic Editor: Adrian Manea

Copyright © 2012 S. A. Muhammad et al. This is an open access article distributed under the Creative Commons Attribution License, which permits unrestricted use, distribution, and reproduction in any medium, provided the original work is properly cited.

Oxidative stress has been implicated in various pathologies, including hypertension, atherosclerosis, diabetes, and chronic renal disease. The current work was designed with the aim of investigating the potentials of antioxidants copper, manganese, and zinc in the treatment of hypertension in Wistar rats. The rats were fed 8% NaCl diet for 5 weeks and treatment with supplements in the presence of the challenging agent for additional 4 weeks. The supplementation significantly decreased the blood pressure as compared with hypertensive control. The result also indicated significant decreased in the levels of total cholesterol, triglyceride, low-density lipoprotein cholesterol and very low-density lipoprotein cholesterol, malondialdehyde, insulin and increase in the high-density lipoprotein cholesterol, total antioxidant activities, and nitric oxide of the supplemented groups relative to the hypertensive control. The average percentage protection against atherogenesis indicated $47.13 \pm 9.60\%$ for all the supplemented groups. The mean arterial blood pressure showed significant positive correlation with glucose, total cholesterol, triglyceride, low-density lipoprotein cholesterol, very low-density lipoprotein cholesterol, atherogenic index, insulin resistance and malondialdehyde while high density lipoprotein-cholesterol and total antioxidant activities showed negative correlation. The result therefore indicated strong relationship between oxidative stress and hypertension and underscores the role of antioxidant minerals in reducing oxidative stress, dyslipidemia, and insulin resistance associated with hypertension.

1. Introduction

Hypertension is one of the most common diseases worldwide and a major cause of death from cardiovascular failure. Due to associated morbidity and mortality, hypertension is a public health problem [1], and thus the need to search for proper preventive and management strategies should be the concern of health care providers. Increased vascular oxidative stress could be involved in the pathogenesis of hypertension [2, 3] a major risk factor for cardiovascular disease and mortality in the developed and developing countries. The onset of hypertension is caused by complex interactions between genetic predisposition and environmental factors [4]. Increased salt intake may aggravate the rise in blood pressure and the development of consequential end-organ damage [5].

The novel concept that structural and functional abnormalities in the vasculature, including endothelial dysfunction, increased oxidative stress, and decreased antioxidant activities, may antedate hypertension and contribute to its pathogenesis, has gained support in recent years [6]. Animal studies have generally supported the hypothesis that increased blood pressure is associated with increased oxidative stress [7]. Elevated lipid peroxidation byproducts and decreased activity of antioxidant systems have been reported in hypertensive subjects [8]. Several studies have indicated an increase in O_2^- levels in hypertension [9] and implicate NADPH oxidase as a source of excess O_2^- [10, 11].

Angiotensin II has been shown to be a potent activator of NADPH oxidase activity in vascular smooth muscle, endothelial cells, and cardiomyocytes [12]. A common finding in all types of hypertension as well as diabetes and

metabolic syndrome is endothelial dysfunction, characterized by an imbalance in the expression of and sensitivity to vasodilator and vasoconstrictor agents resulting in increased vascular tone and thus an increase in resistance to flow [13, 14].

Copper, manganese, and zinc are commonly referred to as antioxidant minerals that are required for the activity of some antioxidant enzymes. Hiroyuki et al. [15] reported that zinc deficiency might play a crucial role in the development of genetic hypertension presumably through the oxidative stress caused by hypertension. It is known that superoxide anion rapidly inactivates the endothelium-derived vasodilator, nitric oxide, thereby promoting vasoconstriction [16]. Consequently, attempts to counteract the hypertensive effects of reactive oxygen species have led to the use of exogenous antioxidants to improve vascular function and reduce blood pressure in animal models [17] and human hypertension [18, 19]. Thus, evaluation of potential effect of antioxidants copper, manganese, and zinc in the management of hypertension form the basis of this study.

2. Methods

2.1. Chemicals and Reagents. Analytical graded chemicals and reagents were used for this research. Copper sulphate and manganese sulphate were sourced from May and Baker, England, while zinc sulphate was from J.T. Baker chemical company, Philipsburg, New Jersey.

2.2. Experimental Animals. Male wistar rats weighing between 150–180 g were purchased from the Faculty of Veterinary Medicine, Usmanu Danfodiyo University, Sokoto, Nigeria and were allowed to acclimatize for two weeks before the commencement of the experiment. The animals were grouped into six groups of 5 rats each and they were fed pelletized growers' feed (Vital feed, Jos, Nigeria) and allowed access to water *ad libitum* throughout the experimental period. The experimental protocol was approved by the Ethical Committee of the Usmanu Danfodiyo University, Sokoto, Nigeria.

2.3. Induction of Hypertension. The rats were placed on a high-salt diet (8% NaCl) except normotensive control for 9 weeks by adding 8% NaCl to the feed [20]. Treatment commenced from the 6th week of salt loading.

2.4. Measurement of Blood Pressure. Blood pressure was monitored weekly by the tail-cuff method using noninvasive Ugo Basile, series 58500 Blood Pressure Recorder. Average of four readings was taken for each rat, and the temperature of the rat was monitored throughout the measurement period. Mean arterial blood pressure was calculated according to the following equation: $DP + (1/3) (SP - DP)$ where SP and DP are systolic and diastolic pressure, respectively.

2.5. Preparation of Supplements. Copper, manganese, and zinc were prepared by dissolving copper sulphate, manganese

sulphate, and zinc sulphate in distilled water to obtain 2.5 mg/mL of copper, 2.4 mg/mL of manganese, and 11 mg/mL of zinc, respectively. All the supplements were prepared just prior to administration.

2.6. Grouping of Animals and Treatment

Group I Normal untreated /distilled water.

Group II Hypertensive control/distilled water.

Group III Salt-loaded treated with 4 mg/kg of copper.

Group IV Salt-loaded treated with 10 mg/kg of manganese.

Group V Salt-loaded treated with 20 mg/kg of zinc.

Group VI Salt-loaded treated with 4 mg/kg of copper, 10 mg/kg of manganese, and 20 mg/kg of zinc.

The concentrations of the supplements were selected based on the recommended dietary allowance and the appropriate dosages administered orally to the treated groups according to their body weight by intubation using intravenous cannula tube for 4 weeks. Twenty four hours after the last treatment, the animals were anaesthetized with chloroform vapour and fasting blood samples were collected through cardiac puncture into labelled tubes for biochemical analyses. Weight changes of the rats were monitored throughout the experimental period.

2.7. Estimation of Biochemical Parameters. The blood sample was allowed to clot and centrifuged at 4000 g for ten minutes and the serum obtained was used for the estimation of glucose, lipid profile, total antioxidant status, insulin, superoxide dismutase, catalase, and nitric oxide. The animals were sacrificed and the liver of each rat was dissected out, rinsed with ice-cold saline to remove the blood. 10% homogenate was prepared in ice-cold 0.1 M Tris buffer, pH 7.4 using homogenizer. The homogenate was centrifuged at 4000 g for 15 minutes. The supernatants were used for estimation of thiobarbituric acid reactive substance (TBARS) and glutathione peroxidase activity.

The fasting serum glucose level was estimated by glucose oxidase method [21]. Serum total cholesterol [22], triglyceride [23] and high-density lipoprotein cholesterol [24] were determined by enzymatic method.

Serum low-density lipoprotein cholesterol and very low density lipoprotein cholesterol was calculated by the formula of friedewald et al. [25]. Atherogenic index was calculated as the ratio of LDL cholesterol to HDL cholesterol [26].

Colorimetric method was used for the estimation of serum total antioxidant status [27] and tissue malondialdehyde [28].

Cayman's Superoxide Dismutase Assay Kit was used for the estimation of SOD. The assay utilizes a tetrazolium salt for the detection of superoxide radicals generated by xanthine oxidase and hypoxanthine at 450 nm. One unit of SOD is defined as the amount of enzyme needed to exhibit 50% dismutation of the superoxide radicals.

The catalase activity was estimated using Cayman's Catalase Assay Kit. The method is based on the reaction of the enzyme with methanol in the presence of an optimal concentration of H_2O_2 . The formaldehyde produced is measured with 4-amino-3-hydrazino-5-mercapto-1,2,4-triazole (Purpald) as the chromogen at 540 nm.

Glutathione peroxidase activity was assayed using Cayman's Assay Kit. This assay measures glutathione peroxidase activity indirectly by a coupled reaction with glutathione reductase. Oxidized glutathione, produced upon reduction of hydroperoxide by glutathione peroxidase, is recycled to its reduced state by glutathione reductase and NADPH. The oxidation of NADPH to $NADP^+$ is accompanied by a decrease in absorbance at 340 nm.

Nitric oxide was estimated by Cayman's Assay Kit. The assay provides an accurate and convenient method for measurement of total nitrate/nitrite concentration in a simple two-step process. The first step is the conversion of nitrate to nitrite utilizing nitrate reductase. The second step is the addition of the Griess reagent which converts nitrite into a deep purple azo compound.

Insulin was estimated by SPI biorat insulin enzyme immunoassay kit. The assay is based on the competition between unlabelled rat insulin and acetylcholinesterase linked to rat insulin (tracer) for limited specific guinea-pig anti-rat insulin antiserum sites. The plate was then washed and Ellman's reagent added to the wells, and the acetylcholinesterase tracer acts on the Ellman's reagent to form a yellow compound which was determined at 405nm.

Insulin resistance index was calculated by Homeostasis Model Assessment—Insulin Resistance (HOMA-IR) [29].

HOMA-IR

$$= \frac{\text{Fasting glucose (mmol/L)} \times \text{Fasting insulin } (\mu\text{U/mL})}{22.5} \quad (1)$$

Percentage protection against atherogenesis was calculated using the following equation

$$\frac{\text{Atherogenic index (AI) of Hypertensive control (HC) - AI of treated group}}{\text{Atherogenic index (AI) of Hypertensive control (HC)}} \times 100 \quad (2)$$

2.8. Statistical Analysis. Values are expressed as mean \pm standard deviation for 5 rats in each group. The result were analysed statistically using one way analysis of variance (ANOVA), followed by Dunnett's multiple comparison test using GraphPad Instat software. Differences were considered significant when $P < 0.05$.

3. Results

The weight gain of rats (Figure 1) indicated that salt-loaded untreated control gain more weight (53.89 ± 2.50) than the treated groups and normotensive control. Supplementation showed significant ($P < 0.01$) effect on the weight changes of the rats as compared to the hypertensive control.

There was significant ($P < 0.05$) increase in mean arterial blood pressure of the salt-loaded rats (Figure 2). Supplementation caused significant decrease in the mean arterial blood pressure of the treated groups relative to the hypertensive control.

The effect of mineral elements in SBP, DBP, and MABP is presented in Figure 3. The result indicated significant ($P < 0.05$) increase in the % reduction of SBP between the minerals combined (11.02%) group and groups supplemented with copper (7.36%), manganese (6.59%), and zinc (7.73%), respectively while there was no significant ($P > 0.05$) difference in the % reduction of DBP and MABP between the minerals combined group and copper-, manganese-, and zinc- supplemented groups. The % reduction in DBP of copper-, zinc-, and manganese-treated groups indicated 21.71%, 20.68%, and 18.29%, respectively, while mineral combined was 24.47%. The group treated with

TABLE 1: Effect of antioxidant minerals on glucose, insulin and insulin resistance in salt-induced hypertensive.

Group	Glucose (mmol/L)	Insulin ($\mu\text{U/mL}$)	HOMA-IR
I	4.28 ± 0.31	2.98 ± 1.42	0.56 ± 0.23
II	6.50 ± 0.83^p	17.01 ± 4.04^p	4.81 ± 0.68^p
III	5.62 ± 0.72^y	4.94 ± 1.51^a	1.21 ± 0.26^a
IV	5.66 ± 0.75^p	$9.68 \pm 2.76^{a,p}$	$2.48 \pm 0.46^{a,p}$
V	5.66 ± 0.66^p	$11.06 \pm 4.50^{\beta,p}$	$2.93 \pm 0.42^{a,p}$
VI	4.63 ± 0.21^a	6.56 ± 1.47^a	$1.34 \pm 0.24^{a,y}$

HOMA-IR: Homeostasis Model Assessment-Insulin Resistance, I-normotensive control, II-hypertensive control, III-group treated with copper, IV-group treated with manganese, V-group treated with zinc, VI-group treated with all the minerals.

Values are expressed as Mean \pm SD; $n = 5$. $^aP < 0.01$ when compared with grp II, $^bP < 0.05$ when compared with grp II, $^pP < 0.01$ when compared with grp I, $^yP < 0.05$ when compare with grp I by Dunnette's multiple comparison test.

mineral combined showed 18.52% reduction in MABP, zinc (15.38%), and copper (14.68%) while manganese-treated group, 13.80%, was the lowest in the group.

Salt loading caused significant increase in serum glucose, insulin, and insulin resistance (Table 1), and supplementations with the mineral elements reverse the trend.

Effect of supplementation on serum lipid profile and atherogenic index is presented in Table 2. The result indicated significant decrease in the levels of TC, TG, LDL-C, VLDL-C, and AI and increase in HDL-C as compared with salt-loaded untreated group.

TABLE 2: Effect of antioxidant minerals on lipid profile and atherogenic index.

Group	TC (mg/dL)	TG (mg/dL)	HDL-C (mg/dL)	LDL-C (mg/dL)	VLDL-C (mg/dL)	AI
I	78.08 ± 4.03	63.89 ± 5.17	40.44 ± 5.30	24.53 ± 4.85	12.77 ± 1.03	0.61 ± 0.16
II	123.64 ± 7.47 ^p	121.10 ± 12.14 ^p	30.36 ± 2.23 ^p	69.05 ± 5.83 ^p	24.21 ± 2.42 ^p	2.27 ± 0.20 ^p
III	109.82 ± 3.43 ^{β,p}	70.87 ± 4.63 ^α	41.45 ± 2.74 ^{α,p}	54.18 ± 3.14 ^α	14.17 ± 0.92 ^α	1.30 ± 0.11 ^{α,p}
IV	108.38 ± 5.18 ^{α,p}	65.97 ± 4.76 ^α	39.98 ± 6.42 ^α	55.26 ± 5.96 ^{β,p}	13.18 ± 0.95 ^α	1.39 ± 0.36 ^{α,p}
V	102.19 ± 11.64 ^{α,p}	83.50 ± 8.33 ^{α,p}	38.05 ± 3.12 ^β	46.69 ± 10.9 ^{α,p}	16.69 ± 1.66 ^{α,p}	1.23 ± 0.33 ^{α,p}
VI	94.02 ± 5.24 ^{α,p}	80.02 ± 12.06 ^{α,γ}	41.14 ± 1.23 ^α	36.86 ± 5.40 ^{α,γ}	16.00 ± 2.41 ^{α,γ}	0.89 ± 0.14 ^α

TC: total cholesterol, TG: triglyceride, HDL-C: high-density lipoprotein cholesterol, LDL-C: low-density lipoprotein cholesterol, VLDL-C: very low density lipoprotein cholesterol, AI: atherogenic index, I: normotensive control, II: hypertensive control, III: group treated with copper, IV: group treated with manganese, V: group treated with zinc, and VI: group treated with all the minerals.

Values are expressed as Mean ± SD; $n = 5$. ^α $P < 0.01$ when compared with group II, ^β $P < 0.05$ when compared with group II, ^p $P < 0.01$ when compared with group I, and ^γ $P < 0.05$ when compared with group I by Dunnett's multiple comparison test.

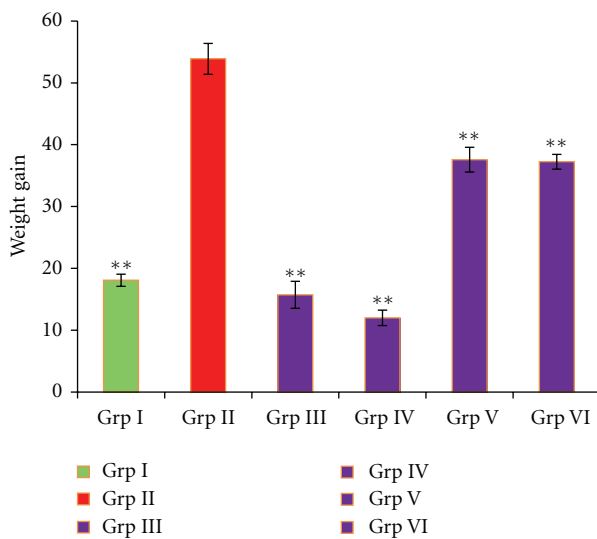


FIGURE 1: Weight gain of salt-induced hypertensive treated with antioxidant minerals. Grp I: normal untreated, Grp II: hypertensive untreated, Grp III: salt loaded treated with copper, Grp IV: salt loaded treated with manganese, Grp V: salt loaded treated with zinc, and Grp VI: salt loaded treated with minerals combined ** $P < 0.01$ when compared with group II.

The % protection against atherogenesis (Figure 4) indicated significant ($P < 0.01$) increase in the % protection in the group supplemented with minerals combined as compared to the copper, manganese, and zinc groups. The group treated with minerals combined showed the highest protection of 60.79% while the group supplemented with manganese showed the lowest protection of 38.76%.

Effect of supplementation on total antioxidant status, nitric oxide, and MDA (Table 3) showed significant increase in the levels of TAS between untreated group and manganese ($P < 0.05$) and mineral combined ($P < 0.01$) groups. The result also indicated significant ($P < 0.01$) decrease in the tissue MDA of the supplemented groups as compared with untreated control. Endothelial function was also improved following supplementation.

The result of effect of supplementation on antioxidant enzymes is presented in Table 4. The result indicated that

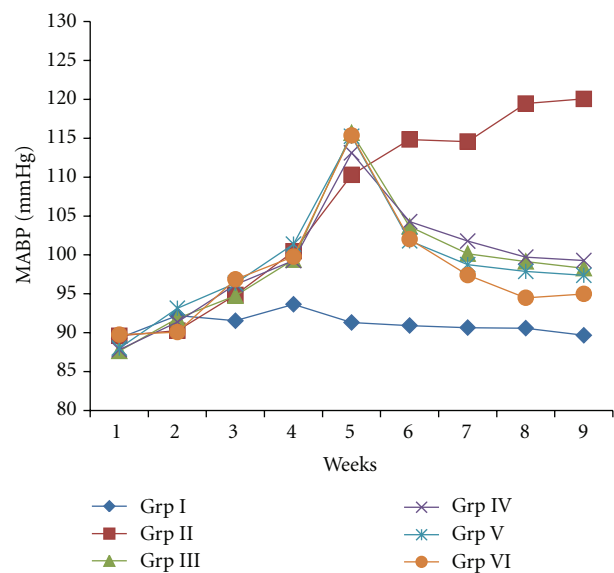


FIGURE 2: Effect of salt diet and antioxidant supplementation on mean arterial blood pressure of salt-loaded rats. Week 1–5: salt diet only, week 6–9: salt diet plus supplements, MABP-mean arterial blood pressure Grp I: normal untreated, Grp II: hypertensive untreated, Grp III: salt loaded treated with copper, Grp IV: salt loaded treated with manganese, Grp V: salt loaded treated with zinc, and Grp VI: salt-loaded treated with minerals combined.

supplementation increased the activities of cat, Gpx, and SOD as compared with hypertensive control.

Correlation coefficient (r) of MABP against glucose, insulin resistance, lipid profile, and oxidative stress markers is presented in Figure 5. The result showed significant positive correlation between MABP and glucose, insulin, insulin resistance, TC, TG, LDL-C, VLDL-C, AI, and MDA while HDL-C, TAS, SOD, Cat, and GPx showed negative correlation with MABP.

4. Discussion

Hypertension is among the top most risk factors for cardiovascular disease [30]. In this model, a diet containing 8% NaCl was used to induce hypertension in wistar rats

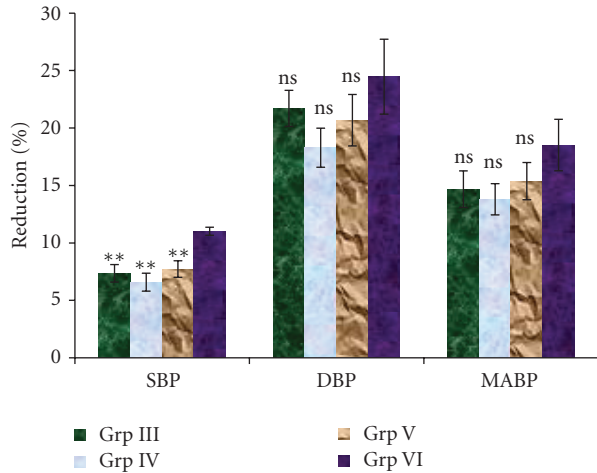


FIGURE 3: The mean percentage reduction in blood pressure of supplemented groups. SBP: systolic blood pressure, DBP: diastolic blood pressure, MABP: mean arterial blood pressure, Grp III: salt-loaded treated with copper, Grp IV: salt-loaded treated with manganese, Grp V: salt loaded treated with zinc, and Grp VI: salt loaded treated with minerals combined. ** $P < 0.01$ and ns: not significant when compared with Grp VI.

TABLE 3: Effect of antioxidant minerals on total antioxidant, nitric oxide, and lipid peroxidation.

Group	Nitric oxide (μM)	TAS (mmol/L)	MDA (nmol/mg tissue)
I	28.14 \pm 3.85	1.64 \pm 0.24	0.382 \pm 0.04
II	17.70 \pm 3.07 ^p	0.70 \pm 0.17 ^p	1.210 \pm 0.22 ^p
III	31.55 \pm 6.16 ^a	0.99 \pm 0.28 ^p	0.549 \pm 0.11 ^a
IV	22.00 \pm 5.62	1.13 \pm 0.26 ^{b-p}	0.569 \pm 0.08 ^a
V-	18.81 \pm 3.01 ^y	1.00 \pm 0.15 ^p	0.545 \pm 0.11 ^a
VI	30.81 \pm 5.67 ^a	1.40 \pm 0.06 ^a	0.512 \pm 0.14 ^a

TAS: total antioxidant status, MDA: malondialdehyde, I: normotensive control, II: hypertensive control, III: group treated with copper, IV: group treated with manganese, V: group treated with zinc, and VI: group treated with all the minerals.

Values are expressed as Mean \pm SD; $n = 5$. ^a $P < 0.01$ when compared with group II, ^b $P < 0.05$ when compared with group II, ^p $P < 0.01$ when compared with group I, and ^y $P < 0.05$ when compare with group I by Dunnette's multiple comparison test.

for 5 weeks and salt-loaded diet with supplementation for additional 4 weeks. High salt has been reported to cause hypertension in rats [20, 31]. The mechanism by which high-salt diets induced hypertension could be due to increase in the level of circulating sodium which cause cells to release water due to osmotic pressure which elevates the pressure on blood vessel walls [32]. Other possible mechanisms could be in part due to an increase in the plasma's capacity to inhibit Na^+ , K^+ -Adenosine Triphosphatase which raises the blood pressure by inhibiting the sodium-calcium exchange pump in vascular smooth muscle [33], or that sodium diet is associated with increased intrarenal angiotensin II [34] which may result in renal vasoconstriction and increased renal O_2^- production due to activation of NADPH oxidase.

TABLE 4: Effect of supplementation on antioxidant enzymes.

Group	Catalase (nmol/min/mL)	GPx (nmol/min/mL)	SOD (U/mL)
I	26.27 \pm 4.47	95.76 \pm 9.75	5.21 \pm 1.46
II	14.52 \pm 3.16 ^p	28.01 \pm 7.26 ^p	2.86 \pm 0.62 ^y
III	19.41 \pm 3.14 ^y	49.15 \pm 9.72 ^{a-p}	4.83 \pm 1.06 ^b
IV	21.67 \pm 4.27 ^b	49.40 \pm 7.71 ^{a-p}	5.13 \pm 0.94 ^b
V	21.05 \pm 2.95 ^b	47.62 \pm 9.38 ^{a-p}	5.82 \pm 1.31 ^a
VI	23.71 \pm 3.30 ^a	68.00 \pm 7.93 ^{a-p}	4.89 \pm 1.29 ^b

GPx: glutathione peroxidase, SOD: superoxide dismutase, I: normotensive control, II: hypertensive control, III: group treated with copper, IV: group treated with manganese, V: group treated with zinc, and VI: group treated with all the minerals.

Values are expressed as Mean \pm SD; $n = 5$. ^a $P < 0.01$ when compared with group II, ^b $P < 0.05$ when compared with group II, ^p $P < 0.01$ when compared with group I, and ^y $P < 0.05$ when compare with group I by Dunnette's multiple comparison test.

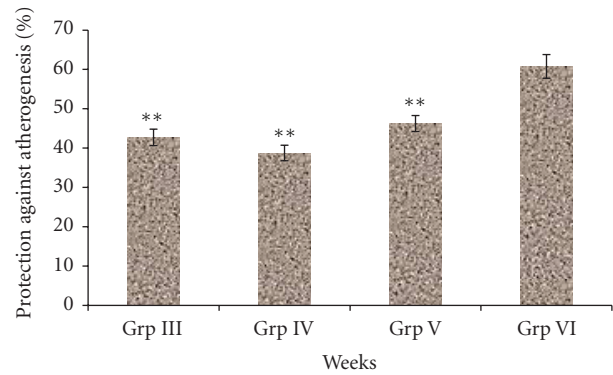


FIGURE 4: Percentage protection against atherogenesis of salt-induced hypertensive rats supplemented with minerals Grp I: normal untreated, Grp II: hypertensive untreated, Grp III: salt loaded treated with copper, Grp IV: salt loaded treated with manganese, Grp V: salt loaded treated with zinc, Grp VI: salt loaded treated with minerals combined ** $P < 0.01$ when compared with Grp VI.

Overproduction of superoxide anions and other free radicals due to activation of NADPH oxidase may overwhelm the antioxidant capability and cause imbalances between oxidant and antioxidant status which may result in oxidative stress. The result indicated that salt loading increased the arterial blood pressure of the rats and supplementation with antioxidant minerals prevents the elevation of blood pressure. The observation confirms the report that salt loading to various strains of rats such as Sprague-Dawley rats [20] and wistar rats [35] result in increased blood pressure.

The group supplemented with minerals combined nearly normalized the mean arterial blood pressure which indicates that combination therapy appears to be more effective in blood pressure reduction than single antioxidant mineral supplementation.

The blood pressure lowering effect of copper, manganese, and zinc in this model could be attributed to their free radical scavenging properties which decrease nitric oxide quenching

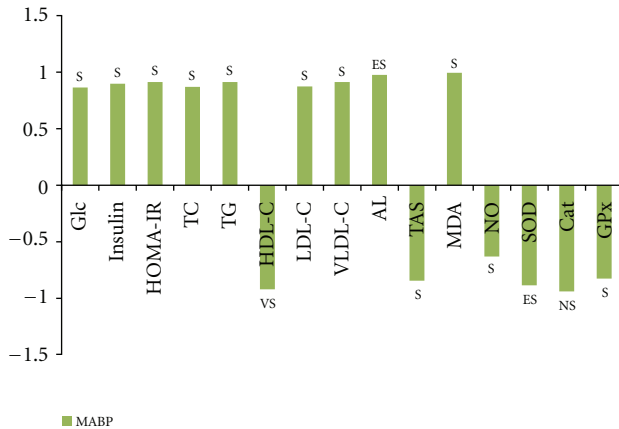


FIGURE 5: Correlation coefficient (r) of MABP against glucose, insulin resistance, lipid profile, and oxidative stress markers. MABP: mean arterial blood pressure, Glc: glucose, HOMA-IR: Homeostasis Model Assessment-Insulin Resistance, GPx: glutathione peroxidase, SOD: superoxide dismutase, TC: total cholesterol, TG: triglyceride, HDL-C: high-density lipoprotein cholesterol, LDL-C: low density lipoprotein cholesterol, VLDL-C: very low-density lipoprotein cholesterol, AI: atherogenic index, vit: vitamin, TAS: total antioxidant status, MDA: malondialdehyde, NO: nitric oxide, ES: extremely significant, VS: very significant, S: significant, and NS: not significant.

by superoxide anion, decrease NADPH oxidase activity, or increase superoxide dismutase activity since these minerals form an essential and integral part of superoxide dismutase. The result of the current work confirms the report that zinc supplementation lowers the blood pressure of salt-loaded hypertensive rats [36].

The increased levels of triglyceride, total cholesterol, low-density lipoprotein cholesterol, and very low-density lipoprotein-cholesterol and decrease in the high-density lipoprotein-cholesterol observed in hypertensive rats compared to the supplemented group corroborated with several studies [37, 38]. The possible mechanism underlying the relationship between increased levels of HDL-C and decreased LDL-C and cardiovascular outcome of hypertension following supplementation in this study could be due to increased synthesis or decreased degradation of HDL-C that may decrease the oxidized lipid species in LDL particles, thereby protecting them from atherogenesis. This might indeed reflect the starting point for the protection against atherosclerosis. The result also showed decreased in the levels of glucose, insulin, insulin resistance, malondialdehyde, and increased nitric oxide of the supplemented groups as compared with hypertensive control. The improved endothelial function and insulin sensitivity observed in the supplemented groups confirms the role of antioxidant copper, manganese and zinc in the management of hypertension. Thus, the exact molecular mechanisms underlying antioxidant effects of these minerals on insulin sensitivity and endothelial function were not fully determined in this model but could be mediated through oxidative stress suppression which resulted in improving antioxidant status and endothelial function as evidenced by the decreased level

of lipid peroxidation index, malondialdehyde, and increased nitric oxide, a measure of endothelial function.

The results of the study suggest that salt loading induces hypertension via oxidative stress, since it elicits lipid peroxidation and influence, the activities of antioxidant enzymes in the rats. This is indicated by the increase in the total antioxidant status and activities of superoxide dismutase, catalase, and glutathione peroxidase following supplementation with antioxidant minerals which was overwhelmed due to oxidative stress induced by salt.

Attempt was also made to correlate the mean arterial blood pressure with all the biochemical parameters assessed in our model in order to determine the degree of association between these variables. The result indicated significant positive correlation between mean arterial blood pressure and glucose, total cholesterol, triglyceride, low density lipoprotein-cholesterol, very low-density lipoprotein cholesterol, atherogenic index, insulin resistance, and malondialdehyde while high-density lipoprotein cholesterol, total antioxidant status, catalase, superoxide dismutase, and glutathione peroxidase showed significant negative correlation.

The positive correlation between MABP and malondialdehyde suggest that increase in blood pressure resulted in more production of thiobarbituric acid reactive substances, and supplementation decreased both MABP and MDA. The negative correlation between MABP and total antioxidant status, catalase, SOD, and glutathione peroxidase is evidence that increase in the MABP downregulated the activities of these enzymes and decreased the TAS which could be attributed to the production of excess free radicals, but supplementation ameliorate, the effects.

These observations further confirmed the role of oxidative stress in hypertension, and supplementations with antioxidant minerals have the potential to prevent or delay the cardiovascular complications of hypertension since our results provides antioxidant protection. However, it is not clear whether increase in the amount of reactive oxygen species is a consequence of hypertension or otherwise.

5. Conclusion

The result confirmed the role of oxidative stress in hypertension and underscores the role of copper, manganese, and zinc in delaying and treatment of cardiovascular complications of hypertension.

References

- [1] C. J. L. Murray and A. D. Lopez, "Mortality by cause for eight regions of the world: global burden of disease study," *Lancet*, vol. 349, no. 9061, pp. 1269–1276, 1997.
- [2] R. Rodrigo, W. Passalacqua, J. Araya, M. Orellana, and G. Rivera, "Implications of oxidative stress and homocysteine in the pathophysiology of essential hypertension," *Journal of Cardiovascular Pharmacology*, vol. 42, no. 4, pp. 453–461, 2003.
- [3] K. Miyajima, S. Minatoguchi, Y. Ito et al., "Reduction of QTc dispersion by the angiotensin II receptor blocker valsartan may be related to its anti-oxidative stress effect in patients with

- essential hypertension," *Hypertension Research*, vol. 30, no. 4, pp. 307–313, 2007.
- [4] B. R. Winkelmann, J. Hager, W. E. Kraus et al., "Genetics of coronary heart disease: current knowledge and research principles," *American Heart Journal*, vol. 140, no. 4, pp. S11–S26, 2000.
 - [5] B. Rassler, "The renin-angiotensin system in the development of salt-sensitive hypertension in animal models and humans," *Pharmaceuticals*, vol. 3, no. 4, pp. 940–960, 2010.
 - [6] S. Oparil, M. A. Zaman, and D. A. Calhoun, "Pathogenesis of hypertension," *Annals of Internal Medicine*, vol. 139, no. 9, pp. 761–776, 2003.
 - [7] E. Grossman, "Does increased oxidative stress cause hypertension?" *Diabetes care*, vol. 31, pp. S185–S189, 2008.
 - [8] K. Yasunari, K. Maeda, M. Nakamura, and J. Yoshikawa, "Oxidative stress in leukocytes is a possible link between blood pressure, blood glucose, and C-reacting protein," *Hypertension*, vol. 39, no. 3, pp. 777–780, 2002.
 - [9] F. Lacy, D. T. O'Connor, and G. W. Schmid-Schönbein, "Plasma hydrogen peroxide production in hypertensives and normotensive subjects at genetic risk of hypertension," *Journal of Hypertension*, vol. 16, no. 3, pp. 291–303, 1998.
 - [10] C. Berry, C. A. Hamilton, M. J. Brosnan et al., "Investigation into the sources of superoxide in human blood vessels: angiotensin II increases superoxide production in human internal mammary arteries," *Circulation*, vol. 101, no. 18, pp. 2206–2212, 2000.
 - [11] R. M. Touyz and E. L. Schiffrin, "Increased generation of superoxide by angiotensin II in smooth muscle cells from resistance arteries of hypertensive patients: role of phospholipase D-dependent NAD(P)H oxidase-sensitive pathways," *Journal of Hypertension*, vol. 19, no. 7, pp. 1245–1254, 2001.
 - [12] Y. Taniyama and K. K. Griendling, "Reactive oxygen species in the vasculature: molecular and cellular mechanisms," *Hypertension*, vol. 42, no. 6, pp. 1075–1081, 2003.
 - [13] D. Versari, E. Daghini, A. Viridis, L. Ghiadoni, and S. Taddei, "Endothelium-dependent contractions and endothelial dysfunction in human hypertension," *British Journal of Pharmacology*, vol. 157, no. 4, pp. 527–536, 2009.
 - [14] M. Félétou, R. Köhler, and P. M. Vanhoutte, "Endothelium-derived vasoactive factors and hypertension: possible roles in pathogenesis and as treatment targets," *Current Hypertension Reports*, vol. 12, no. 4, pp. 267–275, 2010.
 - [15] Y. Hiroyuki, S. Masamichi, and W. Osamu, "Zinc deficiency and hypertension," in *Proceedings of the 18th Symposium on Trace Nutrients Research*, pp. 67–71, 2001.
 - [16] J. Zicha, Z. Dobešová, and J. Kuneš, "Relative deficiency of nitric oxide-dependent vasodilation in salt-hypertensive Dahl rats: the possible role of superoxide anions," *Journal of Hypertension*, vol. 19, no. 2, pp. 247–254, 2001.
 - [17] X. Chen, R. M. Touyz, J. B. Park, and E. L. Schiffrin, "Antioxidant effects of vitamins C and E are associated with altered activation of vascular NADPH oxidase and superoxide dismutase in stroke-prone SHR," *Hypertension*, vol. 38, no. 3, pp. 606–611, 2001.
 - [18] S. J. Duffy, N. Gokce, M. Holbrook et al., "Effect of ascorbic acid treatment on conduit vessel endothelial dysfunction in patients with hypertension," *American Journal of Physiology*, vol. 280, no. 2, pp. H528–H534, 2001.
 - [19] M. Boshtam, M. Rafiei, K. Sadeghi, and N. Sarraf-Zadegan, "Vitamin E can reduce blood pressure in mild hypertensives," *International Journal for Vitamin and Nutrition Research*, vol. 72, no. 5, pp. 309–314, 2002.
 - [20] N. Tian, K. D. Thrasher, P. D. Gundy, M. D. Hughson, and R. D. Jr Manning, "Antioxidant treatment prevents renal damage and dysfunction and reduces arterial pressure in salt-sensitivity hypertension," *Hypertension*, vol. 45, no. 5, pp. 934–939, 2005.
 - [21] P. Trinder, "Determination of blood glucose in blood using glucose oxidase with an alternative oxygen acceptor," *Annals of Clinical Biochemistry*, vol. 6, pp. 24–25, 1969.
 - [22] C. C. Allain, L. S. Poon, and C. S. G. Chan, "Enzymatic determination of total serum cholesterol," *Clinical Chemistry*, vol. 20, no. 4, pp. 470–475, 1974.
 - [23] N. W. Tietz, "Serum triglyceride determination," in *Clinical Guide to Laboratory Tests*, pp. 554–556, W.B. Saunders, Philadelphia, Pa, USA, 2nd edition, 1990.
 - [24] M. Burstein, H. R. Scholnick, and R. Morfin, "Rapid method for the isolation of lipoproteins from human serum by precipitation with polyanions," *Journal of Lipid Research*, vol. 11, no. 6, pp. 583–595, 1970.
 - [25] W. T. Friedewald, R. I. Levy, and D. S. Fredrickson, "Estimation of the concentration of low-density lipoprotein cholesterol in plasma, without use of the preparative ultracentrifuge," *Clinical Chemistry*, vol. 18, no. 6, pp. 499–502, 1972.
 - [26] R. D. Abbott, P. W. F. Wilson, W. B. Kannel, and W. P. Castelli, "High density lipoprotein cholesterol, total cholesterol screening, and myocardial infarction. The Framingham Study," *Arteriosclerosis*, vol. 8, no. 3, pp. 207–211, 1988.
 - [27] D. Koracevic, G. Koracevic, V. Djordjevic, S. Andrejevic, and V. Cosic, "Method for the measurement of antioxidant activity in human fluids," *Journal of Clinical Pathology*, vol. 54, no. 5, pp. 356–361, 2001.
 - [28] W. G. Niehaus and B. Samuelsson, "Formation of malonaldehyde from phospholipid arachidonate during microsomal lipid peroxidation," *European Journal of Biochemistry*, vol. 6, no. 1, pp. 126–130, 1968.
 - [29] D. R. Matthews, J. P. Hosker, and A. S. Rudenski, "Homeostasis model assessment: insulin resistance and β -cell function from fasting plasma glucose and insulin concentrations in man," *Diabetologia*, vol. 28, no. 7, pp. 412–419, 1985.
 - [30] S. Kadiri, "Tackling cardiovascular disease in Africa," *British Medical Journal*, vol. 331, no. 7519, pp. 711–712, 2005.
 - [31] T. Ogihara, T. Asano, K. Ando et al., "High-salt diet enhances insulin signaling and induces insulin resistance in Dahl salt-sensitive rats," *Hypertension*, vol. 40, no. 1, pp. 83–89, 2002.
 - [32] B. M. S. Matthew, "Phenotypic expression of hypertension in rodent models through dietary manipulation," *Research diets*, pp. 1–3, 2008.
 - [33] P. Meneton, X. Jeunemaitre, H. E. De Wardener, and G. A. Macgregor, "Links between dietary salt intake, renal salt handling, blood pressure, and cardiovascular diseases," *Physiological Reviews*, vol. 85, no. 2, pp. 679–715, 2005.
 - [34] H. Kobori, A. Nishiyama, Y. Abe, and L. G. Navar, "Enhancement of intrarenal angiotensinogen in Dahl salt-sensitive rats on high salt diet," *Hypertension*, vol. 41, no. 3 I, pp. 592–597, 2003.
 - [35] S. Kagota, A. Tamashiro, Y. Yamaguchi et al., "Downregulation of vascular soluble guanylate cyclase induced by high salt intake in spontaneously hypertensive rats," *British Journal of Pharmacology*, vol. 134, no. 4, pp. 737–744, 2001.
 - [36] O. S. Adeniyi and A. A. Fasanmade, "Effect of dietary zinc supplementation on salt induced hypertension in rats," *International Journal of Pharmacology*, vol. 2, no. 5, pp. 485–491, 2006.

- [37] N. K. Lakshmana, J. Deepthi, Y. N. Rao, and K. M. Deedi, "Study of lipid profile, serum magnesium and blood glucose in hypertension," *Biology and Medicine*, vol. 2, no. 1, pp. 6–16, 2010.
- [38] U. K. Biswas and A. Kumar, "A study on lipid profile, oxidation stress and carbonic anhydrase activity in patients with essential hypertension," *Journal of Clinical and Diagnostic Research*, vol. 4, no. 6, pp. 3414–3420, 2010.

Research Article

Protective Effects of Aspirin from Cardiac Hypertrophy and Oxidative Stress in Cardiomyopathic Hamsters

Rong Wu,¹ David Yin,¹ Nataliya Sadekova,¹ Christian F. Deschepper,² Jacques de Champlain,¹ and Helene Girouard¹

¹ Department of Pharmacology, Faculty of Medicine, Université de Montréal, Pavillon Roger-Gaudry, 2900 Edouard Montpetit, Montréal QC, Canada H3T 1J4

² Clinical Research Institute of Montreal (CRIM), 110 Pine Ave. West, Montréal QC, Canada H2W 1R7

Correspondence should be addressed to Helene Girouard, helene.girouard@umontreal.ca

Received 10 April 2012; Revised 31 May 2012; Accepted 1 June 2012

Academic Editor: Adrian Manea

Copyright © 2012 Rong Wu et al. This is an open access article distributed under the Creative Commons Attribution License, which permits unrestricted use, distribution, and reproduction in any medium, provided the original work is properly cited.

Objective. To evaluate the capacity of chronic ASA therapy to prevent cardiac alterations and increased oxidative stress in cardiomyopathic hamsters. **Methods and Results.** Male Syrian cardiomyopathic and age-matched inbred control hamsters received ASA orally from the age of 60 days. Animals were sacrificed at the age of 150, 250, and 350 days to evaluate the time course of cardiac hypertrophy and cardiovascular tissue superoxide anion (O_2^-) production. At the age of 150 days, the ventricular weight over body weight ratio, resting heart rate, and cardiovascular O_2^- production were much higher in cardiomyopathic hamsters than those in control. At the age of 250 days, in addition to the continual deterioration of these parameters with age, the blood pressure started to fall and the signs of heart failure appeared. In these cardiomyopathic hamsters, chronic ASA treatment (a) completely prevented elevated O_2^- production and the NAD(P)H oxidase activity, (b) significantly slowed down the development of the cardiac hypertrophy and fibrosis. **Conclusions.** Chronic ASA treatment significantly prevents the deterioration of cardiac function and structure as well as the increased oxidative stress in the cardiomyopathic hamster. Our findings suggest that ASA presents a therapeutic potential to prevent cardiac dysfunction.

1. Introduction

The Syrian golden hamster of the cardiomyopathic strain is a model of hereditary cardiomyopathy that mimics the gradual progression of congestive heart failure in humans [1]. This animal model has a progressive nonpressure overload cardiac disease originated from a genetically transmitted metabolic anomaly that induces degenerative lesions in all striated muscles with particular consistency and intensity in the heart [2]. This type of cardiomyopathy is characterized by ventricular hypertrophy which progresses into dilated congestive heart failure in the later stages of the disease. The pathologic development can be divided into four temporal phases: pre-necrotic (25–30 days), necrotic (70–75 days), hypertrophic (125–150 days) with progressing dilatation (225–250 days), and severe heart failure (325–350 days) [1].

The physiopathology of the disease state is not fully understood, but previous studies have shown an overactivated renin-angiotensin system which is characterized by higher plasma and ventricular angiotensin II concentrations [3], higher ventricular angiotensin converting enzyme (ACE) activity [4], and an upregulation of cardiac angiotensin II AT1 receptor in the cardiomyopathic hamsters [5]. Administration of ACE inhibitors such as quinapril [4] or captopril [6] preserves contractile function and/or increases survival rate in these animals.

Previous data suggest that the vascular renin-angiotensin system and the oxidative stress play a critical role in the generation of cardiomyopathies and heart failure [7]. Ang II has been shown to increase the cardiovascular tissue NAD(P)H oxidase activity and to stimulate the cardiovascular O_2^- production [8]. This oxidative mechanism is thought to play an important role in Ang-II-mediated trophic cardiovascular

changes such as cardiovascular tissue hypertrophy and in hypertension [9].

Aspirin (acetylsalicylic acid (ASA)) is an anti-inflammatory and cardiovascular protective drug with potent inhibitory properties on cyclo-oxygenases which are responsible for the arachidonic acid metabolism and prostaglandin production. Although ASA has no direct effect on cardiovascular function, this drug has been reported to provide effective beneficial protection against many cardiovascular pathological conditions such as atherosclerosis, ischemic heart diseases, and myocardial infarction. Our previous studies have demonstrated that ASA is a potent antioxidative agent which markedly reduced the vascular O_2^- production by reducing the vascular NAD(P)H oxidase activity in normal and hypertensive rats [10]. Thus, our hypothesis is that ASA, by inhibiting NAD(P)H oxidase activity, prevents cardiovascular structural and functional alterations in the cardiomyopathic hamster.

The aims of this study are to evaluate the cardioprotective and antioxidant effects of chronic administration of ASA during the development of cardiac structural and functional alterations in the cardiomyopathic hamster.

2. Methods

2.1. Animals. Studies were performed on 36 male cardiomyopathic hamsters (CM, CHF 146) and an equivalent number of their age-matched male Syrian inbred control (Cntrl, CHF148) purchased from the Canadian Hybrid Farm (NS, Canada). The animals were housed individually in a temperature-controlled room with a 6:00 am to 6:00 pm light-dark cycle. Each type of animals was separated into placebo and ASA-treated groups. The ASA treatment started at the age of 60 days and continued until the end of the experiment (except when specified otherwise). The animals were given free access to drinking water. For the placebo groups, their drinking water was free of any drug, whereas aspirin was added in the drinking water of treated hamsters. The concentration of aspirin in drinking water was adjusted upon each animal's drinking volume to ensure a treatment dose of 100 mg/kg/day. Six hamsters from each group were sacrificed at the age of 150 days, 250 days and 350 days.

The blood pressure and heart rate were measured with the femoral artery cannulation method under general anaesthesia with a mixture of ketamine/xylazine (90/5 mg/kg i.m.) just before the animal decapitation. The catheter was connected to a pressure transducer (MX860, Medex Inc. Carlsbad, CA) for continuous recording of arterial blood pressure and pulse rate for more than 10 mins via a patient monitor (model 206EL, Protocol Systems, Inc., Beaverton, OR). The heart and thoracic aorta were then quickly excised and immersed in ice-cold Krebs-Hepes buffer solution containing (mmol/L): NaCl 99.01, KCl 4.69, CaCl₂ 1.87, MgSO₄ 1.20, K₂HPO₄ 1.03, NaHCO₃ 25.0, Na-Hepes 20.0, glucose 11.1 (saturated with 95% O₂ and 5% CO₂, pH 7.40). After the heart was washed and dissected, the ventricle was weighed and the aortic periadventitial tissue was carefully removed. The part of the cardiac apex was

cut into 0.5 mm thick and roughly 10 mg slices while the aorta was cut into 2 mm ring segments for O₂ measurement. The rest of cardiac and aortic tissues were frozen in liquid nitrogen and kept at -80°C until assayed.

In a preliminary study, eight 250-day-old CM hamsters were treated with placebo or ASA (100 mg/kg/day) for 7 days. Compared with placebo-treated group, the ASA treatment did not modify any cardiovascular parameters (ventricle/body weight ratio, heart rate, or blood pressure). However a reduction of ventricular and aortic O_2^- production was observed (data not shown).

All experimental procedures were performed in accordance with the guidelines of the Canadian Council for Animal Care and monitored by an institutional care committee.

2.2. Superoxide Anion Measurement. The superoxide anion (O_2^-) production was measured using the lucigenin-enhanced chemiluminescence method as described previously [11]. Briefly, after 10 min equilibration in Krebs-Hepes buffer at room temperature, the aortic ring or the myocardial slice was transferred to a scintillation vial containing 5 $\mu\text{mol/L}$ lucigenin to determine the basal O_2^- level. The chemiluminescence was recorded every minute for 15 minutes by a liquid scintillation counter (Wallac 1409, Turku, Finland) switched to the out-of-coincidence mode. At the end of the count, the fresh cardiac tissue and aortic ring were weighed. The data were expressed as cpm per mg tissue.

To evaluate the intrinsic NAD(P)H oxidase activity, an NAD(P)H oxidase inhibitor, diphenyleneiodonium (DPI, 100 $\mu\text{mol/L}$) was used to determine DPI-inhibitable production of O_2^- . Aortic rings or cardiac slices were incubated first with DPI for 10 min at room temperature before O_2^- production was evaluated. DPI-inhibitable production of O_2^- was calculated as the difference in production of O_2^- observed in the presence and in the absence of DPI.

2.3. NAD(P)H Oxidase Subunit p47phox Western Blot Analysis. Frozen ventricular tissue was crushed in liquid nitrogen. Lyses and Western blots were performed as described previously [12] with 20 μg of proteins loaded on gels. Proteins were separated (Mini Gel Protean II System, Bio-Rad) and then transferred electrophoretically to nitrocellulose paper at 70 V for 90 min. After transfer, the membranes were washed twice and then incubated in PBS containing 5% dehydrated milk at room temperature for 2 h. The blots were then incubated with specific antibody against p47phox (H195, sc-14015, Santa Cruz Biotechnology) with a 1/2000 dilution. The antibody-antigen complexes were detected by second antibody (goat anti-rabbit IgG-HRP, 1: 4000, Santa Cruz Biotechnology). Membranes were exposed to Kodak X-Omat blue films (Kodak, Rochester, NY, USA) for 2 min. The gels were scanned and the densitometry of the bands was assessed using Scion image 4.0.2 (Scion Corporation, Frederick, MD, USA). Results for each condition were divided by the values of normal inbred hamsters without aspirin treatment to estimate the relative magnitude of changes. The β -actin (42 kDa) was used as our loading control for p47phox

expression experiments. All reagents used in buffer solution were purchased from Sigma Chemical Co.

2.4. Ventricular Fibrosis. Hearts were fixed in formalin for 24 h. Two cross-sections of the heart were obtained at 1-mm intervals midway between the base and the apex of the heart. Ventricular fibrosis was determined from the tissues obtained from the two cross sections. These tissues were dehydrated and embedded in paraffin, and 4 μ m sections were cut. A representative section from the two cross-sections of each heart was stained with picrosirius red. These sections were mounted on a slide for projection to a magnification of 20x. A digital image of the entire section was obtained using computer software (Aperio Technologies, CA, USA). The extent of fibrosis in the myocardium was assessed using the positive pixel count algorithm as the area of collagen staining which was expressed as a percentage of the total myocardial tissue area.

2.5. Data Analysis. Data are expressed as mean \pm SEM. Statistical comparisons were made by one-way ANOVA followed by Tukey test for multivariance. The critical level of significance was set at $P < 0.05$.

3. Results

3.1. Body Weight and Cardiac Hypertrophy. Compared with inbred control hamsters, the body weight of the CM hamsters was significantly lower in all age groups (Figure 1(a)). The body weight of both strains (control and CM hamsters) remained stable during the study period and was not modified by ASA treatment.

Cardiac hypertrophy was evaluated by measuring the ratio of cardiac ventricular weight over body weight at the ages of 150, 250, and 350 days (Figure 1(b)). The ventricle/body weight ratio remained low and stable in the inbred control animals during the whole study period. This ratio progressively increased with age in CM hamsters from the initial value of 3.41 ± 0.06 at 150 days to 3.63 ± 0.01 at 250 days and 4.07 ± 0.10 at 350 days ($P < 0.01$ each compared with its previous data). ASA treatment reduced this ventricle/body weight ratio since age of 150 days and then partially prevented the increase of this ratio with age in CM hamsters (Figure 1(b)). ASA treatment did not show any effect on the ventricle/body weight ratio in inbred control hamsters.

3.2. Heart Rate and Blood Pressure. Heart rate (HR) was stable in inbred control hamsters during the whole study period (HR varied from 199 to 214 with an average of 205 ± 5 beat/min), while the HR was higher in CM hamster than the one of their age-matched inbred control animals since the age of 150 days (210 ± 6 beat/min) and reached to even a higher level at age of 350 days (241 ± 4 beat/min) ($P < 0.01$ versus Control) (Figure 2(a)). ASA treatment slowed down significantly HR increase in CM hamsters. Nevertheless, administration of ASA did not show any modification of the HR in the inbred control animals.

The systolic (SBP) and diastolic (DBP) blood pressure were similar between control and CM hamsters at the age of 150 days (control $123/82$ versus CM $120/79$ mmHg). Thereafter, these pressures continually decreased with age to a SBP of 110 ± 5 and 82 ± 3 mmHg and DBP of 75 ± 3 and 56 ± 4 mmHg in 250- and 350-day-old CM hamsters, respectively, which were significantly lower than those of age-matched control ($P < 0.01$). Meanwhile, the blood pressures remained stable in inbred control animals. ASA treatment significantly prevented blood pressure lowering in CM hamsters without modifying blood pressures in age-matched inbred control hamsters (Figure 2(b)).

Starting at the age of 250 days, the CM hamsters began to show some signs of heart failure such as reduced food intake, oedema, and ascites (data not shown).

3.3. Ventricular Fibrosis. The extent of fibrosis in ventricular tissues was assessed in 350-day-old control and CM hamsters treated either with placebo or ASA. The percentage of the tissue occupied by fibrosis was much higher in CM group ($16.5 \pm 1.4\%$) when compared with the control ($5.1 \pm 0.8\%$, $P < 0.01$, Figure 3). This high level of fibrosis in CM hamsters was reduced by 35% ($P < 0.01$ versus placebo-treated CM) after ASA treatment, but no change was observed in ASA-treated control group.

3.4. Ventricular and Aortic Superoxide Anion Production. The cardiac ventricular and aortic tissue O_2^- production was evaluated in inbred control and CM hamster at the ages of 150, 250, and 350 days. Ventricular O_2^- production was higher in CM hamster than in their age-matched control. This high level of O_2^- production increased continually with age in CM group from a basal level of 243 ± 16 cpm/mg tissue at the age of 150 days to 299 ± 19 cpm/mg tissue at the age of 350 days, while the O_2^- level remained low and stable in the control group (Figure 4(a)). ASA treatment normalized the elevated ventricular O_2^- production in all age groups of CM hamsters ($P < 0.01$ versus age-matched placebo-treated CM), but only slightly reduced the O_2^- production in all age groups of inbred control animals.

Similar results were observed about the aortic O_2^- production (Figure 4(b)). The aortic O_2^- production was 727 ± 55 , 749 ± 17 , and 741 ± 38 cpm/mg tissue in 150-, 250- and 350-day-old control animals, respectively. Compared with the controls, the aortic O_2^- production was elevated by 20%, 26%, and 31% ($P < 0.01$) in the age-matched CM hamsters. ASA treatment completely normalized this elevated O_2^- production level to 692 ± 28 , 742 ± 38 , and 755 ± 29 cpm/mg tissue in the 3 age groups of CM hamsters ($P < 0.01$ versus placebo-treated CM). However, ASA treatment did not show significant effect in the inbred control groups.

3.5. NAD(P)H Oxidase Activity and Expression of Cardiac NAD(P)H Oxidase Subunit p47phox. The NAD(P)H oxidase activity was estimated by DPI-inhibitable production of O_2^- anion in ventricular and aortic tissues from 350-day-old control and CM hamsters. The DPI-inhibitable O_2^- production was significantly increased in ventricular and

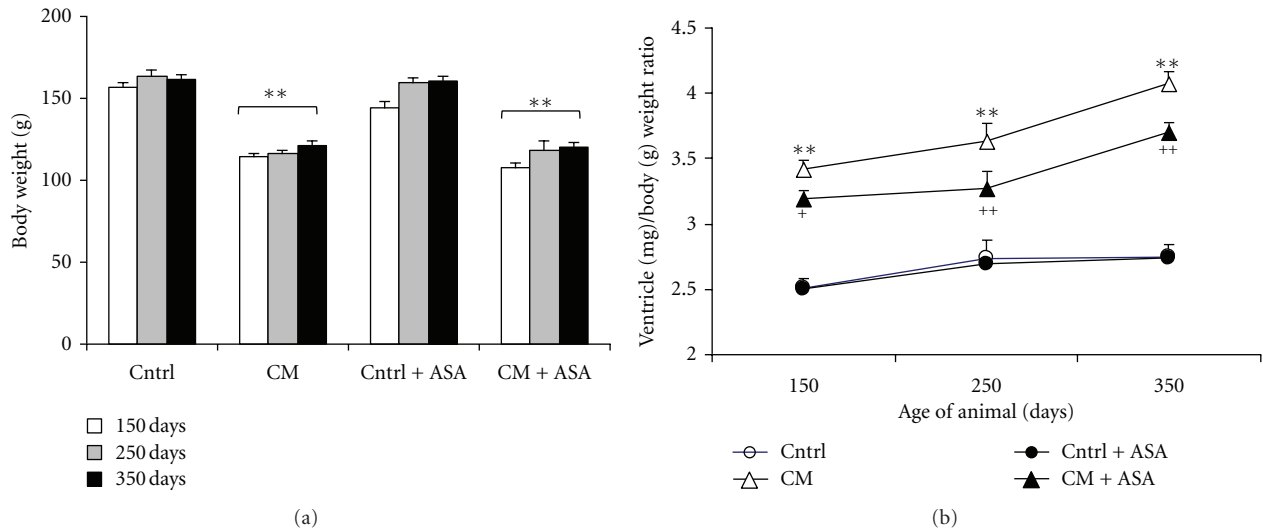


FIGURE 1: Time course of body weight (a) and the cardiac ventricular weight (mg)/body weight (g) ratio (b) in control (Cntrl) and cardiomyopathic (CM) hamster treated with placebo or 100 mg/kg/day acetylsalicylic acid (+ASA). ** $P < 0.01$ versus control, + $P < 0.05$, ++ $P < 0.01$ versus CM hamsters.

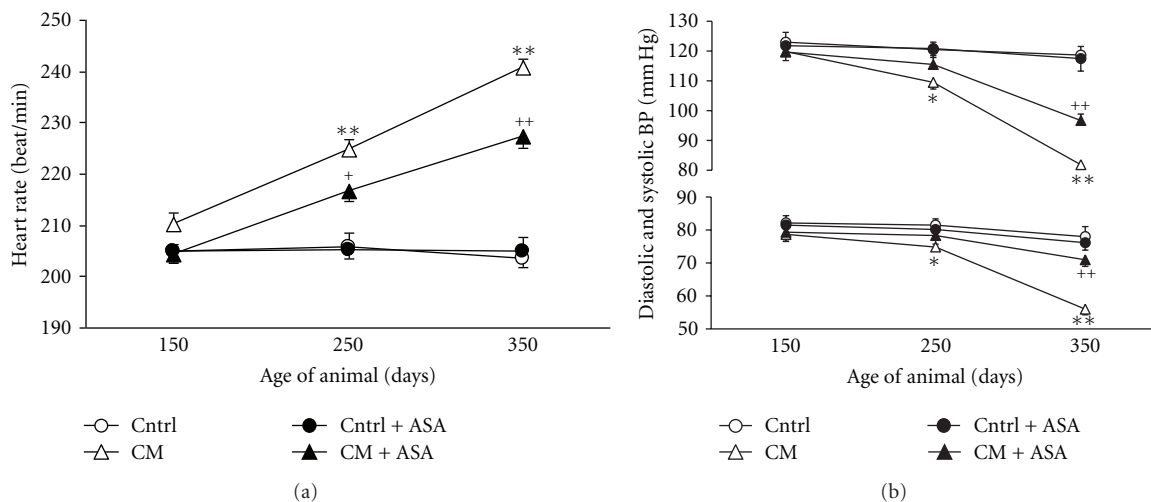


FIGURE 2: Selected hemodynamic parameters at the ages of 150, 250, and 350 days. (a) Heart rate in control (Cntrl) and cardiomyopathic (CM) hamsters with (+ASA) or without ASA treatment. (b) Systolic and diastolic blood pressure in the same animals. * $P < 0.05$, ** $P < 0.01$ versus control, ++ $P < 0.01$ versus placebo-treated CM hamsters.

aortic tissues of CM hamsters by 47 and 32% compared to the normal values of 130 ± 14 and 497 ± 25 cpm/mg tissue obtained in the same tissues from inbred control animals (Figures 5(a) and 5(b)). ASA treatment normalized these elevated ventricular and aortic DPI-inhibitable productions of O_2^- in CM hamsters, but did not affect the O_2^- production in inbred control animals.

The expression of cardiac tissue NAD(P)H oxidase subunit p47 was measured in 350-day-old control and CM hamsters by Western blot method. The ratio of the expression of p47phox in CM over their inbred controls was 1.18 ± 0.04 in CM group ($P < 0.01$). ASA treatment reduced this elevated ratio of expression to near control level ($P < 0.05$) (Figure 6).

4. Discussion

In the present study, the cardiomyopathy progressed with age in the CM hamsters. At the age of 150 days, the cardiac function was still in a compensatory stage presenting only cardiac hypertrophy and tachycardia. Thereafter, the SBP and DBP started to fall with age and signs of heart failure such as reduction of food intake, oedema, and ascites began to appear. These age-related cardiac damages are consistent with previous reports [1, 13]. Meanwhile, the cardiovascular tissue O_2^- production was significantly elevated in the CM hamsters with an increased NAD(P)H oxidase activity and expression of the subunit p47phox of NAD(P)H oxidase.

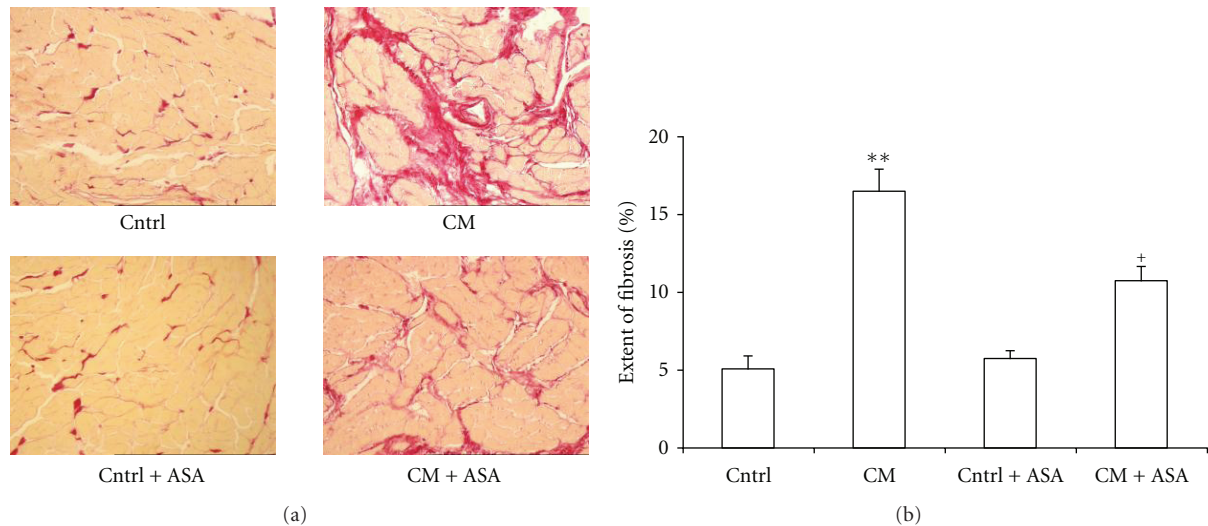


FIGURE 3: (a) Representative cross-sectional tissue slices of hearts stained with picrosirius red show minimal fibrosis in control (Cntrl) and importantly increased fibrosis in 350-day-old cardiomyopathic hearts (CM). ASA treatment significantly reduced the cardiomyotic fibrosis in the CM hamsters (CM + ASA), but did not show any effect on control (Cntrl + ASA), (b) Percentage of the tissue occupied by fibrosis in whole ventricular section of 350-day-old untreated or ASA-treated control or cardiomyopathic hamsters. ** $P < 0.01$ versus control, ⁺ $P < 0.05$ versus CM hamsters.

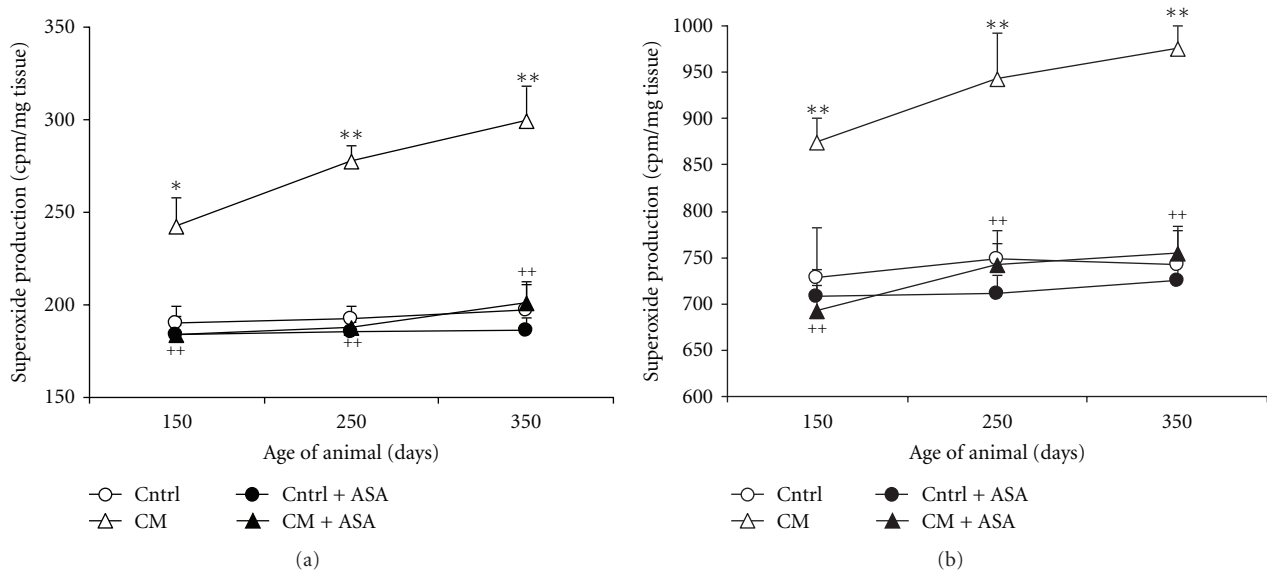


FIGURE 4: Time course of ventricular (a) and aortic (b) production of O_2^- in control (Cntrl) and cardiomyopathic (CM) hamsters with (+ASA) or without acetylsalicylic acid treatment. * $P < 0.05$, ** $P < 0.01$ versus control, ⁺⁺ $P < 0.01$ CM + ASA versus CM hamsters.

An important finding from the present study is that chronic ASA treatment significantly slowed down the development of cardiac hypertrophy by reducing ventricle/body weight ratio and the extent of ventricular fibrosis in Syrian CM hamster. Moreover, ASA treatment prevented HR increase as well as blood pressure decrease suggesting improvement of both chronotropic and inotropic cardiac functions. Consistent with our previous report [10], ASA treatment demonstrated a potent antioxidative effect in the present animal model by completely normalizing the elevated cardiac and aortic tissue O_2^- production in CM

hamsters. The DPI-inhibitable O_2^- production and the expression of the subunit p47phox of NAD(P)H oxidase were both reduced by ASA treatment suggesting that the antioxidative effect of ASA is probably mainly mediated by reduction of the NAD(P)H oxidase activity and expression. Our results also indicated that the DPI-inhibitable O_2^- production significantly contributes to the total cardiovascular tissue O_2^- production. Nevertheless, DPI is not a specific inhibitor of NADPH oxidase as it could also inhibit the NO synthase and cytochrome P450. These two enzymes could potentially modify the level of superoxide and other

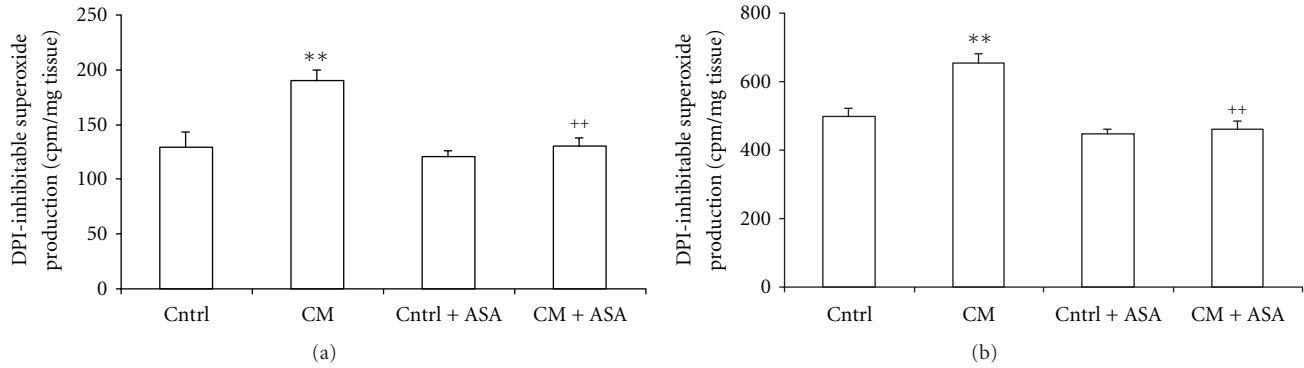


FIGURE 5: Diphenyleneiodonium (DPI)-inhibitable O_2^- production in ventricular slices (a) or aortic rings (b) from control (Cntrl) and cardiomyopathic (CM) hamsters treated with placebo or acetylsalicylic acid (+ASA). ** $P < 0.01$ versus control, ++ $P < 0.01$ versus CM hamsters.

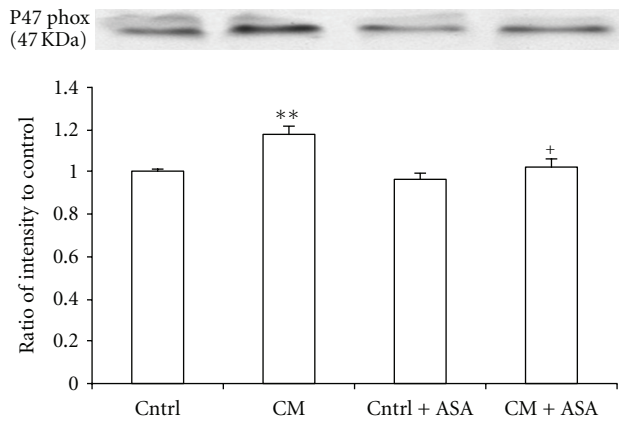


FIGURE 6: The ratio of cardiac tissue NAD(P)H oxidase subunit p47phox expression over their control determined by Western blot in cardiomyopathic (CM) hamsters treated with placebo or 100 mg/kg/day acetylsalicylic acid (+ASA). ** $P < 0.01$ versus control, + $P < 0.05$ versus CM hamsters.

reactive oxygen species by changing the NO level or on the P450-related metabolism. These nonspecific effects of DPI could result in an imprecise estimation of the contribution of NADPH oxidase to the oxidative stress with the use of the DPI-inhibitable superoxide production only. However, the increased expression of p47phox strongly suggests an increased NADPH oxidase activity.

The pathophysiology of the cardiomyopathy in the Syrian hamster appears to be multifactorial [7]. Overactivation of the renin-angiotensin II system has been reported in this CM model, in which a high level of angiotensin converting enzyme activity and AT1 receptors in the cardiovascular tissues was observed at an early age [4, 5]. These upregulations could lead to dysfunction of coronary vasculature, promoting vasospasms and transient ischemia. The latter was assumed to lead the early phase of myocardial necrosis and myolysis [14]. Increasing evidence indicates that activation of angiotensin II system can increase cardiovascular tissue O_2^- production and oxidative stress through the NAD(P)H oxidase pathway [8, 15]. It is well known that

oxidative-stress-mediated cardiac injury is implicated in the pathophysiology and development of cardiomyopathy and heart failure through inducing cellular injury and apoptosis, depressing myocardial contractility, and damaging coronary endothelial function, and myocardial blood supply [7, 16].

ASA has been reported to provide effective beneficial protection against many cardiovascular pathological conditions, such as atherosclerosis, ischemic heart diseases, and myocardial infarction. Our previous studies have demonstrated that ASA is a potent antioxidative agent that remarkably reduced O_2^- production in cardiovascular tissues and prevented the development of hypertension, vascular hypertrophy, insulin resistance in numerous pathologic conditions including SHR, chronically glucose-fed rats, and Ang II infusion-induced hypertension models [17, 18]. Moreover, ASA treatment abolished chronic Ang II infusion-induced oxidative stress, cardiac hypertrophy and hypertension in rats. It is worth noticing that ASA does not have any effect on cardiac functions such as contractility, heart rate and hypertrophy in healthy animals. Indeed, acute ASA administration did not show any effect on cardiovascular function or O_2^- production [10]. Our previous studies have demonstrated that all those beneficial cardiovascular effects of ASA are preventive and require long-term treatment. In the present study, short term ASA treatment (1 week) did not ameliorate cardiovascular functions or reduce cardiac hypertrophy in CM hamsters. Based on all these elements, we presume that the protective cardiovascular effects of ASA on the CM hamsters are indirect and probably mediated by its antioxidative properties. Our previous results also indicated that the antioxidative and cardiovascular protective properties of ASA were probably mediated by its effect on COX-2 and were not shared by other anti-inflammatory drugs with non-selective COX inhibitory property such as ibuprofen, indomethacin or salicylic acid [19].

In the present study, only early started (at age of 60 days) long-term ASA treatment slowed down the cardiac hypertrophic development and partially prevented the deterioration of the cardiac function. During this early age, the pathology changes in CM hamsters are characterised by coronary spasm, cardiac micronecrosis, and absence of any

sign of cardiac function damage [20]. At that moment, the antioxidative property of ASA could protect and improve the endothelial function, reduce the vasospasm and cardiac ischemia, and prevent the micronecrosis, which slow down the cardiac hypertrophy and heart failure development.

The pathophysiology of the cardiomyopathy in the Syrian hamster is not well understood. Our results demonstrate that long-term ASA treatment can slow down the deterioration of cardiac functions suggesting that oxidative stress might play an important role in the development of heart failure in this CM model. However, although ASA treatment normalizes the cardiovascular O_2^- production and NADPH oxidase activity, it can only partially prevent the deterioration of the cardiac functions. These results suggest that some oxidative stress-independent mechanism might be involved in the disease development.

It is worth to notice that the body weight of CM hamsters was significantly lower than that of control animal in the present study. This could result in an overestimation of the cardiac hypertrophy in CM hamsters. However, the ventricle/body weight ratios clearly demonstrate the development of hypertrophy over time as well as the protective effect of ASA which does not have any effect on body weight.

In conclusion, the long-term ASA treatment significantly prevents cardiac structure and function alterations in the CM hamster. It seems that the preventive effects of ASA are mediated by its antioxidative properties. Thus, our findings suggest a potentially beneficial therapeutic use of ASA in treatment of heart failure.

Acknowledgments

The authors would like to express their gratitude to Diane Papin and Sylvie Picard for their technical expertise as well as to Dr. Chantal Lambert for her helpful comments. This study was supported by funds from the Canadian Institutes in Health Research (CIHR) grants to J. Champlain and H. Girouard and the Canada Foundation for Innovation (CFI) to H. Girouard. J. Champlain was the holder of a J. C. Edwards career investigatorship. H. Girouard was the holder of an operating grants from the Fonds de Recherche en Santé du Québec (FRSQ), Natural Science and Engineering Research Council of Canada (NSERC), and a new investigator award from the FRSQ and the HSFC.

References

- [1] E. G. Hunter, V. Hughes, and J. White, "Cardiomyopathic hamsters, CHF 146 and CHF 147: a preliminary study," *Canadian Journal of Physiology and Pharmacology*, vol. 62, no. 11, pp. 1423–1428, 1984.
- [2] D. Chemla, E. Scalbert, P. Desche, and Y. Lecarpentier, "Cardiomyopathy in the Syrian hamster. Physiological and therapeutic aspects," *Archives des Maladies du Cœur et des Vaisseaux*, vol. 84, no. 4, pp. 85–87, 1991.
- [3] F. Nakamura, M. Nagano, R. Kobayashi et al., "Chronic administration of angiotensin II receptor antagonist, TCV-116, in cardiomyopathic hamsters," *American Journal of Physiology*, vol. 267, no. 6, pp. H2297–H2304, 1994.
- [4] S. J. Haleen, R. E. Weishaar, R. W. Overhiser et al., "Effects of quinapril, a new angiotensin converting enzyme inhibitor, on left ventricular failure and survival in the cardiomyopathic hamster. Hemodynamic, morphological, and biochemical correlates," *Circulation Research*, vol. 68, no. 5, pp. 1302–1312, 1991.
- [5] C. Lambert, Y. Massillon, and S. Meloche, "Upregulation of cardiac angiotensin II AT1 receptors in congenital cardiomyopathic hamsters," *Circulation Research*, vol. 77, no. 5, pp. 1001–1007, 1995.
- [6] H. Hirakata, F. M. Fouad-Tarazi, F. M. Bumpus et al., "Angiotensins and the failing heart. Enhanced positive inotropic response to angiotensin I in cardiomyopathic hamster heart in the presence of captopril," *Circulation Research*, vol. 66, no. 4, pp. 891–899, 1990.
- [7] N. Escobales and M. J. Crespo, "Early pathophysiological alterations in experimental cardiomyopathy: the Syrian cardiomyopathic hamster," *Puerto Rico Health Sciences Journal*, vol. 27, no. 4, pp. 307–314, 2008.
- [8] K. K. Griendling, C. A. Minieri, J. D. Ollerenshaw, and R. W. Alexander, "Angiotensin II stimulates NADH and NADPH oxidase activity in cultured vascular smooth muscle cells," *Circulation Research*, vol. 74, no. 6, pp. 1141–1148, 1994.
- [9] J. F. Reckelhoff and J. C. Romero, "Role of oxidative stress in angiotensin-induced hypertension," *American Journal of Physiology*, vol. 284, no. 4, pp. R893–R912, 2003.
- [10] R. Wu, D. Lamontagne, and J. de Champlain, "Antioxidative properties of acetylsalicylic acid on vascular tissues from normotensive and spontaneously hypertensive rats," *Circulation*, vol. 105, no. 3, pp. 387–392, 2002.
- [11] T. Munzel, H. Sayegh, B. A. Freeman, M. M. Tarpey, and D. G. Harrison, "Evidence for enhanced vascular superoxide anion production in nitrate tolerance. A novel mechanism underlying tolerance and cross-tolerance," *Journal of Clinical Investigation*, vol. 95, no. 1, pp. 187–194, 1995.
- [12] K. Matrougui, Y. E. Eskildsen-Helmond, A. Fiebeler et al., "Angiotensin II stimulates extracellular signal-regulated kinase activity in intact pressurized rat mesenteric resistance arteries," *Hypertension*, vol. 36, no. 4, pp. 617–621, 2000.
- [13] N. R. Bastien, A. V. Juneau, J. Ouellette, and C. Lambert, "Chronic AT1 receptor blockade and angiotensin-converting enzyme (ACE) inhibition in (CHF 146) cardiomyopathic hamsters: effects on cardiac hypertrophy and survival," *Cardiovascular Research*, vol. 43, no. 1, pp. 77–85, 1999.
- [14] S. M. Factor, T. Minase, S. Cho, R. Dominitz, and E. H. Sonnenblick, "Microvascular spasm in the cardiomyopathic Syrian hamster: a preventable cause of focal myocardial necrosis," *Circulation*, vol. 66, no. 2, pp. 342–354, 1982.
- [15] H. Hitomi, H. Kiyomoto, and A. Nishiyama, "Angiotensin II and oxidative stress," *Current Opinion in Cardiology*, vol. 22, no. 4, pp. 311–315, 2007.
- [16] M. J. Thomson, M. P. Frenneaux, and J. C. Kaski, "Antioxidant treatment for heart failure: friend or foe?" *QJM*, vol. 102, no. 5, pp. 305–310, 2009.
- [17] A. El Midaoui, R. Wu, and J. de Champlain, "Prevention of hypertension, hyperglycemia and vascular oxidative stress by aspirin treatment in chronically glucose-fed rats," *Journal of Hypertension*, vol. 20, no. 7, pp. 1407–1412, 2002.
- [18] R. Wu, M. A. Laplante, and J. de Champlain, "Prevention of angiotensin II-induced hypertension, cardiovascular hypertrophy and oxidative stress by acetylsalicylic acid in rats," *Journal of Hypertension*, vol. 22, no. 4, pp. 793–801, 2004.
- [19] R. Wu, M. A. Laplante, and J. de Champlain, "Cyclooxygenase-2 inhibitors attenuate angiotensin II-induced oxidative stress,

hypertension, and cardiac hypertrophy in rats," *Hypertension*, vol. 45, no. 6, pp. 1139–1144, 2005.

- [20] N. Escobales and M. J. Crespo, "Angiotensin II-dependent vascular alterations in young cardiomyopathic hamsters: role for oxidative stress," *Vascular Pharmacology*, vol. 44, no. 1, pp. 22–28, 2006.

Review Article

Cell Stress Proteins in Atherothrombosis

**Julio Madrigal-Matute, Roxana Martinez-Pinna,
Carlos Ernesto Fernandez-Garcia, Priscila Ramos-Mozo, Elena Burillo,
Jesus Egido, Luis Miguel Blanco-Colio, and Jose Luis Martin-Ventura**

Vascular Research Laboratory, IIS-Fundación Jiménez Díaz, Universidad Autónoma de Madrid, 28040 Madrid, Spain

Correspondence should be addressed to Julio Madrigal-Matute, jmadrigal@fjd.es

Received 30 March 2012; Accepted 14 May 2012

Academic Editor: Ana Fortuno

Copyright © 2012 Julio Madrigal-Matute et al. This is an open access article distributed under the Creative Commons Attribution License, which permits unrestricted use, distribution, and reproduction in any medium, provided the original work is properly cited.

Cell stress proteins (CSPs) are a large and heterogeneous family of proteins, sharing two main characteristics: their levels and/or location are modified under stress and most of them can exert a chaperon function inside the cells. Nonetheless, they are also involved in the modulation of several mechanisms, both at the intracellular and the extracellular compartments. There are more than 100 proteins belonging to the CSPs family, among them the thioredoxin (TRX) system, which is the focus of the present paper. TRX system is composed of several proteins such as TRX and peroxiredoxin (PRDX), two thiol-containing enzymes that are key players in redox homeostasis due to their ability to scavenge potential harmful reactive oxygen species. In addition to their main role as antioxidants, recent data highlights their function in several processes such as cell signalling, immune inflammatory responses, or apoptosis, all of them key mechanisms involved in atherothrombosis. Moreover, since TRX and PRDX are present in the pathological vascular wall and can be secreted under prooxidative conditions to the circulation, several studies have addressed their role as diagnostic, prognostic, and therapeutic biomarkers of cardiovascular diseases (CVDs).

1. Introduction

The vast majority of the proteins require further assistance for acquiring proper maturation and stability; this process described in the late 80s is facilitated through the activity of a family of proteins called “molecular chaperones” or cell stress proteins (CSPs) [1]. This large and diverse group of proteins composed by more than 20 families of proteins and more than 100 proteins includes the heat shock proteins (HSPs) and the thioredoxin (TRX) system. The role of HSPs in cardiovascular diseases (CVDs) has been thoroughly reviewed [2]. In the present paper, we will focus on the role of the TRX system, specifically TRX and peroxiredoxins (PRDXs), in atherothrombosis. For this purpose, we have followed the PRISMA chart displayed in Supplementary Figure 1 (see Supplementary Figure 1 in supplementary material available online at doi:10.1155/2012/232464).

2. The Thioredoxin System

The TRX system mainly comprises TRX, TRX reductase, TRX interacting protein ((TXNIP), vitamin D3-upregulated

protein-1 ((VDUP)-1) or TRX-binding protein (TRXBP)), and the PRDXs [3]. The TRX system is involved in protein assembly and plays a key role in cellular redox maintenance.

Under physiological conditions, intra- and extracellular reactive oxygen species (ROS) modulate metabolic, signaling, and transcriptional processes within the cell. However, pathological dysregulation of the redox balance could contribute to CVDs [4, 5]. Cellular redox homeostasis is tightly regulated by the coordinated action of NADPH oxidases, the TRX system and glutathione (GSH) [6], among others. The TRX system and GSH are thiol reduction systems with a key role in the defense against excessive ROS production, as well as in the modulation of signaling processes such as inflammation, cellular proliferation, and apoptosis [7–9]. These molecules maintain the intracellular milieu in a reduced state. GSH is used by the GSH peroxidase to reduce peroxides, producing oxidized GSH (GSSG) while GSH reductase reduces this oxidized form to GSH. The antioxidant properties of TRX result from PRDX action, which recycle H_2O_2 through reduction of several hydroperoxides into water and alcohol (Figure 1).

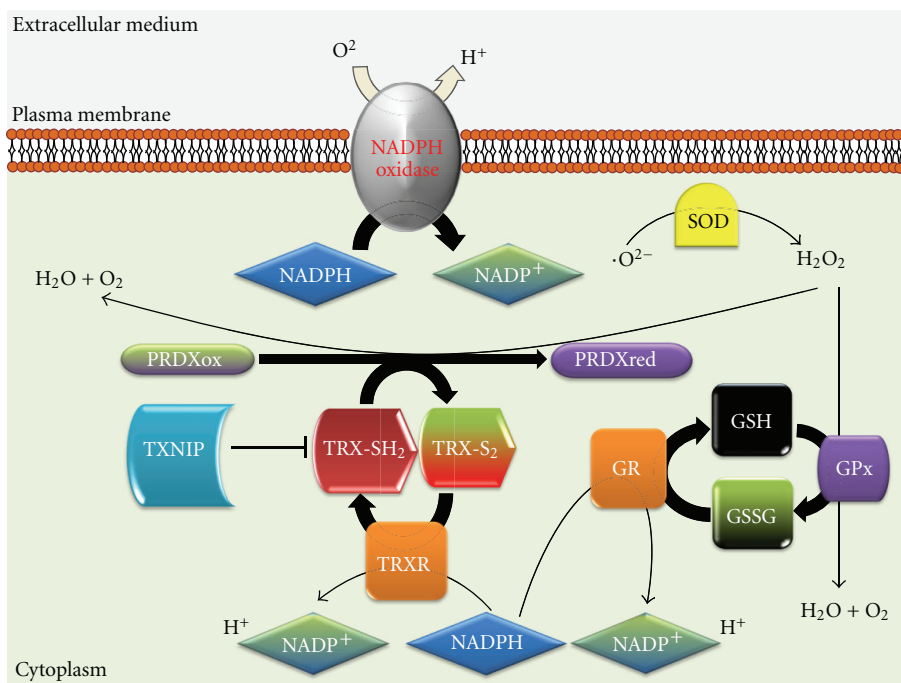


FIGURE 1: Schematic diagram showing the maintenance of the cellular redox homeostasis by the NADPH oxidase, GSH, and the TRX system. PRDXox-oxidized PRDX; PRDXred-reduced PRDX; TRX-S₂-oxidized TRX; TRX-SH₂-reduced TRX; GR-GSH reductase; GPx-GSH peroxidase.

Depending on their cellular location, TRX/PRDX may exert different functions than their known chaperone and antioxidant activities. This process can be described with the so-called “Moonlighting proteins” theory [10]. This idea supports the notion that one gene = one protein = one function is simple and old-fashioned because large number of proteins have two or more functions. This theory might not apply to every protein but it seems to be right for TRX/PRDX. Under certain circumstances, mainly pro-oxidative conditions, TRX and PRDX could be released to the extracellular milieu [11, 12] although their trafficking mechanisms are not yet fully described.

2.1. Intracellular TRX. TRXs are a class of small redox molecules (~12 kDa) present in prokaryotes and eukaryotes and are essential for cellular viability [13]. So far, 3 human TRX variants have been characterized codified by different genes. TRX1 is localized under resting conditions in the cytosol but can be translocated upon stress conditions [14] (e.g., it can be found in an oxidized form in the nucleus of exponential growing cells [15] (Figure 2)), TRX2 is mitochondrial [16, 17], and SpTRX [18] is abundantly expressed in spermatozoa. TRX has a redox active disulfide/dithiol site within 2 conserved Cys residues [19], and it functions as an antioxidant molecule by protecting cells against H₂O₂ [20], regulating heme-oxygenase 1 (HO-1) expression [21], or inducing manganese superoxide dismutase (MnSOD) in the mitochondria [22]. Moreover, it has a protective role against nitric-oxide- (NO-) induced stress, regulating NO synthases activity [23] and through other NO regulating processes [24]. In addition to its role as antioxidant protein, TRX interacts with numerous signaling molecules (including

apoptosis signal-regulating kinase 1 (ASK1) and TXNIP) and transcription factors such as nuclear factor-kappa B (NF-κB) and activating protein 1 (AP-1). TRX function can be regulated by redox modification (e.g., NO increases S-nitrosylation of TRX stimulating TRX activity [25]) or by TXNIP binding [26] (reducing TRX activity), among other mechanisms.

Regarding intracellular TRX *in vivo* functions, as TRX-1 KO mice are lethal, some information has been obtained from studies performed in TRX transgenic (Tg) mice [27]. TRX overexpression in mice protects placenta from oxidative stress and fetal growth by augmenting glucose availability [28], and it also functions as a shelter against apoptosis induced by extensive oxidation in diabetic embryopathy [29] or streptozotocin-induced diabetic osteopenia [30]. Furthermore, TRX is able to protect the lung injury provoked by diesel exhaust particles (DEPs) derived from diesel engine-powered automobiles and industrial machines. This protective role, played through AKT modulation, is reflected in the augmented TRX levels in control cells induced by DEP [31]. Also, mediated by AKT signaling, TRX protects neurons against apoptosis during brain focal ischemia [32].

Thus, the major role of TRX in the redox balance is supported by the numerous data regarding the protection exerted by TRX against excessive oxidative damage in different diseases and the embryonic lethality of KO mice for TRX.

2.2. Intracellular PRDX. PRDXs are a recent discovery among the peroxidases lacking the hemo group. PRDX protein levels are very abundant, around 0.1–1% of total soluble protein in mammals, and they are ubiquitously distributed in all organisms [12, 33]. PRDXs are thiol-specific enzymes

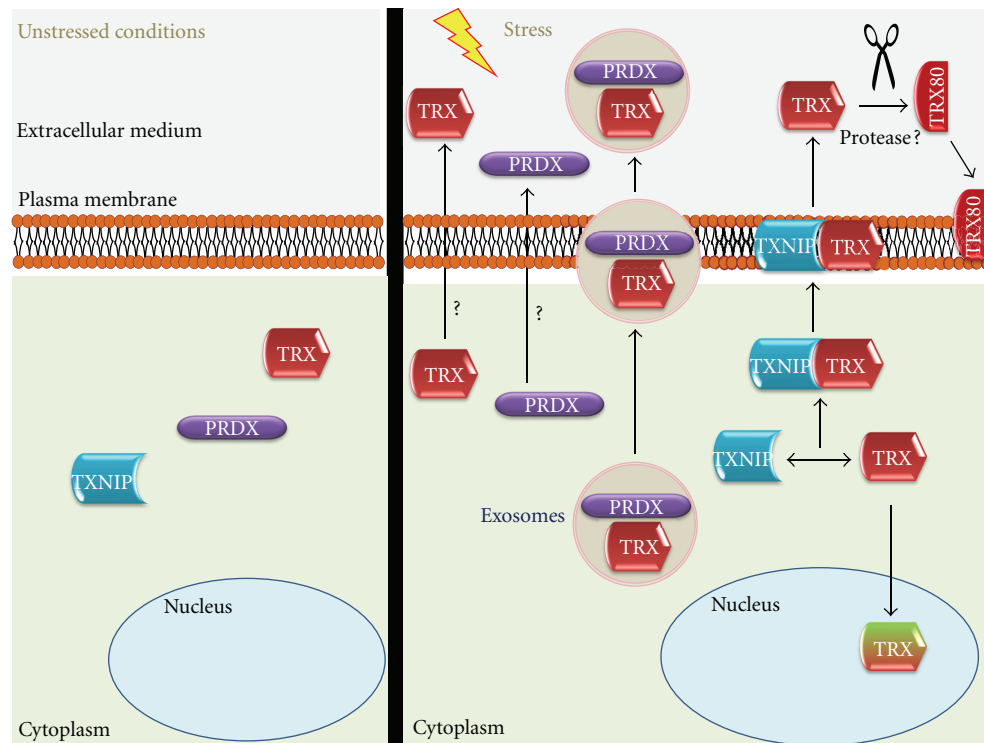


FIGURE 2: Schematic diagram showing PRDX1/TRX main cellular location under nonstress conditions (left), under oxidative stress (right) and trafficking mechanisms (right).

lacking selenium, and they use their active sites to reduce peroxides and scavenge ROS [12]. Mammal cells express 6 PRDX isoforms (PRDX 1–6): 1, 2, and 6 are cytosolic, and 3 and 5 are mitochondrial, while 4 is described as a secretory protein in most tissues [34]. Every isoform contains a conserved Cys residue, which is the primary site for H_2O_2 oxidation, and they can be further classified according to their Cys residues (PRDX1–4 belongs to the 2-Cys subfamily, PRDX5 or atypical 2-Cys and PRDX6 or 1-Cys PRDX) [35].

PRDXs scavenge H_2O_2 more efficiently than other systems such as catalase due to its higher affinity for H_2O_2 [36]. PRDX can modulate NADPH oxidase activity through H_2O_2 inactivation [37]. In addition, PRDX can also reduce peroxynitrites levels through peroxynitrites reductases [38]. Among the mechanisms modifying PRDX functions, several posttranslational modifications have been described, such as nitrosylation [39], glutathionylation [40], phosphorylation, and the hyperoxidation of its active site [41], which stimulates its chaperone activity [42]. For example, under low H_2O_2 concentrations produced in conditions of cellular homeostasis PRDX forms low-molecular-weight oligomers, exerting peroxidase activity. However, under significant changes in H_2O_2 concentration, PRDX experiences structural changes and forms high-molecular-weight oligomers and acquires chaperone activity [43, 44]. Similarly to TRX, PRDX interacts with several proteins (e.g., cyclophilin A, macrophage inhibitory factor, etc.) and can modulate the function of these binding proteins, in a dependent or independent manner of the PRX redox status [35].

Mice lacking PRDX1 are viable with a phenotype characterized by hemolytic anemia caused by an increased ROS

production by red blood cells (RBCs). Furthermore, PRDX1 has tumor suppressor properties as PRDX1 KO mice show an increased rate in malignant tumors as they age, which can be explained by the excessive accumulation of damaged tissue due to extreme ROS production [45]. Similarly to PRDX1 KO mice, targeted disruption of PRDX2 causes cysteine oxidation of several proteins on RBCs membranes, which finally results in augmented levels of denatured protein, cell toxification, and hemolysis [46]. PRDX2 also has been identified as a tumor suppressor gene [47]. Accordingly, PRDX3 (also known as MER5) KO mice are characterized by increased ROS production in macrophages and develop more severe lung injury upon Lipopolisaccharide (LPS) induction, possibly due to an excessive DNA and protein oxidative damage and inflammatory cell infiltration [48]. In fact, it has been calculated that almost 90% of H_2O_2 targets PRDX3 within the mitochondrial matrix, playing a major role in redox signaling in the mitochondria [49], protecting the cells against apoptosis induced by excessive damage to mitochondrial macromolecules [50]. PRDX3 absence is also involved in mitochondrial dysregulation associated with obesity, through increased protein carbonylation and ROS production [51]. It is noteworthy that PRDX3 KO adipocytes accumulate more fat than wild type due to hypertrophy and defects in the levels of enzymes implicated in glucose/lipid metabolism [51]. PRDX4 is mostly a secretory protein, while it is attached to the endoplasmic reticulum (ER) membrane of spermatogenic cells in mature testes. In these cells PRDX4 protects from cell death through its antioxidant properties, nonetheless PRDX4 KO spermatozoa shows normal fertilization [52]. To our knowledge there is no PRDX5 KO strain,

although it has been described that PRDX5 overexpression prevents ROS production and p53-dependent apoptosis [53]. Nevertheless, KO mice for PRDX6, the only 1-Cys member of the peroxiredoxin family, were more vulnerable to ischemic reperfusion injury as shown by increased infarct size and higher amount oxidative stress [54]. In agreement, PRDX6 overexpression functions as a shelter in mouse lungs against toxicity of hyperoxia [55].

On the whole, the plethora of data regarding the different isoforms of PRDX demonstrate that every subunit, independently of its location, is a member of one of the major cellular systems in charge of scavenging prooxidant species and thus in the maintenance of cellular redox status.

2.3. Extracellular TRX. TRX expression can be augmented very fast under stress and is secreted by normal and tumor cells although its secretion does not seem to follow a classical Golgi apparatus pathway [11]. TRX location is regulated by TXNIP binding [26] and facilitates TRX transport from cytoplasm to the membrane under oxidative stress [14]. Another mechanism that can be involved in TRX active secretion is the exosomal pathway. Exosomes are small microparticles released by cells upon activation or apoptosis. These vesicles have been implicated in thrombosis, diabetes, inflammation, atherosclerosis, and vascular cell proliferation [56]. Proteomic studies have described the presence of TRX in exosomes in B cells [57], bladder cancer cells [58], colorectal cancer cells [59], and urine [60] (Figure 2).

There is also a truncated form of TRX that corresponds to the last 80–84 amino acids from the N-terminal end, named TRX80, and it is present in plasma where it was firstly identified as a stimulating factor of eosinophils cytotoxicity [61]. It is possibly a result of protease activity but this process is still unknown (Figure 2). Recombinant TRX80 is a potent mitogenic cytokine for peripheral blood mononuclear cells (PBMCs), an effect not shared by TRX [62]. TRX80 differs from TRX because it forms a dimer lacking reductase activity and its activity is independent of the Cys residues from the TRX active site. The main cellular target for TRX80 are PBMCs in which it induces a Th1 response via IL12 production [63].

Extracellular TRX is present in the circulation and its levels are increased under oxidative stress or inflammation [64] (Figure 2). TRX has been pointed out as a biomarker in numerous oxidative and inflammatory diseases such as rheumatoid arthritis (RA) in which plasma TRX levels of normal subjects were significantly lower than those of RA patients and correlated with RA disease activity and C-reactive protein [65]. TRX levels were increased in patients with systemic inflammatory stress syndrome (SIRS)/sepsis compared to control subjects [66].

2.4. Extracellular PRDX. PRDX1 can be found inside the Golgi apparatus on endothelial cells (ECs) [67], and under phorbol 12-myristate 13-acetate (PMA) stimulation PRDX1 is translocated to the cellular membrane [68], as also showed for PRDX6 in polymorphonuclear cells (PMNs) [69] (Figure 2). PRDX might also be secreted by lung cancer cells

through a nonclassical pathway [70, 71]. Nonetheless, the extracellular function of PRDX is still unknown. Unlike the well-described function of intracellular PRDX1, membrane PRDX6 helps in the maintenance of an optimal NADPH oxidase activity [69]. A number of chaperones, including TRX and HSPs, are released by stressed or dying cells, acting as an endogenous warning system through binding of these signals to receptors on the outer membrane [72–75]. Most of these signals are recognized by Toll-like receptor 4 (TLR4) [74, 75]. Accordingly, PRDX1 binds TLR4 and stimulates proinflammatory cytokine production in macrophages and dendritic cells, which suggests that PRDX could be acting as damage-associated molecular-pattern molecule (DAMP). Its trafficking seems to be dependent on PRDX binding to *protein kinase C* (PKC) through microvesicles [76]. In fact, exosomes can be participating in active transport of PRDX since proteomic studies have described PRDX in exosomes in B cells [57], bladder cancer cells [58], breast cancer cells [77], breast milk [78], colorectal cancer cells [59], and saliva [79] (Figure 2).

Thus, it is tempting to speculate that extracellular levels of PRDX/TRX result from a cellular response to high oxidant conditions in the outer milieu.

3. TRX/PRDX in Atherothrombosis

Atherothrombosis is an immune-inflammatory disease, originated by the subendothelial accumulation of LDLs, that can be oxidized by ROS. Oxidative stress is involved not only in the first stages of atherogenesis by modifying LDLs or NO, but also in later stages of atherothrombosis by modulating the expression of proteases that weakens the fibrous cap [80, 81]. ROS overproduction also produces direct damage to macromolecules such as lipids, nucleic acids, and proteins [82]. Furthermore, ROS can act as signaling molecules by inducing the activation of several cells from the vasculature. For example, through LDL oxydation and/or direct cell targeting, ROS can induce endothelial dysfunction and further leucocyte activation, deposition, and extravasation. In addition, ROS are clearly involved in the activation of vascular smooth muscle cells (VSMCs) from the lesion and sustain foam cell formation. Thus, pathological ROS overproduction is a main feature in atherogenesis and plaque rupture, which finally results in almost 70% of the clinical events [83].

Among the different systems involved in the redox maintenance in the vasculature, one of the most active is the TRX system. It is present in ECs [14, 84], VSMCs [85, 86], monocytes/macrophages [87, 88], RBCs [89, 90], and PMNs [90, 91]. Since TRX and PRDX are present in the atherosclerotic plaque and they can modulate different mechanisms involved in CVDs, several studies have addressed their role as diagnostic, prognostic, and therapeutic biomarkers.

3.1. TRX. TRX is abundantly expressed in the vasculature, and its levels are increased under oxidative stress, possibly as a response mechanism to augmented ROS production [19]. Besides, TRX expression in the endothelium and

in macrophages is augmented in atherosclerotic patients [92] and in arteries damaged by the balloon model [93]. More recently, TRX has been pointed as a possible marker for unstable atherosclerotic plaques due to its association with oxidative stress and intraplaque hemorrhage in culprit lesions [94]. TRX reductase is as well overexpressed in atherosclerotic plaques, maybe synthesized by macrophages engulfing oxLDLs [95].

The antioxidant effects of TRX are shown when overexpressed in mouse hearts, protecting them from myocardial infarction and displaying significantly improved postischemic ventricular recovery [96]. The positive effects of TRX in myocardial infarction are also due to its neoangiogenic properties as shown in different murine models [97, 98].

On the other hand, TRX can function as a signaling molecule by decreasing pressure-overload cardiac hypertrophy [99], maybe through upregulation of miR-98 [100]. However, there is a controversy about this matter because almost at the same time it was published another article in which the authors described that activation of TRX participates in the development of pressure-overload cardiac hypertrophy. In this respect, animals overexpressing TXNIP developed less hypertrophy [101]. Furthermore, transverse aortic constriction increased TRX activity accompanied by a 40% reduction in TXNIP levels [101]. Whether variations in TXNIP and TRX levels/activity reflect an increase in oxidative stress or they act as signaling molecules is still a matter to elucidate [102].

Recent studies have shown that extracellular TRX can inhibit interleukin-1 expression stimulated by LPS in monocyte-derived macrophages [103]. Besides, TRX1 administration has beneficial effects on myosin-induced autoimmune myocarditis through inhibition of inflammatory mediators and macrophage infiltration [104] and TRX1 also protects from reperfusion-induced arrhythmias [105]. Furthermore, TRX administration has been also shown to be beneficial in cerebral ischemia/reperfusion injury reducing the infarcted area through its antioxidant properties [106]. As an additional support for the beneficial effects of TRX in therapeutics, it is to note that TRX-1 gene delivery protects hypertensive rats from myocardial infarction through HO-1/B-cell lymphoma 2 (BCL-2) [107].

Regarding cardiovascular diseases, TRX levels are elevated in plasma from atherothrombotic patients [108, 109], and high homocysteine plus low TRX is related to CAD severity [110]. Furthermore, TRX was elevated in patients following angioplasty, and there was an association with increased TRX levels and decreased rate of restenosis at follow-up angiography (6 months) [111]. We have recently reported an increase in serum TRX from abdominal aortic aneurysm (AAA) patients compared with control subjects. Besides, TRX correlates with AAA size and expansion rate which suggests that TRX could be a good biomarker of AAA evolution [91].

3.2. PRDX. PRDX expression can be modified by prooxidative stimulus such as LPS or the phorbol ester 12-O-tetradecanoylphorbol-13-acetate (TPA) [88, 112]. Attention to

PRDX as a major regulator of H_2O_2 homeostasis is growing [34]. In cells stimulated with platelet-derived growth factor (PDGF) or tumor necrosis factor alpha, PRDX overexpression or silencing provoked, respectively, reduction or increase of H_2O_2 levels [113]. Moreover, through H_2O_2 scavenging, PRDX can inhibit the NF- κ B pathway and consequently the inflammatory response [114]. Different PRDX isoforms seem to modulate different cellular responses. For example, transfection of VSMCs from rat pulmonary artery with an expression plasmid for PRDX1 increases proliferation rate significantly [115]. PRDX1 also diminishes leucocytes activation and adhesion to vascular endothelium. Double KO mice for PRDX1 and ApoE chow fed showed larger atherosclerotic lesions and macrophages enriched than ApoE KO mice [116]. KO mice for PRDX2/ApoE showed exacerbated atherosclerotic lesion formation dependent both on vascular and hematopoietic cells. Besides, immune cells accumulation in the atherosclerotic lesions is increased due to PRDX2 absence and also redox-dependent signaling PRDX2 [117]. Moreover, PRDX2 modulates PDGF signaling, inhibiting thereby cell proliferation and migration [113, 118]. Using different *in vivo* models, it was shown that CD36 KO mice produce lower levels of ROS, along with an increase in heme-oxygenase1 (HO-1) and PRDX2. Furthermore, NF-E2-related factor-2 (Nrf2), a transcription factor in charge of the transcriptional regulation of HO-1 and PRDX2, knockdown led to increased ROS production and a prothrombotic phenotype under $FeCl_3$ treatment, a similar phenotype to that of PRDX2 KO mice [119]. Regarding PRDX2 and vascular diseases, it has been recently shown that PRDX2 is overexpressed in ruptured AAA tissue compared with nonruptured [120]. This could be associated with the increased oxidative stress observed in AAA tissue, which produces 2.5 times higher superoxide than adjacent non-AAA tissue and 10 times higher than nonpathological aorta [121].

Besides, PRDX3 overexpression prevents ventricular remodeling and cardiac failure after myocardial infarction in mice [122]. As mentioned above, PRDX6 protects mice against ischemic reperfusion injury [54]. Although, little is known about circulating levels of PRDX, we have recently described high PRDX1 levels in serum from AAA patients [90]. Besides, PRDX1 levels correlated positively with size and expansion rate of AAA, suggesting its potential role as diagnostic and prognostic biomarker for AAA.

4. Conclusion

On the whole, we have summarized several findings that demonstrate the major role of the TRX system in the maintenance of the redox status in CVDs. Furthermore, the extracellular levels of PRDX/TRX seem to be related with a prooxidative scenario and there is growing data suggesting their potential role as biomarkers for oxidative-stress-related diseases. Finally, their value as useful therapeutic tools is being tested and future studies are necessary to validate their prospective beneficial effects in CVDs.

Acknowledgments

This work was supported by the Spanish Ministerio de Ciencia y Tecnología (SAF 2010-21852), Ministerio de Sanidad y Consumo, Instituto de Salud Carlos III, Redes RECAVA (RD06/0014/0035), Ministerio de Sanidad y Consumo, Instituto de Salud Carlos III (PI10/00072), and Sociedad Española de Arteriosclerosis and Fundación Lilly.

References

- [1] S. M. Hemmingsen, C. Woolford, S. M. Van der Vies et al., "Homologous plant and bacterial proteins chaperone oligomeric protein assembly," *Nature*, vol. 333, no. 6171, pp. 330–334, 1988.
- [2] J. Madrigal-Matute, J. L. Martin-Ventura, L. M. Blanco-Colio, J. Egido, J. B. Michel, and O. Meilhac, "Heat-shock proteins in cardiovascular disease," *Advances in Clinical Chemistry*, vol. 54, pp. 1–43, 2011.
- [3] G. Powis, M. Briehl, and J. Oblong, "Redox signalling and the control of cell growth and death," *Pharmacology and Therapeutics*, vol. 68, no. 1, pp. 149–173, 1995.
- [4] R. Albertini, R. Moratti, and G. De Luca, "Oxidation of low-density lipoprotein in atherosclerosis from basic biochemistry to clinical studies," *Current Molecular Medicine*, vol. 2, no. 6, pp. 579–592, 2002.
- [5] Y. Lavrovsky, B. Chatterjee, R. A. Clark, and A. K. Roy, "Role of redox-regulated transcription factors in inflammation, aging and age-related diseases," *Experimental Gerontology*, vol. 35, no. 5, pp. 521–532, 2000.
- [6] C. J. World, H. Yamawaki, and B. C. Berk, "Thioredoxin in the cardiovascular system," *Journal of Molecular Medicine*, vol. 84, no. 12, pp. 997–1003, 2006.
- [7] A. Holmgren, "Antioxidant function of thioredoxin and glutaredoxin systems," *Antioxidants and Redox Signaling*, vol. 2, no. 4, pp. 811–820, 2000.
- [8] G. Powis and W. R. Montfort, "Properties and biological activities of thioredoxins," *Annual Review of Biophysics & Biomolecular Structure*, vol. 30, pp. 421–455, 2001.
- [9] Z. A. Wood, L. B. Poole, and P. A. Karplus, "Peroxiredoxin evolution and the regulation of hydrogen peroxide signaling," *Science*, vol. 300, no. 5619, pp. 650–653, 2003.
- [10] C. J. Jeffery, "Moonlighting proteins," *Trends in Biochemical Sciences*, vol. 24, no. 1, pp. 8–11, 1999.
- [11] A. Rubartelli, A. Bajetto, G. Allavena, E. Wollman, and R. Sitia, "Secretion of thioredoxin by normal and neoplastic cells through a leaderless secretory pathway," *Journal of Biological Chemistry*, vol. 267, no. 34, pp. 24161–24164, 1992.
- [12] S. G. Rhee, H. Z. Chae, and K. Kim, "Peroxiredoxins: a historical overview and speculative preview of novel mechanisms and emerging concepts in cell signaling," *Free Radical Biology and Medicine*, vol. 38, no. 12, pp. 1543–1552, 2005.
- [13] I. Slaby and A. Holmgren, "Thioredoxin reductase-dependent insulin disulfide reduction by phage T7 DNA polymerase reflects dissociation of the enzyme into subunits," *Journal of Biological Chemistry*, vol. 264, no. 28, pp. 16502–16506, 1989.
- [14] C. World, O. N. Spindel, and B. C. Berk, "Thioredoxin-interacting protein mediates TRX1 translocation to the plasma membrane in response to tumor necrosis factor- α : a key mechanism for vascular endothelial growth factor receptor-2 transactivation by reactive oxygen species," *Arteriosclerosis, Thrombosis, and Vascular Biology*, vol. 31, no. 8, pp. 1890–1897, 2011.
- [15] J. C. Spielberger, A. D. Moody, and W. H. Watson, "Oxidation and nuclear localization of thioredoxin-1 in sparse cell cultures," *Journal of Cellular Biochemistry*, vol. 104, no. 5, pp. 1879–1889, 2008.
- [16] G. Spyrou, E. Enmark, A. Miranda-Vizuete, and J. Å. Gustafsson, "Cloning and expression of a novel mammalian thioredoxin," *Journal of Biological Chemistry*, vol. 272, no. 5, pp. 2936–2941, 1997.
- [17] T. Tanaka, F. Hosoi, Y. Yamaguchi-Iwai et al., "Thioredoxin-2 (TRX-2) is an essential gene regulating mitochondria-dependent apoptosis," *EMBO Journal*, vol. 21, no. 7, pp. 1695–1703, 2002.
- [18] A. Miranda-Vizuete, J. Ljung, A. E. Damdimopoulos et al., "Characterization of sptx, a novel member of the thioredoxin family specifically expressed in human spermatozoa," *Journal of Biological Chemistry*, vol. 276, no. 34, pp. 31567–31574, 2001.
- [19] H. Nakamura, K. Nakamura, and J. Yodoi, "Redox regulation of cellular activation," *Annual Review of Immunology*, vol. 15, pp. 351–369, 1997.
- [20] H. Nakamura, M. Matsuda, K. Furuke et al., "Adult T cell leukemia-derived factor/human thioredoxin protects endothelial F-2 cell injury caused by activated neutrophils or hydrogen peroxide," *Immunology Letters*, vol. 42, no. 1-2, pp. 75–80, 1994.
- [21] W. L. Trigona, I. K. Mullarky, Y. Cao, and L. M. Sordillo, "Thioredoxin reductase regulates the induction of haem oxygenase-1 expression in aortic endothelial cells," *Biochemical Journal*, vol. 394, no. 1, pp. 207–216, 2006.
- [22] K. C. Das, Y. Lewis-Molock, and C. W. White, "Elevation of manganese superoxide dismutase gene expression by thioredoxin," *American Journal of Respiratory Cell and Molecular Biology*, vol. 17, no. 6, pp. 713–726, 1997.
- [23] J. Zhang, Y. D. Li, J. M. Patel, and E. R. Block, "Thioredoxin overexpression prevents NO-induced reduction of NO synthase activity in lung endothelial cells," *American Journal of Physiology, Lung Cellular and Molecular Physiology*, vol. 275, no. 2, pp. L288–L293, 1998.
- [24] L. E. Shao, T. Tanaka, R. Gribi, and J. Yu, "Thioredoxin-related regulation of NO/NOS activities," *Annals of the New York Academy of Sciences*, vol. 962, pp. 140–150, 2002.
- [25] J. Haendeler, J. Hoffmann, A. M. Zeiher, and S. Dimmeler, "Antioxidant effects of statins via S-nitrosylation and activation of thioredoxin in endothelial cells: a novel vasculoprotective function of statins," *Circulation*, vol. 110, no. 7, pp. 856–861, 2004.
- [26] E. Junn, S. H. Han, J. Y. Im et al., "Vitamin D3 up-regulated protein 1 mediates oxidative stress via suppressing the thioredoxin function," *Journal of Immunology*, vol. 164, no. 12, pp. 6287–6295, 2000.
- [27] M. Matsui, M. Oshima, H. Oshima et al., "Early embryonic lethality caused by targeted disruption of the mouse thioredoxin gene," *Developmental Biology*, vol. 178, no. 1, pp. 179–185, 1996.
- [28] T. Umekawa, T. Sugiyama, T. Kihira et al., "Overexpression of thioredoxin-1 reduces oxidative stress in the placenta of transgenic mice and promotes fetal growth via glucose metabolism," *Endocrinology*, vol. 149, no. 8, pp. 3980–3988, 2008.
- [29] Y. Kamimoto, T. Sugiyama, T. Kihira et al., "Transgenic mice overproducing human thioredoxin-1, an antioxidative and anti-apoptotic protein, prevents diabetic embryopathy," *Diabetologia*, vol. 53, no. 9, pp. 2046–2055, 2010.
- [30] Y. Hamada, H. Fujii, R. Kitazawa, J. Yodoi, S. Kitazawa, and M. Fukagawa, "Thioredoxin-1 overexpression in transgenic

- mice attenuates streptozotocin-induced diabetic osteopenia: a novel role of oxidative stress and therapeutic implications," *Bone*, vol. 44, no. 5, pp. 936–941, 2009.
- [31] M. Kaimul Ahsan, H. Nakamura, M. Tanito, K. Yamada, H. Utsumi, and J. Yodoi, "Thioredoxin-1 suppresses lung injury and apoptosis induced by diesel exhaust particles (DEP) by scavenging reactive oxygen species and by inhibiting DEP-induced downregulation of Akt," *Free Radical Biology and Medicine*, vol. 39, no. 12, pp. 1549–1559, 2005.
 - [32] F. Zhou, M. Gomi, M. Fujimoto et al., "Attenuation of neuronal degeneration in thioredoxin-1 overexpressing mice after mild focal ischemia," *Brain Research*, vol. 1272, pp. 62–70, 2009.
 - [33] Z. A. Wood, E. Schröder, J. R. Harris, and L. B. Poole, "Structure, mechanism and regulation of peroxiredoxins," *Trends in Biochemical Sciences*, vol. 28, no. 1, pp. 32–40, 2003.
 - [34] H. Z. Chae, H. J. Kim, S. W. Kang, and S. G. Rhee, "Characterization of three isoforms of mammalian peroxiredoxin that reduce peroxides in the presence of thioredoxin," *Diabetes Research and Clinical Practice*, vol. 45, no. 2-3, pp. 101–112, 1999.
 - [35] S. G. Rhee and H. A. Woo, "Multiple functions of peroxiredoxins: peroxidases, sensors and regulators of the intracellular messenger H_2O_2 , and protein chaperones," *Antioxidants and Redox Signaling*, vol. 15, no. 3, pp. 781–794, 2011.
 - [36] A. V. Peskin, F. M. Low, L. N. Paton, G. J. Maghzal, M. B. Hampton, and C. C. Winterbourn, "The high reactivity of peroxiredoxin 2 with H_2O_2 is not reflected in its reaction with other oxidants and thiol reagents," *Journal of Biological Chemistry*, vol. 282, no. 16, pp. 11885–11892, 2007.
 - [37] P. J. Leavey, C. Gonzalez-Aller, G. Thurman et al., "A 29-kDa protein associated with p67phox expresses both peroxiredoxin and phospholipase A2 activity and enhances superoxide anion production by a cell-free system of NADPH oxidase activity," *Journal of Biological Chemistry*, vol. 277, no. 47, pp. 45181–45187, 2002.
 - [38] J. Uwayama, A. Hirayama, T. Yanagawa et al., "Tissue Prx I in the protection against Fe-NTA and the reduction of nitroxyl radicals," *Biochemical and Biophysical Research Communications*, vol. 339, no. 1, pp. 226–231, 2006.
 - [39] J. Fang, T. Nakamura, D. H. Cho, Z. Gu, and S. A. Lipton, "S-nitrosylation of peroxiredoxin 2 promotes oxidative stress-induced neuronal cell death in Parkinson's disease," *Proceedings of the National Academy of Sciences of the United States of America*, vol. 104, no. 47, pp. 18742–18747, 2007.
 - [40] H. Z. Chae, H. Oubrahim, J. W. Park, S. G. Rhee, and P. B. Chock, "Protein glutathionylation in the regulation of peroxiredoxins: a family of thiol-specific peroxidases that function as antioxidants, molecular chaperones, and signal modulators," *Antioxidants & Redox Signaling*, vol. 16, no. 6, pp. 506–523, 2012.
 - [41] K. S. Yang, S. W. Kang, H. A. Woo et al., "Inactivation of human peroxiredoxin I during catalysis as the result of the oxidation of the catalytic site cysteine to cysteine-sulfinic acid," *Journal of Biological Chemistry*, vol. 277, no. 41, pp. 38029–38036, 2002.
 - [42] S. Barranco-Medina, J. J. Lázaro, and K. J. Dietz, "The oligomeric conformation of peroxiredoxins links redox state to function," *FEBS Letters*, vol. 583, no. 12, pp. 1809–1816, 2009.
 - [43] J. C. Lim, H. I. Choi, Y. S. Park et al., "Irreversible oxidation of the active-site cysteine of peroxiredoxin to cysteine sulfonic acid for enhanced molecular chaperone activity," *Journal of Biological Chemistry*, vol. 283, no. 43, pp. 28873–28880, 2008.
 - [44] S. G. Rhee, W. Jeong, T. S. Chang, and H. A. Woo, "Sulfinic acid reductase specific to 2-Cys peroxiredoxin: its discovery, mechanism of action, and biological significance," *Kidney international. Supplement*, no. 106, pp. S3–S8, 2007.
 - [45] C. A. Neumann, D. S. Krause, C. V. Carman et al., "Essential role for the peroxiredoxin Prdx1 in erythrocyte antioxidant defence and tumour suppression," *Nature*, vol. 424, no. 6948, pp. 561–565, 2003.
 - [46] T. H. Lee, S. U. Kim, S. L. Yu et al., "Peroxiredoxin II is essential for sustaining life span of erythrocytes in mice," *Blood*, vol. 101, no. 12, pp. 5033–5038, 2003.
 - [47] S. Agrawal-Singh, F. Isken, K. Agelopoulos et al., "Genome-wide analysis of histone H3 acetylation patterns in AML identifies PRDX2 as an epigenetically silenced tumor suppressor gene," *Blood*, vol. 119, no. 10, pp. 2346–2357, 2012.
 - [48] L. Li, W. Shoji, H. Takano et al., "Increased susceptibility of MER5 (peroxiredoxin III) knockout mice to LPS-induced oxidative stress," *Biochemical and Biophysical Research Communications*, vol. 355, no. 3, pp. 715–721, 2007.
 - [49] A. G. Cox, C. C. Winterbourn, and M. B. Hampton, "Mitochondrial peroxiredoxin involvement in antioxidant defence and redox signalling," *Biochemical Journal*, vol. 425, no. 2, pp. 313–325, 2010.
 - [50] T. S. Chang, C. S. Cho, S. Park, S. Yu, W. K. Sang, and G. R. Sue, "Peroxiredoxin III, a mitochondrion-specific peroxidase, regulates apoptotic signaling by mitochondria," *Journal of Biological Chemistry*, vol. 279, no. 40, pp. 41975–41984, 2004.
 - [51] J. Y. Huh, Y. Kim, J. Jeong et al., "Peroxiredoxin 3 is a key molecule regulating adipocyte oxidative stress, mitochondrial biogenesis, and adipokine expression," *Antioxidants & Redox Signaling*, vol. 16, no. 3, pp. 229–243, 2012.
 - [52] Y. Iuchi, F. Okada, S. Tsunoda et al., "Peroxiredoxin 4 knockout results in elevated spermatogenic cell death via oxidative stress," *Biochemical Journal*, vol. 419, no. 1, pp. 149–158, 2009.
 - [53] Y. Zhou, K. H. Kok, A. C. S. Chun et al., "Mouse peroxiredoxin V is a thioredoxin peroxidase that inhibits p53-induced apoptosis," *Biochemical and Biophysical Research Communications*, vol. 268, no. 3, pp. 921–927, 2000.
 - [54] N. Nagy, G. Malik, A. B. Fisher, and D. K. Das, "Targeted disruption of peroxiredoxin 6 gene renders the heart vulnerable to ischemia-reperfusion injury," *American Journal of Physiology, Heart and Circulatory Physiology*, vol. 291, no. 6, pp. H2636–H2640, 2006.
 - [55] Y. Manevich and A. B. Fisher, "Peroxiredoxin 6, a 1-Cys peroxiredoxin, functions in antioxidant defense and lung phospholipid metabolism," *Free Radical Biology and Medicine*, vol. 38, no. 11, pp. 1422–1432, 2005.
 - [56] L. C. P. Azevedo, M. A. Pedro, and F. R. M. Laurindo, "Circulating microparticles as therapeutic targets in cardiovascular diseases," *Recent Patents on Cardiovascular Drug Discovery*, vol. 2, no. 1, pp. 41–51, 2007.
 - [57] S. I. Buschow, B. W. M. Van Balkom, M. Aalberts, A. J. R. Heck, M. Wauben, and W. Stoorvogel, "MHC class II-associated proteins in B-cell exosomes and potential functional implications for exosome biogenesis," *Immunology and Cell Biology*, vol. 88, no. 8, pp. 851–856, 2010.
 - [58] J. L. Welton, S. Khanna, P. J. Giles et al., "Proteomics analysis of bladder cancer exosomes," *Molecular and Cellular Proteomics*, vol. 9, no. 6, pp. 1324–1338, 2010.
 - [59] D. S. Choi, J. M. Lee, W. P. Gun et al., "Proteomic analysis of microvesicles derived from human colorectal cancer cells,"

- Journal of Proteome Research*, vol. 6, no. 12, pp. 4646–4655, 2007.
- [60] P. A. Gonzales, T. Pisitkun, J. D. Hoffert et al., “Large-scale proteomics and phosphoproteomics of urinary exosomes,” *Journal of the American Society of Nephrology*, vol. 20, no. 2, pp. 363–379, 2009.
 - [61] A. J. Dessein, H. L. Lenzi, and J. C. Bina, “Modulation of eosinophil cytotoxicity by blood mononuclear cells from healthy subjects and patients with chronic schistosomiasis mansoni,” *Cellular Immunology*, vol. 85, no. 1, pp. 100–113, 1984.
 - [62] K. Pekkari, R. Gurunath, E. S. J. Arner, and A. Holmgren, “Truncated thioredoxin is a mitogenic cytokine for resting human peripheral blood mononuclear cells and is present in human plasma,” *Journal of Biological Chemistry*, vol. 275, no. 48, pp. 37474–37480, 2000.
 - [63] K. Pekkari, J. Avila-Carino, A. Bengtsson, R. Gurunath, A. Scheynius, and A. Holmgren, “Truncated thioredoxin. (Trx80) induces production of interleukin-12 and enhances CD14 expression in human monocytes,” *Blood*, vol. 97, no. 10, pp. 3184–3190, 2001.
 - [64] N. Kondo, Y. Ishii, Y. W. Kwon et al., “Redox-sensing release of human thioredoxin from t lymphocytes with negative feedback loops,” *Journal of Immunology*, vol. 172, no. 1, pp. 442–448, 2004.
 - [65] T. Jikimoto, Y. Nishikubo, M. Koshiba et al., “Thioredoxin as a biomarker for oxidative stress in patients with rheumatoid arthritis,” *Molecular Immunology*, vol. 38, no. 10, pp. 765–772, 2002.
 - [66] S. K. Leaver, N. S. MacCallum, V. Pingle et al., “Increased plasma thioredoxin levels in patients with sepsis: positive association with macrophage migration inhibitory factor,” *Intensive Care Medicine*, vol. 36, no. 2, pp. 336–341, 2010.
 - [67] A. L. Mowbray, D. H. Kang, G. R. Sue, W. K. Sang, and H. Jo, “Laminar shear stress up-regulates peroxiredoxins (PRX) in endothelial cells: PRX 1 as a mechanosensitive antioxidant,” *Journal of Biological Chemistry*, vol. 283, no. 3, pp. 1622–1627, 2008.
 - [68] C. Lehel, Z. Oláh, G. Petrovics, G. Jakab, and W. B. Anderson, “Influence of various domains of protein kinase C ϵ on its PMA-induced translocation from the golgi to the plasma membrane,” *Biochemical and Biophysical Research Communications*, vol. 223, no. 1, pp. 98–103, 1996.
 - [69] D. R. Ambruso, M. A. Ellison, G. W. Thurman, and T. L. Leto, “Peroxiredoxin 6 translocates to the plasma membrane during neutrophil activation and is required for optimal NADPH oxidase activity,” *Biochimica et Biophysica Acta*, vol. 1823, no. 2, pp. 306–315, 2012.
 - [70] J. W. Chang, S. H. Lee, Y. Lu, and Y. J. Yoo, “Transforming growth factor- β 1 induces the non-classical secretion of peroxiredoxin-I in A549 cells,” *Biochemical and Biophysical Research Communications*, vol. 345, no. 1, pp. 118–123, 2006.
 - [71] W. C. Jong, H. L. Seung, Y. J. Ju et al., “Peroxiredoxin-I is an autoimmunogenic tumor antigen in non-small cell lung cancer,” *FEBS Letters*, vol. 579, no. 13, pp. 2873–2877, 2005.
 - [72] S. Yoshida, T. Katoh, T. Tetsuka, K. Uno, N. Matsui, and T. Okamoto, “Involvement of thioredoxin in rheumatoid arthritis: its costimulatory roles in the TNF- α -induced production of IL-6 and IL-8 from cultured synovial fibroblasts,” *Journal of Immunology*, vol. 163, no. 1, pp. 351–358, 1999.
 - [73] C. Hunter-Lavin, E. L. Davies, M. M. F. V. G. Bacelar, M. J. Marshall, S. M. Andrew, and J. H. H. Williams, “Hsp70 release from peripheral blood mononuclear cells,” *Biochemical and Biophysical Research Communications*, vol. 324, no. 2, pp. 511–517, 2004.
 - [74] A. Asea, M. Rehli, E. Kabingu et al., “Novel signal transduction pathway utilized by extracellular HSP70. Role of toll-like receptor (TLR) 2 and TLR4,” *Journal of Biological Chemistry*, vol. 277, no. 17, pp. 15028–15034, 2002.
 - [75] M. T. Lotze, H. J. Zeh, A. Rubartelli et al., “The grateful dead: damage-associated molecular pattern molecules and reduction/oxidation regulate immunity,” *Immunological Reviews*, vol. 220, no. 1, pp. 60–81, 2007.
 - [76] P. Westermann, M. Knoblich, O. Maier, C. Lindschau, and H. Haller, “Protein kinase C bound to the Golgi apparatus supports the formation of constitutive transport vesicles,” *Biochemical Journal*, vol. 320, no. 2, pp. 651–658, 1996.
 - [77] S. Staubach, H. Razawi, and F. G. Hanisch, “Proteomics of MUC1-containing lipid rafts from plasma membranes and exosomes of human breast carcinoma cells MCF-7,” *Proteomics*, vol. 9, no. 10, pp. 2820–2835, 2009.
 - [78] C. Admyre, S. M. Johansson, K. R. Qazi et al., “Exosomes with immune modulatory features are present in human breast milk,” *Journal of Immunology*, vol. 179, no. 3, pp. 1969–1978, 2007.
 - [79] M. Gonzalez-Begne, B. Lu, X. Han et al., “Proteomic analysis of human parotid gland exosomes by multidimensional protein identification technology (MudPIT),” *Journal of Proteome Research*, vol. 8, no. 3, pp. 1304–1314, 2009.
 - [80] D. Harrison, K. K. Griendling, U. Landmesser, B. Hornig, and H. Drexler, “Role of oxidative stress in atherosclerosis,” *American Journal of Cardiology*, vol. 91, no. 3, pp. A7–A11, 2003.
 - [81] Y. Lu and L. M. Wahl, “Oxidative stress augments the production of matrix metalloproteinase-1, cyclooxygenase-2, and prostaglandin E2 through enhancement of NF- κ B activity in lipopolysaccharide-activated human primary monocytes,” *Journal of Immunology*, vol. 175, no. 8, pp. 5423–5429, 2005.
 - [82] J. Blumberg, “Use of biomarkers of oxidative stress in research studies,” *Journal of Nutrition*, vol. 134, no. 11, pp. 3188S–3189S, 2004.
 - [83] R. Virmani, A. P. Burke, A. Farb, and E. D. Kolodgie, “Pathology of the Vulnerable Plaque,” *Journal of the American College of Cardiology*, vol. 47, no. 8, supplement, pp. C13–C18, 2006.
 - [84] H. Jo, H. Song, and A. Mowbray, “Role of NADPH oxidases in disturbed flow- and BMP4-induced inflammation and atherosclerosis,” *Antioxidants and Redox Signaling*, vol. 8, no. 9–10, pp. 1609–1619, 2006.
 - [85] A. Qu, C. Jiang, M. Xu et al., “PGC-1 α attenuates neointimal formation via inhibition of vascular smooth muscle cell migration in the injured rat carotid artery,” *American Journal of Physiology, Cell Physiology*, vol. 297, no. 3, pp. C645–C653, 2009.
 - [86] D. A. Popowich, A. K. Vavra, C. P. Walsh et al., “Regulation of reactive oxygen species by p53: implications for nitric oxide-mediated apoptosis,” *American Journal of Physiology, Heart and Circulatory Physiology*, vol. 298, no. 6, pp. H2192–H2200, 2010.
 - [87] B. Sahaf and A. Rosén, “Secretion of 10-kDa and 12-kDa thioredoxin species from blood monocytes and transformed leukocytes,” *Antioxidants and Redox Signaling*, vol. 2, no. 4, pp. 717–726, 2000.
 - [88] A. Hess, N. Wijayanti, A. P. Neuschäfer-Rube, N. Katz, T. Kietzmann, and S. Immenschuh, “Phorbol ester-dependent activation of peroxiredoxin i gene expression via a protein

- kinase C, Ras, p38 mitogen-activated protein kinase signaling pathway," *Journal of Biological Chemistry*, vol. 278, no. 46, pp. 45419–45434, 2003.
- [89] M. K. Cha and I. H. Kim, "Thioredoxin-linked peroxidase from human red blood cell: evidence for the existence of thioredoxin and thioredoxin reductase in human red blood cell," *Biochemical and Biophysical Research Communications*, vol. 217, no. 3, pp. 900–907, 1995.
- [90] R. Martinez-Pinna, P. Ramos-Mozo, J. Madrigal-Matute et al., "Identification of peroxiredoxin-1 as a novel biomarker of abdominal aortic aneurysm," *Arteriosclerosis, Thrombosis, and Vascular Biology*, vol. 31, no. 4, pp. 935–943, 2011.
- [91] R. Martinez-Pinna, J. S. Lindholt, L. M. Blanco-Colio et al., "Increased levels of thioredoxin in patients with abdominal aortic aneurysms (AAAs). A potential link of oxidative stress with AAA evolution," *Atherosclerosis*, vol. 212, no. 1, pp. 333–338, 2010.
- [92] M. Okuda, N. Inoue, H. Azumi et al., "Expression of glutaredoxin in human coronary arteries: its potential role in antioxidant protection against atherosclerosis," *Arteriosclerosis, Thrombosis, and Vascular Biology*, vol. 21, no. 9, pp. 1483–1487, 2001.
- [93] Y. Takagi, Y. Gon, T. Todaka et al., "Expression of thioredoxin is enhanced in atherosclerotic plaques and during neointima formation in rat arteries," *Laboratory Investigation*, vol. 78, no. 8, pp. 957–966, 1998.
- [94] K. Nishihira, A. Yamashita, T. Imamura et al., "Thioredoxin in coronary culprit lesions: possible relationship to oxidative stress and intraplaque hemorrhage," *Atherosclerosis*, vol. 201, no. 2, pp. 360–367, 2008.
- [95] C. Furman, A. K. Rundlöf, G. Larigauderie et al., "Thioredoxin reductase 1 is upregulated in atherosclerotic plaques: specific induction of the promoter in human macrophages by oxidized low-density lipoproteins," *Free Radical Biology and Medicine*, vol. 37, no. 1, pp. 71–85, 2004.
- [96] T. Türoczi, V. W. H. Chang, R. M. Engelman, N. Maulik, Y. S. Ho, and D. K. Das, "Thioredoxin redox signaling in the ischemic heart: an insight with transgenic mice overexpressing Trx1," *Journal of Molecular and Cellular Cardiology*, vol. 35, no. 6, pp. 695–704, 2003.
- [97] S. M. Samuel, M. Thirunavukkarasu, S. V. Penumathsa et al., "Thioredoxin-1 gene therapy enhances angiogenic signaling and reduces ventricular remodeling in infarcted myocardium of diabetic rats," *Circulation*, vol. 121, no. 10, pp. 1244–1255, 2010.
- [98] R. S. Adluri, M. Thirunavukkarasu, L. Zhan et al., "Thioredoxin 1 enhances neovascularization and reduces ventricular remodeling during chronic myocardial infarction: a study using thioredoxin 1 transgenic mice," *Journal of Molecular and Cellular Cardiology*, vol. 50, no. 1, pp. 239–247, 2011.
- [99] M. Yamamoto, G. Yang, C. Hong et al., "Inhibition of endogenous thioredoxin in the heart increases oxidative stress and cardiac hypertrophy," *Journal of Clinical Investigation*, vol. 112, no. 9, pp. 1395–1406, 2003.
- [100] Y. Yang, T. Ago, P. Zhai, M. Abdellatif, and J. Sadoshima, "Thioredoxin 1 negatively regulates angiotensin II-Induced cardiac hypertrophy through upregulation of miR-98/let-7," *Circulation Research*, vol. 108, no. 3, pp. 305–313, 2011.
- [101] J. Yoshioka, P. C. Schulze, M. Cupesi et al., "Thioredoxin-interacting protein controls cardiac hypertrophy through regulation of thioredoxin activity," *Circulation*, vol. 109, no. 21, pp. 2581–2586, 2004.
- [102] C. J. Lowenstein, "Exogenous thioredoxin reduces inflammation in autoimmune myocarditis," *Circulation*, vol. 110, no. 10, pp. 1178–1179, 2004.
- [103] L. Billiet, C. Furman, G. Larigauderie et al., "Extracellular human thioredoxin-1 inhibits lipopolysaccharide-induced interleukin-1 β expression in human monocyte-derived macrophages," *Journal of Biological Chemistry*, vol. 280, no. 48, pp. 40310–40318, 2005.
- [104] W. Liu, H. Nakamura, K. Shioji et al., "Thioredoxin-1 ameliorates myosin-induced autoimmune myocarditis by suppressing chemokine expressions and leukocyte chemotaxis in mice," *Circulation*, vol. 110, no. 10, pp. 1276–1283, 2004.
- [105] M. Aota, K. Matsuda, N. Isowa, H. Wada, J. Yodoi, and T. Ban, "Protection against reperfusion-induced arrhythmias by human thioredoxin," *Journal of Cardiovascular Pharmacology*, vol. 27, no. 5, pp. 727–732, 1996.
- [106] I. Hattori, Y. Takagi, H. Nakamura et al., "Intravenous administration of thioredoxin decreases brain damage following transient focal cerebral ischemia in mice," *Antioxidants and Redox Signaling*, vol. 6, no. 1, pp. 81–87, 2004.
- [107] S. Koneru, S. V. Penumathsa, M. Thirunavukkarasu, L. Zhan, and N. Maulik, "Thioredoxin-1 gene delivery induces heme oxygenase-1 mediated myocardial preservation after chronic infarction in hypertensive rats," *American Journal of Hypertension*, vol. 22, no. 2, pp. 183–190, 2009.
- [108] S. Miyamoto, T. Sakamoto, H. Soejima et al., "Plasma thioredoxin levels and platelet aggregability in patients with acute myocardial infarction," *American Heart Journal*, vol. 146, no. 3, pp. 465–471, 2003.
- [109] J. Hokamaki, H. Kawano, H. Soejima et al., "Plasma thioredoxin levels in patients with unstable angina," *International Journal of Cardiology*, vol. 99, no. 2, pp. 225–231, 2005.
- [110] Y. Wu, L. Yang, and L. Zhong, "Decreased serum levels of thioredoxin in patients with coronary artery disease plus hyperhomocysteinemia is strongly associated with the disease severity," *Atherosclerosis*, vol. 212, no. 1, pp. 351–355, 2010.
- [111] C. M. Wahlgren and K. Pekkari, "Elevated thioredoxin after angioplasty in peripheral arterial disease," *European Journal of Vascular and Endovascular Surgery*, vol. 29, no. 3, pp. 281–286, 2005.
- [112] N. Wijayanti, S. Naidu, T. Kietzmann, and S. Immenschuh, "Inhibition of phorbol ester-dependent peroxiredoxin I gene activation by lipopolysaccharide via phosphorylation of RelA/p65 at serine 276 in monocytes," *Free Radical Biology and Medicine*, vol. 44, no. 4, pp. 699–710, 2008.
- [113] M. H. Choi, I. K. Lee, G. W. Kim et al., "Regulation of PDGF signalling and vascular remodelling by peroxiredoxin II," *Nature*, vol. 435, no. 7040, pp. 347–353, 2005.
- [114] S. G. Rhee, S. W. Kang, W. Jeong, T. S. Chang, K. S. Yang, and H. A. Woo, "Intracellular messenger function of hydrogen peroxide and its regulation by peroxiredoxins," *Current Opinion in Cell Biology*, vol. 17, no. 2, pp. 183–189, 2005.
- [115] K. Ihida-Stansbury, D. M. McKean, S. A. Gebb et al., "Regulation and functions of the paired-related homeobox gene PRX1 in pulmonary vascular development and disease," *Chest*, vol. 128, no. 6, supplement, p. S591, 2005.
- [116] J. Kisucka, A. K. Chauhan, I. S. Patten et al., "Peroxiredoxin1 prevents excessive endothelial activation and early atherosclerosis," *Circulation Research*, vol. 103, no. 6, pp. 598–605, 2008.

- [117] J.-G. Park, J.-Y. Yoo, S.-J. Jeong et al., "Peroxiredoxin 2 deficiency exacerbates atherosclerosis in apolipoprotein E-deficient mice," *Circulation Research*, vol. 109, no. 7, pp. 739–749, 2011.
- [118] S. W. Kang, S. G. Rhee, T. S. Chang, W. Jeong, and M. H. Choi, "2-Cys peroxiredoxin function in intracellular signal transduction: therapeutic implications," *Trends in Molecular Medicine*, vol. 11, no. 12, pp. 571–578, 2005.
- [119] W. Li, M. Febbraio, S. P. Reddy, D. Y. Yu, M. Yamamoto, and R. L. Silverstein, "CD36 participates in a signaling pathway that regulates ROS formation in murine VSMCs," *Journal of Clinical Investigation*, vol. 120, no. 11, pp. 3996–4006, 2010.
- [120] S. Urbonavicius, J. S. Lindholt, H. Vorum, G. Urbonaviciene, E. W. Henneberg, and B. Honoré, "Proteomic identification of differentially expressed proteins in aortic wall of patients with ruptured and nonruptured abdominal aortic aneurysms," *Journal of Vascular Surgery*, vol. 49, no. 2, pp. 455–463, 2009.
- [121] F. J. Miller Jr., W. J. Sharp, X. Fang, L. W. Oberley, T. D. Oberley, and N. L. Weintraub, "Oxidative stress in human abdominal aortic aneurysms: a potential mediator of aneurysmal remodeling," *Arteriosclerosis, Thrombosis, and Vascular Biology*, vol. 22, no. 4, pp. 560–565, 2002.
- [122] S. Matsushima, T. Ide, M. Yamato et al., "Overexpression of mitochondrial peroxiredoxin-3 prevents left ventricular remodeling and failure after myocardial infarction in mice," *Circulation*, vol. 113, no. 14, pp. 1779–1786, 2006.

Research Article

Blockade of TGF- β 1 Signalling Inhibits Cardiac NADPH Oxidase Overactivity in Hypertensive Rats

José Luis Miguel-Carrasco,¹ Ana Baltanás,¹ Carolina Cebrián,¹ María U. Moreno,¹ Begoña López,¹ Nerea Hermida,¹ Arantxa González,¹ Javier Dotor,² Francisco Borrás-Cuesta,² Javier Díez,^{1,3} Ana Fortuño,¹ and Guillermo Zalba¹

¹ Division of Cardiovascular Sciences, Centre for Applied Medical Research, University of Navarra, 31008 Pamplona, Spain

² Division of Hepatology and Gene Therapy, Centre for Applied Medical Research, University of Navarra, 31008 Pamplona, Spain

³ Department of Cardiology and Cardiac Surgery, University Clinic, University of Navarra, 31008 Pamplona, Spain

Correspondence should be addressed to Ana Fortuño, afortuno@unav.es

Received 15 December 2011; Accepted 21 March 2012

Academic Editor: Adrian Manea

Copyright © 2012 José Luis Miguel-Carrasco et al. This is an open access article distributed under the Creative Commons Attribution License, which permits unrestricted use, distribution, and reproduction in any medium, provided the original work is properly cited.

NADPH oxidases constitute a major source of superoxide anion ($\cdot\text{O}_2^-$) in hypertension. Several studies suggest an important role of NADPH oxidases in different effects mediated by TGF- β 1. In this study we show that chronic administration of P144, a peptide synthesized from type III TGF- β 1 receptor, significantly reduced the cardiac NADPH oxidase expression and activity as well as in the nitrotyrosine levels observed in control spontaneously hypertensive rats (V-SHR) to levels similar to control normotensive Wistar Kyoto rats. In addition, P144 was also able to reduce the significant increases in the expression of collagen type I protein and mRNA observed in hearts from V-SHR. In addition, positive correlations between collagen expression, NADPH oxidase activity, and nitrotyrosine levels were found in all animals. Finally, TGF- β 1-stimulated Rat-2 exhibited significant increases in NADPH oxidase activity that was inhibited in the presence of P144. It could be concluded that the blockade of TGF- β 1 with P144 inhibited cardiac NADPH oxidase in SHR, thus adding new data to elucidate the involvement of this enzyme in the profibrotic actions of TGF- β 1.

1. Introduction

Hypertension is associated with multiple functional and structural cardiovascular alterations [1, 2]. Among others, these alterations are characterized by the progressive accumulation of fibrillar collagen, namely, collagen type I, in the myocardium of animals and humans with arterial hypertension and left ventricular hypertrophy [3]. Although the exact mechanism by which physiological collagen turns into pathological fibrotic tissue is still unknown, there are many studies that suggest an important role of the local production of the transforming growth factor β 1 (TGF- β 1) [4]. TGF- β 1 acts as a key fibrogenic cytokine in many tissues by enhancing extracellular matrix synthesis [5].

Currently, *in vitro* studies have described that the activation of the nicotinamide adenine dinucleotide phosphate (NADPH) oxidase system has a role in TGF- β 1-induced

effects [6–9]. Moreover, the association of the NADPH oxidase with TGF- β 1-induced fibrosis has been also observed in several experimental models [10–13]. The NADPH oxidase has been shown as a major source of superoxide anion ($\cdot\text{O}_2^-$) [14]. It consists of a membrane bound cytochrome formed by a small subunit (p22phox) and a big (NOX1-5, Duox1-2) subunit, and in some cases, cytoplasmic subunits that upon phosphorylation bind to the cytochrome [15]. In the heart of rats, Nox2 and Nox4 NADPH isoforms are expressed. There is evidence that the Nox2-dependent form of the enzyme is inducible and generates $\cdot\text{O}_2^-$, especially by humoral activation [15, 16]. The Nox4-dependent enzyme seems to be constitutively active and may directly generate hydrogen peroxide (H_2O_2) [17, 18].

It has been described that the synthetic peptide P144, encompassing amino acids 730–743 from the human membrane-proximal ligand-binding domain of TGF- β 1

type III receptor, also called betaglycan, acts as a competitor of TGF- β 1 type III receptor, sequestering TGF- β 1. P144 is able to inhibit fibrosis in a rat model of hepatic failure as well as in a murine model of scleroderma [19, 20]. Furthermore, our group has recently demonstrated that P144 prevents myocardial fibrosis and collagen type I synthesis in experimental hypertension [21].

The possible interrelationship between TGF- β 1 and the NADPH oxidase in cardiac damage has not yet been studied in an experimental model of hypertension. Given that TGF- β 1 is a major contributor to the development of structural alterations in target organs of hypertension [22], we investigated whether the chronic treatment with P144 inhibits cardiac NADPH oxidase and whether this effect is associated with the cardiac antifibrotic properties of the peptide.

2. Material and Methods

2.1. Animals. The study was in agreement with the Guide for the Care and Use of Laboratory Animals published by the US National Institutes of Health (NIH Publication no. 85–23, revised 1996) [23], and was approved by the Ethical Committee for Animal Experimentation of the University of Navarra (090/05; 100/07). Rats were provided by Harlan UK Limited (Bicester, UK). Ten-week-old male spontaneously hypertensive rats (SHR) ($n = 10$, V-SHR) received vehicle (saline solution) intraperitoneally for 12 weeks, and then were sacrificed at the age of 22 weeks. In addition, 10-week-old WKY ($n = 10$, P144-WKY) and 10-week-old SHR ($n = 10$, P144-SHR) were treated with intraperitoneal P144 for 12 weeks and then sacrificed. The peptide was dissolved in saline solution, and the concentration was adjusted for the body weight to obtain an average daily dose of 1 mg/kg body weight/day. This dose was selected because it had been demonstrated previously in rodents that P144 exhibits hepatic and cutaneous antifibrotic activity at doses above 0.5 mg/kg body weight/day [15, 16]. All rats were housed in individual cages with free access to standard rat chow and tap water in a quiet room with constant temperature (20–22°C) and humidity (50–60%). Before they were sacrificed by decapitation, the rats were weighed and anaesthetized with Ketamine 75 mg/kg (Imalgene 1000, Merial) and Xylazine 5 mg/kg (Rompun, Bayer).

2.2. Measurement of Blood Pressure. Systolic blood pressure (SBP) and diastolic blood pressure (DBP) were measured in all rats every 2 weeks by the standard tail-cuff method using an LE5007 Pressure Computer (Letica Scientific Instruments).

2.3. Preparation of Tissue Samples. After sacrifice, hearts were carefully excised and frozen at -80°C for mRNA, enzymatic activity, and protein analysis.

For NADPH oxidase activity and Western blot studies, hearts were homogenated on ice in phosphate buffer saline (50 mM K_2HPO_4 , 50 mM KH_2PO_4 , 0.001 mM EDTA, and

proteases inhibitor pH = 7) with a glass/glass motor-driven tissue homogenizer for 2 minutes. The homogenate was centrifuged at 2000 g for 10 minutes. The pellet was discarded, and the supernatant was stored at -80°C . Protein concentration was determined by the Lowry methodology.

2.4. NADPH Oxidase Activity. Chemiluminescence assays with 10 $\mu\text{mol/L}$ lucigenin and 200 $\mu\text{mol/L}$ NADPH were used to measure $\cdot\text{O}_2^-$ production in 200 μg of tissue homogenate. Luminescence was recorded during 10 minutes in a tube luminometer (Berthold Detection System, Sirius). A buffer blank was subtracted from each reading, and the value of the area under the curve was used to quantify chemiluminescence. Data are expressed as relative light units (RLUs) produced per second per mg of protein.

2.5. Western Blot. To analyze the nitrotyrosine (NT) levels and the expression of collagen type I and Nox4 and Nox2 NADPH oxidase isoforms, proteins were separated by electrophoresis. Membranes were incubated with specific antibodies against Nox4 and Nox2 isoforms (Santa Cruz Biotechnology, INC Santa Cruz), NT (Upstate Biotechnology, Millipore), and collagen type I (Biogenesis) overnight at 4°C at a dilution of 1:1000. The membranes were incubated with appropriated peroxidase-conjugated secondary antibodies (GE Healthcare) for 1 hour at room temperature (1:25000 anti-rabbit for Nox4, 1:10000 anti-mouse for Nox2, 1:10000 anti-mouse for collagen type I, and 1:20000 anti-mouse for NT). Protein expression was visualized with the ECL-Advanced chemiluminescence system (Amersham Biosciences). Bands were analyzed using the Chemidoc Detection System and the Quantity One software (Bio-Rad) obtaining densitometric arbitrary units (AU). The blots were reprobed with a monoclonal α -tubulin antibody (Santa Cruz Biotechnology, INC Santa Cruz) as a control for loading. Data are expressed as the relative expression to α -tubulin.

2.6. Real-Time RT-PCR. The messenger RNA (mRNA) was isolated from total RNA with the Oligotex mRNA KIT (Quiagen). A real-time PCR reaction was performed using TaqMan Gene Expression probes: Nox4 (Rn 00585380), Nox2 (Rn 00576710), p22phox (Rn 00577357), p47phox (Rn 00586945), TGF- β 1 (Rn 00572010), fibronectin (Rn 00569575), type I collagen (Rn01463848), biglycan (Rn 01529736), connective tissue growth factor (CTGF, Rn 00573960), lysyl oxidase (LOX, Rn 01491829), and 18S ribosomal RNA (Hs 03003631). Data were normalized to 18S ribosomal RNA expression. Relative expression of mRNA was determined by the $2^{-\Delta\Delta\text{CT}}$ method [24].

2.7. Cell Cultures and In Vitro Experiments. The Rat-2 fibroblast cell line was purchased from American Type Culture Collection and maintained in Dulbecco's modified Eagle's medium (Invitrogen) supplemented with 10% fetal bovine serum (FBS, Invitrogen), Penicillin-Streptomycin solution (Invitrogen), and Fungizone (Invitrogen). Rat-2 cells were seeded at a density of 5.25×10^5 cells in T-25 tissue culture flasks (Nunc) and allowed to adhere overnight. Cells

were then incubated in reduced-serum medium (1% FBS) for 24 h prior to TGF- β 1 stimulation. Four conditions were used: (i) cells incubated in reduced serum media, (ii) cells incubated in reduced serum media containing TGF- β 1 (10 ng/mL), (iii) cells incubated in reduced serum media containing P144 (200 μ g/mL), and (iv) cells incubated in reduced serum media containing TGF- β 1 (10 ng/mL) and P144 (200 μ g/mL), for 24 h prior to harvesting. After treatment, cells were trypsinized and pelleted. The cell pellets were washed in phosphate-buffered solution (Invitrogen) and centrifuged at 1100 g for 5 min at 4°C and then used for protein extraction.

NADPH oxidase activity was performed as above. In this case, $\cdot\text{O}_2^-$ production was measured on 10 μ g of cell protein.

2.8. Statistical Analysis. Results are given as mean \pm SEM. To analyze the differences among the four groups, a one-way ANOVA followed by a Scheffe's test was performed once normality had been proven (Shapiro-Wilks test); otherwise, a nonparametric test (Kruskal-Wallis) followed by a Mann-Whitney *U*-test (adjusting the alpha-level by Bonferroni inequality) was used. Bivariate associations were performed by Pearson's correlation test. The statistical analysis was carried out using the computer program SPSS for Windows version 15.0.

3. Results

3.1. Effects of P144 on Blood Pressure. Values of SBP and DBP were elevated in V-SHR (SBP: 246.7 ± 3.6 mmHg; DBP: 208.6 ± 5.9 mmHg) at the age of 22 weeks compared with V-WKY (SBP: 175.0 ± 3.5 mmHg; DBP: 128.7 ± 7.1 mmHg; $P < 0.01$). Interestingly, at the age of 22 weeks, blood pressure values were lower ($P < 0.01$) in P144-SHR (SBP: 215.6 ± 5.9 mmHg; DBP: 191.9 ± 4.5 mmHg) than in V-SHR, although they were still higher ($P < 0.01$) than in V-WKY. No significant differences were observed between P144-WKY (SBP: 160.8 ± 5.2 mmHg; DBP: 126.9 ± 4.3 mmHg) and V-WKY.

3.2. Effects of P144 on Cardiac NADPH Oxidase. Cardiac NADPH oxidase activity was higher ($P < 0.05$) in V-SHR than in V-WKY (Figure 1). The administration of P144 reduced ($P < 0.05$) NADPH oxidase activity in P144-SHR to the V-WKY levels. No differences were found between P144-WKY and V-WKY (Figure 1). Accordingly, cardiac mRNA and protein levels of Nox2 (Figure 2) were higher ($P < 0.05$) in V-SHR than in V-WKY. Compared with V-SHR, the administration of P144 reduced mRNA and protein levels of Nox2 (Figure 2) in P144-SHR ($P < 0.01$) to levels similar to V-WKY. Other NADPH oxidase subunits associated with Nox2 NADPH oxidase isoform were also evaluated at mRNA level. Cardiac abundance of p22phox and p47phox was higher ($P < 0.01$) in V-SHR (2.26 ± 0.15 AU and 2.23 ± 0.21 AU, respectively) than in V-WKY (1.00 ± 0.09 AU for p22phox and 1.00 ± 0.08 AU for p47phox). In the same line as the NADPH oxidase activity results, the administration of P144 reduced ($P < 0.01$) the mRNA expression of p22phox

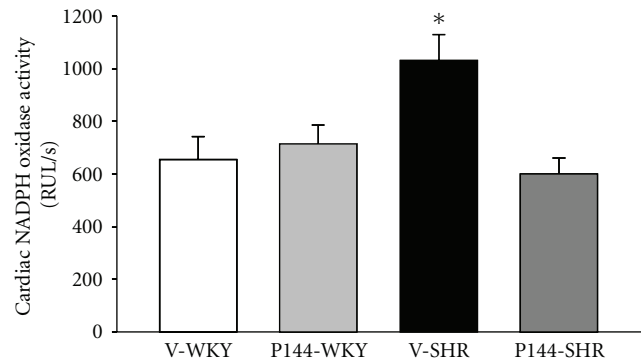


FIGURE 1: Effect of P144 on cardiac NADPH oxidase activity. Cardiac NADPH oxidase-dependent $\cdot\text{O}_2^-$ production was determined by chemiluminescence in the presence of NADPH 200 μ mol/L, and it is expressed as relative light units per second (RLU/s). Histogram represents mean \pm SEM ($n = 10$). V-WKY means vehicle-treated normotensive rat; P144-WKY, P144-treated WKY rat; V-SHR, vehicle-treated spontaneously hypertensive rat, P144-SHR, P144-treated SHR. * $P < 0.05$ versus the other groups.

and p47phox on P144-SHR group (1.47 ± 0.1 AU and 0.99 ± 0.23 AU, respectively) to levels similar to V-WKY.

Interestingly, cardiac mRNA and protein levels of Nox4 NADPH oxidase isoform (Figure 3) were higher ($P < 0.05$) in V-SHR than in V-WKY. Compared with V-SHR, the administration of P144 reduced expression of Nox4 (Figure 3) in P144-SHR ($P < 0.01$) to levels similar to V-WKY.

3.3. Effects of P144 on Cardiac Levels of Nitrotyrosine. Since nitrosylation of proteins is considered a consequence of oxidative stress, the levels of nitrotyrosinated proteins were quantified by Western blot. Following the same pattern that the NADPH oxidase activity determined in heart homogenates, the NT levels were higher ($P < 0.05$) in the V-SHR group than in V-WKY (Figure 4(a)). Similarly, the administration of P144 reduced ($P < 0.05$) the levels of NT expression in P144-SHR. The levels of nitrotyrosinated proteins were similar between V-WKY and P144-SHR.

A direct correlation was found between the cardiac NADPH oxidase activity and NT levels in all the rats ($r = 0.407$, $P < 0.01$), suggesting that the NADPH oxidase overactivity may play an important role in the development of cardiac oxidative stress in this model of hypertension (Figure 4(b)).

3.4. Effects of P144 on Cardiac Collagen Metabolism. Cardiac collagen type I protein expression and mRNA levels were higher ($P < 0.05$) in V-SHR than in V-WKY (Figure 5). The administration of P144 reduced cardiac collagen type I protein expression in P144-SHR. No differences were found between P144-WKY and V-WKY (Figure 5).

The mRNA expression of TGF- β 1, CTGF, fibronectin, biglycan and LOX was higher ($P < 0.01$) in V-SHR than in V-WKY. The chronic administration of P144 resulted in a decreased expression ($P < 0.05$) of the mRNA levels of these molecules (Figure 6).

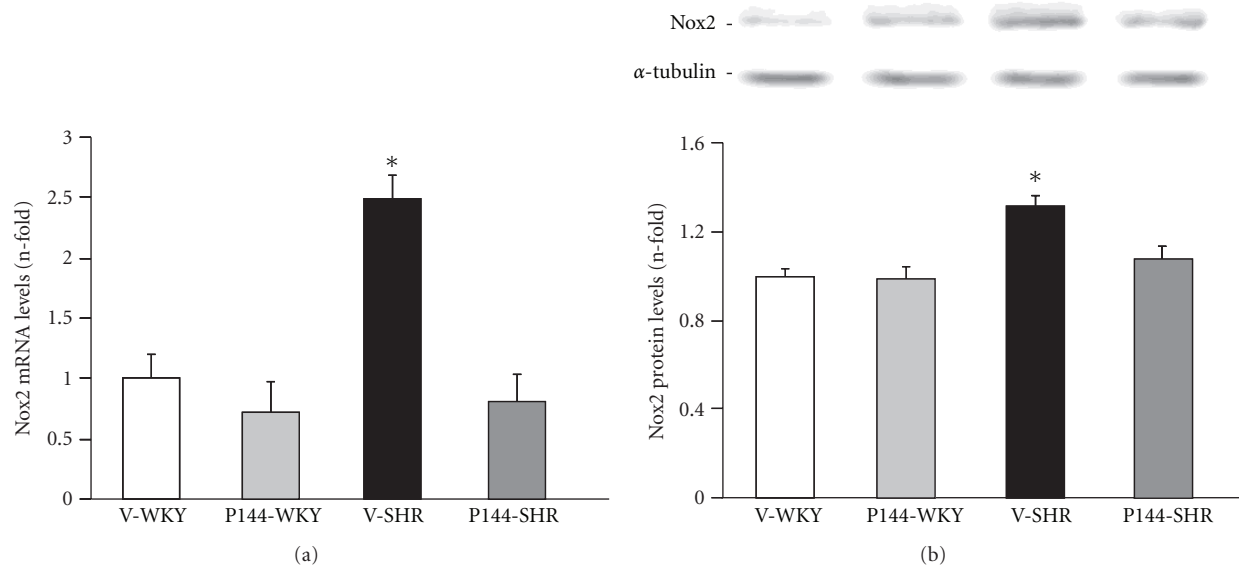


FIGURE 2: Effect of P144 on cardiac Nox2 subunit expression. (a) mRNA levels of Nox2 expressed as a ratio of gene to 18S values from rat heart. (b) Expression of the Nox2 protein levels relative to α -tubulin in the rat heart. Representative western blot of the four groups of rats are shown at the upper part. Histograms represent mean \pm SEM ($n = 10$). V-WKY means vehicle-treated normotensive rat; P144-WKY, P144-treated WKY rat; V-SHR, vehicle-treated spontaneously hypertensive rat; P144-SHR, P144-treated SHR. * $P < 0.05$ versus the other groups.

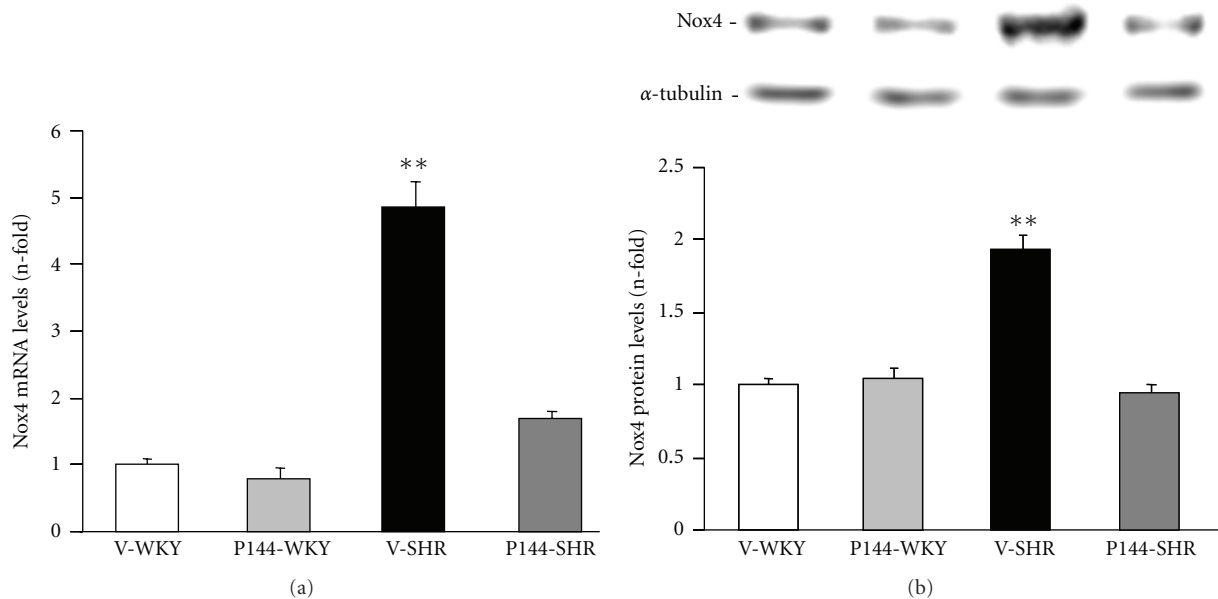


FIGURE 3: Effect of P144 on cardiac Nox4 subunit expression. (a) mRNA levels of Nox4 expressed as a ratio of gene to 18S values from rat heart. (b) Expression of Nox4 protein levels relative to α -tubulin in the rat heart. Representative western blot of the four groups of rats is shown at the upper part. Histograms represent mean \pm SEM ($n = 10$). V-WKY means vehicle-treated normotensive rat; P144-WKY, P144-treated WKY rat; V-SHR, vehicle-treated spontaneously hypertensive rat; P144-SHR, P144-treated SHR. ** $P < 0.01$ versus the other groups.

Moreover, combining data from all groups, direct positive correlations were found between collagen type I protein expression and parameters assessing oxidative stress, that is, NT levels ($r = 0.384$, $P < 0.01$) and NADPH oxidase activity ($r = 0.372$, $P < 0.05$).

3.5. In Vitro Findings. *In vitro* studies showed that TGF- β 1 stimulated ($P < 0.05$) the NADPH oxidase activity in Rat-2 fibroblasts (Figure 7). Interestingly, P144 completely prevented the TGF- β 1-induced NADPH oxidase activity (Figure 7).

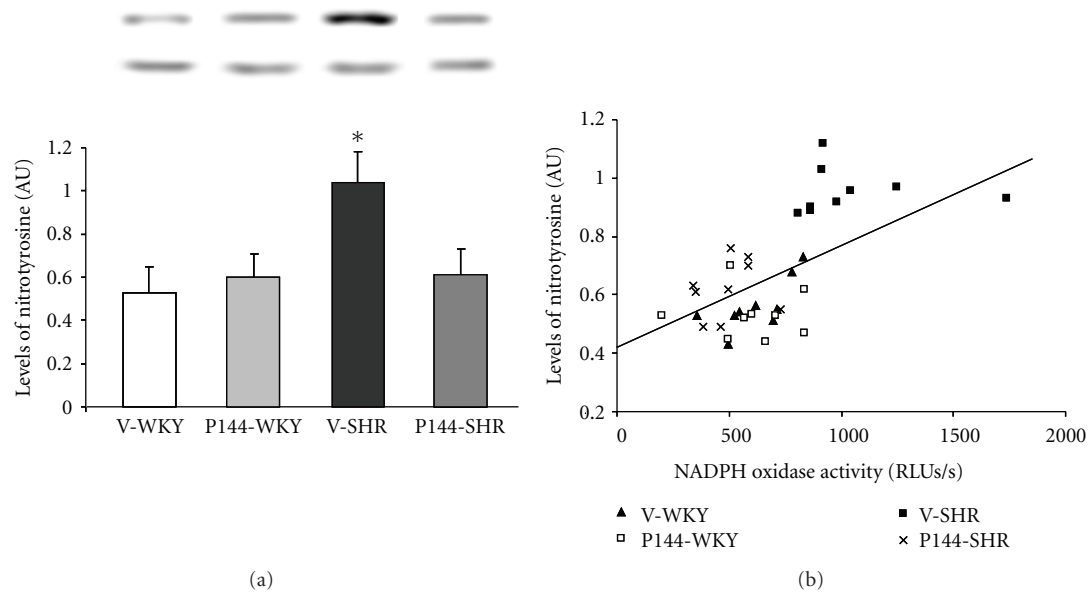


FIGURE 4: Effect of P144 on cardiac levels of nitrotyrosine (NT). (a) Levels of NT relative to α -tubulin in the rat heart. Representative western blot of the four groups of rats are shown at the upper part. Histogram represents mean \pm SEM ($n = 10$). (b) Positive correlation of cardiac NADPH oxidase activity and levels of NT in all the rats ($r = 0.407$; $P = 0.001$; $y = 0.0004x + 0.3797$). RLU/s means relative light units per second. V-WKY means vehicle-treated normotensive rat; P144-WKY, P144-treated WKY rat; V-SHR, vehicle-treated spontaneously hypertensive rat; P144-SHR, P144-treated SHR. * $P < 0.05$ versus the other groups.

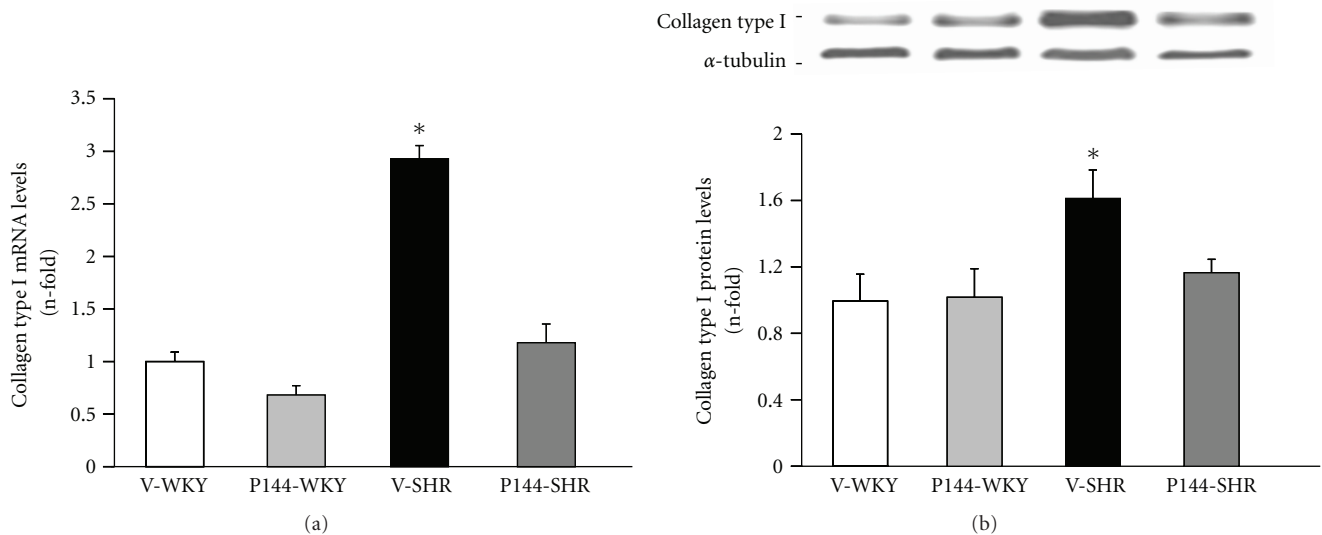


FIGURE 5: Effect of P144 on cardiac collagen type I expression. (a) mRNA levels of collagen type I expressed as a ratio of gene to 18S values from rat heart. (b) Expression of the collagen type I protein relative to α -tubulin in the rat heart. Representative western blot of the four groups of rats are shown at the upper part. Histograms represent mean \pm SEM ($n = 10$). V-WKY means vehicle-treated normotensive rat; P144-WKY, P144-treated WKY rat; V-SHR, vehicle-treated spontaneously hypertensive rat; P144-SHR, P144-treated SHR. * $P < 0.05$ and * $P < 0.05$ versus the other groups.

4. Discussion

The main findings of this study are as follows: (i) the chronic administration of P144 inhibits NADPH oxidase activity and expression, as well as NT-assessed oxidative stress in the heart

of SHR; (ii) the chronic administration of P144 prevents the excessive expression of cardiac collagen type I and molecules related to collagen synthesis in the same rats; (iii) P144 is able to block the TGF- β 1-induced NADPH oxidase activity in cultured rat fibroblasts. Collectively, these findings suggest

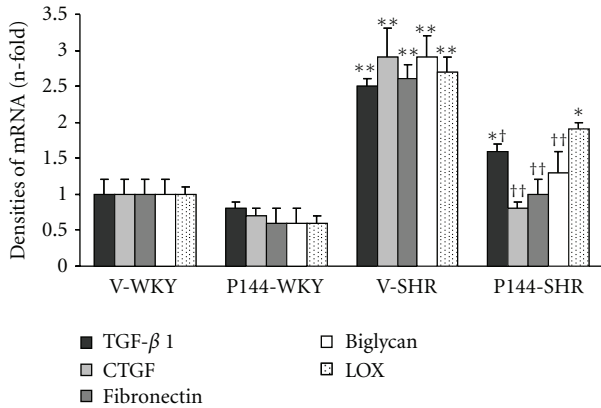


FIGURE 6: Cardiac mRNA levels of genes assessing collagen metabolism. Cardiac mRNA expression of TGF- β 1, connective tissue growth factor (CTGF), fibronectin, biglycan, and lysyl oxidase (LOX) as a ratio of gene to 18S values. Histogram represents mean \pm SEM ($n = 10$). V-WKY means vehicle-treated normotensive rat; P144-WKY, P144-treated WKY rat; V-SHR, vehicle-treated spontaneously hypertensive rat; P144-SHR, P144-treated SHR. * $P < 0.05$ and ** $P < 0.01$ versus V-WKY; $^{\dagger}P < 0.05$ and $^{\dagger\dagger}P < 0.01$ versus V-SHR.

that interference with the TGF- β 1-NADPH oxidase axis by P144 may contribute to the cardiac antifibrotic action of this peptide.

Accumulating evidence indicates that NADPH oxidase activity is increased in several animal models of heart disease [25, 26]. In our study, increased NADPH oxidase activity in V-SHR associated with upregulated Nox2 and associated subunits, namely, p22phox and p47phox. In addition, the elevation of cardiac NT levels in untreated V-SHR was associated with a parallel increase in NADPH oxidase activity, indicating an increase in oxidative stress in the heart of V-SHR, presumably by NADPH oxidase activation. Interestingly, an increased expression of Nox4 isoform was also observed in the heart of V-SHR. Given that it has been demonstrated that Nox4 NADPH oxidase isoform generates mainly H_2O_2 [17], we can speculate that increased cardiac NADPH oxidase activity on V-SHR was due to upregulation of Nox2 isoform and its cytosolic components.

The TGF- β 1 type III receptor or betaglycan is the most abundant TGF- β 1 binding protein at the cell surface [27]. Betaglycan potentiates TGF- β 1 binding to the signaling type I and type II receptors and, therefore, may be involved in ligand presentation [28]. Most of the research to prevent fibrosis in hypertensive heart disease has been focused on the effectiveness of drugs interfering with the angiotensin II-aldosterone-TGF- β 1 axis [29, 30]. In this context, our group has developed a synthetic peptide from the sequence of the extracellular region of human betaglycan, the P144, which was predicted as a potential binder to TGF- β 1 by a computer program [31]. We have recently demonstrated that P144 prevents myocardial fibrosis and collagen type I synthesis in SHR [21].

Diverse experimental approaches have suggested a key role of TGF- β 1 in the activation of the NADPH oxidase. A study in apolipoprotein E-deficient mice demonstrated that

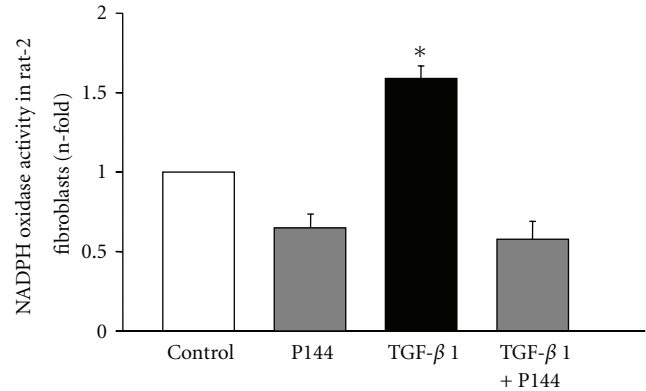


FIGURE 7: Effect of P144 on TGF- β -1-induced NADPH oxidase activity in Rat-2 fibroblasts. Cells were incubated with 10 ng/mL TGF- β 1 (TGF- β 1), 200 μ g/mL P144 (P144), and TGF- β 1 and P144 (TGF- β 1+P144). Data are expressed as fold increase versus control cells incubated in the absence of TGF- β 1 and P144 (Control). Histogram represents mean \pm SEM ($n = 10$). * $P < 0.05$ versus the other groups.

elevated systemic TGF- β 1 levels cause vascular alterations through the NADPH oxidase activation [32]. In addition, the treatment with benidipine of Dahl salt-sensitive rats with heart failure prevented the cardiac dysfunction and remodeling, which was associated with the suppression of TGF- β 1 and inhibited the expression of NADPH oxidase subunits [33]. In rat ventricular myocytes, the oxidative stress caused by the NADPH oxidase system mediated the cardiomyocyte contractile dysfunction caused by TGF- β 1 [34]. In agreement with these studies, we have observed that the treatment with P144 prevented the NADPH oxidase overactivity observed in SHR. In addition, our data showed that the reduction of NADPH oxidase activity by chronic treatment with P144 was associated with a significant reduction of the NADPH oxidase subunit abundance and diminished NT levels in the heart of P144-SHR. Thus, P144 treatment appears to limit oxidative stress by lowering NADPH oxidase abundance in the SHR heart to the levels of the control strain. Studies in adult rat cardiac fibroblasts have shown that NADPH oxidase inhibition blocked the angiotensin II-stimulated collagen production [4]. Finally, the generation of reactive oxygen species in response to Rac has been demonstrated in Rat-2 fibroblasts [35]. Findings from the current study expanded these data by showing that P144 inhibits the ability of TGF- β 1 to stimulate NADPH oxidase activity in the same cell line of rat fibroblasts.

Several studies have shown that a reduction in NADPH oxidase activation was associated with reversed cardiac damage in several experimental models [33, 36, 37]. In fact, Wu et al. demonstrated that the antioxidant properties of acetylsalicylic acid were closely associated with its protective effect against angiotensin II-induced cardiac hypertrophy [26]. In addition, the combination of pioglitazone and candesartan exerted beneficial effects on cardiac fibrosis by attenuating the NADPH oxidase activity [37]. The results of the current study allow us to suggest that the antifibrotic

actions of P144 in experimental hypertension may be associated with its ability to block the TGF- β -1-induced NADPH oxidase activation. Nevertheless, further experiments should be performed to better address this possibility.

Some limitations of the current study must be recognized. First, the dose of 1 mg/kg body weight/day was selected to study the effects of P144 on NADPH oxidase-mediated TGF- β 1 effects. It was previously demonstrated that P144 exhibits hepatic and cutaneous antifibrotic activity at doses above 0.5 mg/kg body weight per day in rodents [19]. In fact, other groups of SHR and WKY rats were previously treated with P144 at the dose of 0.5 mg/kg body weight per day, and no antifibrotic effect at cardiac level was observed (data not shown). Second, although we did not determine H₂O₂ production, it has been proposed that levels of Nox4 protein expression may be representative of Nox4-dependent H₂O₂ production. Finally, to better understand the link between NADPH oxidase and collagen production, further data from *in vitro* studies would be necessary.

In conclusion, the present results support that P144, a peptide synthesized from type III TGF- β 1 receptor, prevented NADPH oxidase-dependent oxidative stress and fibrosis in hearts of SHR. Thus, P144 may be interesting as a therapeutic agent for the protection of the heart against oxidative stress and fibrosis in hypertension. Further studies should be performed to better address this possibility.

Abbreviations

NADPH:	Nicotinamide adenine dinucleotide phosphate
TGF- β 1:	Transforming growth factor- β 1
$\cdot\text{O}_2^-$:	Superoxide anion
SHR:	Spontaneously hypertensive rats
NT:	Nitrotyrosine
CTGF:	Connective tissue growth factor
LOX:	Lysyl oxidase
SBP:	Systolic blood pressure
DBP:	Diastolic blood pressure.

Acknowledgments

This paper was funded through the agreement between the Foundation for Applied Medical Research (FIMA) and UTE project CIMA, the Department of Education of Government of Navarra (87/2007), the Ministry of Science and Innovation (RECAVA RD06/0014/0008) (SAF2008-04228), and the European Union (MEDIA project grant HEALTH-F2-2010-261409). The authors thank Ana Montoya, Raquel Ros, Idoia Rodríguez, and the Morphology and Imaging Department for their technical support.

References

- [1] M. J. Brown and S. Haydock, "Pathoetiology, epidemiology and diagnosis of hypertension," *Drugs*, vol. 59, no. 2, pp. 1–12, 2000.
- [2] G. A. Mensah, J. B. Croft, and W. H. Giles, "The heart, kidney, and brain as target organs in hypertension," *Current Problems in Cardiology*, vol. 28, pp. 156–193, 2003.
- [3] J. Díez, A. González, B. López, and R. Querejeta, "Mechanisms of disease: pathologic structural remodeling is more than adaptive hypertrophy in hypertensive heart disease," *Nature Clinical Practice Cardiovascular Medicine*, vol. 2, no. 4, pp. 209–216, 2005.
- [4] P. J. Lijnen, V. V. Petrov, and R. H. Fagard, "Induction of cardiac fibrosis by transforming growth factor- β 1," *Molecular Genetics and Metabolism*, vol. 71, no. 1-2, pp. 418–435, 2000.
- [5] W. A. Border and N. A. Noble, "Transforming growth factor β in tissue fibrosis," *New England Journal of Medicine*, vol. 331, no. 19, pp. 1286–1292, 1994.
- [6] E. Mata-Greenwood, A. Grobe, S. Kumar, Y. Noskina, and S. M. Black, "Cyclic stretch increases VEGF expression in pulmonary arterial smooth muscle cells via TGF- β 1 and reactive oxygen species: as requirement for NAD(P)H oxidase," *American Journal of Physiology*, vol. 289, no. 2, pp. L288–L298, 2005.
- [7] I. Cucoranu, R. Clempus, A. Dikalova et al., "NAD(P)H oxidase 4 mediates transforming growth factor- β 1-induced differentiation of cardiac fibroblasts into myofibroblasts," *Circulation Research*, vol. 97, no. 9, pp. 900–907, 2005.
- [8] M. M. Murillo, I. Carmona-Cuenca, G. Del Castillo et al., "Activation of NADPH oxidase by transforming growth factor- β in hepatocytes mediates up-regulation of epidermal growth factor receptor ligands through a nuclear factor- κ B-dependent mechanism," *Biochemical Journal*, vol. 405, no. 2, pp. 251–259, 2007.
- [9] V. J. Thannickal and B. L. Fanburg, "Activation of an H₂O₂-generating NADH oxidase in human lung fibroblasts by transforming growth factor β 1," *Journal of Biological Chemistry*, vol. 270, no. 51, pp. 30334–30338, 1995.
- [10] Y. Ishikawa, T. Nishikimi, K. Akimoto, K. Ishimura, H. Ono, and H. Matsuoka, "Long-term administration of Rho-kinase inhibitor ameliorates renal damage in malignant hypertensive rats," *Hypertension*, vol. 47, no. 6, pp. 1075–1083, 2006.
- [11] X. P. Liu, Y. J. Pang, W. W. Zhu et al., "Benazepril, an angiotensin-converting enzyme inhibitor, alleviates renal injury in spontaneously hypertensive rats by inhibiting advanced glycation end-product-mediated pathways," *Clinical and Experimental Pharmacology and Physiology*, vol. 36, no. 3, pp. 287–296, 2009.
- [12] T. Namikoshi, N. Tomita, M. Satoh et al., "Olmesartan ameliorates renovascular injury and oxidative stress in Zucker obese rats enhanced by dietary protein," *American Journal of Hypertension*, vol. 20, no. 10, pp. 1085–1091, 2007.
- [13] S. Ohtomo, M. Nangaku, Y. Izuhara, S. Takizawa, C. V. Y. D. Strihou, and T. Miyata, "Cobalt ameliorates renal injury in an obese, hypertensive type 2 diabetes rat model," *Nephrology Dialysis Transplantation*, vol. 23, no. 4, pp. 1166–1172, 2008.
- [14] A. M. Briones and R. M. Touyz, "Oxidative stress and hypertension: current concepts," *Current Hypertension Reports*, vol. 12, no. 2, pp. 135–142, 2010.
- [15] K. Bedard and K. H. Krause, "The NOX family of ROS-generating NADPH oxidases: physiology and pathophysiology," *Physiological Reviews*, vol. 87, no. 1, pp. 245–313, 2007.
- [16] A. Nabeebaccus, M. Zhang, and A. M. Shah, "NADPH oxidases and cardiac remodelling," *Heart Failure Reviews*, vol. 16, no. 1, pp. 5–12, 2011.
- [17] K. D. Martyn, L. M. Frederick, K. Von Loehneysen, M. C. Dinanier, and U. G. Knaus, "Functional analysis of Nox4 reveals unique characteristics compared to other NADPH oxidases," *Cellular Signalling*, vol. 18, no. 1, pp. 69–82, 2006.
- [18] S. I. Dikalov, A. E. Dikalova, A. T. Bikineyeva, H. H. H. W. Schmidt, D. G. Harrison, and K. K. Griendling, "Distinct roles

- of Nox1 and Nox4 in basal and angiotensin II-stimulated superoxide and hydrogen peroxide production," *Free Radical Biology and Medicine*, vol. 45, no. 9, pp. 1340–1351, 2008.
- [19] B. Santiago, I. Gutiérrez-Cañas, J. Dotor et al., "Topical application of a peptide inhibitor of transforming growth factor- β 1 ameliorates bleomycin-induced skin fibrosis," *Journal of Investigative Dermatology*, vol. 125, no. 3, pp. 450–455, 2005.
 - [20] I. J. Ezquerro, J. J. Lasarte, J. Dotor et al., "A synthetic peptide from transforming growth factor β type III receptor inhibits liver fibrogenesis in rats with carbon tetrachloride liver injury," *Cytokine*, vol. 22, no. 1-2, pp. 12–20, 2003.
 - [21] N. Hermida, B. López, A. González et al., "A synthetic peptide from transforming growth factor- β 1 type III receptor prevents myocardial fibrosis in spontaneously hypertensive rats," *Cardiovascular Research*, vol. 81, no. 3, pp. 601–609, 2009.
 - [22] J. Dabek, A. Kułach, B. Monastyrska-Cup, and Z. Gasior, "Transforming growth factor β and cardiovascular diseases: the other facet of the "protective cytokine"," *Pharmacological Reports*, vol. 58, no. 6, pp. 799–805, 2006.
 - [23] US National Institutes of Health, *Guide for the Care and Use of Laboratory Animals*, NIH Publication no. 85-23, Washington, DC, USA, 1996.
 - [24] K. J. Livak and T. D. Schmittgen, "Analysis of relative gene expression data using real-time quantitative PCR and the 2- $\Delta\Delta$ CT method," *Methods*, vol. 25, no. 4, pp. 402–408, 2001.
 - [25] M. C. Wendt, A. Daiber, A. L. Kleschyov et al., "Differential effects of diabetes on the expression of the gp91 phox homologues nox1 and nox4," *Free Radical Biology and Medicine*, vol. 39, no. 3, pp. 381–391, 2005.
 - [26] R. Wu, M. A. Laplante, and J. De Champlain, "Prevention of angiotensin II-induced hypertension, cardiovascular hypertrophy and oxidative stress by acetylsalicylic acid in rats," *Journal of Hypertension*, vol. 22, no. 4, pp. 793–801, 2004.
 - [27] J. Massagué and B. Like, "Cellular receptors for type β transforming growth factor. Ligand binding and affinity labeling in human and rodent cell lines," *Journal of Biological Chemistry*, vol. 260, no. 5, pp. 2636–2645, 1985.
 - [28] F. López-Casillas, J. L. Wrana, and J. Massagué, "Betaglycan presents ligand to the TGF β signaling receptor," *Cell*, vol. 73, no. 7, pp. 1435–1444, 1993.
 - [29] W. Arozal, K. Watanabe, P. T. Veeraveedu et al., "Effects of angiotensin receptor blocker on oxidative stress and cardio-renal function in streptozotocin-induced diabetic rats," *Biological and Pharmaceutical Bulletin*, vol. 32, no. 8, pp. 1411–1416, 2009.
 - [30] K. Nagata, F. Somura, K. Obata et al., "AT1 receptor blockade reduces cardiac calcineurin activity in hypertensive rats," *Hypertension*, vol. 40, no. 2, pp. 168–174, 2002.
 - [31] J. Esparza-López, J. L. Montiel, M. M. Vilchis-Landeros, T. Okadome, K. Miyazono, and F. López-Casillas, "Ligand binding and functional properties of betaglycan, a co-receptor of the transforming growth factor- β superfamily. Specialized binding regions for transforming growth factor- β and inhibin A," *Journal of Biological Chemistry*, vol. 276, no. 18, pp. 14588–14596, 2001.
 - [32] A. Buday, P. Orsy, M. Godó et al., "Elevated systemic TGF- β impairs aortic vasomotor function through activation of NADPH oxidase-driven superoxide production and leads to hypertension, myocardial remodeling, and increased plaque formation in apoE $-/-$ mice," *American Journal of Physiology*, vol. 299, no. 2, pp. H386–H395, 2010.
 - [33] T. Ohno, N. Kobayashi, K. Yoshida, H. Fukushima, and H. Matsuoka, "Cardioprotective effect of benidipine on cardiac performance and remodeling in failing rat hearts," *American Journal of Hypertension*, vol. 21, no. 2, pp. 224–230, 2008.
 - [34] S. Li, X. Li, H. Zheng, B. Xie, K. R. Bidasee, and G. J. Rozanski, "Pro-oxidant effect of transforming growth factor- β 1 mediates contractile dysfunction in rat ventricular myocytes," *Cardiovascular Research*, vol. 77, no. 1, pp. 107–117, 2008.
 - [35] C. H. Woo, Z. W. Lee, B. C. Kim, K. S. Ha, and J. H. Kim, "Involvement of cytosolic phospholipase A2, and the subsequent release of arachidonic acid, in signalling by Rac for the generation of intracellular reactive oxygen species in Rat-2 fibroblasts," *Biochemical Journal*, vol. 348, no. 3, pp. 525–530, 2000.
 - [36] I. Papparella, G. Ceolotto, L. Berto et al., "Vitamin C prevents zidovudine-induced NAD(P)H oxidase activation and hypertension in the rat," *Cardiovascular Research*, vol. 73, no. 2, pp. 432–438, 2007.
 - [37] T. Nakamura, E. Yamamoto, K. Kataoka et al., "Beneficial effects of pioglitazone on hypertensive cardiovascular injury are enhanced by combination with candesartan," *Hypertension*, vol. 51, no. 2, pp. 296–301, 2008.

Research Article

Ginkgo Biloba Extract EGB761 Protects against Aging-Associated Diastolic Dysfunction in Cardiomyocytes of D-Galactose-Induced Aging Rat

Jing Liu,¹ Junhong Wang,¹ Xiangjian Chen,² Changqing Guo,³ Yan Guo,¹ and Hui Wang⁴

¹ Department of Gerontology, The First Affiliated Hospital of Nanjing Medical University, Nanjing, Jiangsu 210029, China

² Institute of Cardiovascular Disease, The First Affiliated Hospital of Nanjing Medical University, Nanjing, Jiangsu 210029, China

³ Department of Cardiology, Anyang Sixth People Hospital, Anyang, Henan 455000, China

⁴ Department of Cardiology, The Shengze Hospital of Jiangsu Province, SuZhou 215002, China

Correspondence should be addressed to Yan Guo, guoyan51@hotmail.com and Hui Wang, wangnuo@263.net

Received 30 November 2011; Revised 6 March 2012; Accepted 13 March 2012

Academic Editor: Ana Fortuno

Copyright © 2012 Jing Liu et al. This is an open access article distributed under the Creative Commons Attribution License, which permits unrestricted use, distribution, and reproduction in any medium, provided the original work is properly cited.

The aim of the present study was to make use of the artificially induced aging model cardiomyocytes to further investigate potential anti-aging-associated cellular diastolic dysfunction effects of EGB761 and explore underlying molecular mechanisms. Cultured rat primary cardiomyocytes were treated with either D-galactose or D-galactose combined with EGB761 for 48 h. After treatment, the percentage of cells positive for SA- β -gal, AGEs production, cardiac sarcoplasmic reticulum calcium pump (SERCA) activity, the myocardial sarcoplasmic reticulum calcium uptake, and relative protein levels were measured. Our results demonstrated that in vitro stimulation with D-galactose induced AGEs production. The addition of EGB761 significantly decreased the number of cells positive for SA- β -gal. Furthermore, decreased diastolic $[Ca^{2+}]_i$, curtailment of the time from the maximum concentration of Ca^{2+} to the baseline level and increased reuptake of Ca^{2+} stores in the SR were also observed. In addition, the level of p-Ser16-PLN protein as well as SERCA was markedly increased. The study indicated that EGB761 alleviates formation of AGEs products on SERCA2a in order to mitigate myocardial stiffness on one hand; on other hand, improve SERCA2a function through increase the amount of Ser16 sites PLN phosphorylation, which two hands finally led to ameliorate diastolic dysfunction of aging cardiomyocytes.

1. Introduction

Diastolic heart failure (DHF) is most commonly seen in elderly patients and women with a history of diabetes, hypertension, obesity, cardiac ischemia, and so on. Existing research revealed that elevated oxidative stress, NAD(P)H oxidase expression, protein carbonyl formation, protein oxidation, and protein modification as well as enhanced AGE level have been found in aged cardiac myocytes [1]. The major cause for DHF is cardiac aging, which is referred to as a dramatic decline in cardiac pump function with advanced age and resulted in diastolic dysfunction [2, 3]. Due to lack of understanding the mechanism of cardiac diastolic dysfunction, current clinical treatment for patients

with DHF is disappointing [4–6]. Therefore, understanding mechanism of aging myocardial diastolic dysfunction in molecular level is especially important for the specific therapeutic targets of DHF association with aging.

D-galactose is a reducing sugar that reacts readily with the free amines of amino acids in proteins and peptides both in vitro and in vivo to form advanced glycation endproducts (AGEs) [4]. AGE is increased during aging and has been linked to the pathogenesis of many age-associated pathologies such as diabetes, arteriosclerosis, nephropathy, infection, and Alzheimer's disease [5]. Our previous study demonstrated that D-galactose injection led to accelerated aging phenotypes manifested by an increased AGEs level, and aging rats fed with D-galactose present

significant cardiac remodeling compared with adult rats, which was manifested by increased left ventricular posterior wall and interventricular septal thickness and by increased left ventricular weight and impaired diastolic function. The contents of MDA, mtDNA, and AGEs were significantly increased; however, the contents of SOD and GSH-PX were decreased. Therefore, we have simulated aging process in vivo by D-galactose intervention in order to study aging-related cardiac diastolic dysfunction.

The incidence of cardiac diastolic dysfunction is related to an elevated myocardial stiffness and the resting tension (F_{passive}) which led to diastolic capacity decline. The increase in myocardial stiffness is mainly related to AGEs cross-linking with collagen deposition on myocardial interstitium, whereas the latter is mainly related to abnormal myocardial sarcoplasmic reticulum calcium transport regulatory proteins which led the intracellular calcium overload in diastolic phase [6]. Dysregulation of intracellular calcium homeostasis plays a significant role in the aged myocardial cell, which leads to diastolic heart failure. An excessive increase in the intracellular concentration of Ca^{2+} and impaired translocating calcium ions from the cytosol to the lumen of the sarcoplasmic reticulum would result in Ca^{2+} overload and thus produce myocardial diastolic dysfunction [2].

As intracellular calcium is mainly regulated by the activity of myocardial sarcoplasmic reticulum calcium transport regulatory proteins, removal of calcium from the cytosol may be delayed by a decrease in the activity of sarco/endoplasmic reticulum calcium adenosine triphosphate (SERCA) or an increase in the level of activity of phospholamban (PLN), which is a SERCA-inhibitory protein [7]. SERCA and PLN dysfunction may lead to intracellular calcium overload, which further arouse diastolic dysfunction [8].

EGB761 is a standard extract from the leaves of Ginkgo biloba (Yinxing) containing 24% ginkgo-flavone glycosides (e.g., kaempferol, quercetin, and isorhamnetin derivatives) and 6% terpenoid (e.g., ginkgolides A, B, C, J and bilobalide) [9]. Numerous studies have shown that the flavonoid components scavenge superoxide, hydroxyl radicals, and nitric oxide (NO) and protect myocardia from ischemia-reperfusion injury [10–13], and the terpenoid constituents also showed their cardioprotective effects independent from the free radical-scavenging properties [14].

The cardioprotective effects of EGB761 have been demonstrated in various in vivo and in vitro animal models and humans. The existing literature [12, 15], including our prophase research, has highlighted that EGB761 has particular antiaging effects on cardiomyocytes by inhibiting nonenzymatic glycation and reducing the deposition of AGEs in myocardium tissues [12, 16]. However, due to cardiac aging which is referred to diastolic dysfunction, it is unclear yet whether EGB761 can regulate myocardial sarcoplasmic reticulum calcium transport regulatory proteins to improve the diastolic function of aging cardiomyocytes. In this study, we then aimed to investigate the possible action and its molecular mechanisms in cultured D-galactose-induced aging rat cardiomyocytes of treatment EGB761.

2. Materials and Methods

2.1. Drugs and Reagents. Standard EGB761 preparation that we used mainly contains 4.2 mg flavonoid from Dr. Willmar Schwabe Pharmaceuticals (Karlsruhe, Germany); D-galactose and caffeine were purchased from Sigma Aldrich Inc (G5388; C1778); Dulbecco's modified Eagle's medium (DMEM) and fetal calf serum (FCS) were purchased from Gibco Invitrogen (31600-034; 16000044); senescence β -galactosidase (β -gal) staining kit was purchase from Cell Signaling (no. 9860); rat AGEs ELISA kit was purchased from ADL Technology Inc (E0263r). The enhanced chemiluminescence (ECL) Western blotting detection kit was purchased from Pierce Rockford, IL, USA. Other materials used are specified in detail in the following sections.

2.2. Primary Culture of Cardiomyocytes. Neonatal cardiomyocytes were obtained from 20 Sprague-Dawley rats aged 1–2 days. Cardiac tissue was harvested using previously described protocols with minor modifications [17]. The ventricles from the rats were minced and dissociated in 0.06% trypsin at 37°C. The dissociated myocytes were placed into DMEM supplemented with 20% fetal calf serum and 100 U/mL penicillin and streptomycin in a 50 mL Corning cell culture flask for 1.5 h at 37°C with 5% CO_2 , which minimized nonmyocyte cells by adhesion to the bottom of the flask. The nonattached myocytes were then removed and plated ($5\text{--}6 \times 10^5/\text{mL}$) into a six-well culture cluster at 37°C in room air with 5% CO_2 . After incubation for 48 h, 80% of the attached myocytes were beating spontaneously and were used for further experiments. All procedures were performed in accordance with the Guide for the Care and Use of Laboratory Animals (National Institutes of Health Publication no. 85-23, revised 1996).

2.3. D-Galactose Treatment Protocol. The treatment protocol for D-galactose induction was as previously described [18]. Once the attached myocytes were beating spontaneously, the DMEM supplemented with 20% fetal calf serum was removed, and DMEM supplemented with 5 g/L D-galactose was added to the cardiomyocytes in the culture cluster for a further 48 h incubation period. In addition, for the cardioprotection study, EGB761 plus D-galactose was added into the culture media at concentrations of 5, 10, and $20 \mu\text{g} \cdot \text{mL}^{-1}$ throughout the treatment.

2.4. SA β -Gal Staining. Senescence-associated β -gal (SA- β -gal) activity was measured with the β -gal staining kit at pH 6.0 according to the instructions from the manufacturer. Briefly, cells were washed in phosphate buffered saline (PBS), fixed for 10–15 min at room temperature with 1 mL of fixative solution and incubated overnight at 37°C with the staining solution mix. Cells were observed for development of the blue coloration with a microscope at a magnification of $\times 400$.

2.5. AGEs ELISA Assay. The AGEs assay was performed with AGEs ELISA kit according to the instructions from the

manufacturer. The reagents of the test kit were placed at room temperature for 30 min and diluted 1 : 20 with distilled water. Aliquots of 100 μL of the standards and samples were added to blank micropores and 50 μL enzyme marker solution was added. Microtiter plates were incubated at 37°C for 60 min and then washed five times and put aside for 10–20 s each time. The A and B substrate solutions (50 μL) were added into the microtiter plates for 15 min dark reactions at 37°C. The reaction was terminated by the addition of 50 μL stop solution, and the optical density (OD) at 450 nm was determined by an ultra microplate reader (ELX 808 IU, Bio-Tek Instruments Inc.). An AGEs standard curve was generated and the AGEs values of the samples were calculated from the standard curve.

2.6. Measurement of Cardiac SERCA Activity. SERCA activity was determined by a modified p-nitrophenyl phosphate (p-NPP) method routinely used in our laboratory [19]. Briefly, cardiomyocytes were homogenized and centrifuged at 4°C for 15 min. A 10 μL aliquot of supernatant was preincubated for 10 min at 37°C with 80 μL buffer solution containing: 10 μL MgCl_2 , 10 μL EGTA, 10 μL KCl, 30 or 40 μL HEPES (pH 7.4), and 10 μL 0.01% TritonX-100, either with or without 10 μL CaCl_2 . The phosphatase reaction was started by the addition of 10 μL 10 mM p-NPP disodium salt hexahydrate and stopped after 30 min by the addition of 100 μL 500 mM Tris (pH 8.7) and 55 mM EDTA. The liberated p-nitrophenol was measured by an ultra microplate reader (ELX 808 IU) at a wavelength of 405 nm and a standard curve was generated. The SERCA activity was expressed as the amount of p-nitrophenol produced per gram of protein in a minute ($\mu\text{mol/g/min}$).

2.7. Measurement of $[\text{Ca}^{2+}]_i$ and SR Ca^{2+} Load. Field myocyte on the cell culture dishes (Corning Inc) and $[\text{Ca}^{2+}]_i$ were measured as previously described [19], using Fura-2/AM (2.0 μM , Invitrogen) for 30 min at 37°C. SR Ca^{2+} load was measured as the $\Delta[\text{Ca}^{2+}]_i$ amplitude upon rapid exposure to 10 mM caffeine. The ratio of background-corrected fluorescence at 340 nm excitation to 380 nm excitation (F340/F380 ratio) was regarded as $[\text{Ca}^{2+}]_i$. The time from the maximum concentration of Ca^{2+} to the baseline level was regarded as the time of SR Ca^{2+} uptake.

2.8. Western Blot. Cells were lysed with ice-cold Cell Lysis Reagent containing protease and phosphatase inhibitors (Bi Yun Tian, China, P0013) to extract cytoplasm proteins. The protein concentrations of the cytoplasm were determined by bicinchoninic acid (BCA) protein concentration determination. Equal amounts of protein extracts were separated to 16% SDS/PAGE and blotted onto a polyvinylidene difluoride (PVDF) membranes (Millipore, Technology Inc). The membrane was blocked and probed overnight at 4°C with primary antibodies against SERCA2a (1:1000, ARB Inc.) and Ser16/Thr17-phosphorylated phospholamban (p-PLN) (1:1000, Abcam Inc/1:100, Santa Cruz Inc) and GAPDH (1:3000, Sigma), followed by incubation with horseradish-peroxidase-conjugated secondary antibody for

1 h at room temperature. Blots were developed using an ECL detection system and exposed to X-ray film. Normalized bands densities were analyzed by Gel-pro analyzer software and expressed as ratios to GAPDH.

2.9. Statistical Analysis. All data are presented as mean \pm standard deviation (SD). Statistical analysis was performed by ANOVA for multiple comparisons. Origin 7.0 (OriginLab, USA) was used to perform all statistical analysis. In each case, $P < 0.05$ was considered statistically significant.

3. Results

3.1. EGB761 Prevented against Increased Numbers of SA β -Gal-Positive Cells and Formation of AGEs. To investigate whether cardiomyocytes-treated D-galactose showed a senescent phenotype, we examined the numbers of SA β -gal-positive cells in all groups of cardiomyocytes. In D-galactose-induced cardiomyocytes, the ratio of SA β -gal-positive cardiomyocytes was significantly increased than that of control cardiomyocytes. The addition of EGB761 significantly decreased the number of cells positive for SA- β -gal in a dose-dependent manner, with an optimal concentration of 20 $\mu\text{g}\cdot\text{mL}^{-1}$ ($n = 20$ number of rats each group and $n = 6$ experimental replicates; $P < 0.05$ versus D-galactose).

Meanwhile, AGEs are considered as one of the important markers in cardiac aging. In the present study, AGEs content was significantly increased in the D-galactose-treated group. Significantly decreased AGEs level was observed in different concentrations of EGB761 treatment groups ($n = 20$ number of rats each group and $n = 6$ experimental replicates; $P < 0.05$ versus D-galactose) (Table 1 and Figure 1).

3.2. The Effect of EGB761 on the Intracellular $[\text{Ca}^{2+}]_i$ and SR Ca^{2+} Load. Intracellular Ca^{2+} overload is suggested to be one of the main factors involved in DHF. We then used the Ca^{2+} indicator Fluo2/AM to determine the effect of AGEs on the intracellular $[\text{Ca}^{2+}]_i$, the time that Ca^{2+} uptake into sarcoplasmic reticulum and SR Ca^{2+} load. In the D-galactose group, an increased diastolic $[\text{Ca}^{2+}]_i$ was observed, and the time from the maximum concentration of Ca^{2+} to the baseline level was prolonged compared with the controls ($P < 0.05$). After perfusion with 10 mM caffeine, the amplitude of the caffeine-induced calcium transient ($\Delta[\text{Ca}^{2+}]_i$) also declined in D-galactose-treated group. However, above-mentioned effects were reversed by 20 $\mu\text{g}\cdot\text{mL}^{-1}$ EGB761 ($n = 20$ number of rats each group and $n = 6$ experimental replicates; $P < 0.05$ versus D-galactose). Representative changes in the ratio are shown in Table 2.

3.3. The Effect of EGB761 on SERCA Activity in Cardiomyocytes. To investigate the mechanism of EGB761 on intracellular $[\text{Ca}^{2+}]_i$ and SR Ca^{2+} load, the SR Ca^{2+} -ATPase (SERCA) activity in the cardiomyocytes was measured (Table 3). An obvious suppression of SERCA activity was observed in the D-galactose group, and this inhibition effect was attenuated by 20 $\mu\text{g}\cdot\text{mL}^{-1}$ EGB761 treatment ($n = 20$

TABLE 1: Effects of EGB761 on the numbers of SA β -gal-positive cell and formation of AGEs.

Group	Control (<i>N</i> = 20)	5 g·L ⁻¹ D-galactose (<i>N</i> = 20)	5 g·L ⁻¹ D-galactose + 5 μ g·mL ⁻¹ EGB761 (<i>N</i> = 20)	5 g·L ⁻¹ D-galactose + 10 μ g·mL ⁻¹ EGB761 (<i>N</i> = 20)	5 g·L ⁻¹ D-galactose + 20 μ g·mL ⁻¹ EGB761 (<i>N</i> = 20)
The percentage of SA β -gal-positive cell (%)	17.15 \pm 2.9	75.6 \pm 4.9 ^a	57.7 \pm 7.9 ^b	49.7 \pm 9.2 ^c	34.0 \pm 6.6 ^d
AGEs content (pg/mL)	93.22 \pm 26.14	702.58 \pm 32.16 ^a	404.36 \pm 32.94 ^b	356.77 \pm 25.32 ^c	248.72 \pm 77.26 ^d

(Data are means \pm SD, *n* = 6 experimental replicates, ^a*P* < 0.05 Versus control group; ^b*P* < 0.05, ^c*P*, ^d*P* < 0.05 Versus D-galactose group).

TABLE 2: Effects of EGB761 on intracellular diastolic [Ca²⁺]_i, the time from the maximum concentration of Ca²⁺ to the baseline level and SR Ca²⁺ load (Δ [Ca²⁺]_i (%)).

Group	Control (<i>N</i> = 20)	5 g·L ⁻¹ D-galactose (<i>N</i> = 20)	5 g·L ⁻¹ D-galactose + 20 μ g·mL ⁻¹ EGB761 (<i>N</i> = 20)
([Ca ²⁺] _i) _D	0.59 \pm 0.06	0.71 \pm 0.08 ^a	0.61 \pm 0.07 ^b
<i>t</i> _{β(ms)}	775.15 \pm 121.68	1000.95 \pm 129.34 ^a	834.36 \pm 301.85 ^d
Δ [Ca ²⁺] _i (%)	0.53 \pm 0.19	0.11 \pm 0.02 ^a	0.47 \pm 0.16 ^b

(Data are means \pm SD, *n* = 6 experimental replicates, ^a*P* < 0.05 versus control group; ^b*P* < 0.05 versus D-galactose group).

TABLE 3: Effects of EGB761 on sarcoplasmic reticulum calcium pump (SERCA2a) activity.

Group	SERCA2a activity (μ mol/g/min)
Control	2.68 \pm 0.35
5 g·L ⁻¹ D-galactose	1.60 \pm 0.28 ^a
5 g·L ⁻¹ D-galactose + 20 μ g·mL ⁻¹ EGB761	2.43 \pm 0.44 ^b

(Data are means \pm SD, *n* = 6 experimental replicates, ^a*P* < 0.05 versus control group; ^b*P* < 0.05 versus D-galactose group).

number of rats each group and *n* = 6 experimental replicates; *P* < 0.05 versus D-galactose).

3.4. The Effect of EGB761 on Sarcoplasmic Reticulum Calcium Transport Regulatory Proteins Expression in Cardiomyocytes. In order to investigate the underlying mechanisms of EGB761 protecting against aging-associated diastolic dysfunction in cardiomyocytes, protein levels of calcium transport regulatory proteins were measured by Western blot. As shown in Figure 2, an approximately 60% downregulation of SERCA2a protein expression was observed in D-galactose-treated cardiomyocytes, while it was increased in addition of EGB761 compared with the D-galactose group (*P* < 0.05). Since the inhibitory effect of PLN on SERCA2a was dependent on the phosphorylation level of PLN, p-Ser¹⁶-PLN and p-Thr¹⁷-PLN protein expressions were then measured. As shown in Figure 2, the level of p-Ser¹⁶-PLN protein expression was markedly decreased by 54% in the D-galactose-treated cardiomyocytes compared with the control group, while it was increased in the EGB761 group (*P* < 0.05 versus D-galactose). However, the level of p-Thr¹⁷-PLN protein expression showed no significant changes in any groups (*n* = 20 number of rats and *n* = 6 experimental replicates; *P* < 0.05 versus D-galactose).

4. Discussion

With the discovery of in vivo derived AGEs and then several cell-surface AGE-binding proteins, much research has been devoted to studying AGE formation and the potential biological effects of AGEs [20]. Several earlier reports showed that free radicals were increased in D-galactose-treated animals and suggested that the increased free radicals may account for the underlining mechanism responsible for the acceleration of aging [21, 22]. However, data in earlier study from Song et al. has shown that the aging change is not D-galactose specific and aminoguanidine as an AGE inhibitor preventing sugar-induced aging changes suggests that glycation, rather than free radicals, is the major cause of aging in this model [4]. In our current study, myocardial cells chronic incubation with D-galactose has been used as an artificially induced cardiomyocytes aging model for AGEs formation and to further investigate potential anti-aging-associated diastolic dysfunction effects of EGB761 and underlying molecular mechanisms.

The senescent phenotypes are associated with a typical gene expression profile [23]; a senescent morphology increases in senescence-associated β -galactosidase (SA β -gal) activity [24]. Our data showed that the numbers of SA β -gal-positive cells were significantly increased in all of cardiomyocytes after D-galactose treatment for 48 h. Meanwhile, intracellular AGEs content was significantly elevated compared with control group. It is confirmed that D-galactose-induced cardiomyocytes aging model was successfully established in vitro. It is in agreement with those ideas in the previous literature that is accumulation of AGEs may associate with aging [1]. When EGB761 was included, however, the numbers of SA β -gal-positive cells and intracellular AGEs content were significantly decreased, which may indicate that EGB761 can attenuate the intracellular formation of AGEs and delay the cellular senescence.

Relaxation dysfunction has been indicated in the aging myocardium [25]. At the cellular level, depressed relaxation

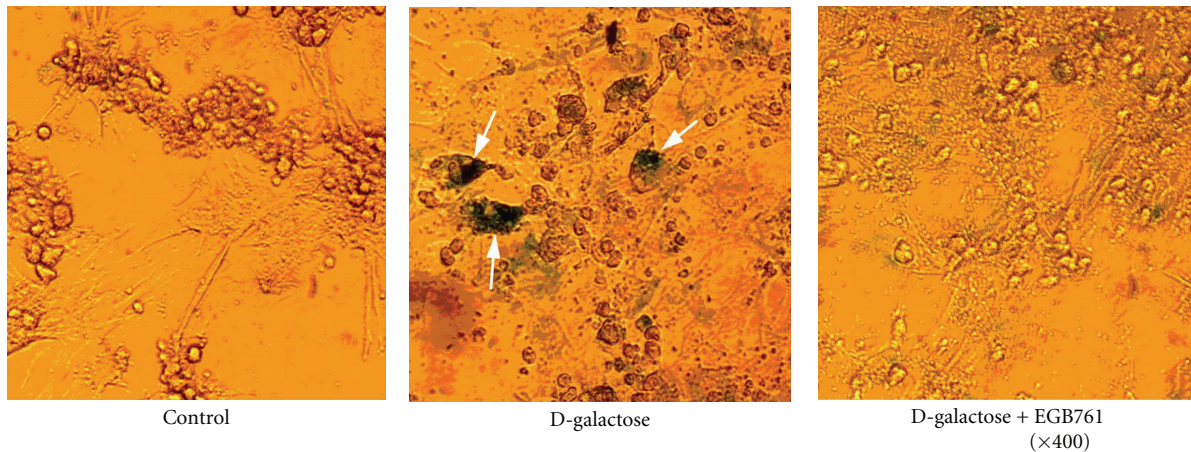


FIGURE 1: Response of neonatal rat cardiomyocytes to $5 \text{ g} \cdot \text{L}^{-1}$ D-galactose and $5 \text{ g} \cdot \text{L}^{-1}$ D-galactose combined with $20 \mu\text{g} \cdot \text{mL}^{-1}$ EGB761 for 48 h. Phase-contrast images showing morphologic changes and stained cells. (SA- β -gal positive cells; Blue, magnification $\times 400$).

reflects impaired removal of cytosolic Ca^{2+} and reduced cardiac SR Ca^{2+} loading. Data from our present study depicted that AGEs accumulated on cardiomyocytes lead to impaired intracellular Ca^{2+} handling, which is the main cause of increased diastolic $[\text{Ca}^{2+}]_i$ and a prolonged relaxation duration in aged cardiomyocytes. Meanwhile, similar with the results previous reported by Petrova et al. [26]. As early as 1996, it was reported that all of these Ca^{2+} removal systems are functionally inhibited in diabetes [27]. Our results also demonstrated that caffeine-induced Ca^{2+} transients, an indication of the reserve of Ca^{2+} in the SR, were significantly reduced. However, given EGB761 could increase reuptake of Ca^{2+} stores in the SR, curtailment of the time of SR Ca^{2+} uptake and a decrease in the diastolic $[\text{Ca}^{2+}]_i$ in cardiomyocytes. These findings have suggested that EGB761 may protect against aging-associated diastolic dysfunction in cardiomyocytes.

Simultaneously Ca^{2+} cycling is a critical determinant of cardiomyocyte contractility and dilation. In mammalian, during relaxation, about 70% of cytosolic Ca^{2+} is partly taken back into the sarcoplasmic reticulum by SERCA2a under the regulation of PLN and partly extruded to the external medium through the action of plasma membrane Ca^{2+} ATPase (PMCA, 2%) and the $\text{Na}^+/\text{Ca}^{2+}$ exchanger (NCX, 28%) [28]. Thus, changed level and/or activity of SERCA2a protein and/or its regulatory protein PLN may influence the homeostasis of cardiac intracellular Ca^{2+} [29]. As the PLN phosphorylation status is the key factor regulating the function of SERCA, the main phosphorylation status of Ser16 and Thr17 sites of PLN was investigated in our study [30]. Our data revealed a significant suppression of SERCA2a function including the activity and protein level due to AGEs accumulation. It is consistent with the results of Bidasee et al. They have shown for the first time that prolongation of cardiac relaxation rate may be attributed to diabetes-induced increase in formation of AGEs (crosslinking as well as noncrosslinking) on SERCA2a in diabetic cardiomyopathy rat. In addition, they also have found that the formation of

AGEs may decrease the amount of serine-16 and threonine-17 phosphorylation of PLN [31].

However, in case of EGB761 additive, the effect of suppression was relieved. Followed by the next experiment, in order to determine which phosphorylation residue of PLN was involved in EGB761 protecting against aging-associated diastolic dysfunction in cardiomyocytes, we determined the amount of p-Ser16-PLN and p-Thr17-PLN protein. Our data showed that decreased p-Ser16-PLN protein level was observed in D-galactose-treated cardiomyocytes; while it was increased in the EGB761 group compared with the D-galactose group ($P < 0.05$). However, the protein level of p-Thr17-PLN showed no significant changes in any of the groups compared with the control cells ($P > 0.05$). Thus, these results may imply that the activity and phosphorylation status of SERCA and PLN are involved in the pathogenesis of cardiac diastolic dysfunction. It was possible that EGB761 could upregulate SERCA2a function through improvement of the amount of Ser16 sites PLN phosphorylation, further improving the homeostasis impairment of intracellular Ca^{2+} .

Since standard EGB761 preparation that we used mainly contains 4.2 mg flavonoid and other unknown complex composition, our results are consistent with the reports demonstrating that flavonoid components exhibit better effects than ginkgolides and bilobalides on protection of SERCA2a function through increasing the amount of Ser16 sites PLN phosphorylation, which decline the intracellular calcium overload [32]. Abdel-Kader et al. also have confirmed that quercetin showed a similar antioxidant effect as EGB761, suggesting that ginkgo-flavone glycosides may be the major components of EGB761 and other unknown complex compositions effect on the endoplasmic reticulum, and other phenotypes tested in our paper may be multifactorial, including its antioxidant, antiglycemic and other properties [32, 33]. In our present study, we treat EGB761 plus D-galactose incubation cardiomyocytes that can effectively and extensively counteract this action of aging-associated diastolic dysfunction. It may be indicated that EGB761

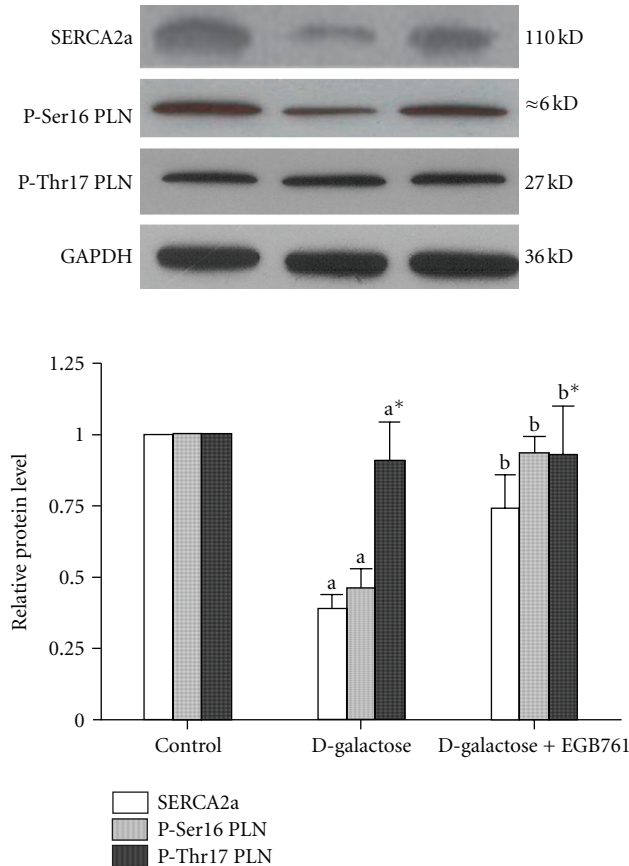


FIGURE 2: Effect of EGB761 on SERCA2a, Ser16-phosphorylated PLN (p-Ser16 PLN), Thr17-phosphorylated PLN (p-Thr17 PLN) protein levels. Representative immunoblots for SERCA2a: p-Ser16 PLN, p-Thr17 PLN, and GAPDH in samples obtained from the control (lane 1), D-galactose (lane 2), D-galactose + EGB761 (lane 3). Summarized data showing SERCA2a, p-Ser16 PLN, and p-Thr17 PLN protein expression normalized. Values are expressed as mean \pm SD ($n = 4$, $^aP < 0.05$ versus control group; $^bP < 0.05$ versus D-galactose group).

extract may be a hypothetical preventive therapy in ageing and AGE-related disease and may potentially protect the heart from AGEs formation [11].

Taken together, due to cardiac diastolic dysfunction which is related to an elevated myocardial stiffness and the resting tension (F_{passive}), it is possible that EGB761 at least partially attenuates the nonenzymatic glycation formation AGEs (crosslinking as well as noncrosslinking) on SERCA2a in cardiomyocytes on one hand, so that it mitigates myocardial stiffness. On other hand, it improves SERCA2a function through increasing the amount of Ser16 sites PLN phosphorylation, which declines the intracellular calcium overload in diastolic phase. The two hands effects of EGB761 may possibly protect against aging-associated diastolic dysfunction in cardiomyocytes. In this case, the EGB761 extract or some of its compounds may be a novel therapeutic strategy in the prevention of the cardiac alterations in diastolic dysfunction for the patients in clinical practice.

5. Conclusions

In summary, EGB761, as an “antiaging” herb, has been used in China for thousands of years which can treat aging-associated diseases. Our work is the first one to directly prove the anti-aging-associated diastolic dysfunction efficacy of EGB761 in cardiomyocytes in vitro. EGB761 may alleviate myocardial stiffness and the resting tension (F_{passive}), thus, protecting against aging-associated diastolic dysfunction in cardiomyocytes.

Authors' Contribution

J. Liu and J. Wang contributed equally to this work.

Acknowledgments

This work was supported by grants from the National Natural Science Foundation of China (nos. 30772781 and 30900602), National Natural Science Foundation of Jiangsu Province (BK2011382), and “Sixth-Peak Talent” of Jiangsu Province (2011WSN-029) to Professor Y. Guo.

References

- [1] S. Y. Li, M. Du, E. K. Dolence et al., “Aging induces cardiac diastolic dysfunction, oxidative stress, accumulation of advanced glycation endproducts and protein modification,” *Aging Cell*, vol. 4, no. 2, pp. 57–64, 2005.
- [2] G. A. Silberman, T. H. M. Fan, H. Liu et al., “Uncoupled cardiac nitric oxide synthase mediates diastolic dysfunction,” *Circulation*, vol. 121, no. 4, pp. 519–528, 2010.
- [3] J. Ren, Q. Li, S. Wu, S. Y. Li, and S. A. Babcock, “Cardiac overexpression of antioxidant catalase attenuates aging-induced cardiomyocyte relaxation dysfunction,” *Mechanisms of Ageing and Development*, vol. 128, no. 3, pp. 276–285, 2007.
- [4] X. Song, M. Bao, D. Li, and Y. M. Li, “Advanced glycation in d-galactose induced mouse aging model,” *Mechanisms of Ageing and Development*, vol. 108, no. 3, pp. 239–251, 1999.
- [5] F. Safciuc, A. Constantin, A. Manea et al., “Advanced glycation end products, oxidative stress and metalloproteinases are altered in the cerebral microvasculature during aging,” *Current Neurovascular Research*, vol. 4, no. 4, pp. 228–234, 2007.
- [6] L. Van Heerebeek, N. Hamdani, M. L. Handoko et al., “Diastolic stiffness of the failing diabetic heart: importance of fibrosis, advanced glycation end products, and myocyte resting tension,” *Circulation*, vol. 117, no. 1, pp. 43–51, 2008.
- [7] S. Dhar, D. Koul, and G. E. D'Alonzo, “Current concepts in diastolic heart failure,” *Journal of the American Osteopathic Association*, vol. 108, no. 4, pp. 203–209, 2008.
- [8] E. Picht, J. DeSantiago, S. Huke, M. A. Kaetzel, J. R. Dedman, and D. M. Bers, “CaMKII inhibition targeted to the sarcoplasmic reticulum inhibits frequency-dependent acceleration of relaxation and Ca^{2+} current facilitation,” *Journal of Molecular and Cellular Cardiology*, vol. 42, no. 1, pp. 196–205, 2007.
- [9] Y. C. Yeh, T. J. Liu, L. C. Wang et al., “A standardized extract of Ginkgo biloba suppresses doxorubicin-induced oxidative stress and p53-mediated mitochondrial apoptosis in rat testes,” *British Journal of Pharmacology*, vol. 156, no. 1, pp. 48–61, 2009.

- [10] J. Shen, J. Wang, B. Zhao, J. Hou, T. Gao, and W. Xin, "Effects of EGb 761 on nitric oxide and oxygen free radicals, myocardial damage and arrhythmia in ischemia-reperfusion injury in vivo," *Biochimica et Biophysica Acta*, vol. 1406, no. 3, pp. 228–236, 1998.
- [11] J. G. Shen and D. Y. Zhou, "Efficiency of ginkgo biloba extract (EGb 761) in antioxidant protection against myocardial ischemia and reperfusion injury," *Biochemistry and Molecular Biology International*, vol. 35, no. 1, pp. 125–134, 1995.
- [12] C. Mozet, R. Martin, K. Welt, and G. Fitz, "Cardioprotective effect of EGb 761 on myocardial ultrastructure of young and old rat heart and antioxidant status during acute hypoxia," *Aging*, vol. 21, no. 1, pp. 14–21, 2009.
- [13] R. Schneider, K. Welt, W. Aust, H. Löster, and G. Fitzl, "Cardiac ischemia and reperfusion in spontaneously diabetic rats with and without application of EGb 761: II. Interstitium and microvasculature," *Histology and Histopathology*, vol. 24, no. 5, pp. 587–598, 2009.
- [14] T. Liebgott, M. Miollan, Y. Berchadsky, K. Drieu, M. Culcasi, and S. Pietri, "Complementary cardioprotective effects of flavonoid metabolites and terpenoid constituents of Ginkgo biloba extract (EGb 761) during ischemia and reperfusion," *Basic Research in Cardiology*, vol. 95, no. 5, pp. 368–377, 2000.
- [15] C. Schiborr, G. P. Eckert, J. Weissenberger et al., "Cardiac oxidative stress and inflammation are similar in SAMP8 and SAMR1 mice and unaltered by curcumin and Ginkgo biloba extract intake," *Current Pharmaceutical Biotechnology*, vol. 11, no. 8, pp. 861–867, 2010.
- [16] D. Jezova, R. Duncko, M. Lassanova, M. Kriska, and F. Moncek, "Reduction of rise in blood pressure and cortisol release during stress by Ginkgo biloba extract (EGb 761) in healthy volunteers," *Journal of Physiology and Pharmacology*, vol. 53, no. 3, pp. 337–348, 2002.
- [17] Y. Maejima, S. Adachi, H. Ito, K. Hirao, and M. Isobe, "Induction of premature senescence in cardiomyocytes by doxorubicin as a novel mechanism of myocardial damage," *Aging Cell*, vol. 7, no. 2, pp. 125–136, 2008.
- [18] B. Chen, Y. Zhong, W. Peng, Y. Sun, and W. J. Kong, "Age-related changes in the central auditory system: comparison of d-galactose-induced aging rats and naturally aging rats," *Brain Research C*, vol. 1344, pp. 43–53, 2010.
- [19] X. L. Xu, X. J. Chen, H. Ji et al., "Astragaloside IV improved intracellular calcium handling in hypoxia-reoxygenated cardiomyocytes via the sarcoplasmic reticulum Ca^{2+} -ATPase," *Pharmacology*, vol. 81, no. 4, pp. 325–332, 2008.
- [20] J. V. Valencia, S. C. Weldon, D. Quinn et al., "Advanced glycation end product ligands for the receptor for advanced glycation end products: biochemical characterization and formation kinetics," *Analytical Biochemistry*, vol. 324, no. 1, pp. 68–78, 2004.
- [21] H. M. Hsieh, W. M. Wu, and M. L. Hu, "Genistein attenuates d-galactose-induced oxidative damage through decreased reactive oxygen species and NF- κ B binding activity in neuronal PC12 cells," *Life Sciences*, vol. 88, no. 1-2, pp. 82–88, 2011.
- [22] X. Zhang, W. Liu, X. Niu, and L. An, "Systemic administration of catalpol prevents d-galactose induced mitochondrial dysfunction in mice," *Neuroscience Letters*, vol. 473, no. 3, pp. 224–228, 2010.
- [23] J. Pedro De Magalhães, F. Chainiaux, F. De Longueville et al., "Gene expression and regulation in H_2O_2 -induced premature senescence of human foreskin fibroblasts expressing or not telomerase," *Experimental Gerontology*, vol. 39, no. 9, pp. 1379–1389, 2004.
- [24] G. P. Dimri, X. Lee, G. Basile et al., "A biomarker that identifies senescent human cells in culture and in aging skin in vivo," *Proceedings of the National Academy of Sciences of the United States of America*, vol. 92, no. 20, pp. 9363–9367, 1995.
- [25] D. Bernhard and G. Laufer, "The aging cardiomyocyte: a mini-review," *Gerontology*, vol. 54, no. 1, pp. 24–31, 2008.
- [26] R. Petrova, Y. Yamamoto, K. Muraki et al., "Advanced glycation endproduct-induced calcium handling impairment in mouse cardiac myocytes," *Journal of Molecular and Cellular Cardiology*, vol. 34, no. 10, pp. 1425–1431, 2002.
- [27] D. Lagadic-Gossmann, K. J. Buckler, K. Le Prigent, and D. Feuvray, "Altered Ca^{2+} handling in ventricular myocytes isolated from diabetic rats," *American Journal of Physiology*, vol. 270, no. 5, pp. H1529–H1537, 1996.
- [28] D. M. Bers, "Cardiac excitation-contraction coupling," *Nature*, vol. 415, no. 6868, pp. 198–205, 2002.
- [29] E. Vafiadaki, V. Papalouka, D. A. Arvanitis, E. G. Kranias, and D. Sanoudou, "The role of SERCA2a/PLN complex, Ca^{2+} homeostasis, and anti-apoptotic proteins in determining cell fate," *Pflugers Archiv European Journal of Physiology*, vol. 457, no. 3, pp. 687–700, 2009.
- [30] K. F. Frank, B. Bölk, E. Erdmann, and R. H. G. Schwinger, "Sarcoplasmic reticulum Ca^{2+} -ATPase modulates cardiac contraction and relaxation," *Cardiovascular Research*, vol. 57, no. 1, pp. 20–27, 2003.
- [31] K. R. Bidasee, Y. Zhang, C. H. Shao et al., "Diabetes increases formation of advanced glycation end products on Sarco(endo)plasmic reticulum Ca^{2+} -ATPase," *Diabetes*, vol. 53, no. 2, pp. 463–473, 2004.
- [32] R. Abdel-Kader, S. Hauptmann, U. Keil et al., "Stabilization of mitochondrial function by Ginkgo biloba extract (EGb 761)," *Pharmacological Research*, vol. 56, no. 6, pp. 493–502, 2007.
- [33] J. Renugadevi and S. Milton Prabu, "Quercetin protects against oxidative stress-related renal dysfunction by cadmium in rats," *Experimental and Toxicologic Pathology*, vol. 62, no. 5, pp. 471–481, 2010.

Research Article

Phytochemical Activation of Nrf2 Protects Human Coronary Artery Endothelial Cells against an Oxidative Challenge

Elise L. Donovan,¹ Joe M. McCord,² Danielle J. Reuland,¹
Benjamin F. Miller,¹ and Karyn L. Hamilton¹

¹ Department of Health and Exercise Science, Colorado State University, 220 Moby B Complex 1582, Fort Collins, CO 80523, USA

² Pulmonary Sciences and Critical Care Medicine, University of Colorado, Denver Anschutz Medical Campus Research Building 29th Floor, 12700 E. 19th Avenue, Aurora, CO 80045, USA

Correspondence should be addressed to Karyn L. Hamilton, karyn.hamilton@colostate.edu

Received 22 December 2011; Accepted 16 March 2012

Academic Editor: Adrian Manea

Copyright © 2012 Elise L. Donovan et al. This is an open access article distributed under the Creative Commons Attribution License, which permits unrestricted use, distribution, and reproduction in any medium, provided the original work is properly cited.

Activation of NF-E2-related factor 2 (Nrf2) is a potential therapeutic intervention against endothelial cell oxidative stress and associated vascular disease. We hypothesized that treatment with the phytochemicals in the patented dietary supplement Protandim would induce Nrf2 nuclear localization and phase II antioxidant enzyme protein in human coronary artery endothelial cells (HCAECs), protecting against an oxidant challenge in an Nrf2-dependent manner. Protandim treatment induced Nrf2 nuclear localization, and HO-1 (778% of control \pm 82.25 P < 0.01), SOD1 (125.9% of control \pm 6.05 P < 0.01), NQO1 (126% of control \pm 6.5 P < 0.01), and GR (119.5% of control \pm 7.00 P < 0.05) protein expression in HCAEC. Treatment of HCAEC with H₂O₂ induced apoptosis in 34% of cells while pretreatment with Protandim resulted in only 6% apoptotic cells (P < 0.01). Nrf2 silencing significantly decreased the Protandim-induced increase in HO-1 protein (P < 0.01). Nrf2 silencing also significantly decreased the protection afforded by Protandim against H₂O₂-induced apoptosis (P < 0.01 compared to no RNA, and P < 0.05 compared to control RNA). These results show that Protandim induces Nrf2 nuclear localization and antioxidant enzyme expression, and protection of HCAEC from an oxidative challenge is Nrf2 dependent.

1. Introduction

Oxidative stress has been implicated in many chronic diseases including Alzheimer's, diabetes and coronary artery disease (CAD) [1–4]. Increased production of reactive oxygen species (ROS) and oxidative damage in the vascular endothelium contribute to CAD initiation and progression. Specifically, increased vascular superoxide causes oxidation of lipids, decreased nitric oxide availability, increased expression of adhesion molecules and inflammatory mediators, and recruitment of monocytes to the endothelium [5–8]. Endothelium-bound superoxide dismutase is also decreased in CAD patients compared to healthy controls, impairing the cellular response to excessive ROS production [9]. Atherosclerotic coronary arteries isolated from humans display increased superoxide production compared

to nonatherosclerotic human coronary arteries, and in a mouse model of atherosclerosis, attenuation of superoxide production by decreased expression of NADPH oxidase (NOX) results in a decrease in atherosclerotic lesion size [10, 11].

Initial studies examining the effects of decreasing oxidative stress in several diseases, including cardiovascular disease, have used exogenous antioxidant supplements such as vitamins C and E. However, the protective effect of exogenous antioxidants has been disappointing and in some cases supplementation increased mortality [12–14]. A novel approach to decreasing disease-associated oxidative stress involves augmenting endogenous antioxidant defense systems rather than relying on exogenous antioxidant supplementation. Protandim is a commercially available dietary supplement consisting of phytochemicals derived from five

widely studied medicinal plants including silymarin from milk thistle, curcumin from turmeric, bacopa extract, ashwagandha, and green tea extract. The five phytochemical components of Protandim have a synergistic effect to induce phase II antioxidant enzymes and protect cells from oxidative stress through activation of the transcription factor NF-E2-related factor 2 (Nrf2) [15, 16].

Nrf2 is constitutively expressed but is marked for ubiquitination by association with Kelch-like ECH-associated protein 1 (Keap1) in the cytosol. Activation of Nrf2 occurs when it is released from Keap1 and translocates to the nucleus. In the nucleus, Nrf2 heterodimerizes with small Maf or Jun proteins and binds to the antioxidant response element (ARE) in the promoter region of several hundred genes including many phase II antioxidant enzymes subsequently initiating transcription [17, 18]. Protandim likely activates Nrf2 through activation of various kinases with subsequent Nrf2 phosphorylation [16, 19].

Although acute activation of Nrf2 occurs *in vivo* in response to oxidized phospholipid signaling, increased ROS production, hyperglycemia, and shear stress [20–22], in chronic disease states the antioxidant response is often insufficient to maintain redox balance and prevent disease progression [22–24]. For example, Landmesser et al. report increased SOD activity in young hypercholesterolemic subjects compared to age-matched controls [9]. In contrast, decreased SOD activity was observed in coronary arteries from CAD patients compared to age-matched controls [9]. Data show that upregulation of phase II antioxidant enzymes can protect against oxidative stress *in vitro* and in humans [16, 25, 26]. It was also recently reported that Protandim protected a human saphenous vein *ex vivo* culture from oxidative stress-induced hyperplasia and vessel wall thickening [27]. Thus, phytochemical-induced Nrf2 activation is a potential therapeutic intervention against endothelial cell oxidative stress and associated vascular disease initiation and progression. Limited research (8 publications) exists examining whether Protandim treatment can minimize the pathologies associated with chronic diseases. The effects of Protandim on Nrf2 and oxidative stress in human coronary vascular cells have not been investigated.

The purpose of this study was to determine (1) if treatment with Protandim induces Nrf2 nuclear translocation and phase II antioxidant enzyme protein expression in human coronary artery endothelial cells (HCAEC), (2) if treatment with Protandim protects HCAEC from apoptosis induced by an oxidant challenge, and (3) if Nrf2 mediates Protandim induced protection from an oxidative challenge. We hypothesized that Protandim treatment would induce Nrf2 nuclear localization and phase II antioxidant enzyme protein expression, and Protandim treatment prior to an oxidant challenge would afford cells protection in a Nrf2 dependent manner.

2. Materials and Methods

2.1. Materials. HCAEC and cell culture reagents, PrimeFect siRNA transfection reagent and PrimeFect diluent

were purchased from Lonza (Walkersville, MD). Heme oxygenase-1 (HO-1) antibody was from Affinity Bioreagents (Golden, CO), nitroquinone oxidoreductase (NQO1), and glutathione reductase (GR) antibodies, and appropriate HRP-conjugated secondary antibodies were purchased from AbCam, (Cambridge, MA). Nrf2, Cu-Zn superoxide dismutase (SOD1), and actin antibodies, HRP- and FITC-conjugated appropriate secondary antibodies, and Nrf2 siRNA, and control RNA were purchased from Santa Cruz Biotech (Santa Cruz, CA). The Santa Cruz Nrf2 siRNA is a pool of 3 19–25 nt siRNA duplexes. Sequence one 5' to 3' sense: GCAUGCACGUGAUGAGAtt, antisense: UCUUCAUCACGUAGCAUGCtt, sequence two 5' to 3' sense: CUCCUACUGUGAUGUGAAAtt, antisense: UUU-CACAUCACAGUAGGAGtt, sequence three 5' to 3' sense: GUGUCAGUAUGUUGAAUctt, antisense: UGAUUCACAUACUGACACtt. The Pierce BCA assay kit for determining protein concentrations, protease and phosphatase inhibitors, and SuperSignal West Dura substrate were from Thermo Scientific (Rockford, IL). TUNEL assay kits were from Roche (Indianapolis, IN).

2.2. Culture of HCAEC. Primary HCAECs were grown in endothelial cell growth medium (EBM-2) containing 5% FBS and manufacturer-recommended supplemental growth factors, antibiotics, and antimycotics. All assays were performed on cells at 80–100% confluence, between passages 3 and 12, and were repeated at least 3 times in duplicate or triplicate.

2.3. Protandim and H₂O₂ Preparation and Treatment. Protandim is a phytochemical composition containing *W. somnifera*, *B. monniera* (45% bacosides), *S. marianum*, *Ca. sinesis* (98% polyphenols and 45% (–)-epigallocatechin-3-gallate), and curcumin (95%) from turmeric (*Cu. longa*) (LifeVantage Corp., Salt Lake City, UT). Protandim extract was prepared by mixing 500 mg Protandim in 5 mL 95% ethanol. The mixture was rocked overnight at room temperature and then centrifuged for 15 min at 3,000 × g. The resulting supernatant contains ethanol extracted Protandim at a concentration of 100 mg/mL. The Protandim extract was diluted to 20 µg/mL with complete cell culture medium for all treatments following initial concentration response experiments that showed 20 µg/mL was the lowest concentration that significantly stimulated phase II antioxidant enzyme protein expression. Cells not treated with Protandim were treated with 95% ethanol as a vehicle control, with a maximum ethanol concentration in the growth medium of 0.02% (2 µL in 10 mL). H₂O₂ (30% W/W) was diluted in complete cell growth medium to a final concentration of 1.25 µM for all treatments. Protandim treatments ranged from 1 hr to 12 hrs as indicated, and H₂O₂ treatments were 4 hrs.

2.4. Western Blot Analyses. HCAEC were seeded in 65 mm polystyrene cell culture dishes and grown to at least 80% confluence prior to Protandim treatment. Following treatment, cells were scraped in RIPA buffer (50 mM Tris, 0.15 M NaCl, 1% Na deoxycholic acid, 1 mM EGTA, 1% NP40) containing protease and phosphatase inhibitors and sonicated

3 × 10 secs. Protein concentrations were determined using a BCA assay, and samples were diluted with Laemmli sample buffer. Samples were separated on 10% polyacrylamide gels at 125 v and transferred to nitrocellulose membranes (BioRad, Hercules, CA) for 1 hr at 50 v. Membranes were blocked for 1 hr in Superblock (Thermo Scientific, Rockford, IL) then incubated with primary antibodies against HO-1 (1:500), SOD1 (1:500), NQO1 (1:1000), GR (1:5000), and β -actin (1:1000) followed by the appropriate HRP-conjugated secondary antibodies. Membranes were developed by chemiluminescence using SuperSignal West Dura substrate (Thermo Scientific, Rockford, IL), with digital images obtained using the Biospectrum UVP system. All signals were normalized to β -actin obtained from the same blot and expressed as the percent of the vehicle control (no Protandim) condition.

2.5. Immunocytochemistry for Nrf2 Nuclear Localization. HCAECs were grown to confluence on coverslips in 35 mm polystyrene cell culture plates coated with 2 $\mu\text{g}/\text{cm}^2$ fibronectin prior to Protandim treatment. Cells were initially treated with Protandim for 1 hr, 2 hrs, 4 hrs, 8 hrs, and 12 hrs to determine the optimal duration of treatment for visualizing Nrf2 nuclear localization. Following time course experiments, all Protandim treatments were for 1 hr. Cells were washed with PBS, fixed for 30 min in 4% paraformaldehyde, washed with PBS, and then permeabilized in cold acetone for 30 min. Cells were blocked for 1 hr in 5% bovine serum albumin with 0.5% goat serum and then incubated with Nrf2 primary antibody (1:100) for 1 hr at room temperature. Cells were washed with PBS then incubated for 45 min in FITC-conjugated secondary antibody at room temperature in the dark. The coverslips were mounted on slides using DAPI containing mounting medium for identification of cell nuclei and visualized by fluorescence microscopy (Nikon TE2000) using Metamorph data acquisition software (Molecular Devices, Sunnyvale, CA).

2.6. TUNEL Assay to Assess Apoptosis. A TdT-mediated dUTP nick end labeling (TUNEL) assay was used to assess HCAEC apoptosis in response to an oxidative challenge. Cells were grown to confluence on fibronectin-coated coverslips prior to Protandim and H_2O_2 treatment. Cells were washed with PBS, fixed for 30 min in 4% paraformaldehyde, washed again with PBS, then permeabilized for 2 min in 0.1% Triton X-100 with 0.1% sodium citrate. Cells were washed again with PBS and incubated in TUNEL reagent for 1.5 hrs. The coverslips were then mounted on slides using DAPI containing mounting medium to identify cell nuclei. Signals were visualized using fluorescence microscopy (Nikon TE2000).

2.7. Nrf2 Silencing. Prior to transfection, 250 μL PrimeFect diluent was mixed with 5 μL PrimeFect transfection reagent and incubated at room temperature for 15 min. Nrf2 siRNA or control RNA was added to the transfection solution for a final concentration of 50 nM and incubated at room

temperature for 15 min. The transfection solution was applied to cells grown to 70–80% confluence in antibiotic free medium, along with 1.25 mL antibiotic free growth medium. The volume of transfection reagent used caused minimal distress to the cells as assessed by minimal changes to cell morphology. After 24 hrs, the transfection solution was removed and the cells were rinsed with PBS, treated with Protandim, and assayed as indicated.

2.8. Statistical Analysis. Unpaired *t*-tests were used to compare control versus Protandim treatments. A two by three treatment (Protandim and no Protandim) by condition (no RNA, control RNA, and Nrf2 siRNA) ANOVA with *a priori* linear contrasts of means was used to analyze Nrf2 silencing experiments. Percent protection was analyzed using one-way ANOVA. Statistical significance was set at $P < 0.05$.

3. Results

3.1. Antioxidant Enzyme Protein Expression Is Elevated in Response to Protandim Treatment. HCAEC were treated with Protandim concentrations of 0 to 50 $\mu\text{g}/\text{mL}$ in 5 $\mu\text{g}/\text{mL}$ increments to determine a profile of Nrf2 activation as measured by HO-1 protein content. HO-1 protein went from barely detectable in control conditions to 8–10-fold greater in cells treated with 20–30 $\mu\text{g}/\text{mL}$ (Figure 1(a)). Concentrations higher than 30 $\mu\text{g}/\text{mL}$ induced morphological changes. In all subsequent treatments 20 $\mu\text{g}/\text{mL}$ Protandim was used. HO-1 protein was visible after 1 hr of Protandim treatment and became significant and sustained from 4 hrs through the longest treatment period of 12 hrs (data not shown). To confirm treatment concentration and duration on multiple antioxidant enzymes we determined that 20 $\mu\text{g}/\text{mL}$ Protandim for 12 hrs induced HO-1 (778% of control \pm 82.25 $P < 0.01$), SOD1 (125.9% of control \pm 6.05 $P < 0.01$), NQO1 (126% of control \pm 6.5 $P < 0.01$), and GR (119.5% of control \pm 7.00 $P < 0.05$) (Figure 1(b)). All subsequent treatments used Protandim at a concentration of 20 $\mu\text{g}/\text{mL}$ for 12 hrs unless otherwise noted.

3.2. Protandim Stimulates Nrf2 Nuclear Localization. HCAECs were treated with Protandim for up to 12 hrs and subsequently visualized using immunocytochemistry to determine Nrf2 nuclear localization. Nrf2 content and nuclear localization were elevated as soon as 1 hr after Protandim treatment initiation. Induction remained with treatments of 2, 4, 8, and 12 hrs (12 hrs was the longest treatment duration examined) (Figure 2).

3.3. Protandim Protects HCAEC from Oxidative Challenge Induced Apoptosis. HCAECs were treated for 12 hrs with Protandim or vehicle control followed by a 4 hr exposure to 1.25 μM H_2O_2 and induction of apoptosis was measured by TUNEL assay. Protandim was removed prior to H_2O_2 exposure. In vehicle controls apoptosis was induced in 34% of cells (Figures 3(a) and 3(b)) while only 6% of cells treated

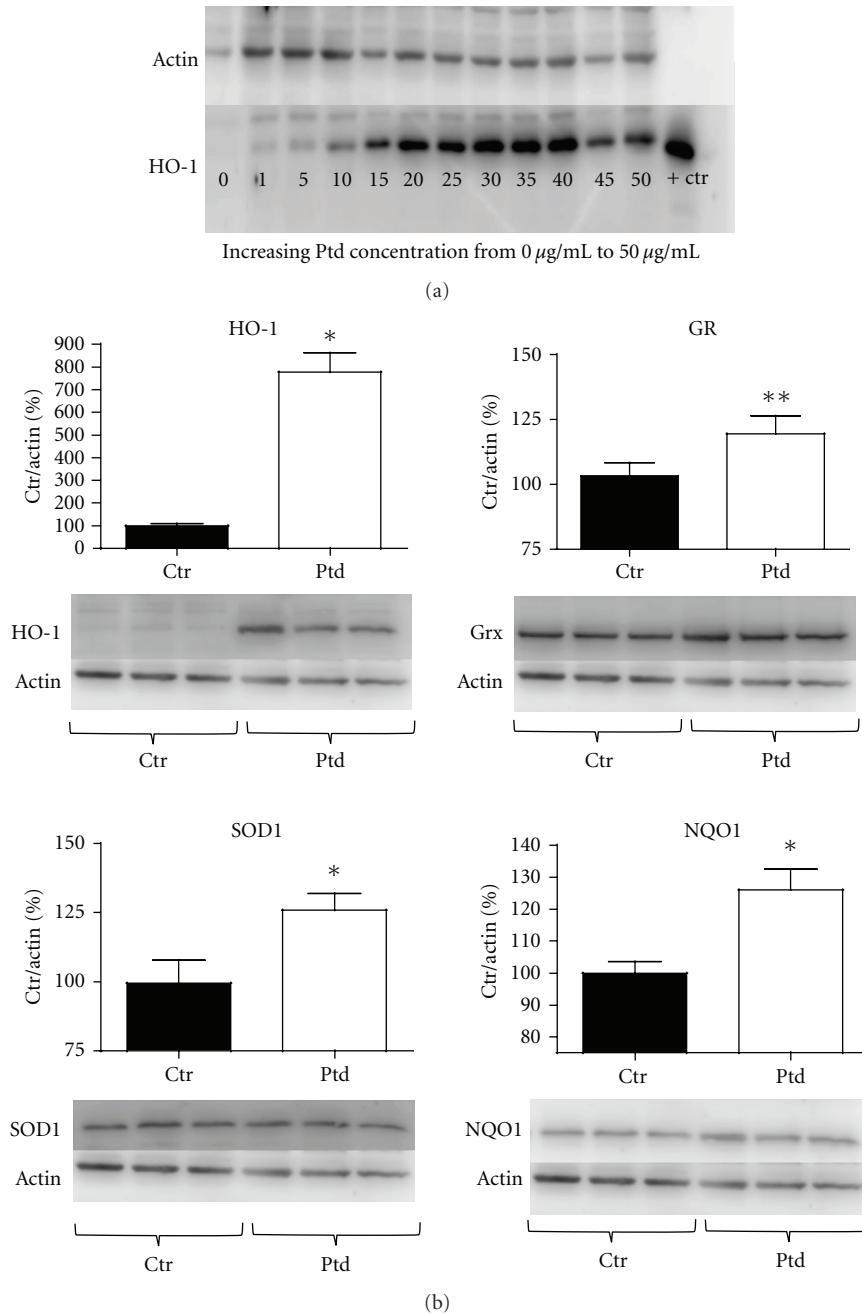


FIGURE 1: Protandim treatment induces phase II antioxidant enzyme protein expression in HCAEC. (a) HCAECs were treated with 1–50 $\mu\text{g}/\text{mL}$ of Protandim for 12 hrs prior to measuring HO-1 protein expression. The HO-1 signal was verified using a purified HO-1 protein extract positive control. (b) Following determination of the appropriate concentration of Protandim, HCAECs were treated with 20 $\mu\text{g}/\text{mL}$ Protandim for 12 hrs then protein expression of HO-1, GR, SOD-1, and NQO1 was determined by Western blot. All bands were normalized to β -actin as a loading control and expressed as a percent of the control (vehicle) condition ($n = 16$ treatments). * $P < 0.01$ compared to control (no Protandim), ** $P < 0.05$ compared to control (no Protandim). Data are presented as mean \pm SE. Ptd: Protandim, Ctr: No Protandim, + Ctr: HO-1 positive control.

with Protandim prior to H₂O₂ were apoptotic ($P < 0.01$ compared to vehicle control) (Figures 3(a) and 3(b)).

3.4. Nrf2 Silencing Diminishes Protandim-Induced Increases in HO-1 and Protection from an Oxidative Challenge. Nrf2 was silenced using siRNA prior to Protandim treatment to

determine if Protandim induced increases in antioxidant enzyme expression and protection occur through Nrf2 activation. Nrf2 silencing prior to Protandim treatment significantly inhibited ($P < 0.01$) Protandim-induced HO-1 protein expression compared to both the no RNA condition, and control RNA condition. (Figures 4(a) and 4(b)). There

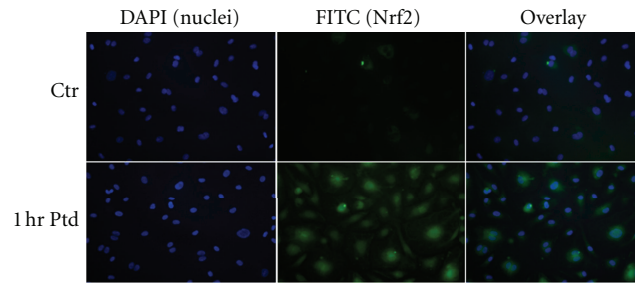


FIGURE 2: Protandim induced Nrf2 expression and nuclear localization. HCAECs were treated with Protandim for 1 hr, following which immunofluorescence was used to visualize changes in Nrf2 expression and localization. Following Protandim treatment Nrf2 signal was greater and became visible in the nucleus. Ptd: Protandim, Ctr: no Protandim.

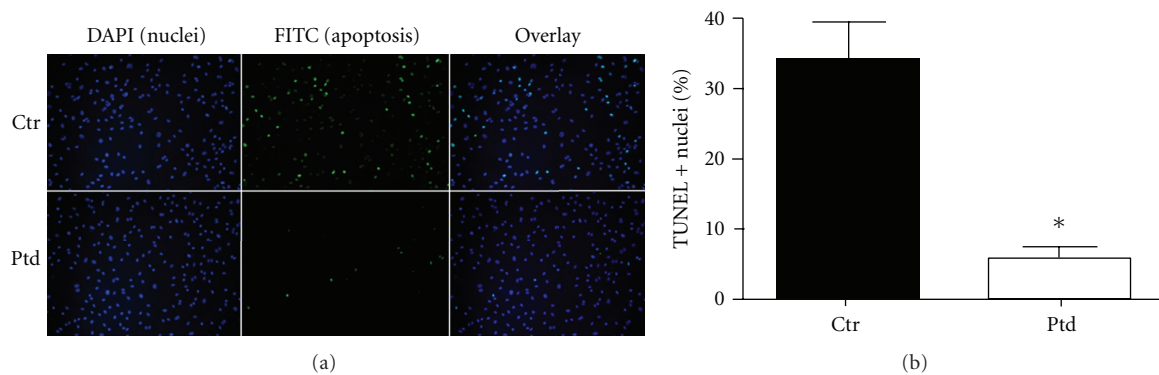


FIGURE 3: Protandim treatment protects HCAEC against an oxidative stress. HCAEC were treated with Protandim for 12 hrs, followed by H_2O_2 4 hrs. (a) Treatment of HCAEC with Protandim prior to an oxidative challenge resulted in significantly fewer apoptotic nuclei as determined by TUNEL assay. (b) Approximately 35% of cells underwent apoptosis without Protandim treatment prior to an oxidative challenge while pre-treatment with Protandim resulted in approximately 5% of cells undergoing apoptosis in response to the same oxidative challenge ($n = 18$ fields) $*P < 0.01$ compared to control (no Protandim). Data are presented as mean \pm SE percent of TUNEL positive (+) nuclei. Ptd: Protandim, Ctr: no Protandim.

were no differences between no RNA and control RNA conditions with or without Protandim.

Nrf2 was then silenced prior to Protandim treatment and an oxidative challenge. In cells receiving no RNA and cells that received control RNA, 30–40% of cells underwent apoptosis (Figures 5(a) and 5(b)). Nrf2 siRNA treatment prior to H_2O_2 resulted in apoptosis in 80% of cells ($P < 0.0001$) compared to no RNA conditions and control RNA (Figures 5(a) and 5(b)). In both no RNA and control RNA conditions, Protandim treatment prior to H_2O_2 resulted in significantly fewer apoptotic cells ($P < 0.0001$) (Figure 5(b)). The number of apoptotic cells in the no RNA condition compared to the control RNA condition was not significantly different with or without Protandim ($P = 0.413$ no Protandim, $P = 0.093$ with Protandim). Protandim prior to Nrf2 siRNA also significantly protected cells from apoptosis ($P = 0.023$); however the amount of protection afforded by the Protandim in this condition was significantly less than in no RNA and control RNA conditions ($P < 0.01$ and $P < 0.05$, resp.) (Figure 5(c)).

4. Discussion

The novel findings of this study were that Protandim treatment of HCAEC induced Nrf2 nuclear localization and

phase II antioxidant enzyme expression, Protandim treatment prior to an oxidative challenge was protective against apoptosis, and this protection was dependent on Nrf2. Our data show that the phytochemical components of Protandim increase Nrf2 in the cytosol and nucleus of HCAEC within an hour of treatment. In cardiac myocytes we have observed increases in Nrf2 within 15 minutes of Protandim treatment (unpublished data). Nrf2 remains elevated through treatment durations up to 12 hours, which was the longest duration examined. These data show for the first time an immediate, substantial, and sustained effect of Protandim on Nrf2 in HCAEC.

4.1. Protandim Induction of Antioxidant Enzymes. The components in Protandim work synergistically to activate Nrf2 and induce antioxidant enzyme expression. HO-1 mRNA was increased to 500 percent of control in response to 40 μ g/mL Protandim in MIN6 cells and 1,000 percent of control in response to 20 μ g/mL Protandim in SK-N-MC cells [16]. However, when each phytochemical component of Protandim was tested individually at the low concentration found in Protandim extract, the maximum increase in HO-1 mRNA was less than 200% of control [16]. While we observed significant increases in protein expression of

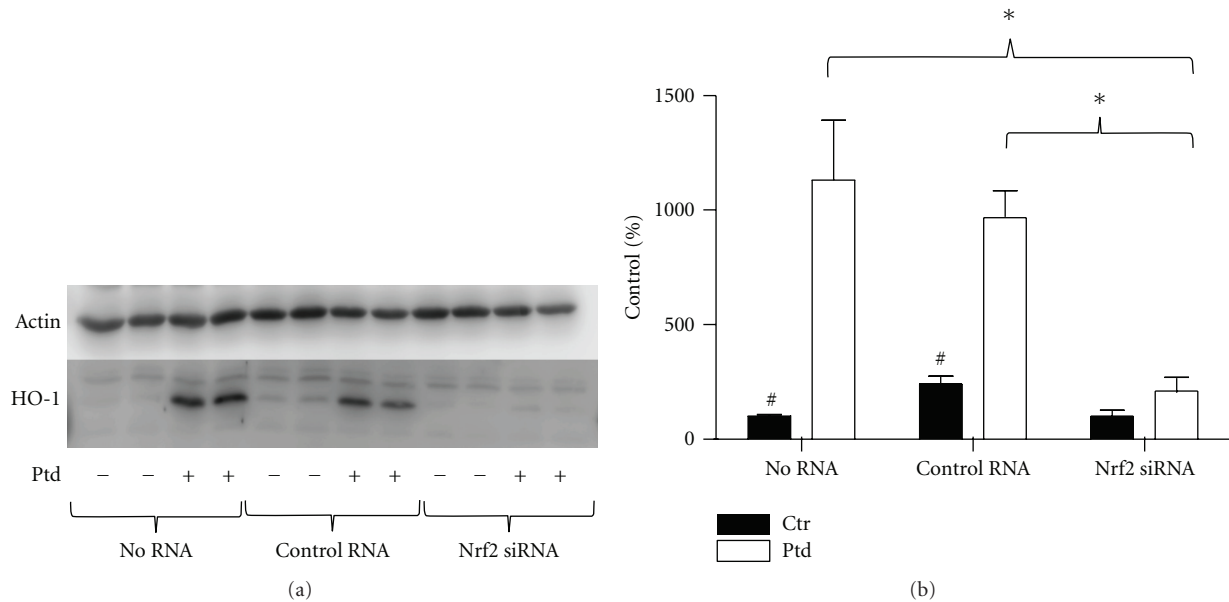


FIGURE 4: Silencing of Nrf2 abrogated Protandim-induced increases in HO-1 expression. (a) Cells were treated with no RNA, control RNA, or Nrf2 siRNA prior to 12 hrs Protandim, then HO-1 expression determined by Western blotting. (b) HO-1 expression in response to Protandim treatment was elevated over 1,000% of control in the no RNA and control RNA conditions, while increases in HO-1 expression in the Nrf2 siRNA condition were negligible. ($n = 6$ treatments per condition). Data are presented as mean \pm SE percent of control (no RNA, no Protandim) condition. * $P < 0.01$ # $P < 0.01$ compared to within RNA condition Protandim treatment. Ptd: Protandim, Ctr: No Protandim.

multiple antioxidant enzymes (approximately 125% of control for SOD1, GR, and NQO1), the Protandim-induced increase in HO-1 was over 700% of control. Until recently, the antioxidant properties of HO-1 were thought to be through production of the ROS scavenger bilirubin, but data now suggest HO-1 may have other antioxidant qualities and be important in multiple cell types in the vasculature. Kadl et al. found that cell death in macrophages was exacerbated in the absence of Nrf2 or with inhibition of HO-1 activity [21]. It has also been demonstrated in macrophages that HO-1 functions as an antioxidant by decreasing heme availability, which decreases expression of the NADPH oxidase heme containing subunit gp91^{phox} and subsequently decreases superoxide production [28].

Decreasing NOX superoxide production has important implications in both macrophages and endothelial cells. Substantial evidence exists demonstrating a role for NOX and increased superoxide production in obesity and atherosclerosis. Compared to nonobese controls, overweight, and obese subjects demonstrate increased NOX subunit expression and augmented oxidative stress in the vascular endothelium [29]. NOX subunit expression is elevated in lesions of coronary arteries in bypass graft patients, particularly in the vicinity of macrophages, and NOX expression levels correlate with severity of atherosclerosis [10]. Superoxide produced by any mechanism including NOX is rapidly converted to H₂O₂. Our experiments used H₂O₂ as an oxidative stress to induce apoptosis in HCAEC. While the concentration of H₂O₂ used in our experiments was chosen based on consistent induction of apoptosis in 30–50% of untreated cells, H₂O₂ is a relevant oxidant *in vivo* [30].

Whether HO-1 also functions as a protective antioxidant in endothelial cells through decreasing heme availability, inhibiting NOX, and decreasing superoxide production, or via an alternative mechanism also is yet to be determined. Greater baseline HO-1 expression in aortic endothelial cells also results in decreased effects of oxidized phospholipids on inflammatory genes [31], suggesting that presence of HO-1 may delay progression of disease-related phenotypic changes when cells are faced with chronic lipid and oxidative stresses. While it was beyond the scope of this study, determining whether HO-1 is essential to the Nrf2-dependent Protandim induced protection against an oxidative challenge is warranted.

SOD1, GR, and NQO1 were also significantly elevated in HCAEC in response to Protandim though the effect was not as large as that seen with HO-1. These are the first data indicating increases in GR and NQO1 in response to Protandim; increases in SOD1 expression and activity have been previously reported [15, 27]. In erythrocytes isolated from human subjects following 120 days of Protandim supplementation, SOD activity was increased by 30% [15]. In an *ex vivo* preparation of human saphenous veins, Protandim treatment increased SOD activity 3-fold, HO-1 activity 7-fold, and catalase activity 12-fold [27]. Catalase has been shown to be increased by Protandim and to mediate protective effects in erythrocytes and saphenous vein preparations, as well as protect against skin cancer development in an animal model [15, 27, 32]. Collectively, these data suggest that the antioxidant enzymes increase following Protandim treatment in a cell type specific manner.

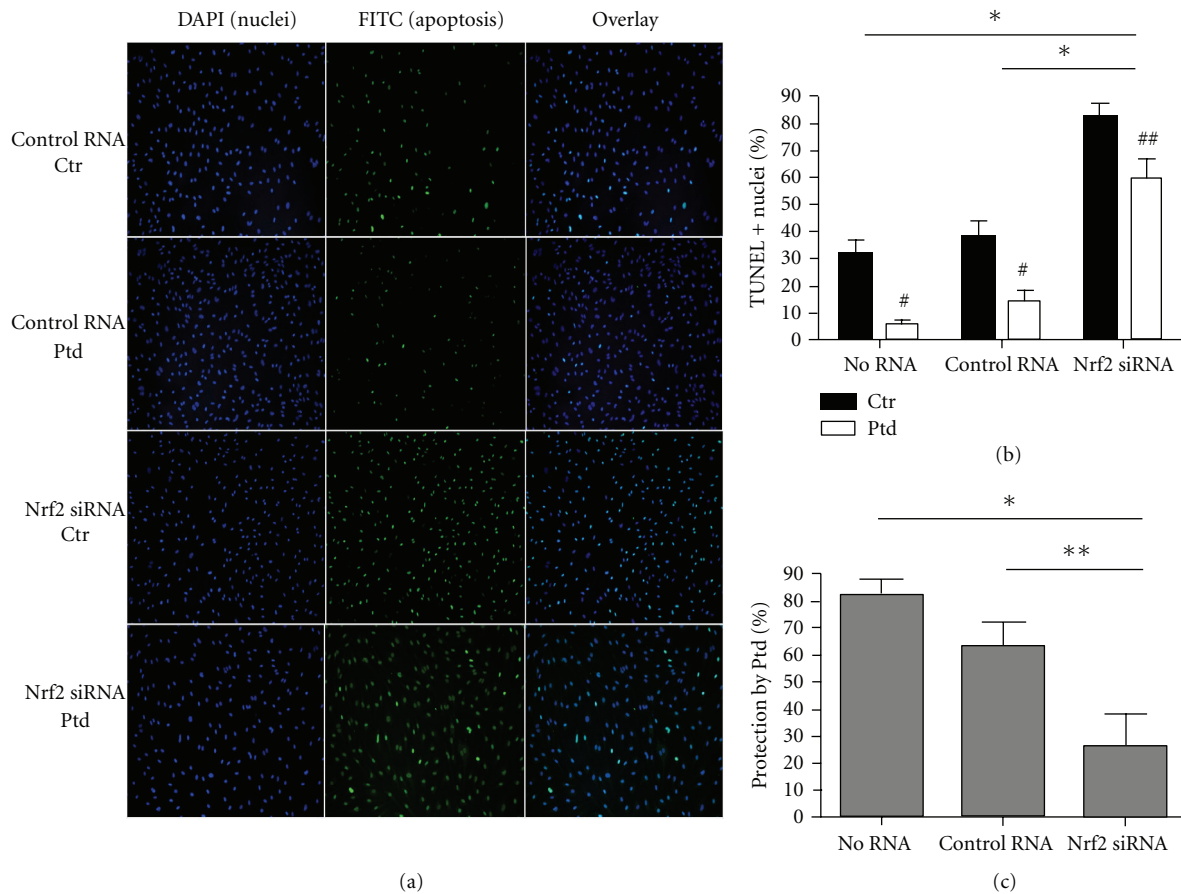


FIGURE 5: Protandim treatment following Nrf2 silencing protected HCAEC against an oxidative challenge; however, protection following Nrf2 silencing was significantly diminished compared to controls. (a) Silencing of Nrf2 resulted in a significant increase in the number of cells undergoing apoptosis in response to an oxidative challenge regardless of Protandim. (b) In no RNA, control RNA, and Nrf2 RNA conditions, significantly fewer cells underwent apoptosis when treated with Protandim prior to an oxidative stress. The no RNA condition and control RNA were not significantly different from each other with or without Protandim. In Nrf2 siRNA conditions, % TUNEL-positive (+) nuclei were significantly higher than no RNA and control RNA conditions with and without Protandim- ($n = 15-19$ fields) (c) The percent protection by Protandim was not significantly different between no RNA and control RNA conditions. The protection afforded by Protandim in the Nrf2 siRNA condition was significantly less compared to both no RNA and control RNA conditions. Data are presented as means \pm SE. * $P < 0.01$ between indicated groups, ** $P < 0.05$ between indicated groups. [#] $P < 0.01$ compared to within RNA condition control (no Protandim), ^{##} $P < 0.05$ compared to within RNA condition control (no Protandim). Ptd: Protandim, Ctr: No Protandim.

4.2. Nrf2 Mediated Protection against an Oxidative Challenge by Protandim. Protandim treatment protected HCAEC from H_2O_2 -induced apoptosis, an effect that was significantly diminished but not abrogated with silencing of Nrf2 prior to Protandim treatment. There are multiple potential explanations for this observation. First, diminished but incomplete protection may be due to the rapid turnover rate in Nrf2. Nrf2 is constitutively expressed and rapidly degraded. In unstimulated cells the half-life of Nrf2 is less than 30 minutes [33]. The delivered Nrf2 siRNA may be diminished prior to the completion of Protandim and H_2O_2 treatments as Nrf2 is rapidly turned over. Second, the amount of siRNA that can be delivered is limited by the ability of the cells to tolerate the transfection procedure. The capacity of the delivered Nrf2 siRNA to silence Nrf2 may be exceeded by the previously noted continuous turnover and subsequent increases in response to Protandim. Finally, antioxidant enzymes can

also be activated independently of Nrf2 by other proteins including p53 and sirtuins [34, 35]. However, our data show that significantly more cells undergo apoptosis in response to an oxidative challenge if Nrf2 is silenced regardless of Protandim treatment indicating the importance of Nrf2 in cytoprotection.

We used apoptosis in endothelial cells as an outcome because it has direct translation to vascular disease development and outcomes. Endothelial cell apoptosis contributes to plaque progression and rupture and may be an independent risk factor for thrombosis [36]. Endothelial cell apoptosis can be induced by oxidized lipids as well as by ROS, and the role of endothelial cell apoptosis in atherosclerosis has been extensively reviewed [37–39].

4.3. Translation and Future Studies. Our data suggest positive effects of Protandim in healthy coronary artery endothelial

cells supporting future examination of how Protandim may affect cells that have been chronically exposed to oxidative and lipid challenges. Most individuals experience transient and/or chronic lipid and oxidative stress in the vasculature throughout life, and it is the accumulated effects that eventually lead to overt vascular disease. Therefore, it is of interest to determine if Protandim can slow or reverse disease related endothelial cell phenotypic changes using *in vivo* models of chronic oxidative stress.

Supplementation with Protandim in humans is safe, with no reported adverse side effects [15, 16]. It has been shown that with oral Protandim supplementation in humans, circulating TBARS, a measure of lipid peroxidation, decrease in 5–12 days, an effect that persists with continued supplementation as measured at 30 and 120 days [15]. In addition, erythrocytes isolated from subjects who ingested Protandim for 120 days had greater SOD and catalase activity compared to controls [15]. The dose ingested by human subjects [15] induces similar increases in antioxidant enzymes compared to the 20 $\mu\text{g}/\text{mL}$ concentration used in our experiments. Thus the effects observed in our cell culture model directly mirror those seen *in vivo* indicating that exposure of cells to the components of Protandim in human subjects is likely similar to what we used *in vitro*. Studies *in vivo* will need to be performed to determine if these results are translatable to intact coronary arteries.

5. Conclusion

Our current investigation shows for the first time that Protandim treatment in HCAEC induces Nrf2 nuclear localization, phase II antioxidant enzyme expression, and Nrf2-dependent protection from an oxidant stress. Oxidative stress has a well-established role in CAD initiation and progression, and our data support further research on phytochemical activation of Nrf2 and the endogenous antioxidant response as a potential therapeutic approach.

Abbreviations

HO-1:	Heme oxygenase-1
Nrf 2:	NF-E2-related factor 2
ROS:	Reactive oxygen species
SOD:	Superoxide dismutase
GR:	Glutathione reductase
NQO1:	NAD(P)H dehydrogenase [quinone] 1
Keap-1:	Kelch-like ECH-associated protein 1
CAD:	Coronary artery disease
HCAEC:	Human coronary artery endothelial cells.

Authors' Contribution

E. L. Donovan, D. J. Reuland, B. F. Miller, and K. L. Hamilton designed research; E. D. conducted research; J. M. McCord provided essential reagents; E. L. Donovan, B. F. Miller, and K. L. Hamilton analyzed data and performed statistical analysis; E. L. Donovan wrote paper. All authors have read and approved the final manuscript.

Acknowledgments

The authors thank Laurie Biela and Dr. Manfred Diehl for their assistance. Funding was provided by CSU Proteomics and Metabolomics Facility Academic Enrichment Program and a Colorado State University CAHS minigrant.

References

- [1] M. F. Walter, R. F. Jacob, B. Jeffers et al., "Serum levels of thiobarbituric acid reactive substances predict cardiovascular events in patients with stable coronary artery disease: a longitudinal analysis of the PREVENT study," *Journal of the American College of Cardiology*, vol. 44, no. 10, pp. 1996–2002, 2004.
- [2] A. P. Robertson, "Chronic oxidative stress as a central mechanism for glucose toxicity in pancreatic islet beta cells in diabetes," *Journal of Biological Chemistry*, vol. 279, no. 41, pp. 42351–42354, 2004.
- [3] C. A. Rottkamp, A. Nunomura, A. K. Raina, L. M. Sayre, G. Perry, and M. A. Smith, "Oxidative stress, antioxidants, and Alzheimer disease," *Alzheimer Disease and Associated Disorders*, vol. 14, supplement 1, pp. S62–S66, 2000.
- [4] D. Harrison, K. K. Griendling, U. Landmesser, B. Hornig, and H. Drexler, "Role of oxidative stress in atherosclerosis," *American Journal of Cardiology*, vol. 91, no. 3, 2003.
- [5] A. C. Carr, M. R. McCall, and B. Frei, "Oxidation of LDL by myeloperoxidase and reactive nitrogen species: reaction pathways and antioxidant protection," *Arteriosclerosis, Thrombosis, and Vascular Biology*, vol. 20, no. 7, pp. 1716–1723, 2000.
- [6] C. P. Judkins, H. Diep, B. R. S. Broughton et al., "Direct evidence of a role for Nox2 in superoxide production, reduced nitric oxide bioavailability, and early atherosclerotic plaque formation in ApoE $^{-/-}$ mice," *American Journal of Physiology, Heart and Circulatory Physiology*, vol. 298, no. 1, pp. H24–H32, 2010.
- [7] S. Lee, N. M. Gharavi, H. Honda et al., "A role for NADPH oxidase 4 in the activation of vascular endothelial cells by oxidized phospholipids," *Free Radical Biology and Medicine*, vol. 47, no. 2, pp. 145–151, 2009.
- [8] M. Rouhanizadeh, J. Hwang, R. E. Clempus et al., "Oxidized-1-palmitoyl-2-arachidonoyl-sn-glycero-3-phosphorylcholine induces vascular endothelial superoxide production: implication of NADPH oxidase," *Free Radical Biology and Medicine*, vol. 39, no. 11, pp. 1512–1522, 2005.
- [9] U. Landmesser, R. Merten, S. Spiekermann, K. Büttner, H. Drexler, and B. Hornig, "Vascular extracellular superoxide dismutase activity in patients with coronary artery disease: relation to endothelium-dependent vasodilation," *Circulation*, vol. 101, no. 19, pp. 2264–2270, 2000.
- [10] D. Sorescu, D. Weiss, B. Lassègue et al., "Superoxide production and expression of Nox family proteins in human atherosclerosis," *Circulation*, vol. 105, no. 12, pp. 1429–1435, 2002.
- [11] A. E. Vendrov, Z. S. Hakim, N. R. Madamanchi, M. Rojas, C. Madamanchi, and M. S. Runge, "Atherosclerosis is attenuated by limiting superoxide generation in both macrophages and vessel wall cells," *Arteriosclerosis, Thrombosis, and Vascular Biology*, vol. 27, no. 12, pp. 2714–2721, 2007.
- [12] G. Bjelakovic, D. Nikolova, L. L. Gluud, R. G. Simonetti, and C. Gluud, "Mortality in randomized trials of antioxidant supplements for primary and secondary prevention: systematic

- review and meta-analysis," *Journal of the American Medical Association*, vol. 297, no. 8, pp. 842–857, 2007.
- [13] I. D. Podmore, H. R. Griffiths, K. E. Herbert, N. Mistry, P. Mistry, and J. Lunec, "Vitamin C exhibits pro-oxidant properties," *Nature*, vol. 392, no. 6676, p. 559, 1998.
 - [14] R. Clarke and J. Armitage, "Antioxidant vitamins and risk of cardiovascular disease. Review of large-scale randomised trials," *Cardiovascular Drugs and Therapy*, vol. 16, no. 5, pp. 411–415, 2002.
 - [15] S. K. Nelson, S. K. Bose, G. K. Grunwald, P. Myhill, and J. M. McCord, "The induction of human superoxide dismutase and catalase in vivo: a fundamentally new approach to antioxidant therapy," *Free Radical Biology and Medicine*, vol. 40, no. 2, pp. 341–347, 2006.
 - [16] K. Velmurugan, J. Alam, J. M. McCord, and S. Pugazhenth, "Synergistic induction of heme oxygenase-1 by the components of the antioxidant supplement Protandim," *Free Radical Biology and Medicine*, vol. 46, no. 3, pp. 430–440, 2009.
 - [17] A. Giudice, C. Arra, and M. C. Turco, "Review of molecular mechanisms involved in the activation of the Nrf2-ARE signaling pathway by chemopreventive agents," *Methods in Molecular Biology*, vol. 647, pp. 37–74, 2010.
 - [18] V. V. Lyakhovich, V. A. Vavilin, N. K. Zenkov, and E. B. Menshchikova, "Active defense under oxidative stress. The antioxidant responsive element," *Biochemistry. Biokhimiia*, vol. 71, no. 9, pp. 962–974, 2006.
 - [19] Y. J. Surh, J. K. Kundu, and H. K. Na, "Nrf2 as a master redox switch in turning on the cellular signaling involved in the induction of cytoprotective genes by some chemopreventive phytochemicals," *Planta Medica*, vol. 74, no. 13, pp. 1526–1539, 2008.
 - [20] M. He, R. C. M. Siow, D. Sugden, L. Gao, X. Cheng, and G. E. Mann, "Induction of HO-1 and redox signaling in endothelial cells by advanced glycation end products: a role for Nrf2 in vascular protection in diabetes," *Nutrition, Metabolism and Cardiovascular Diseases*, vol. 21, no. 4, pp. 277–285, 2011.
 - [21] A. Kadl, A. K. Meher, P. R. Sharma et al., "Identification of a novel macrophage phenotype that develops in response to atherogenic phospholipids via Nrf2," *Circulation Research*, vol. 107, no. 6, pp. 737–746, 2010.
 - [22] E. Warabi, W. Takabe, T. Minami et al., "Shear stress stabilizes NF-E2-related factor 2 and induces antioxidant genes in endothelial cells: role of reactive oxygen/nitrogen species," *Free Radical Biology and Medicine*, vol. 42, no. 2, pp. 260–269, 2007.
 - [23] H. K. Jyrkkänen, E. Kansanen, M. Inkala et al., "Nrf2 regulates antioxidant gene expression evoked by oxidized phospholipids in endothelial cells and murine arteries in vivo," *Circulation Research*, vol. 103, no. 1, pp. e1–e9, 2008.
 - [24] Z. Ungvari, L. Bailey-Downs, T. Gautam et al., "Adaptive induction of NF-E2-related factor-2-driven antioxidant genes in endothelial cells in response to hyperglycemia," *American Journal of Physiology - Heart and Circulatory Physiology*, vol. 300, no. 4, pp. H1133–H1140, 2011.
 - [25] H. Jiang, X. Tian, Y. Guo, W. Duan, H. Bu, and C. Li, "Activation of nuclear factor erythroid 2-related factor 2 cytoprotective signaling by curcumin protect primary spinal cord astrocytes against oxidative toxicity," *Biological and Pharmaceutical Bulletin*, vol. 34, pp. 1194–1197, 2011.
 - [26] S. Liu, W. Hou, P. Yao et al., "Heme oxygenase-1 mediates the protective role of quercetin against ethanol-induced rat hepatocytes oxidative damage," *Toxicol in Vitro*, vol. 26, no. 1, pp. 74–80, 2012.
 - [27] B. Joddar, R. K. Reen, M. S. Firstenberg et al., "Protandim attenuates intimal hyperplasia in human saphenous veins cultured ex vivo via a catalase-dependent pathway," *Free Radical Biology and Medicine*, vol. 50, no. 6, pp. 700–709, 2011.
 - [28] C. Taillé, J. El-Benna, S. Lanone et al., "Induction of heme oxygenase-1 inhibits NAD(P)H oxidase activity by down-regulating cytochrome b558 expression via the reduction of heme availability," *Journal of Biological Chemistry*, vol. 279, no. 27, pp. 28681–28688, 2004.
 - [29] A. E. Silver, S. D. Beske, D. D. Christou et al., "Overweight and obese humans demonstrate increased vascular endothelial NAD(P)H oxidase-p47phox expression and evidence of endothelial oxidative stress," *Circulation*, vol. 115, no. 5, pp. 627–637, 2007.
 - [30] R. R. Brandes and K. Schröder, "Differential vascular functions of Nox family NADPH oxidases," *Current Opinion in Lipidology*, vol. 19, no. 5, pp. 513–518, 2008.
 - [31] C. E. Romanoski, N. Che, F. Yin et al., "Network for activation of human endothelial cells by oxidized phospholipids: a critical role of heme oxygenase 1," *Circulation Research*, vol. 109, pp. e27–e41, 2011.
 - [32] J. Liu, X. Gu, D. Robbins et al., "Protandim, a fundamentally new antioxidant approach in chemoprevention using mouse two-stage skin carcinogenesis as a model," *PloS one*, vol. 4, no. 4, article e5284, 2009.
 - [33] J. Maher and M. Yamamoto, "The rise of antioxidant signaling-The evolution and hormetic actions of Nrf2," *Toxicology and Applied Pharmacology*, vol. 244, no. 1, pp. 4–15, 2010.
 - [34] S. P. Hussain, P. Amstad, P. He et al., "p53-induced up-regulation of MnSOD and GPx but not catalase increases oxidative stress and apoptosis," *Cancer Research*, vol. 64, no. 7, pp. 2350–2356, 2004.
 - [35] P. T. Pfluger, D. Herranz, S. Velasco-Miguel, M. Serrano, and M. H. Tschöp, "Sirt1 protects against high-fat diet-induced metabolic damage," *Proceedings of the National Academy of Sciences of the United States of America*, vol. 105, no. 28, pp. 9793–9798, 2008.
 - [36] F. Xu, Y. Sun, Y. Chen et al., "Endothelial cell apoptosis is responsible for the formation of coronary thrombotic atherosclerotic plaques," *Tohoku Journal of Experimental Medicine*, vol. 218, no. 1, pp. 25–33, 2009.
 - [37] M. Hulsmans and P. Holvoet, "The vicious circle between oxidative stress and inflammation in atherosclerosis," *Journal of Cellular and Molecular Medicine*, vol. 14, no. 1-2, pp. 70–78, 2010.
 - [38] R. S. Frey, M. Ushio-Fukai, and A. B. Malik, "NADPH oxidase-dependent signaling in endothelial cells: role in physiology and pathophysiology," *Antioxidants and Redox Signaling*, vol. 11, no. 4, pp. 791–810, 2009.
 - [39] V. E. A. Stoneman and M. R. Bennett, "Role of apoptosis in atherosclerosis and its therapeutic implications," *Clinical Science*, vol. 107, no. 4, pp. 343–354, 2004.

Research Article

Metformin Rescues the Myocardium from Doxorubicin-Induced Energy Starvation and Mitochondrial Damage in Rats

**Abdelkader E. Ashour,¹ Mohamed M. Sayed-Ahmed,¹
Adel R. Abd-Allah,¹ Hesham M. Korashy,¹ Zaid H. Maayah,¹
Hisham Alkhalidi,² Mohammed Mubarak,² and Abdulqader Alhaider¹**

¹ Department of Pharmacology and Toxicology, College of Pharmacy, King Saud University, P.O. Box 2529, Riyadh 11451, Saudi Arabia

² Department of Pathology, College of Medicine, King Saud University, Riyadh 11461, Saudi Arabia

Correspondence should be addressed to Abdulqader Alhaider, aqahaider@gmail.com

Received 21 November 2011; Revised 11 February 2012; Accepted 26 February 2012

Academic Editor: Martin-Ventura Jose Luis

Copyright © 2012 Abdelkader E. Ashour et al. This is an open access article distributed under the Creative Commons Attribution License, which permits unrestricted use, distribution, and reproduction in any medium, provided the original work is properly cited.

Clinical use of doxorubicin (DOX) is limited by its cardiotoxic side effects. Recent studies established that metformin (MET), an oral antidiabetic drug, possesses an antioxidant activity. However, whether it can protect against DOX-induced energy starvation and mitochondrial damage has not been reported. Our results, in a rat model of DOX-induced cardiotoxicity, show that DOX treatment significantly increased serum levels of LDH and CK-MB, indicators of cardiac injury, and induced expression of hypertrophic gene markers. DOX also caused marked decreases in the cardiac levels of glutathione, CoA-SH and ATP, and mRNA expression of catalase and NQO-1. These biochemical changes were associated with myocardial histopathological and ultrastructural deteriorations, as observed by light and electron microscopy, respectively. Cotreatment with MET (500 mg/kg) eliminated all DOX-induced biochemical, histopathological, and ultrastructural changes. These findings demonstrate that MET successfully prevents DOX-induced cardiotoxicity *in vivo* by inhibiting DOX-induced oxidative stress, energy starvation, and depletion of intramitochondrial CoA-SH.

1. Introduction

The clinical use of doxorubicin (DOX), an anthracycline antibiotic, can have both favorable and unfavorable consequences. On the one hand, DOX is one of the most potent antitumor agents available; on the other hand, its use is limited by development of dose-dependent cardiomyopathy involving cardiomyocyte apoptosis and myocardial fibrosis that may lead to congestive heart failure usually refractory to common medications [1]. Although there is a linear relationship between the cumulative dose received and the incidence of cardiotoxicity, cardiotoxicity may develop in some patients at doses below the generally accepted threshold level [2]. Considerable research has focused on elucidating the mechanisms of DOX-induced cardiomyopathy, aiming at finding ways to prevent the development of cardiotox-

icity. Several mechanisms have been reported, including generation of free radicals and lipid peroxidation of cardiac membranes [3], myocyte damage induced by cardiac calcium overload [4], formation of DOX-iron complex [5], impaired myocardial adrenergic regulation, cellular toxicity of anthracycline metabolites [6], and inhibition of beta-oxidation of long chain fatty acids with the consequent depletion of cardiac ATP [7].

Because of the undisputed key role that DOX plays in the treatment of many neoplastic diseases, one of the research aims being pursued most intensively is the possibility of eliminating its cardiotoxicity or reducing it to an acceptable level. If the cardiac complications resulting from DOX could be prevented or at least reduced, higher doses could potentially be utilized, thereby increasing cancer cure rates. In this regard, various drugs, including L-carnitine [8], dexrazoxane

[9], vitamin E [10], melatonin [11], and resveratrol [12], have been shown to protect against DOX-induced cardiotoxicity. Noticeably, a common theme among these therapeutic approaches is that free radical generation by DOX is being targeted. This highlights the critical role of oxidative stress in DOX-induced cardiac toxicity. This is supported by the findings demonstrating that DOX induces cardiomyocyte apoptosis by reactive oxygen species-dependent mechanism [6, 13]. Interestingly, this pathway has been found to be distinct from apoptosis induced by DOX in tumor cells [14].

The prevalence of glucose intolerance is increased in patients with malignancy [15]. Marks and Bishop [16] have reported that patients with malignant disease had a significantly lower net rate of disappearance of glucose, compared with the control subjects. In addition, DOX itself, at therapeutic doses, has been reported to be highly toxic to endocrine function mainly on insulin secretion [17]. Moreover, glucocorticoids are often included with other agents in cancer treatment to prevent side effects [18, 19]. However, administration of glucocorticoids is commonly associated with impairment of insulin sensitivity, elevations in peripheral glucose levels, and the suppression of the hypothalamic-pituitary-adrenal axis [20]. Insulin resistance is correlated with an enhanced risk for cancer. In addition, the rate of tumor recurrence, metastatic spread, and fatal outcome is higher in cancer patients with hyperglycemia or type II diabetes, as compared with tumor patients without metabolic disease [21]. Taken together, all these previously mentioned findings emphasize the need for an adjuvant drug to be given along with DOX to patients with malignancy, in order to improve glucose tolerance and prevent DOX-induced cardiotoxicity.

Metformin (MET) is an oral biguanide antihyperglycemic drug that is widely used for the management of type 2 diabetes mellitus. Therapeutic effects of MET have been attributed to a combination of improved peripheral uptake and utilization of glucose, decreased hepatic glucose output, decreased rate of intestinal absorption of carbohydrates, and enhanced insulin sensitivity [22, 23]. Beyond its glucose-lowering effects, MET has been shown to exhibit antioxidant properties in various tissues, an effect that is independent of its effect on insulin sensitivity and acts to decrease lipid peroxidation [24, 25]. Further, MET has been demonstrated to exert cardioprotective effects that could be due to its direct beneficial effects on cellular and mitochondrial function and therefore be independent of its insulin-sensitizing effect [26]. Noteworthy, MET has been recently shown to significantly improve left ventricular function and survival via activation of AMP-activated protein kinase (AMPK) in an *in vivo* murine model of heart failure [27].

Based on the aforementioned information, we hypothesized that MET, by virtue of its antioxidant and cardioprotective effects, can protect against DOX-induced cardiomyopathy. The overall objective of the present study was to determine the extent to which MET can protect against DOX-induced-energy starvation and mitochondrial damage and to determine the possible mechanism of this protection. Results from this study may shed the light on the

usefulness of MET, as a safe, clinically approved drug, in such pathological situations.

2. Materials and Methods

2.1. Animals. Adult male Wistar albino rats, weighing 230–250 g, were obtained from the Animal Care Center, College of Pharmacy, King Saud University, Riyadh, Saudi Arabia. Animals were housed in metabolic cages under controlled environmental conditions (25°C and a 12 h light/dark cycle). Animals had free access to pulverized standard rat pellet diet. The protocol of this study has been approved by the Research Ethics Committee of College of Pharmacy, King Saud University, Riyadh, Saudi Arabia.

2.2. Chemicals. DOX was a generous gift from the King Khalid University Hospital drug store. MET, acetyl-CoA, CoA-SH, adenosine triphosphate, and adenosine diphosphate were purchased from Sigma Chemical Company (St. Louis, MO, USA). TRIzol reagent was purchased from Invitrogen Co. (Grand Island, NY, USA). The high-capacity cDNA reverse transcription kits and SYBR Green PCR Master Mix were purchased from Applied Biosystems (Foster City, CA, USA). Metformin was dissolved in normal saline and administered orally at low dose (100 mg/kg) and high dose (500 mg/kg). All other chemicals were of the highest commercially available analytical grade.

2.3. Experimental Design and Treatment Protocol. In this study, the DOX treatment regimen used to develop the cumulative cardiotoxicity was adopted from Beanlands et al. [28] and Sayed-Ahmed et al. [29], while MET dosages (50 and 500 mg/kg, p.o.) were selected based on studies by Anurag and Anuradha [30] and Wang et al. [31], respectively. A total of 60 adult male Wistar albino rats were randomly divided into 6 groups of 10 animals each. In the first group, animals were injected intraperitoneally (i.p.) with normal saline (2.5 mL/kg) and served as a normal control. Animals in the second group were injected, every other day, with DOX (3 mg/kg, i.p.) over a period of 11 days to obtain cumulative dose of 18 mg/kg. Animals in the third and fourth groups received MET (50, 500 mg/kg, p.o., daily), respectively, over a period of 11 days. Animals in the fifth group were injected every other day with DOX (3 mg/kg, i.p.) as in group 2 and daily treated with MET (50 mg/kg, p.o.) over a period of 11 days. Animals in group 6 were injected every other day with DOX (3 mg/kg, i.p.) as in group 2 and daily treated with MET (500 mg/kg, p.o.) over a period of 11 days. Twenty-four hours after receiving the last dose of DOX, animals were anesthetized with light ether anesthesia, and blood samples were obtained from the retro-orbital sinus of the eye. Serum was separated for measurement of lactate dehydrogenase (LDH) and creatine phosphokinase iso-enzyme MB (CK-MB). Immediately after collection of blood samples, animals were sacrificed and hearts were quickly excised, washed with saline, blotted with a filter paper, and homogenized as indicated in the procedures of measurement of each parameter, using a Branson homogenizer (250, VWR Scientific, Danbury, CT, USA).

2.4. Assessment of Serum Levels of Cardiac Enzymes. Serum levels of LDH and CK-MB were determined according to the methods of Buhl and Jackson [32] and Wu and Bowers [33], respectively.

2.5. Determination of CoA-SH and Acetyl-CoA in Isolated Rat Heart Mitochondria. Free CoA-SH and acetyl-CoA were determined in isolated rat heart mitochondria using HPLC as described previously [34]. Briefly, mitochondria were mixed with ice-cold 6% perchloric acid and centrifuged at $300 \times g$ for 5 min at 0.5°C . The resulting supernatant fluid was neutralized to pH 6-7 and then injected into the HPLC apparatus. Chromatographic separation was performed using ODS-Hypersil, 150×4.6 mm i.d., $5 \mu\text{m}$ column (Supelco SA, Gland, Switzerland). The UV detector was adjusted at 254 nm and set at 0.005. A mobile phase of 220 mM potassium phosphate, containing 0.05% dithioglycol (A) and 98% methanol/2% chloroform (B), was used. The flow rate was 0.6 mL/min, and the gradient was as follows: at zero time, 94% A and 6% B; at 8 min, 92% A and 8% B; at 14 min, 87% A and 13% B; at 25 min, 80% A and 20% B; at 40 min, 55% A and 45% B; at 60 min, 94% A and 6% B.

2.6. Measurement of Adenosine Triphosphate in Cardiac Tissue. Adenosine triphosphate (ATP) was determined in heart tissues using high-performance liquid chromatography (HPLC) as described by Botker et al. [35]. In brief, heart tissue was homogenized in ice-cold 6% perchloric acid and centrifuged at 3000 rpm for 15 min at 0.5°C , and the supernatant fluid was injected into the HPLC system (Kontron Instrument, Milano, Italy) after neutralization to pH 6-7. Chromatographic separation was performed at a flow rate of 1.2 mL/min, using ODS-Hypersil, 150×4.6 mm I.D., $5 \mu\text{m}$ column (Supelco SA, Gland, Switzerland) and 75 mM ammonium dihydrogen phosphate as the mobile phase. The peak elution was followed at 254 nm.

2.7. Determination of Reduced Glutathione in Cardiac Tissues. Cardiac tissue levels of the acid-soluble thiols, mainly reduced glutathione (GSH), were assayed spectrophotometrically at 412 nm, according to the method of Ellman [36]. The contents of GSH were expressed as $\mu\text{mol/g}$ wet tissue.

2.8. Histopathology and Electron Microscopy. The heart tissues from all studied groups of rats were analyzed at both histopathological and electron microscopic levels. Three-micron thick sections were performed on the formalin-fixed, paraffin-embedded tissue of the heart, and the sections were stained with routine hematoxylin and eosin stains (H&E). The sections were studied under the optic routine microscope by the histopathologists involved in the study.

The heart tissues submitted for electron microscopy examination were fixed in 3% glutaraldehyde. The tissues were embedded in osmium tetroxide, and the semithin sections were stained with toluidine blue. The adequacy of the sample in each case was checked on the semithin sections. The thin sections were stained with uranyl acetate and lead citrate, then all the sections were examined and photographed by the same histopathologists.

2.9. RNA Preparation and Quantitative Real-Time PCR. To determine the effect of DOX and/or MET on mRNA expression levels of cardiac hypertrophic gene markers (α -MHC and β -MHC) and oxidative stress-mediated genes (glutathione S-transferase- α (GST α), catalase (CAT), NAD(P)H:quinone oxidoreductase 1 (NQO1) and heme oxygenase 1 (HO-1)), we conducted quantitative real-time polymerase chain reaction (qRT-PCR), as follows.

2.9.1. RNA Extraction and cDNA Synthesis. Total RNA from the heart tissue homogenate was isolated using TRIzol reagent (Invitrogen) according to the manufacturer's instructions and quantified by measuring the absorbance at 260 nm; the RNA quality was determined by measuring the 260/280 ratio. Thereafter, first strand cDNA synthesis was performed using the high-capacity cDNA reverse transcription kit (Applied Biosystems), according to the manufacturer's instructions. Briefly, $1.5 \mu\text{g}$ of total RNA from each sample was added to a mix of $2.0 \mu\text{L}$ of 10x reverse transcriptase buffer, $0.8 \mu\text{L}$ of 25x dNTP mix (100 mM), $2.0 \mu\text{L}$ of 10x reverse transcriptase random primers, $1.0 \mu\text{L}$ of MultiScribe reverse transcriptase, and $3.2 \mu\text{L}$ of nuclease-free water. The final reaction mix was kept at 25°C for 10 min, heated to 37°C for 120 min, heated for 85°C for 5 s, and finally cooled to 4°C .

2.9.2. Quantification of mRNA Expression by qRT-PCR. Quantitative analysis of mRNA expression of target genes was performed by RT-PCR through subjecting the resulting cDNA to PCR amplification using 96-well optical reaction plates in the ABI Prism 7500 System (Applied Biosystems). The $25 \mu\text{L}$ reaction mix contained $0.1 \mu\text{L}$ of $10 \mu\text{M}$ forward primer and $0.1 \mu\text{L}$ of $10 \mu\text{M}$ reverse primer (40 nM final concentration of each primer), $12.5 \mu\text{L}$ of SYBR Green Universal Master Mix, $11.05 \mu\text{L}$ of nuclease-free water, and $1.25 \mu\text{L}$ of cDNA sample. The primers used in the current study are listed in Table 1. Assay controls were incorporated onto the same plate, namely, no-template controls to test for the contamination of any assay reagents. The real-time PCR data were analyzed using the relative gene expression (i.e., $\Delta\Delta\text{CT}$) method, as described in Applied Biosystems User Bulletin no. 2. Briefly, the data are presented as the fold change in gene expression normalized to the endogenous reference gene β -actin and relative to a calibrator.

2.10. Statistical Analysis. The data are expressed as mean \pm standard error of the mean (SEM). The significance of differences among groups was evaluated with one-way analysis of variance (ANOVA) followed by the Tukey-Kramer multiple comparison test. *P* values of 0.05 or less were considered significant.

3. Results

3.1. MET Protects against DOX-Induced Cardiac Myocyte Injury. Table 2 shows the effects of DOX, MET, and DOX plus MET on the serum level of cardiotoxicity enzymatic indices, CK-MB and LDH, in rats. Administration of DOX (3 mg/kg) every other day over a period of 11 days resulted

TABLE 1: Primers sequences used for real-time PCR reactions.

Primer set	Sense primer 5' → 3'	Antisense primer 5' → 3'
α -MHC	GGACCACCCATCCTCACTTT	AGCCTCTCATCTCGCATCTC
β -MHC	ACCGCTGAGACAGAGAATGG	GGGTTGGCTTGGATGATTT
GST α	GCTTTACTGTGCAAGGGAGACA	GGAAGGAGGATTCAAGTCAGGA
CAT	CCCGAGTCCAGGCTCTTCT	CGGCCTGTACGTAGGTGTGA
NQO1	CGCAGACCTTGTGATATCCAG	TGTTGCGCTCAATCTCCTCCT
HO-1	ATGGCCTCCCTGTACCACATC	CGTTTCTTCCATCCTTCCAGG
β -Actin	CTGGCACCCAGGACAATG	GCCGATCCACACGGAGTA

TABLE 2: The protective effect of MET against DOX-induced cardiac myocyte injury.

Treatment group	CK-MB (U/L)	LDH (U/L)
Control	331 \pm 16	342 \pm 35
DOX	1125 \pm 94*	1299 \pm 122*
MET, 50 mg/kg	342 \pm 24 [#]	375 \pm 25 [#]
MET, 500 mg/kg	349 \pm 36 [#]	354 \pm 32 [#]
DOX + MET, 50 mg	903 \pm 69*	1030 \pm 67*
DOX + MET, 500 mg	439 \pm 47 [#]	417 \pm 36 [#]

All data represent mean values \pm SEM ($n = 10$).

*indicates significant change from control, at $P < 0.05$.

[#]indicates significant change from DOX, at $P < 0.05$.

TABLE 3: MET rescues the myocardium from DOX-induced depletion of intramitochondrial CoA-SH.

Treatment groups	CoA-SH (nmol/mg protein)	Acetyl-CoA (nmol/mg protein)
Control	3.26 \pm 0.16	13.41 \pm 0.62
DOX	1.89 \pm 0.24*	22.31 \pm 0.89*
MET, 50 mg/kg	2.91 \pm 0.29 [#]	12.19 \pm 0.59 [#]
MET, 500 mg/kg	4.22 \pm 0.20* [#]	8.01 \pm 0.40* [#]
DOX + MET, 50 mg/kg	2.77 \pm 0.16	19.28 \pm 0.93*
DOX + MET, 500 mg/kg	3.06 \pm 0.18 [#]	15.44 \pm 0.78 [#]

All data represent mean values \pm SEM ($n = 10$).

*indicates significant change from control, at $P < 0.05$.

[#]indicates significant change from DOX, at $P < 0.05$.

in a significant 240% and 280% increases in serum LDH and CK-MB, respectively, as compared to the control group. Treatment with MET at dose level either 50 mg/kg or 500 mg/kg for 11 successive days showed nonsignificant changes as compared to the control group. Interestingly, daily administration of MET (500 mg/kg) to DOX-treated rats resulted in a complete reversal of DOX-induced increase in serum CK-MB and LDH to the control values. However, administration of the small dose of MET (50 mg/kg) did not prevent DOX-induced increase in cardiac enzymes.

3.2. MET Rescues the Myocardium from DOX-Induced Depletion of Intramitochondrial CoA-SH. The effects of DOX, MET, and DOX plus MET on the level of CoA-SH and acetyl-CoA in isolated rat heart mitochondria are shown in Table 3. Treatment with DOX resulted in a significant 42% decrease

in CoA-SH level and a significant 66% increase in acetyl-CoA in isolated rat heart mitochondria as compared to the control group. Treatment with MET (500 mg/kg) alone resulted in a significant 30% and 123% increase in CoA-SH level and a significant 40% and 45% decrease in acetyl-CoA as compared to the control and DOX groups, respectively. Interestingly, daily administration of the high dose of MET (500 mg/kg) to DOX-treated rats resulted in a complete prevention of DOX-induced decrease in CoA-SH and increase in acetyl-CoA to the control values.

3.3. MET Protects the Myocardium against DOX-Induced Energy Starvation. Figure 1 shows the effects of DOX, MET, and DOX plus MET on ATP level in cardiac tissues. Treatment with a total cumulative dose of DOX (18 mg/kg) resulted in a significant decrease (31.5%) in ATP level in cardiac tissues as compared to the control group. However, treatment with MET (500 mg/kg) for 11 successive days caused a significant increase (54%) in ATP as compared to the control group. Interestingly, daily administration of MET (500 mg/kg) to DOX-treated rats resulted in a complete reversal of DOX-induced decrease in ATP to the control values. However, administration of the small dose of MET (50 mg/kg) did not alter DOX-induced decrease in ATP level in cardiac tissues.

3.4. MET Reverses the Effect of DOX on Cardiac GSH Level. Figure 2 shows the effects of DOX, MET, and DOX plus MET on GSH level in rat cardiac tissues. Treatment with a total cumulative dose of DOX (18 mg/kg) resulted in a significant 57% decrease in GSH level, as compared to the control group. Treatment with MET at dose level either 50 mg/kg or 500 mg/kg for 11 successive days resulted in a significant and dose-dependent (70% and 102%) increase in GSH level, respectively, as compared to the control group. Daily administration of MET either 50 mg/kg or 500 mg/kg to DOX-treated rats resulted in a complete reversal of DOX-induced decrease in cardiac GSH level to the control values.

3.5. Histopathology and Electron Microscopy. The light microscopic examination of the normal control rat hearts showed normal architecture and cytological features (Figure 3(i)). However, examination of the heart tissues of DOX-alone-treated rats revealed focal mild inflammation of the myocardium (arrows in Figure 3(ii)) that was associated with myocardial fiber injury, in addition to vacuolar changes of the cytoplasm of some myocardial cells

(arrow in Figure 3(ii) B). The inflammatory infiltrate consisted of lymphocytes, plasma cells, and histiocytes, with prominent mononuclear chronic inflammatory appearance that replaced the degenerated myocardial muscle fibers with apparent hypereosinophilia (Figure 3(ii) A and B). Treatment with MET alone (50 or 500 mg/kg) showed no pathological changes in the tested heart tissues, while, in the group that received MET (50 mg/kg) and DOX, the heart tissues showed few mild inflammatory foci with undetected myocardial injury (Figure 3(iii) A and B). The heart tissues of the rats that received MET (500 mg/kg) and DOX revealed almost normal morphological tissue appearance without any detected inflammation or tissue injury (Figure 3(iv) A and B).

The electron microscopic examination of normal control rat hearts revealed normal mitochondria (arrow in Figure 4(i) A) with preserved internal architectures and surrounding organized myofibrils (arrow in Figure 4(i) B). The heart tissues of DOX-treated rats exhibited a prominent component of patchy myofibrillar loss and disarray, in addition to prominent hypercontraction bands with prominent A band loss (Figure 4(ii) A and B). Moreover, the mitochondria showed remarkable abnormalities that included enlargement, contour irregularities, increased spacing between the cristae and disruption of the internal architecture (arrow in Figure 4(ii) B). The group of rats treated with 50 mg/kg or 500 mg/kg of MET illustrated no significant ultrastructural changes. Hearts of rats treated with MET (50 mg/kg) and DOX showed some focal but prominent pathological findings. In this focus, there was an evidence of loss of myofibrils in addition to mitochondrial size and shape variation and many dilated lysosomes (arrow in Figure 4(iii) A). On the contrary, a significant improvement was seen in the ultrastructure of the hearts of rats treated with MET 500 mg/kg and DOX (Figure 4(iv) A and B). The examined sections showed a normal mitochondrial size and shape with normal arrangement of cristae.

3.6. MET Reverses DOX-Mediated Changes in the Levels of Cardiac Hypertrophic Genes. To investigate the effect of MET on the expression of cardiac hypertrophic gene markers, α -MHC and β -MHC mRNA levels were determined in both healthy and DOX-induced cardiotoxic rats using RT-PCR. Figure 5 shows that both doses of MET did not significantly alter the mRNA expression of both α -MHC and β -MHC. On the other hand, DOX-treated rats showed a significant decrease in the mRNA level of α -MHC by approximately 40%, whereas β -MHC mRNA level was induced dramatically 250%. Importantly, administration of MET significantly restored DOX-mediated changes in hypertrophic genes, which was more pronounced at the highest dose (500 mg/kg).

3.7. MET Restores DOX-Mediated Changes in the Levels of Oxidative Stress-Related Genes. To further explore the role of oxidative stress in the cardioprotective effect of MET, we have investigated the effect of MET on the expression of four oxidative stress-mediated genes, GST α , CAT, NQO1, and HO-1. Figure 6 showed that induction of cardiotoxicity by

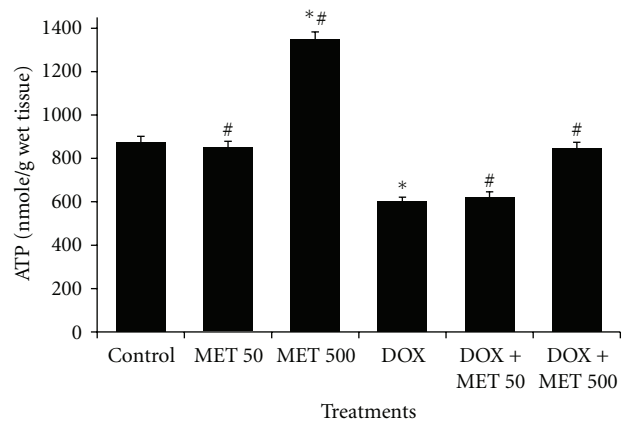


FIGURE 1: MET protects the myocardium against DOX-induced energy starvation. Rats ($n = 10$ /per treatment type) received normal saline, DOX in a total cumulative dose of 18 mg/kg, MET (50 or 500 mg/kg, p.o., daily), or DOX plus either dose of MET. 24 h after receiving the last dose of DOX, ATP was determined in heart tissues using HPLC. Data are presented as mean \pm SEM ($n = 10$). * and # indicate significant change from control and DOX, respectively, at $P < 0.05$ using ANOVA followed by the Tukey-Kramer as a post-ANOVA test.

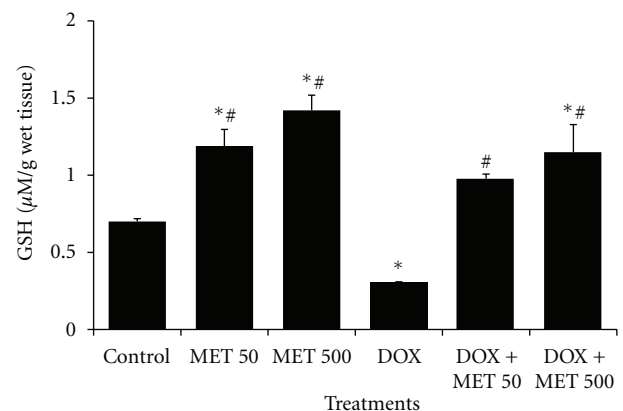


FIGURE 2: MET reverses the effect of DOX on cardiac GSH level. Rats ($n = 10$ /treatment type) received normal saline, DOX in a total cumulative dose of 18 mg/kg, MET (50 or 500 mg/kg, p.o., daily) or DOX plus either dose of MET. 24 h after receiving the last dose of DOX, cardiac tissue level of GSH was determined in rat cardiac tissues. Data are presented as mean \pm SEM ($n = 10$). * and # indicate significant change from control and DOX, respectively, at $P < 0.05$ using ANOVA followed by the Tukey-Kramer as a post-ANOVA test.

DOX was associated with upregulated expression of GST α (A) and HO-1 (B) which was accompanied with a significant decrease in CAT (C) and NQO1 (D) mRNA expression levels as compared to control rats. Although treatment of control rats with MET did not alter the expression of most target genes, treatment of DOX-treated rats with MET significantly restored the DOX-induced modulations of all tested genes in a dose-dependent manner, in that MET induced NQO1 and CAT whereas inhibited GST α and HO-1 mRNA expression in a dose-dependent manner.

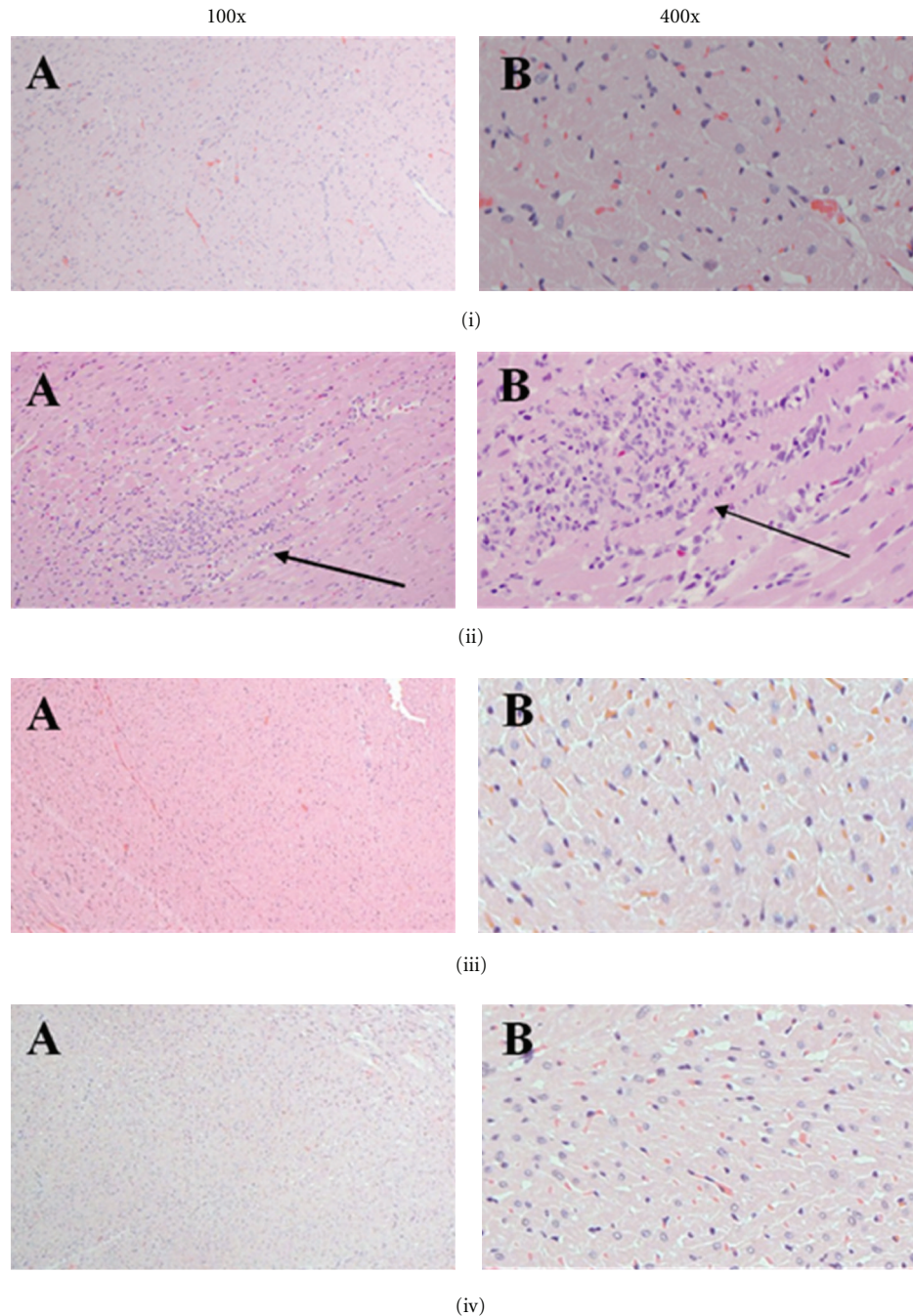


FIGURE 3: MET protects myocardium against DOX-induced histopathological deteriorations. Photos (i) A and B show normal cardiac structure derived from normal control rat. Photos (ii) A and B are derived from heart section of a rat treated with a total cumulative dose of 18 mg/kg DOX and shows myocardial fiber injury as vacuolar changes of the cytoplasm and inflammatory infiltrate consisting of lymphocytes, plasma cells and histiocytes (arrow). Photos (iii) A and B show heart sections derived from a rat treated with MET 50 mg/kg prior to a total cumulative dose of 18 mg/kg DOX. It shows few inflammatory foci with considerable improvement in heart histology. Photos (iv) A and B illustrate heart sections obtained from a rat pretreated with MET 500 mg/kg before a total cumulative dose of 18 mg/kg DOX, revealing almost normal histology with a marked improvement in heart histology. Magnification, 400x in A; 100x in B.

4. Discussion

The most common hypothesis for the mechanism of DOX-induced cardiac injury is the increase of oxidative stress. Free radical generation by DOX, which is usually associated with

a depression of GSH in heart tissue, results in disruption of cellular membrane integrity. This hypothesis is supported by the several reports that have shown that antioxidants, including vitamins E and A, resveratrol, and selenium, protect cardiomyocytes against the toxicity of DOX [37]. On the

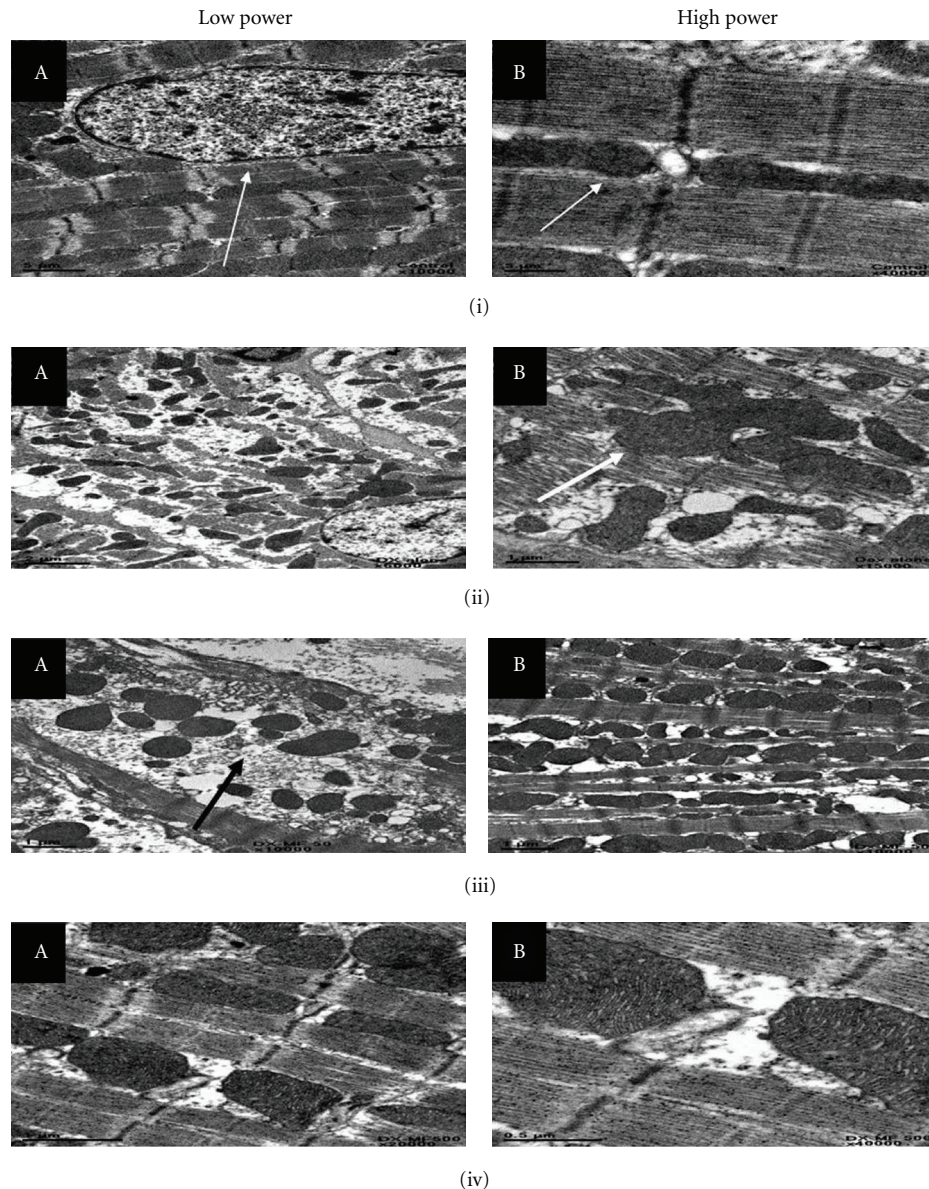


FIGURE 4: MET protects myocardium against DOX-induced ultrastructural deteriorations. Photos (i) A and B show normal ultrastructure of a normal control rat heart. Photos (ii) A and B are EM photo taken for a heart section from a rat treated with a total cumulative dose of 18 mg/kg DOX and show a prominent component of patchy myofibrillar loss and disarray, hypercontraction bands with prominent A band loss. They also show mitochondrial abnormalities, including enlargement and irregular contour. Photos (iii) A and B are photos of ultrastructure of rat heart treated with MET 50 mg/kg prior to a total cumulative dose of 18 mg/kg DOX and show mild improvement in the mitochondrial structure. Photos (iv) A and B are photos of ultrastructure of cardiac muscle derived from a rat treated with MET 500 mg/kg prior to a total cumulative dose of 18 mg/kg DOX, showing almost normal ultrastructure, size, and shape of the myocardial fibers. Magnification, low power in A; high power in B.

other hand, impairment of cardiac high-energy phosphate metabolism has been recognized as an important feature of both acute and chronic DOX cardiotoxic action. These energetic deficits have been associated with compromised mitochondrial function [38]. In this context, oxidative damage to cardiac mitochondria and to cardiomyocytes has been widely implicated as a primary cause for doxorubicin-induced cardiac toxicity [39, 40]. The enhanced generation of ROS by DOX may directly damage mitochondria or alter the synthesis of proteins associated with the mitochondrial elec-

tron transport chain, with the subsequent inhibition of oxidative phosphorylation and decrease in cardiac high-energy phosphate homeostasis [41, 42]. The accumulation of various deficiencies in high-energy phosphate metabolism may be a very critical step for the DOX-induced deterioration of cardiac function and for the onset of chronic clinical cardiotoxicity [43].

The model utilized in the present study has already been established in previous publications that included biomarkers of cardiotoxicity as those reported by Beanlands et al.

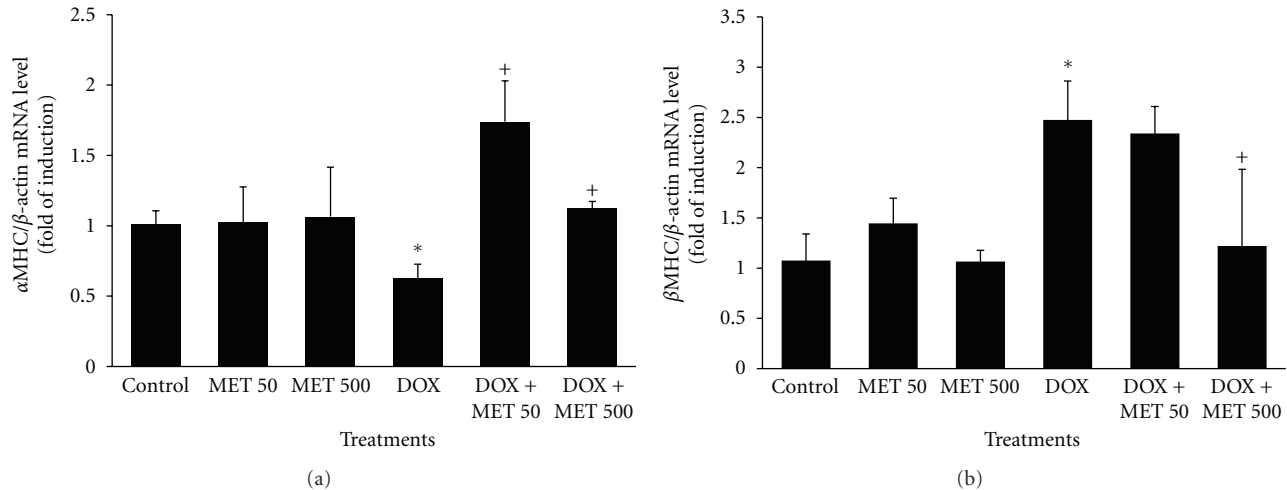


FIGURE 5: MET reverses DOX-mediated changes in the levels of cardiac hypertrophic genes. Rats ($n = 10$ /treatment type) received normal saline, DOX in a total cumulative dose of 18 mg/kg, MET (50 or 500 mg/kg, p.o., daily), or DOX plus either dose of MET. 24 h after receiving the last dose of DOX, total RNA was isolated from rat cardiac tissue using TRIzol methods and quantified spectrophotometrically at 260 nm. The mRNA levels of α -MHC (a) and β -MHC genes (b) were quantified using RT-PCR and normalized to β -actin housekeeping gene. Values represent mean of fold change \pm SEM ($n = 10$). * $P < 0.05$ compared with control rats. † $P < 0.05$ compared with DOX-treated rats.

1994 [28] and Sayed-Ahmed et al. 2010 [29]. In the latter study, rats were injected every other day with doxorubicin (3 mg/kg, i.p.), to obtain treatments with cumulative doses of 6, 12, and 18 mg/kg. The cumulative cardiotoxicity of DOX was clearly featured in that study by the dose-dependent increase in serum cardiac enzymes CK-MB and LDH. At the highest cumulative dose, 18 mg/kg, DOX resulted in a significant increase in CK-MB and LDH and decrease in ATP as well as the expression of apoptotic genes, as compared to the control group. That is why we decided to use that same highest cumulative dose to produce the model of DOX-induced cardiotoxicity on the cellular and molecular levels, rather than functional ones, using the same animal species.

Since DOX causes disruption of cardiac myocyte cell membranes, the release of intracellular proteins, such as LDH and CK-MB, into serum has been used to assay for the presence and extent of cardiac myocyte injury [6, 44]. The levels of these two enzymes were markedly increased by DOX administration in our study. Our results are in a good agreement with previous reports [45, 46]. In addition, histopathological investigation of cardiac tissues from DOX-treated rats showed myocardial mononuclear chronic inflammation that replaced the degenerated muscle fibers affected. Electron microscopic examination revealed the presence of morphological evidences of mitochondrial injury, as well as myofibrillar loss and disruption. Moreover, treatment with DOX increased β -MHC expression and decreased α -MHC expression, as a result of cardiac toxicity. This is consistent with earlier published data [47–50]. All these biochemical and molecular changes and histopathological deteriorations were completely prevented by MET therapy (500 mg/kg, every day). These results suggest that MET therapy during DOX treatment for cancer offers substantial

protection of the heart against DOX-induced injury. The initial damage caused by DOX is believed to be oxidative in nature. This drug can undergo one electron reduction to the corresponding semiquinone, leading to the generation of superoxide radical [51]. DOX interacts with iron, generating a DOX-ferric iron free radical complex, and the resulting complex catalyzes the conversion of hydrogen peroxide to the highly reactive hydroxyl radical. Hydrogen peroxide, lipid peroxides, superoxide radical, and hydroxyl radical can damage membranes, macromolecules, and mitochondria and may cause direct myocardial injury [2, 51]. Notably, mammalian hearts are vulnerable to DOX cardiotoxicity due to limited antioxidant mechanisms that could protect them from oxidative injury [2, 52].

In the present study, total content of GSH, the most important endogenous antioxidant, was assessed as a marker for oxidative stress, since reduced GSH normally represents more than 90% of cellular GSH content [53]. The method used in this study utilized Ellman's reagent which determines total SH-containing compounds, which are mainly represented as reduced GSH [54, 55]. Also, the gene expression of the oxidative stress molecular markers, NQO-1, catalase, HO-1, and GST- α , has been investigated to elaborate more on the oxidative stress pathway. Moreover, it has been reported that DOX itself causes the disappearance of glutathione peroxidase and significantly lowers the levels of GSH in heart tissue. This diminishes the capability of the heart to dispose of hydrogen peroxide, making the heart more susceptible to redox injury [51, 52, 56, 57]. Cardiac tissue level of GSH was demonstrated in our study to be significantly decreased by DOX treatment, which comes in agreement with the previous report by Aleisa et al. [58]. Remarkably, this decrease was completely prevented by the two doses (50

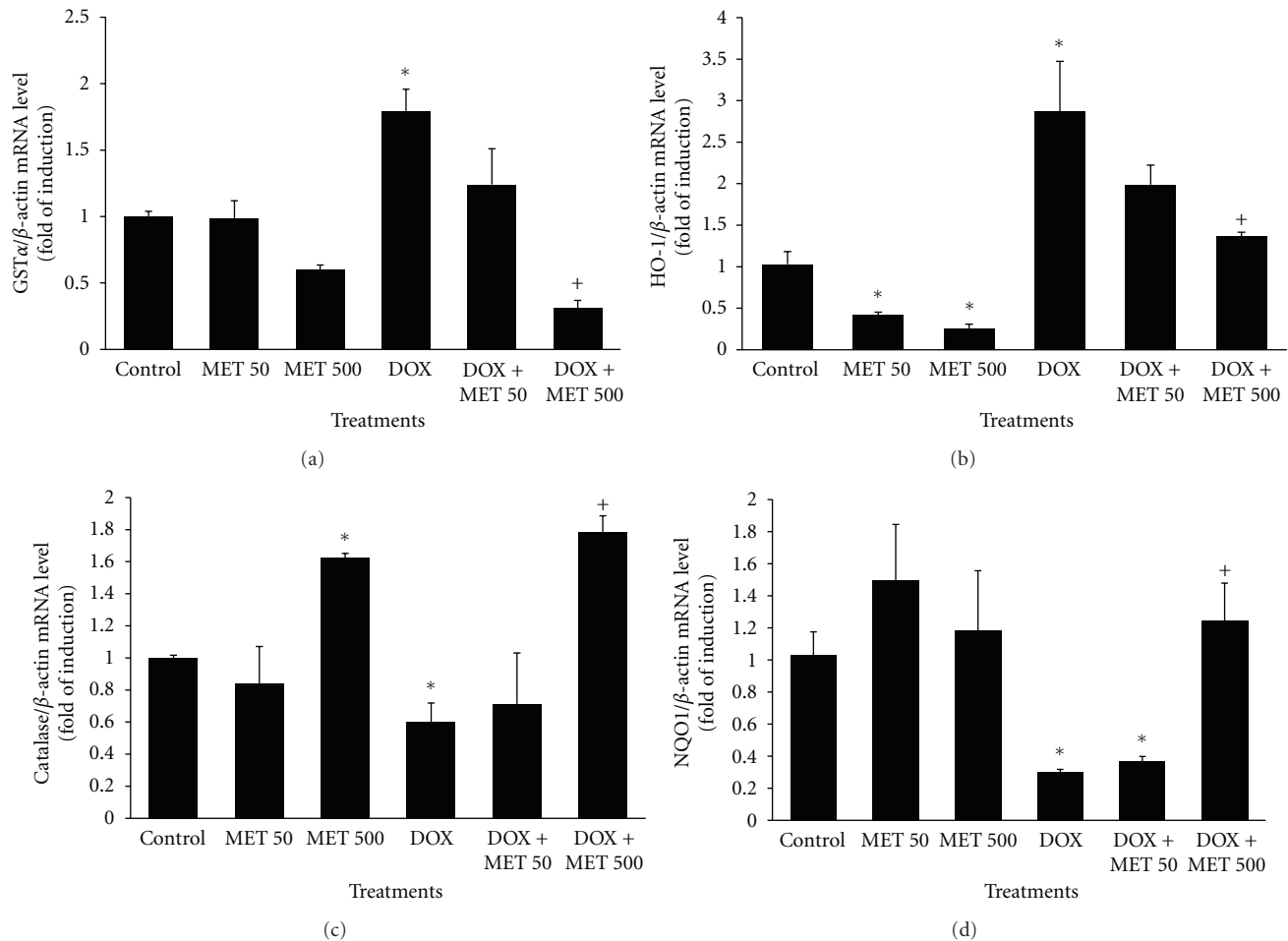


FIGURE 6: MET restores DOX-mediated changes in the levels of oxidative stress-related genes. Rats ($n = 10$ /treatment type) received normal saline, DOX in a total cumulative dose of 18 mg/kg, MET (50 or 500 mg/kg, p.o., daily), or DOX plus either dose of MET. 24 h after receiving the last dose of DOX, total RNA was isolated from rat cardiac tissue using TRIzol methods and quantified spectrophotometrically at 260 nm. The mRNA levels of GST α (a), HO-1 (b), CAT (c), and NQO1 (d) were quantified using RT-PCR and normalized to β -actin housekeeping gene. Values represent mean of fold change \pm SEM ($n = 10$). * $P < 0.05$ compared with control rats. + $P < 0.05$ compared with DOX-treated rats.

and 500 mg/kg/d) of MET, indicating its strong antioxidant activity and its potential cardioprotective efficacy against DOX cardiotoxicity.

DOX also exerted dramatic effects on the expression of molecular oxidative stress markers. It induced the expression of GST α and HO-1 genes and decreased CAT and NQO1 mRNA expression as compared to control rats. DOX treatment is known to enhance the production of the highly reactive lipid peroxidation product 4-hydroxy-2-nonenal (HNE) in cardiac tissue [59]. DOX-induced HNE has been shown to be partially detoxified by conjugation with GSH by GST to form the glutathione conjugate of HNE (GS-HNE) [60]. Induction of GST α gene expression by DOX in the present work reveals that cardiac tissues were defending themselves against DOX toxicity by augmenting the expression of GST α which, in turn, consumed GSH to detoxify DOX. This is evidenced by the significant decrease of cardiac tissue level of GSH by DOX (Figure 2). By virtue of its antioxidant activity, MET released the pressure on cardiac tissue to augment

GST α expression, thereby saving the cardiac levels of GSH (Figure 2).

Moreover, the results showed that CAT, an enzyme responsible for the removal of H₂O₂, gene expression is decreased by DOX treatment, supporting the idea that DOX induces a state of oxidative stress in the heart tissues. NQO1 is cytosolic enzyme that plays an essential role in the detoxification of quinones through two-electron reduction process [61, 62]. In addition, NQO1 helps to maintain endogenous antioxidants, in their active form [63]. It seems that the decrease in NQO1 expression by DOX treatment in our study is attributed to a direct inhibitory effect. This may lead to insufficient NQO1 activity that could have buffered DOX-oxidizing properties. Therefore, the heart was highly exposed to oxidizing species induced by DOX. In the same sense, DOX induced HO-1 gene expression which is the rate-limiting enzyme of heme degradation, and it is a stress-responsive protein that responds to many kinds of chemically or physiologically produced oxidative stress, including GSH

depletion, in various cells and tissues [64, 65]. Hence, the induction of HO-1 gene expression by DOX could be understood as a response of cardiac cells to DOX-induced GSH depletion. MET, alone or along with DOX, decreased HO-1 expression. This could be because MET itself possesses a significant antioxidant activity as shown above. The significant increase in the GSH level and CAT and NQO-1 mRNA expression in heart tissue of animals after treatment with MET supports the above hypothesis that MET ameliorates DOX-induced oxidative stress. These results have extended earlier finding by others that MET substantially increased GSH level in normal rats [24] and protected against the DOX-induced decrease of GSH in mice [58]. Interestingly, Faure et al. [24] showed that this effect was independent of MET effect on insulin activity. More recently, Asensio-Lopez et al. [66] illustrated that MET exerts a protective effect against DOX-induced cardiotoxicity through the involvement of the cardiac system of adiponectin and restoring the activity of antioxidant enzymes in isolated cardiomyocytes *in vitro*.

The most important role of mitochondria in the myocardium is to supply cardiac cells with ATP, a crucial source of energy for contraction and for the maintenance of ion homeostasis, protein synthesis, and other important cellular functions [67]. In that regard, DOX was shown to inhibit long-chain fatty acid oxidation in the heart [68]. Under physiological conditions, long-chain fatty acids are the favored substrates for energy production in the heart [69]. Consequently, inhibition of long-chain fatty acid oxidation results in a deficiency in ATP supply and accumulation of toxic intermediates including long-chain fatty acyl-CoA thioesters and long-chain acyl-carnitine derivatives in cardiac tissues, with subsequent cardiomyopathy and congestive heart failure [70–72]. In the present study, level of ATP in cardiac tissue was markedly reduced by DOX treatment. In addition, DOX significantly decreased level of CoA-SH, an indispensable activator in most of the energy-providing systems (TCA cycle, fatty acid oxidation) [73], and increased that of acetyl-CoA, the main product of β -oxidation of fatty acids. Acetyl-CoA is a strong inhibitor of 3-ketoacyl-CoA thiolase, the enzyme catalyzing the last step in β -oxidation of fatty acids, especially at low concentrations of CoA-SH [74]. Therefore, in the present study, raising the acetyl-CoA/CoA-SH ratio in isolated rat heart mitochondria by DOX could inhibit fatty acid oxidation, with subsequent deleterious effects on cardiac energy supply. Therapy with MET prevented the decrease of ATP and the increase of acetyl-CoA/CoA-SH ratio induced by DOX. These data indicate that MET protects myocardium against DOX-induced energy starvation and depletion of intramitochondrial CoA-SH. In that context, Gundewar et al. [27] have recently reported that MET significantly improves left ventricular function and survival via activation of AMPK in a murine model of heart failure. Activated AMPK phosphorylates a variety of intracellular proteins to increase ATP generation and decrease ATP utilization for processes not immediately critical for survival [75].

Collectively, the data presented in this study suggest that liberation of free radicals induced by DOX treatment causes

oxidative injury to heart tissues and organelles including mitochondria. Since heart is almost entirely dependent on ATP generated by mitochondria for its function and contractility [76], mitochondrial injury, with its subsequent depression of myocardial ATP, contributes to the progression of cardiac toxicity [77]. The oxidative injury to the heart is accentuated by the reduction of the cardiac antioxidant defense, represented by the great reduction of GSH content and CAT and NQO-1 gene expression induced by DOX. Therefore, our data suggest that the protective effect of MET against DOX-induced cardiac toxicity could originate from its antioxidant activity.

5. Conclusion

Results from the present investigation reveal that DOX induces its cardiotoxicity by decreasing cardiac level of CoA-SH and increasing that of acetyl-CoA, with the consequent inhibition of fatty acid oxidation and ATP generation. This is aggravated by the increased susceptibility of the heart to oxidant injury due to DOX-induced reduction of cardiac GSH level, as well as the decrease in CAT and NQO-1 gene expression. Our findings demonstrate that MET prevents all of these biochemical and molecular changes and other histopathological and ultrastructural deteriorations in the cardiac tissues, warranting its coadministration with DOX to ameliorate its cardiotoxicity.

Conflict of Interests

The authors have no personal or financial conflict of interest and have not entered into any agreement that could interfere with their access to the data on the research or upon their ability to analyze the data independently, to prepare papers, and to publish them.

Acknowledgment

This work was supported by a grant from the King Abdulaziz City for Science and Technology (KACST; Grant no. ARP-29-265). The technical assistance of Mr. Jamal Hardelo from the Department of Pharmacology, College of Medicine, King Saud University, is greatly appreciated.

References

- [1] G. Minotti, P. Menna, E. Salvatorelli, G. Cairo, and L. Gianni, "Anthracyclines: molecular advances and pharmacologic developments in antitumor activity and cardiotoxicity," *Pharmacological Reviews*, vol. 56, no. 2, pp. 185–229, 2004.
- [2] M. S. Horenstein, R. S. Vander Heide, and T. J. L'Ecuyer, "Molecular basis of anthracycline-induced cardiotoxicity and its prevention," *Molecular Genetics and Metabolism*, vol. 71, no. 1-2, pp. 436–444, 2000.
- [3] S. Rajagopalan, P. M. Politi, B. K. Sinha, and C. E. Myers, "Adriamycin-induced free radical formation in the perfused rat heart: implications for cardiotoxicity," *Cancer Research*, vol. 48, no. 17, pp. 4766–4769, 1988.
- [4] F. Rossi, W. Filippelli, S. Russo, A. Filippelli, and L. Berrino, "Cardiotoxicity of doxorubicin: effects of drugs inhibiting

- The release of vasoactive substances," *Pharmacology and Toxicology*, vol. 75, no. 2, pp. 99–107, 1994.
- [5] T. Simunek, M. Sterba, O. Popelova, M. Adamcova, R. Hrdina, and V. Gersl, "Anthracycline-induced cardiotoxicity: overview of studies examining the roles of oxidative stress and free cellular iron," *Pharmacological Reports*, vol. 61, no. 1, pp. 154–171, 2009.
 - [6] R. D. Olson and P. S. Mushlin, "Doxorubicin cardiotoxicity: analysis of prevailing hypotheses," *The FASEB Journal*, vol. 4, no. 13, pp. 3076–3086, 1990.
 - [7] M. M. Sayed-Ahmed, S. A. Shouman, B. M. Rezk, M. H. Khalifa, A. M. Osman, and M. M. El-Merzabani, "Propionyl-L-carnitine as potential protective agent against adriamycin-induced impairment of fatty acid beta-oxidation in isolated heart mitochondria," *Pharmacological Research*, vol. 41, no. 2, pp. 143–150, 2000.
 - [8] V. De Leonardis, B. Neri, S. Bacalli, and P. Cinelli, "Reduction of cardiac toxicity of anthracyclines by L-carnitine: preliminary overview of clinical data," *International Journal of Clinical Pharmacology Research*, vol. 5, no. 2, pp. 137–142, 1985.
 - [9] C. F. Seifert, M. E. Nesser, and D. F. Thompson, "Dexrazoxane in the prevention of doxorubicin-induced cardiotoxicity," *Annals of Pharmacotherapy*, vol. 28, no. 9, pp. 1063–1072, 1994.
 - [10] A. Puri, S. K. Maulik, R. Ray, and V. Bhatnagar, "Electrocardiographic and biochemical evidence for the cardioprotective effect of vitamin E in doxorubicin-induced acute cardiotoxicity in rats," *European Journal of Pediatric Surgery*, vol. 15, no. 6, pp. 387–391, 2005.
 - [11] I. Morishima, H. Matsui, H. Mukawa et al., "Melatonin, a pineal hormone with antioxidant property, protects against adriamycin cardiomyopathy in rats," *Life Sciences*, vol. 63, no. 7, pp. 511–521, 1998.
 - [12] E. Tatlidede, O. Sehirli, A. Velioglu-Ogunc et al., "Resveratrol treatment protects against doxorubicin-induced cardiotoxicity by alleviating oxidative damage," *Free Radical Research*, vol. 43, no. 3, pp. 195–205, 2009.
 - [13] E. Delpy, S. N. Hatem, N. Andrieu et al., "Doxorubicin induces slow ceramide accumulation and late apoptosis in cultured adult rat ventricular myocytes," *Cardiovascular Research*, vol. 43, no. 2, pp. 398–407, 1999.
 - [14] S. Wang, E. A. Konorev, S. Kotamraju, J. Joseph, S. Kalivendi, and B. Kalyanaraman, "Doxorubicin induces apoptosis in normal and tumor cells via distinctly different mechanisms: intermediacy of H_2O_2 - and p53-dependent pathways," *Journal of Biological Chemistry*, vol. 279, no. 24, pp. 25535–25543, 2004.
 - [15] A. S. Glicksman and R. W. Rawson, "Diabetes and altered carbohydrate metabolism in patients with cancer," *Cancer*, vol. 9, no. 6, pp. 1127–1134, 1956.
 - [16] P. A. Marks and J. S. Bishop, "The glucose metabolism of patients with malignant disease and of normal subjects as studied by means of an intravenous glucose tolerance test," *The Journal of Clinical Investigation*, vol. 36, no. 2, pp. 254–264, 1957.
 - [17] M. Deleers and E. Goormaghtigh, "Adriamycin effects on insulin secretion, Ca^{2+} movements and glucose oxidation in pancreatic islet cells," *Pharmacological Research Communications*, vol. 17, no. 3, pp. 227–232, 1985.
 - [18] J. P. Ioannidis, P. J. Hesketh, and J. Lau, "Contribution of dexamethasone to control of chemotherapy-induced nausea and vomiting: a meta-analysis of randomized evidence," *Journal of Clinical Oncology*, vol. 18, no. 19, pp. 3409–3422, 2000.
 - [19] R. E. Coleman, "Glucocorticoids in cancer therapy," *Biotherapy*, vol. 4, no. 1, pp. 37–44, 1992.
 - [20] A. Munck, "Glucocorticoid inhibition of glucose uptake by peripheral tissues: old and new evidence, molecular mechanisms, and physiological significance," *Perspectives in Biology and Medicine*, vol. 14, no. 2, pp. 265–269, 1971.
 - [21] Z. Suba and M. Ujjál, "Correlations of insulin resistance and neoplasms," *Magyar onkologia*, vol. 50, no. 2, pp. 127–135, 2006.
 - [22] K. Cusi, A. Consoli, and R. A. DeFronzo, "Metabolic effects of metformin on glucose and lactate metabolism in noninsulin-dependent diabetes mellitus," *Journal of Clinical Endocrinology and Metabolism*, vol. 81, no. 11, pp. 4059–4067, 1996.
 - [23] A. Klip and L. A. Leiter, "Cellular mechanism of action of metformin," *Diabetes Care*, vol. 13, no. 6, pp. 696–704, 1990.
 - [24] P. Faure, E. Rossini, N. Wiernsperger, M. J. Richard, A. Favier, and S. Halimi, "An insulin sensitizer improves the free radical defense system potential and insulin sensitivity in high fructose-fed rats," *Diabetes*, vol. 48, no. 2, pp. 353–357, 1999.
 - [25] G. Kanigur-Sultuybek, M. Guven, I. Onaran, V. Tezcan, A. Cenani, and H. Hatemi, "The effect of metformin on insulin receptors and lipid peroxidation in alloxan and streptozotocin induced diabetes," *Journal of Basic and Clinical Physiology and Pharmacology*, vol. 6, no. 3–4, pp. 271–280, 1995.
 - [26] G. S. Bhamra, D. J. Hausenloy, S. M. Davidson et al., "Metformin protects the ischemic heart by the Akt-mediated inhibition of mitochondrial permeability transition pore opening," *Basic Research in Cardiology*, vol. 103, no. 3, pp. 274–284, 2008.
 - [27] S. Gundewar, J. W. Calvert, S. Jha et al., "Activation of AMP-activated protein kinase by metformin improves left ventricular function and survival in heart failure," *Circulation Research*, vol. 104, no. 3, pp. 403–411, 2009.
 - [28] R. S. B. Beanlands, N. A. Shaikh, W. H. Wen et al., "Alterations in fatty acid metabolism in adriamycin cardiomyopathy," *Journal of Molecular and Cellular Cardiology*, vol. 26, no. 1, pp. 109–119, 1994.
 - [29] M. M. Sayed-Ahmed, O. A. Al-Shabanah, M. M. Hafez, A. M. Aleisa, and S. S. Al-Rejaie, "Inhibition of gene expression of heart fatty acid binding protein and organic cation/carnitine transporter in doxorubicin cardiomyopathic rat model," *European Journal of Pharmacology*, vol. 640, no. 1–3, pp. 143–149, 2010.
 - [30] P. Anurag and C. V. Anuradha, "Metformin improves lipid metabolism and attenuates lipid peroxidation in high fructose-fed rats," *Diabetes, Obesity and Metabolism*, vol. 4, no. 1, pp. 36–42, 2002.
 - [31] X. Wang, X. Jia, T. Chang, K. Desai, and L. Wu, "Attenuation of hypertension development by scavenging methylglyoxal in fructose-treated rats," *Journal of Hypertension*, vol. 26, no. 4, pp. 765–772, 2008.
 - [32] S. N. Buhl and K. Y. Jackson, "Optimal conditions and comparison of lactate dehydrogenase catalysis of the lactate to pyruvate and pyruvate to lactate reactions in human serum at 25, 30, and 37°C," *Clinical Chemistry*, vol. 24, no. 5, pp. 828–831, 1978.
 - [33] A. H. Wu and G. N. Bowers Jr., "Evaluation and comparison of immunoinhibition and immunoprecipitation methods for differentiating MB from BB and macro forms of creatine kinase isoenzymes in patients and healthy individuals," *Clinical Chemistry*, vol. 28, no. 10, pp. 2017–2021, 1982.
 - [34] A. Longo, G. Bruno, S. Curti, A. Mancinelli, and G. Miotto, "Determination of L-carnitine, acetyl-L-carnitine and propionyl-L-carnitine in human plasma by high-performance liquid chromatography after pre-column derivatization with

- 1-aminoanthracene," *Journal of Chromatography B*, vol. 686, no. 2, pp. 129–139, 1996.
- [35] H. E. Botker, H. H. Kimose, P. Helligso, and T. T. Nielsen, "Analytical evaluation of high energy phosphate determination by high performance liquid chromatography in myocardial tissue," *Journal of Molecular and Cellular Cardiology*, vol. 26, no. 1, pp. 41–48, 1994.
 - [36] G. L. Ellman, "Tissue sulfhydryl groups," *Archives of Biochemistry and Biophysics*, vol. 82, no. 1, pp. 70–77, 1959.
 - [37] S. Granados-Principal, J. L. Quiles, C. L. Ramirez-Tortosa, P. Sanchez-Rovira, and M. Ramirez-Tortosa, "New advances in molecular mechanisms and the prevention of adriamycin toxicity by antioxidant nutrients," *Food and Chemical Toxicology*, vol. 48, no. 6, pp. 1425–1438, 2010.
 - [38] K. B. Wallace, "Doxorubicin-induced cardiac mitochondriopathy," *Pharmacology and Toxicology*, vol. 93, no. 3, pp. 105–115, 2003.
 - [39] V. Lee, A. K. Randhawa, and P. K. Singal, "Adriamycin-induced myocardial dysfunction in vitro is mediated by free radicals," *American Journal of Physiology*, vol. 261, no. 4, part 2, pp. H989–H995, 1991.
 - [40] M. F. Xu, P. L. Tang, Z. M. Qian, and M. Ashraf, "Effects by doxorubicin on the myocardium are mediated by oxygen free radicals," *Life Sciences*, vol. 68, no. 8, pp. 889–901, 2001.
 - [41] S. Zhou, C. M. Palmeira, and K. B. Wallace, "Doxorubicin-induced persistent oxidative stress to cardiac myocytes," *Toxicology Letters*, vol. 121, no. 3, pp. 151–157, 2001.
 - [42] J. M. Berthiaume and K. B. Wallace, "Adriamycin-induced oxidative mitochondrial cardiotoxicity," *Cell Biology and Toxicology*, vol. 23, no. 1, pp. 15–25, 2007.
 - [43] M. Tokarska-Schlattner, T. Wallimann, and U. Schlattner, "Alterations in myocardial energy metabolism induced by the anti-cancer drug doxorubicin," *Comptes Rendus*, vol. 329, no. 9, pp. 657–668, 2006.
 - [44] M. Preus, A. S. Bhargava, A. E. Khater, and P. Gunzel, "Diagnostic value of serum creatine kinase and lactate dehydrogenase isoenzyme determinations for monitoring early cardiac damage in rats," *Toxicology Letters*, vol. 42, no. 2, pp. 225–233, 1988.
 - [45] M. A. Abd El-Aziz, A. I. Othman, M. Amer, and M. A. El-Missiry, "Potential protective role of angiotensin-converting enzyme inhibitors captopril and enalapril against adriamycin-induced acute cardiac and hepatic toxicity in rats," *Journal of Applied Toxicology*, vol. 21, no. 6, pp. 469–473, 2001.
 - [46] M. E. Büyükköküroğlu, S. Taysi, M. Buyukavci, and E. Bakan, "Prevention of acute adriamycin cardiotoxicity by dantrolene in rats," *Human and Experimental Toxicology*, vol. 23, no. 5, pp. 251–256, 2004.
 - [47] K. Nakao, W. Minobe, R. Roden, M. R. Bristow, and L. A. Leinwand, "Myosin heavy chain gene expression in human heart failure," *Journal of Clinical Investigation*, vol. 100, no. 9, pp. 2362–2370, 1997.
 - [48] B. D. Lowes, W. Minobe, W. T. Abraham et al., "Changes in gene expression in the intact human heart: downregulation of α -myosin heavy chain in hypertrophied, failing ventricular myocardium," *Journal of Clinical Investigation*, vol. 100, no. 9, pp. 2315–2324, 1997.
 - [49] G. Cooper, "Basic determinants of myocardial hypertrophy: a review of molecular mechanisms," *Annual Review of Medicine*, vol. 48, pp. 13–23, 1997.
 - [50] B. Swynghedauw, S. Besse, P. Assayag et al., "Molecular and cellular biology of the senescent hypertrophied and failing heart," *American Journal of Cardiology*, vol. 76, no. 13, pp. 2D–7D, 1995.
 - [51] C. Myers, "The role of iron in doxorubicin-induced cardiomyopathy," *Seminars in Oncology*, vol. 25, no. 4, supplement 10, pp. 10–14, 1998.
 - [52] R. D. Olson, J. S. MacDonald, and C. J. VanBoxtel, "Regulatory role of glutathione and soluble sulfhydryl groups in the toxicity of adriamycin," *Journal of Pharmacology and Experimental Therapeutics*, vol. 215, no. 2, pp. 450–454, 1980.
 - [53] A. Meister, "Metabolism and functions of glutathione," *Trends in Biochemical Sciences C*, vol. 6, pp. 231–234, 1981.
 - [54] A. Meister and M. E. Anderson, "Glutathione," *Annual Review of Biochemistry*, vol. 52, pp. 711–760, 1983.
 - [55] A. Meister, "On the discovery of glutathione," *Trends in Biochemical Sciences*, vol. 13, no. 5, pp. 185–188, 1988.
 - [56] N. Iliskovic, T. Li, N. Khaper, V. Palace, and P. K. Singal, "Modulation of adriamycin-induced changes in serum free fatty acids, albumin and cardiac oxidative stress," *Molecular and Cellular Biochemistry*, vol. 188, no. 1–2, pp. 161–166, 1998.
 - [57] M. Valko, D. Leibfritz, J. Moncol, M. T. Cronin, M. Mazur, and J. Telser, "Free radicals and antioxidants in normal physiological functions and human disease," *International Journal of Biochemistry and Cell Biology*, vol. 39, no. 1, pp. 44–84, 2007.
 - [58] A. M. Aleisa, S. S. Al-Rejaie, S. A. Bakheet et al., "Effect of metformin on clastogenic and biochemical changes induced by adriamycin in Swiss albino mice," *Mutation Research*, vol. 634, no. 1–2, pp. 93–100, 2007.
 - [59] S. Zhou, A. Starkov, M. K. Froberg, R. L. Leino, and K. B. Wallace, "Cumulative and irreversible cardiac mitochondrial dysfunction induced by doxorubicin," *Cancer Research*, vol. 61, no. 2, pp. 771–777, 2001.
 - [60] P. Alin, U. H. Danielson, and B. Mannervik, "4-hydroxyalk-2-enals are substrates for glutathione transferase," *FEBS Letters*, vol. 179, no. 2, pp. 267–270, 1985.
 - [61] P. Nioi and J. D. Hayes, "Contribution of NAD(P)H:quinone oxidoreductase 1 to protection against carcinogenesis, and regulation of its gene by the Nrf2 basic-region leucine zipper and the arylhydrocarbon receptor basic helix-loop-helix transcription factors," *Mutation Research*, vol. 555, no. 1–2, pp. 149–171, 2004.
 - [62] P. Talalay and A. T. Dinkova-Kostova, "Role of nicotinamide quinone oxidoreductase 1 (NQO1) in protection against toxicity of electrophiles and reactive oxygen intermediates," *Methods in Enzymology*, vol. 382, pp. 355–364, 2004.
 - [63] K. Iida, K. Itoh, Y. Kumagai et al., "Nrf2 is essential for the chemopreventive efficacy of oltipraz against urinary bladder carcinogenesis," *Cancer Research*, vol. 64, no. 18, pp. 6424–6431, 2004.
 - [64] L. A. Applegate, P. Luscher, and R. M. Tyrrell, "Induction of heme oxygenase: a general response to oxidant stress in cultured mammalian cells," *Cancer Research*, vol. 51, no. 3, pp. 974–978, 1991.
 - [65] M. Rizzardini, M. Carelli, M. R. Cabello Porras, and L. Cantoni, "Mechanisms of endotoxin-induced haem oxygenase mRNA accumulation in mouse liver: synergism by glutathione depletion and protection by N-acetylcysteine," *Biochemical Journal*, vol. 304, no. 2, pp. 477–483, 1994.
 - [66] M. C. Asensio-Lopez, A. Lax, D. A. Pascual-Figal, M. Valdes, and J. Sanchez-Mas, "Metformin protects against doxorubicin-induced cardiotoxicity: involvement of the adiponectin cardiac system," *Free Radical Biology and Medicine*, vol. 51, no. 10, pp. 1861–1871, 2011.
 - [67] L. M. Mela-Riker and R. D. Bukoski, "Regulation of mitochondrial activity in cardiac cells," *Annual Review of Physiology*, vol. 47, pp. 645–663, 1985.

- [68] S. Abdel-Aleem, M. M. El-Merzabani, M. Sayed-Ahmed, D. A. Taylor, and J. E. Lowe, "Acute and chronic effects of adriamycin on fatty acid oxidation in isolated cardiac myocytes," *Journal of Molecular and Cellular Cardiology*, vol. 29, no. 2, pp. 789–797, 1997.
- [69] J. R. Neely and H. E. Morgan, "Relationship between carbohydrate and lipid metabolism and the energy balance of heart muscle," *Annual Review of Physiology*, vol. 36, pp. 413–459, 1974.
- [70] R. Bressler, R. Gay, J. G. Copeland, J. J. Bahl, J. Bedotto, and S. Goldman, "Chronic inhibition of fatty acid oxidation: new model of diastolic dysfunction," *Life Sciences*, vol. 44, no. 25, pp. 1897–1906, 1989.
- [71] P. B. Corr, R. W. Gross, and B. E. Sobel, "Amphipathic metabolites and membrane dysfunction in ischemic myocardium," *Circulation Research*, vol. 55, no. 2, pp. 135–154, 1984.
- [72] A. M. Katz and F. C. Messineo, "Lipid-membrane interactions and the pathogenesis of ischemic damage in the myocardium," *Circulation Research*, vol. 48, no. 1, pp. 1–16, 1981.
- [73] G. Peluso, R. Nicolai, E. Reda, P. Benatti, A. Barbarisi, and M. Calvani, "Cancer and anticancer therapy-induced modifications on metabolism mediated by carnitine system," *Journal of Cellular Physiology*, vol. 182, no. 3, pp. 339–350, 2000.
- [74] Y. Olowe and H. Schulz, "Regulation of thiolases from pig heart. Control of fatty acid oxidation in heart," *European Journal of Biochemistry*, vol. 109, no. 2, pp. 425–429, 1980.
- [75] W. W. Winder and D. G. Hardie, "AMP-activated protein kinase, a metabolic master switch: possible roles in Type 2 diabetes," *American Journal of Physiology*, vol. 277, no. 1, part 1, pp. E1–E10, 1999.
- [76] S. Goffart, J. C. von Kleist-Retzow, and R. J. Wiesner, "Regulation of mitochondrial proliferation in the heart: power-plant failure contributes to cardiac failure in hypertrophy," *Cardiovascular Research*, vol. 64, no. 2, pp. 198–207, 2004.
- [77] A. M. Katz, "The myocardium in congestive heart failure," *American Journal of Cardiology*, vol. 63, no. 2, pp. 12A–16A, 1989.